Wireless Communications and Mobile Computing

Health Informatics: Applications of Mobile and Wireless Technologies

Lead Guest Editor: Milos Stojmenovic
Guest Editors: Tom Gedeon, Heng Qi, and Seyed M. Buhari

Health Informatics: Applications of Mobile and Wireless Technologies

Wireless Communications and Mobile Computing

Health Informatics: Applications of Mobile and Wireless Technologies

Lead Guest Editor: Milos Stojmenovic
Guest Editors: Tom Gedeon, Heng Qi, and Seyed M. Buhari

Editorial Board

Contents

Hindawi
Wireless Communications and Mobile Computing
Volume 2019, Article ID 6518784, 1 page
https://doi.org/10.1155/2019/6518784

Editorial

Health Informatics: Applications of Mobile and Wireless Technologies

Milos Stojmenovic,[1] **Tom Gedeon**,[2] **Heng Qi**,[3] **and Seyed M. Buhari**[4]

[1]*Singidunum University, Serbia*
[2]*The Australian National University, Australia*
[3]*Dalian University of Technology, China*
[4]*King Abdul-Aziz University, Saudi Arabia*

Correspondence should be addressed to Milos Stojmenovic; mstojmenovic@singidunum.ac.rs

Received 28 November 2018; Accepted 28 November 2018; Published 3 January 2019

Applying mobile and wireless technologies to the health informatics arena has proven to be a timely topic of interest here. Our special issue has chosen 9 publications from a field of competitive submissions, which we feel best reflect reader's interests, include a high level of novelty, and capture the essence of the topic. We feel that the scope of this special issue will remain of significant interest to the scientific community in the future as the potential applications of these technologies in the field of medicine have not nearly been exhaustively explored.

Conflicts of Interest

Editors declare that they have no conflicts of interest regarding the publication of this Special Issue.

Milos Stojmenovic
Tom Gedeon
Heng Qi
Seyed M. Buhari

Hindawi
Wireless Communications and Mobile Computing
Volume 2018, Article ID 2394384, 14 pages
https://doi.org/10.1155/2018/2394384

Research Article

Wireless TDMA-Based Body Area Network Platform Gathering Multibiosignals Synchronized with Patient's Heartbeat

Tae Min Hwang,[1] Seol Young Jeong,[2] and Soon Ju Kang[1]

[1]*School of Electronics Engineering, College of IT Engineering, Kyungpook National University, 80 Daehakro, Bukgu, Daegu, Republic of Korea*
[2]*School of Computer Science and Engineering, College of IT Engineering, Kyungpook National University, 80 Daehakro, Bukgu, Daegu, Republic of Korea*

Correspondence should be addressed to Soon Ju Kang; sjkang@ee.knu.ac.kr

Received 23 February 2018; Revised 6 October 2018; Accepted 21 October 2018; Published 3 December 2018

Academic Editor: Javier Prieto

In the application of a body area network in medical healthcare, the process of receiving, archiving, and analyzing multibiosignals simultaneously from different devices for each body is very important. For example, to diagnose sleep apnea symptoms, a patient must sleep with dozens of devices, including electroencephalography (EEG), electrocardiogram (ECG), photoplethysmogram (PPG), peripheral oxygen saturation (SpO2), nasal cannula, and bands. Various wireless methods of body area network for acquisition and measurement of body signals have been introduced, but it is difficult to accurately diagnose various biosignals because their measurement frequencies are different from each other, and they are not guaranteed precise synchronization. Because each body biosignal is commonly synchronized with the heartbeat of the patient, precise synchronization of the heartbeat and other measuring cycles of each device is a critical attribute for analyzing the corelation of each biosignal in the body area network. However, it is difficult to guarantee the precise synchronization of multibiosignals by solely using carrier sense multiple access with collision detection- (CSMA/CD-) based wireless protocols, which are mainly used in existing body area networks. This study proposes a method of creating a self-organizing body area network based on wireless Time Division Multiple Access (TDMA) to guarantee the synchronization of multibiosignals and compare its accuracy with the CSMA/CD method.

1. Introduction

As the medical healthcare environment has changed from hospital-centered to home-centered, medical devices have changed accordingly. Classification of these medical devices can be broadly divided into wired and wireless. Wired medical devices have high precision, but they are inconvenient to wear, complicated, and difficult to use by individual patients. Therefore, these wired medical devices are not suitable for a patient living at home. In contrast, wireless medical devices are usually worn by the patient in the form of wearable devices. Because there are no wires, they are convenient to wear and using them is relatively simple. Therefore, they can be used by the patient without assistance. For this reason, interest in wireless medical devices has increased, and studies have been actively conducted. In addition, the body area network for connecting many wireless medical devices has attracted much attention.

The body area network is a short-range wireless communication technology in which devices installed inside and outside the human body can be connected and communicated. Because each device is used in contact with the human body, data such as electrocardiograms, heart rate, and acceleration can be measured according to the device. Therefore, attention has been paid to convenience and usability, and an attempt has been made to provide patient-centered medical services based on measurement of human biometric data in real life. However, for complex medical diagnosis, the following constraints must be considered.

The first is the acquisition of multibiosignals synchronized with the patient's heartbeat. To analyze two or more biosignals at the same time, it is necessary to read various

biosignals from one device or several devices worn in different parts of the body. In this case, because signals arriving from several devices must be synchronized with the measured time, accurate signal analysis can be performed. Therefore, it is necessary to perform a verification process for the received signals when they are measured.

The second is user convenience. The wearable device has an advantage in that it is easy to carry and use. However, when a healthcare medical system is constructed, a user wears a plurality of devices. If many devices need to be manually operated simultaneously, the user will feel rather uncomfortable with the wearable device. Therefore, to take advantage of the wearable device, the body area network-application needs to be configured with minimal user intervention, to be simple and easy to use.

In this paper, we propose a method for constructing a wireless Time Division Multiple Access (TDMA) based body area network platform. The proposed wearable devices constitute a body area network, based on one device to store data and perform time synchronization using periodic sync-signals generated from the central device. The devices periodically receive biometric signal data through the connected peripheral devices. The user receives and stores data from different wearable devices by manipulating the central device without having to manipulate the wearable devices separately. The devices have predefined biosignal channel information, so that the devices can generate and destroy channels without having to exchange prior information about the biosignals, thereby reducing the connection time. Since data can be acquired from the devices by a simple operation, the convenience of the user can be enhanced, and the inconvenience that users may feel using the device can be minimized.

The contribution of this paper is wireless body area network (WBAN) platform that enables users to add or delete wearable devices that measure biomedical signals according to actual pathology. The proposed WBAN can measure various vital signals that are important for time synchronization with heart signal using TDMA wireless communication method. The photoplethysmogram (PPG) signal being compared with the heartbeat signal can measure the blood pressure or pathology diagnosis, so it is particularly important to confirm the time synchronized signal. In this paper, we propose a wearable device that can measure time synchronized signals and make it easy to use in real environment.

Section 2 explains the basic concepts of the method. Section 3 describes the scenario and system requirements of the synchronization method proposed in this study. Section 4 explains the structure and design of the hardware and software for implementation. Section 5 describes the implementation of the method and the scenario used for verification and explains the result of the communication loss ratio of the implemented result. In Section 6, we conclude with future research.

2. Basic Concepts and Related Research

2.1. Body Area Network. As shown in Figure 1, sensors in the body range can be connected, and data can be collected; this data can be sent to the server side and monitored from the outside, so that it can be used in a variety of applications such as emergency situations, remote medical treatment, and exercises [1, 2].

However, because the sensors must be within the human body range, there is a disadvantage in that the size of the installed device is limited, and since the sensor operates in the state in which the user wears it, the consumption of the battery needs to be minimized [3]. Sensors used in the body area network typically require data rates in the order of a few kb/s to several Mb/s (body temp sensor, electrocardiogram (ECG), electroencephalography (EEG), and electromyography (EMG)). Therefore, to transmit each signal in the wireless environment, a sufficient communication protocol should be used for the bandwidth, and there are many protocols that satisfy this (such as ZigBee, Bluetooth SMART, and ANT +).

Within the body area network, sensors are attached to various parts of the body that collect biometric data and deliver it to the gateway. Signals delivered to the gateway can be connected to an external monitoring and alarm system to determine the current patient status in real time. In this study, a system is proposed in which a device attached to a human body forms a cluster; another device acts as a gateway, receiving data from the cluster and delivering it to the outside.

2.2. Wireless Communication Protocol. The communication protocol used for the wireless body area network can be either the carrier sense multiple access with collision detection (CSMA/CD) method or the Time Division Multiple Access (TDMA) method. Table 1 compares the traffic level and synchronization attribute of the protocols.

CSMA/CD is a method of identifying the part where a collision can occur by detecting a carrier wave. It is possible to detect the use of communication, so that it is possible to avoid a collision between different attempts at communication, thus facilitating the configuration of a multicommunication environment constituting a body area network. As a representative MAC protocol using the CSMA/CD method, Bluetooth SMART and ZigBee are used, and body area network research is also actively performed [4, 5].

However, rather than delivering data directly, it is necessary to store the data to be sent to the queue first and to send it when communication is possible. Therefore, if the connection occurs frequently, data may not be transmitted at the desired time, and congestion may occur. Since each sender needs to perform a separate task of synchronizing the receiver with queuing data to be sent, much effort is required in synchronization [4].

The TDMA scheme is a method of using a frequency band without causing a collision, because a plurality of users use the frequency band at the same time. In the TDMA scheme, a frequency band is used only by a predetermined user during a specific period, thereby avoiding collision between users. Therefore, it is advantageous for periodic signal transmission and transmission that is not delayed. It is advantageous in comparison with CSMA/CD when data is transmitted by connecting to a plurality of UEs. Due to these advantages, many studies have been conducted on body area network

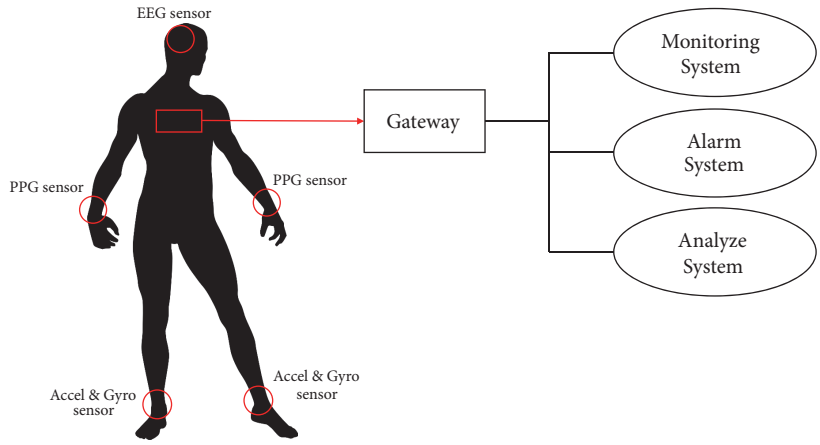

Figure 1: Body area network (BAN) structure.

Table 1: Comparison between TDMA and CSMA/CD.

Protocol	TDMA	CSMA/CD
Preferred traffic level	High	Low
Synchronization	Depends on the latency	Depends on the traffic

using TDMA [3, 6–10]. However, if multiple slots are used adjacent to each other and the transmission timing is not accurately maintained, there is a possibility of causing a collision with a signal of another slot. Therefore, the slot between signals needs to be sufficiently large.

3. Service Scenarios

3.1. Service Scenarios. In this study, each wearable device forms a cluster to read user biometric data and transmit it to the server device in real time, so that the data can be synchronized. By forming a cluster autonomously between the devices in which the user is not required to separately issue commands, the user can minimize the hassle of manipulating the devices and acquiring biosignals, so that convenience is achieved while simultaneously conducting a comprehensive analysis of the signal.

Figure 2 is an illustration of the type of service we want to provide. The user wears each wearable device on the relevant part of the body. Since the type of data that can be measured varies depending on the area in which the device is worn, the user can wear the device on other body parts depending on the purpose of the measurement.

The wearable devices receive the synchronization signal transmitted by the central device periodically and recognize the peripheral devices by transmitting a confirmation message. To distinguish the devices from each other, each device transmits its own device ID and is assigned an address value. Then, the devices in the created organization begin measuring by the measurement start signal of the central device. A channel for each biosignal is created, and the biosignal is transmitted through the corresponding channel.

In this case, because the transmission period for each biosignal is different, the central device first receives the biosignal from the device, stores it in the buffer, and then identifies the data of the channel to be stored in each cycle through the scheduler. The separated data is transferred to a separate analysis module and stored in the SD card or communicated with an external server to transmit data every cycle. The status of the wearer can be known by monitoring the delivered data from the outside in real time.

3.2. Design Requirements. To construct the body area network used in this study, each device must satisfy the following requirements [4].

The first is that it is easy to use. If the user operates all of the devices, the advantages of the wearable device are that it is easy to carry, which does not matter if the device cannot be utilized. Therefore, all the devices should be operable by manipulating the central device of the cluster.

The second is that it can be operated in real time. The data received from each device is inevitably delayed while being immediately transferred through the gateway. In this case, when the data is sent some time after data is accumulated in each device, the entire delay becomes large, so that it is not suitable for situations in which the user's emergency status must be immediately checked. Therefore, it is necessary to acquire each packet of data and send it to the central device immediately.

Next is communication stability. If the communication of each device is not performed properly due to a collision or other factors, incorrect data will be collected, and, if analyzed, a wrong result may be obtained. Therefore, communication should be performed in a stable manner in any situation.

Finally, the system should be secure. Since all the data acquired through the human body network is sensitive information of the individual, it is necessary to maintain the

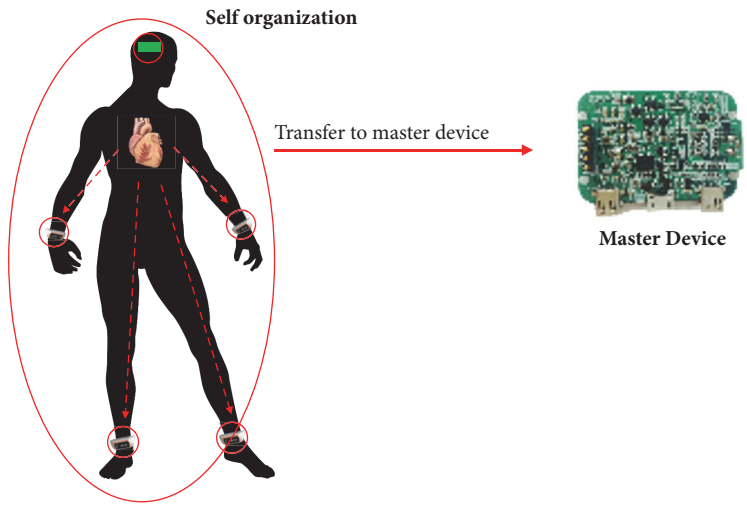

Figure 2: Body area network (BAN) structure.

security of the learning process, measure the data, encrypt it, and transmit it to the other devices.

4. Detailed Structure and Design

4.1. Device Structure. Each worn device plays a role in biometric data collection and delivery. From Figure 3, the user can separately check biometric data, reading through the user interface. Biometric data can be collected regardless of whether or not the organization is formed. In this case, since synchronization with other devices is not necessary, it is possible to measure based on the local time.

Afterwards, it communicates with the center device in an organization with the external device, forms the cluster, and transmits the stored data. Since the channel information of the biometric data of the device is predefined, the devices can form a channel based on the channel information and transmit the data according to the request of the center device. In this case, each organization has a different network value in order to prevent confusion with the external organization, thereby preventing collision with the external organization.

Figure 4 shows the central device of the cluster and the devices connected to each other to receive and manage data according to the synchronization signal. Since the communication is performed by the TDMA method, when the signal transmission timing of the device deviates, there may occur a situation where a collision with a signal from the other device fails. Therefore, to prevent collision between signals, the central device periodically transmits a synchronization signal to prevent collision between the devices, preventing a collision when a new device is added. Then, according to the request of the central device, the devices form a channel to transmit the biosignal to the corresponding channel. In this case, since the center device has different periods for the biosignals, a task for managing the schedule is set separately, and the timing of receiving the data based on the respective synchronization signals is confirmed before receiving the biosignals. After receiving the signal from each device, the scheduler confirms the timing and stores the data by time. If there is no data at the scheduled time, it is determined that a loss has occurred in the transmission process and is marked separately.

After that, communication with the external gateway or wired communication with the analysis module is performed to transmit data, thereby enabling data storage, monitoring, or data analysis to be performed.

4.2. Software Architecture. Figure 5 shows the software structure of the wearable device for implementation. The software of the wearable device includes a main event task to process the entire event, a user interface task to display the state of the current device, a sensing task to perform signal measurement and process communication with the sensor, and there is a communication management task to manage the time slots.

The main event task processes the various events occurring in the device, and it handles the state change of the UI, the start and finish of the sensing task, and the button click event.

The communication management task accepts a connection request from the central device and generates a channel to transmit a biosignal. It also receives specific biometric data from the sensing task and delivers it to the central device.

4.3. Creating and Releasing Organization. The generation of the interdevice organization is based on the synchronization signal of the central device. The central device periodically sends a signal around the synchronization channel.

Figure 6 is a sequence diagram for cluster generation. The device that receives the signal can be divided into two cases, one with, and one without the assigned address. If there is no assigned address, an address allocation request-message is transmitted to the central device in order to allocate a new address. The central device receives the message, checks the empty address, and transmits the value to the device to allocate the address. After this, the device can send a message to the corresponding address. The device to which

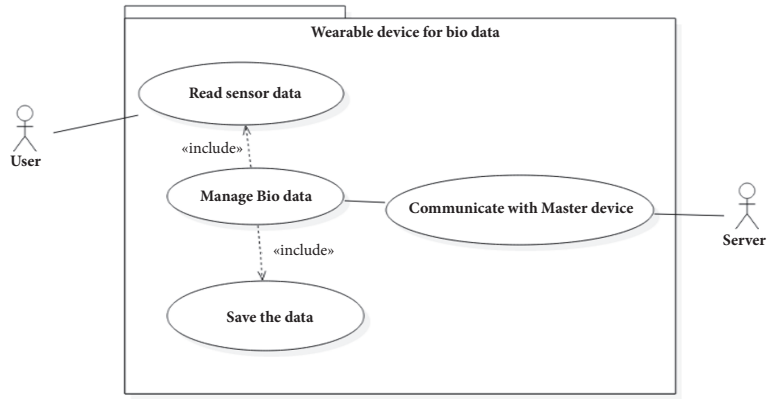

Figure 3: User biodata capture of wearable device.

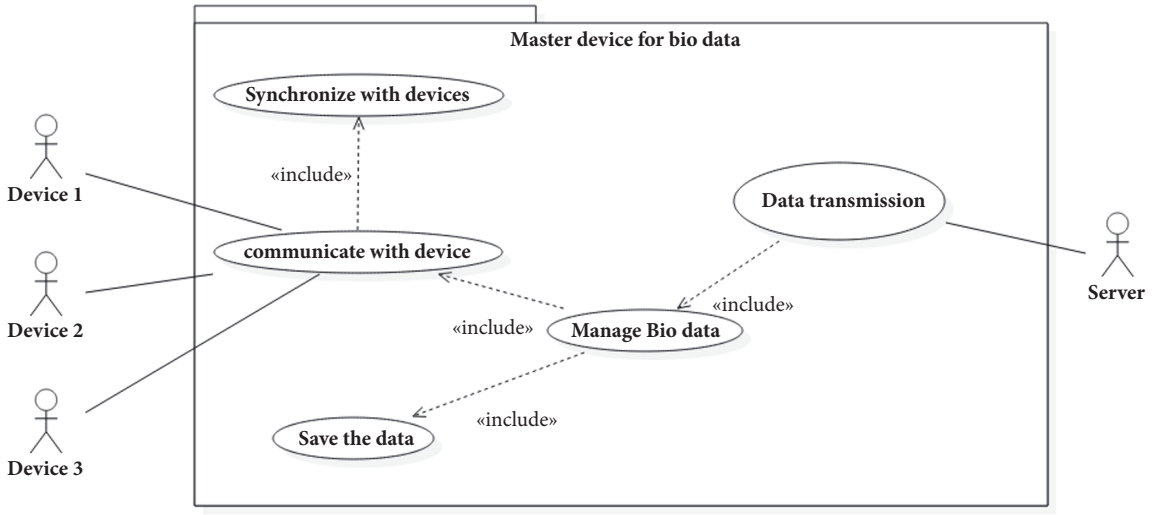

Figure 4: UseCase diagram for connection between devices and data transmission.

the address is allocated transmits a response message to the synchronization signal with a unique device address.

At this time, the unique ID of the device and the sequence value of the synchronization message are stored and sent together in the response message. The central device receives the received message and checks the address of the message and the unique ID stored in the message. If the ID is not included in the organization, the central device stores the unique ID device information for the address together. By storing the device information in this way, when the device makes a data request at a later time, the device can distinguish the measurable biometric signal and make a request.

Many situations can involve the release of the organization, as shown in Figure 7. The first is the release by the decapitating signal of the central device. Like the organization creation, the central device can issue the organization release command to the device registered through the synchronization signal. Upon receiving the declassification command, the device sends a response message, closes the connected channel, and removes the registration information. Upon receiving the response, the central device releases the registration of the corresponding device.

The second is an unresponded state due to distance or battery shortage. The wearable device has a channel-specific watchdog timer. As shown in Figure 8, when the watchdog timer is reset by receiving the synchronization message of the central device and N messages are counted, it is determined that the connection with the central device should be disconnected without receiving the synchronization signal, and the channel connected to the central device is initialized to reduce unnecessary power consumption.

4.4. Timeslot Allocation of TDMA Scheme. In TDMA, one channel is allocated one time slot, as shown in Figure 9. The number of channels that can be connected at one time varies depending on the size of the time slot based on the synchronization signal. When the length of one cycle time is T and the length of the time slot is *t_slot*, as the synchronization signal channel always occupies one slot,

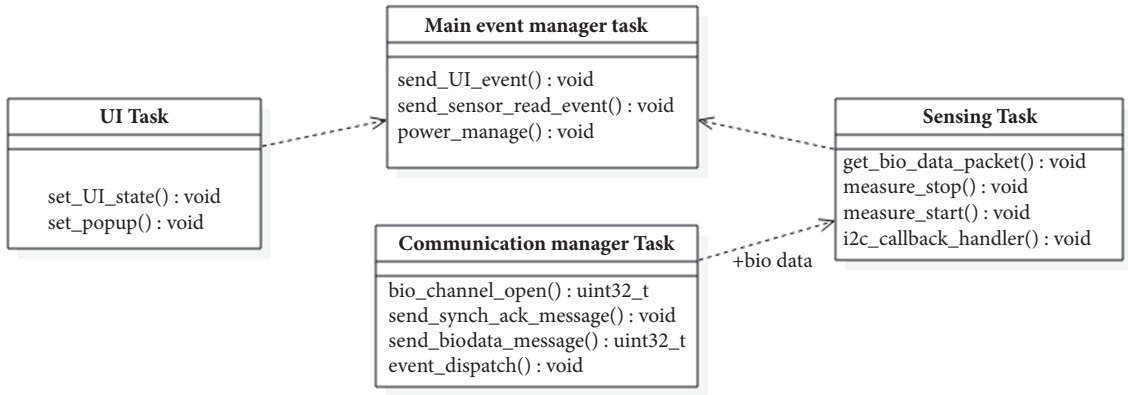

Figure 5: Software structure of wearable device.

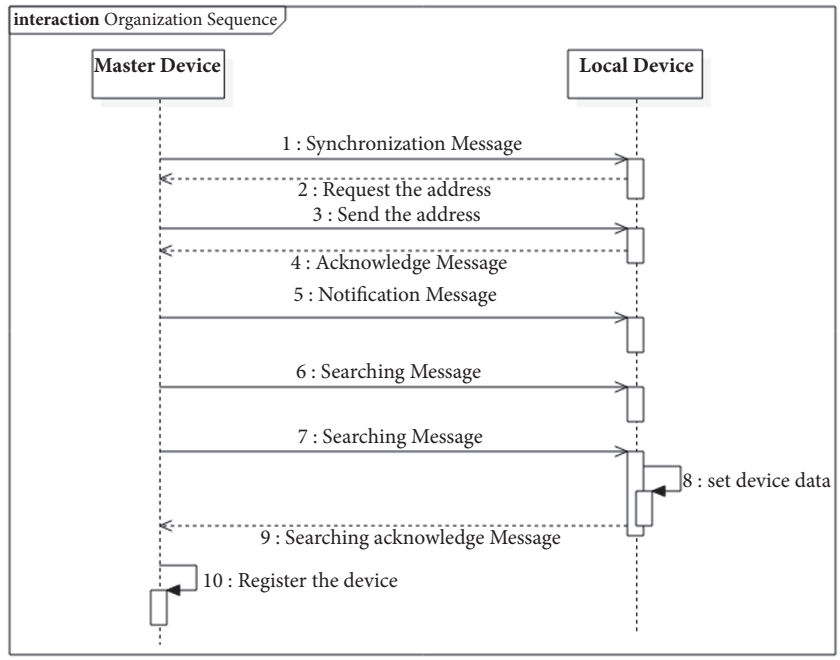

Figure 6: Organization sequence diagram.

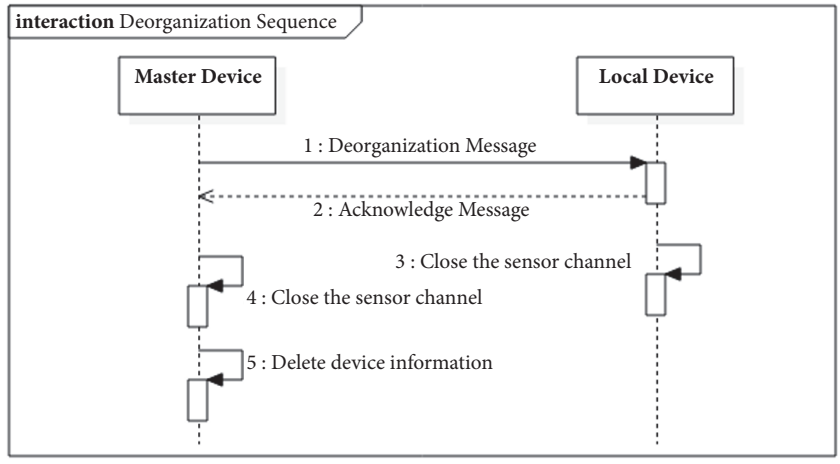

Figure 7: Deorganization sequence diagram.

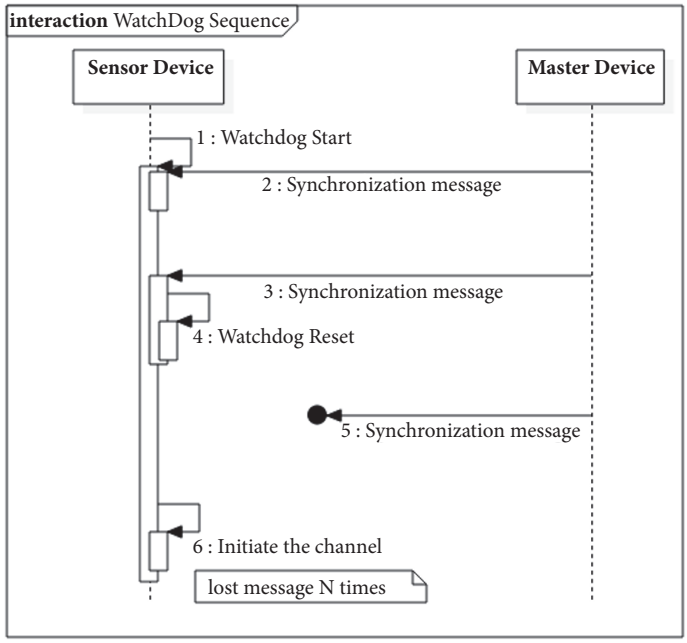

Figure 8: Sequence diagram for watchdog timer of sensor channel.

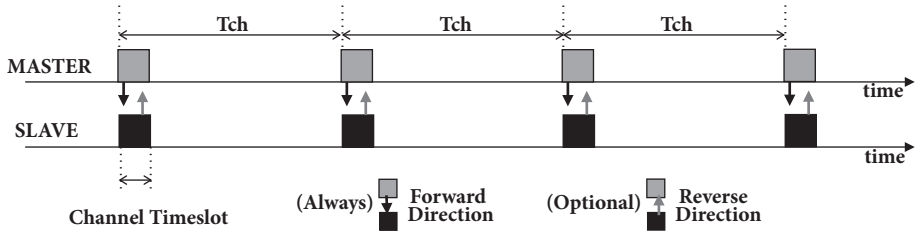

Figure 9: Time slot allocation of TDMA.

the number *n_channel* of the connectable channels can be expressed as follows:

$$n_{channel} = \frac{T}{t_{slot}} - 1$$

$$n_{channel} : Number\ of\ channel$$

$$t_{slot} : Length\ of\ timeslot \quad (1)$$

$$T : Length\ of\ one\ cycle\ time$$

Figure 10 shows the process of transmitting data in a scheduled slot according to the synchronization signal of a central device. The central device transmits a synchronization signal to each of the devices in the first slot of the period. The devices receiving the synchronization signal store the sequence information of the current data based on this signal, and transmit the message, including the biometric data and the sequence number, to the central device side. This process is performed for each device, and as a result, the data from each device can be acquired without collision in one cycle.

At this time, the synchronization signal has the same cycle as the cycle of the signal to be transmitted. This is to distinguish the signals in a cycle based on the synchronization signal and to prevent communication collision in the TDMA.

$$T_{Master} = T_{min}$$

$$T_{Master} :$$

$$Synchronization\ signal\ cycle\ of\ the\ center\ device \quad (2)$$

$$T_{min} : Cycle\ of\ the\ shortest\ signal$$

4.5. Packet Structure of Synchronization Messages. In Table 2, the packet structure of the synchronization message is configured. First, messages sent to the wearable device by the central device are divided into three types—synchronization, organization creation, and organization release. The synchronization message is used for the external synchronization and device information request. The synchronization message includes an address value of a device to which a message is to be sent (an address is blank when sending a notification message to all devices) and an order value.

The organization creation and release message is a message sent to the identified wearable device to command the

Table 2: Synchronization message payload.

Device	Command	Value	Bit 0	1	2	3	4	5	6	7
Main Device	Sync	0xff	addr1	addr2	0xff				sequence1	sequence2
	create channel	0x01	addr1	addr2	0x01	bio data type	device number	network num		
	delete channel	0x02	addr1	addr2	0x02	bio data type	device number	network num		
Sensor Device	Ack device info	0xff	addr1	addr2	0xff	bio data type	device id1	device id2	sequence1	sequence2
	ack channel created	0x01	addr1	addr2	0x01	bio data type	channel number			
	ack channel deleted	0x02	addr1	addr2	0x02	bio data type	channel number			
	nack channel already created	0x03	addr1	addr2	0x02	bio data type	channel number			

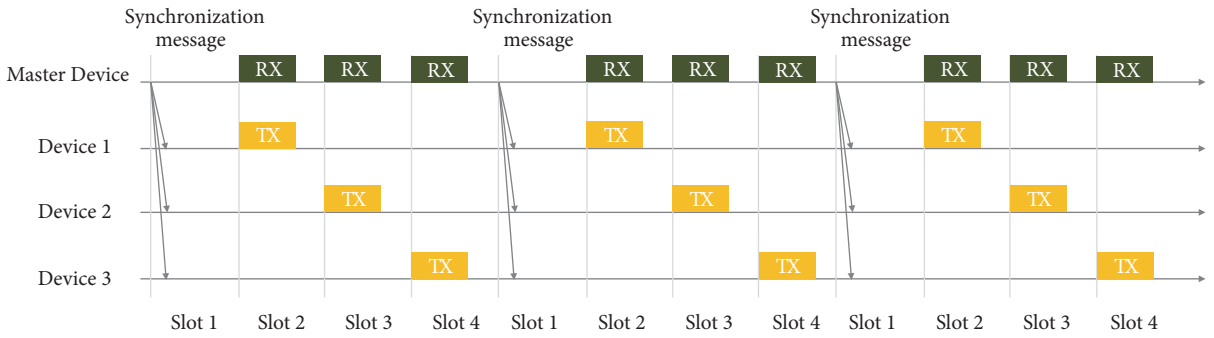

Figure 10: Example of time slot allocation in multidevice connection.

cluster. When sending this message, the following information is transmitted to obtain specific biometric data from each wearable device.

(i) Biometric data type: since the data rate or period required by the biometric data to be measured is different, it is necessary to define the biometric data type in advance so that the central device and the wearable device can directly transmit the biometric data, so that the channel information can be aligned with the center device.

(ii) Cluster network unique number: to prevent overlapping with the other surrounding organization when the organization is created, the unique number of the cluster network managed by the central device is transmitted, setting it as the network unique number of the cluster and preventing it from being included in the.

(iii) Timeslot assignment number: since there is no collision with the different timeslots for each device, the time slot number assigned when connected to the device is delivered.

On the contrary, when the wearable device sends a response message to the central device, the response message can be either a response to the synchronization message, an affirmative response to the organization creation and release command, or a negative response.

When a response to a synchronization message is sent, the following information is also included:

(i) Biometric data type: biometric data that can be measured according to the type of device and the part to be worn are distinguished, and this information is included in the response.

(ii) Device identification number: since the central device knows not only the address assigned to each device but also the device identification number, it can be distinguished, even if the other device responds with the same address.

4.6. Communication between Devices. Based on the synchronization signal of the central device, each device generates a channel and establishes a connection between the devices. Figure 11 shows the channel generation between the central device and the wearable device in the cluster.

First, the central device periodically transmits a synchronization signal to the wearable device in a state in which the synchronization channel is open, thereby confirming the connection state and transmitting/receiving signals. If a connection is needed, the central device transmits a request to the address of the wearable device to request channel creation according to the synchronization period. Upon receiving the message, the wearable device confirms the requested biosignal type, network value, and device number within the signal, and generates a channel corresponding to the request. If it is successful, the response is transmitted to the central device. If the channel creation fails with respect to the request, the channel creation failure-message is also transmitted to the central device. The central device checks the response received from the wearable device, and when the channel is successfully created, the central device receives the data from the wearable device by connecting the corresponding channel.

The wearable device receives the user's biometric data at a predetermined period through the sensor device. Since the received data is stored in the buffer and the data is transmitted every TDMA cycle, there is no need to separately queue the data.

4.7. Signalling and Scheduling. Figure 12 shows the process of reflecting the message exchange process and scheduling between the central device and the wearable device in a sequence diagram. When the center device is connected to the wearable device, the center device registers the cycle of the corresponding biosignal in the schedule. Then, the communication task transfers the synchronization signal to the devices in the cluster. The schedule task stores the signals arriving between this signal and the next synchronization signal in one cycle. The wearable device reads and stores the wearer's vital signs, and delivers the message to the central device at every cycle.

5. Implementation

5.1. Hardware Implementation. In Figure 13, the implementation platform is shown as follows. The

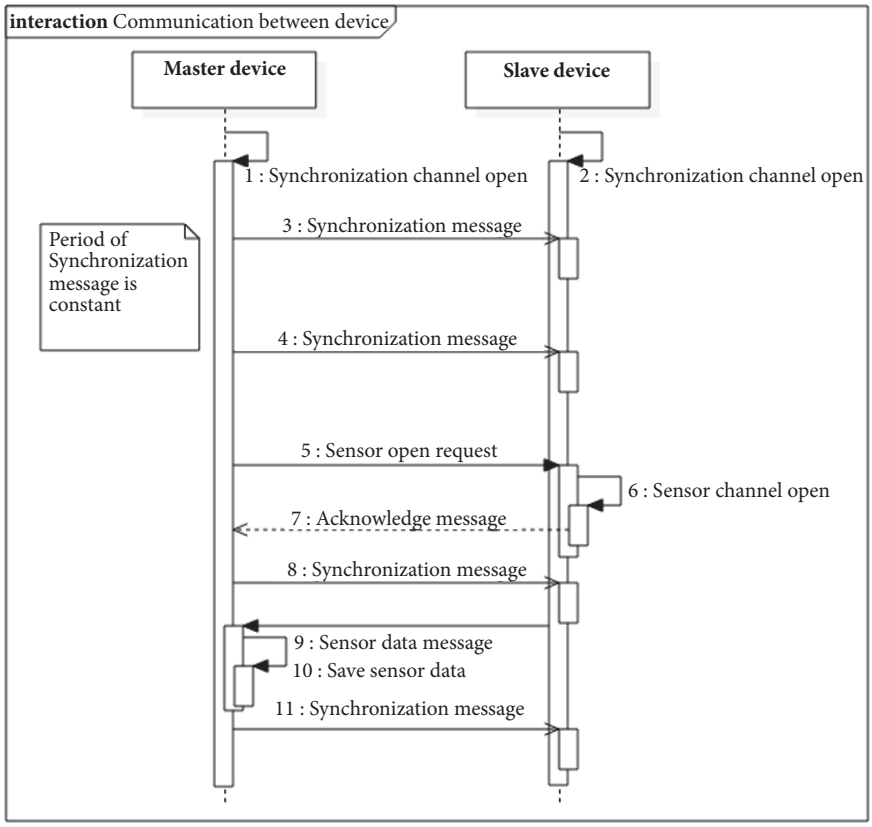

Figure 11: Sequence diagram for communication between organizations.

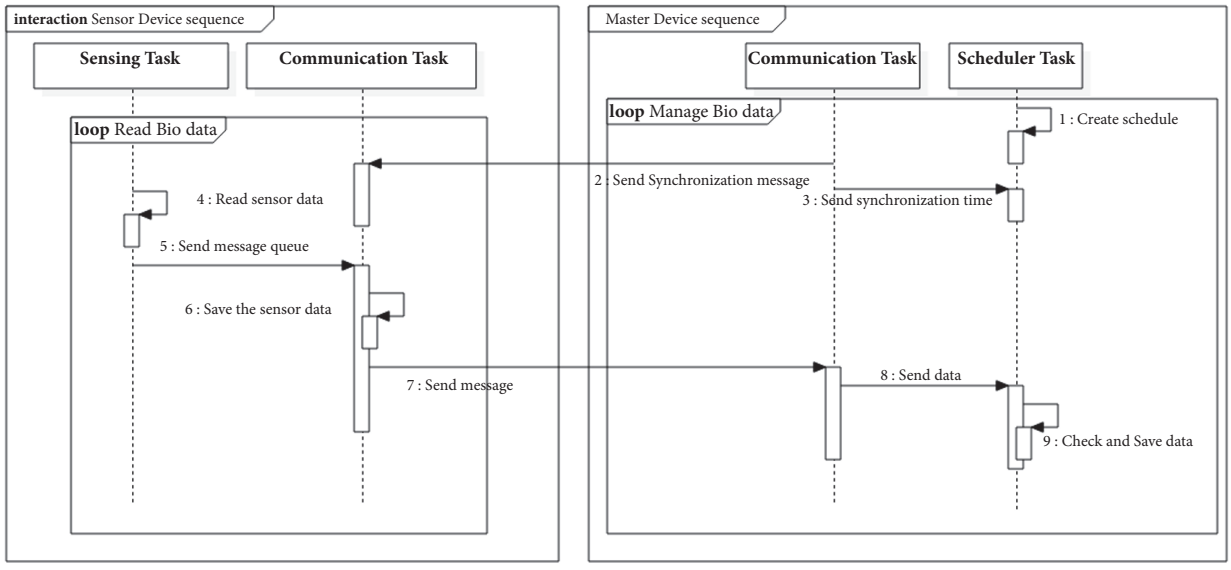

Figure 12: Sequence diagram for saving data of master device.

photoplethysmogram (PPG) module and the acceleration sensor are connected to each wearable device in which the biosignal and acceleration data are read and stored, and data is transmitted to the central device through the RF transceiver. The status of the wearable device can be confirmed by the LCD, and the button is used when operation is required.

The central device is equipped with an oxygen saturation module and can measure the biomedical signal in the center device. The measured data and the data of the wearable device

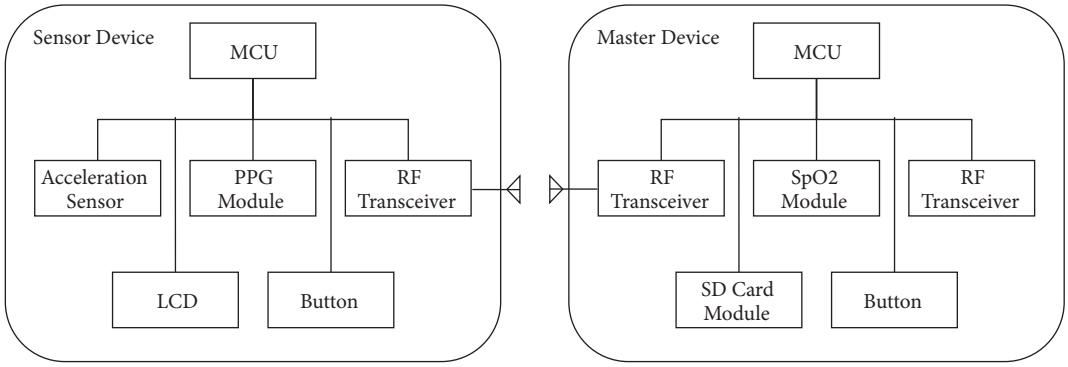

Figure 13: Implemented platform structure.

are collected, and the biomedical signal data array is created and stored in the SD card or transmitted to the outside. In addition, the button is used to check the cluster creation and destruction.

The wearable device and the center device are each configured, as shown in Figure 14. The wearable device is implemented as a wristband to be worn on the user's wrist. The PPG module is connected under the band to measure the PPG signal, and the data is received from the PPG module and transmitted to the central device. The central device receives data from the wearable device while connected to the PC using the nRF52 development kit.

The proposed wearable medical device consists of two parts. The microcontroller unit (MCU) of master device is CortexM4-based nRF52832 chip (frequency: 64 MHz, operating voltage 3.3 V). The sensor device has the EFM32WG990F256 chip (frequency: 48 MHz). As shown in Figure 15, power consumption is an average of 76 uA in the idle state and from minimum 295 uA to maximum 52 mA (average 12 mA) in the sensing and streaming communication state.

5.2. ANT Communication. In this study, the ANT protocol is used to implement wireless TDMA communication. ANT is a type of communication protocol mainly used for medical and health care purposes. ANT has the advantages of simple implementation and low power consumption. It also operates in TDMA and is used within a range of less than 100 meters, similar to BLE. Its data rate was 12.8 kbits/s for broadcast and acknowledging messages and 60 kbits/s for burst mode.

Table 3 shows the performance comparison with major wireless protocols.

Compared with Bluetooth SMART and ZigBee, ANT communication transmits at 12.8 kbits/s when the data rate is broadcast/ACK message, which is somewhat lower than other communication rates. However, since the configuration of nodes is free, it is easy to form interdevice clusters, and, in the case of the system to be used in the paper, data is periodically received from the device, so that data transmission also needs to be performed periodically. Because Bluetooth SMART and ZigBee are CSMA/CD type in this respect, ANT communication is used, because there is a disadvantage in that it is difficult to guarantee the periodicity when several devices transmit signals in a short period.

5.3. PPG Signal. The PPG signal is used in the wearable device for verification. The PPG signal is a signal that indicates the change in the blood volume of the blood vessel due to the heartbeat through the return light by using the principle of absorption, reflection, and scattering by emitting light to the blood vessel. Because the signal form according to the heartbeat during measurement is clearly revealed, and the data measurement period is short, shown in Table 4, it is easy to implement the congested communication environment, and the PPG signal is measured. The PPG signal is measured once every 10 ms and is sent once every 40 ms. One piece of data has a size of 3 bytes.

6. Evaluation

6.1. Evaluation Scenarios. The measurement environment is constructed as shown in Figure 16.

First, the user wears the wearable device on the wrist. In the module of the wearable device, the PPG infrared sensor is connected to the finger, and the PPG signal is measured from the connected PPG sensor and is transmitted to the central device. If the synchronization is performed normally, each wearable device simultaneously measures the PPG signal in real time, such that the increase and decrease in the signal will be similar.

In the ANT protocol environment, two channels are required for each PPG signal to transmit the PPG channel for sufficient performance evaluation. In the ANT protocol, since eight channels are available in one device, three wearable devices are connected in order to use the maximum number of channels. Therefore, there are six ANT channels. For comparison, the Bluetooth protocol also connects three peripherals to the central device.

The performance evaluation method is as follows. The measurement is started according to the signal of the central device when each of the devices is connected. At this time, the central device confirms the signal, and the message order value is sent from the respective wearable devices

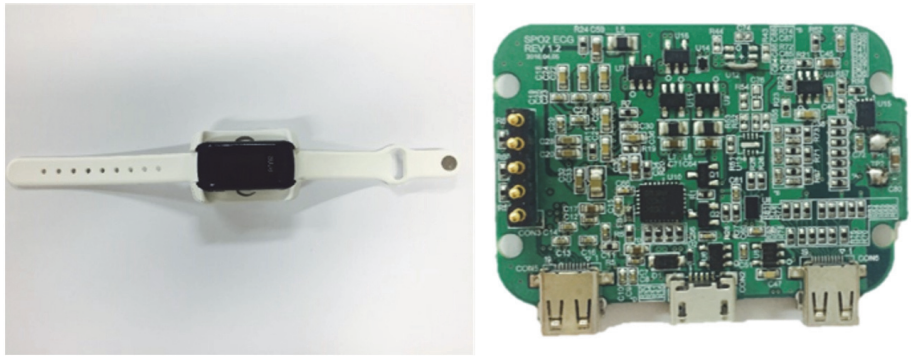

Figure 14: Implemented wearable device (left) and master device (right).

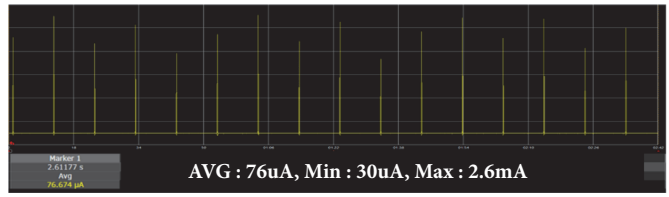

(a) Power consumption in idle state

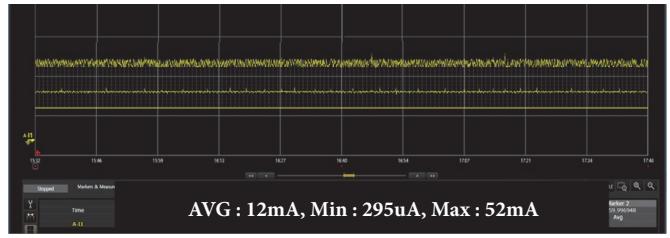

(b) Power consumption in running state (sensing and streaming communication)

Figure 15: Low power consumption of proposed device.

Figure 16: Wearable devices and PPG modules.

and confirms that communication has been performed for every synchronization period. After receiving the data from the wearable device for about five minutes, it checks what percentage of transmissions resulted in error messages. In addition, it confirms how the order value of the Bluetooth SMART protocol and ANT communication is changed compared to the first one, based on one wearable device, and confirms that synchronization is properly performed.

6.2. Comparison of ANT and Bluetooth SMART Communication for PPG Signals. Figures 17 and 18 show graphs displaying the PPG signals received from each wearable device using Bluetooth SMART and ANT protocols, respectively. Figures show the heartbeat signal (blue) and the PPG signals (red, green) of the both wrist. Figure 17 shows that the time synchronization does not match, even though the signal is measured at the same time. The signals of the two wrists have a heart signal and a delay time of 25~35 ms. On the other hand, in case of ANT+, which is a TDMA method, it can be confirmed that the synchronization is exactly performed every 40 ms that generated the signal. Figure 18 shows how the order value changes with time from the reference signal when the PPG signal is received in Bluetooth SMART.

Table 3: Comparison between wireless protocols.

Protocol	*ANT*	*Bluetooth SMART*	*ZigBee*
Standardization	Proprietary	Standard	Standard
Topologies	Point-to-point, star, tree, mesh	Point-to-point, star	Mesh
Range	30 m at 0 dBm	10-100 m	10-100 m
Max data rate	Broadcast/Ack – 12.8 kbit/s Burst – 20 kbit/s Advanced Burst – 60 kbit/s	1 Mbit/s	250 kbit/s
Application throughput	0.5 Hz to 200 Hz	305 kbit/s	
Max nodes in piconet	65536 per shared channel (8 shared channels)	1 master and 7 slaves	Star – 65536

Table 4: PPG (photoplethysmography) specification.

Bio-signal	**Photoplethysmography**
Required Data Rate (kbps)	24
Data size (bytes)	3
Maximum Frequency (Hz)	100
Period (ms)	40

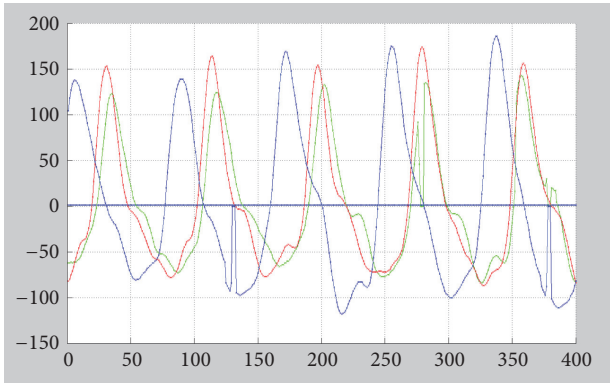

Figure 17: Multiple PPG signal with Bluetooth SMART (CSMA/CD).

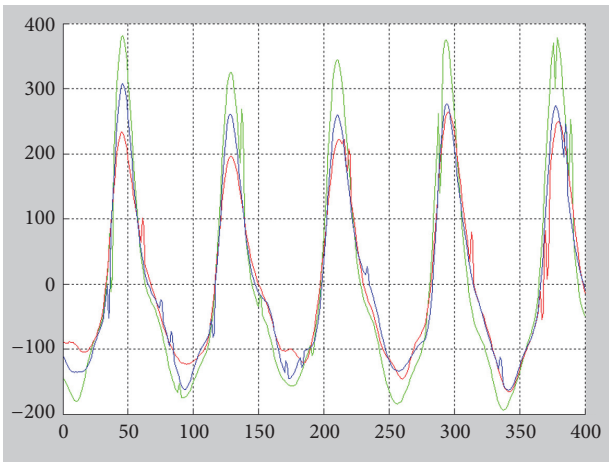

Figure 18: Multiple PPG signal with ANT (TDMA).

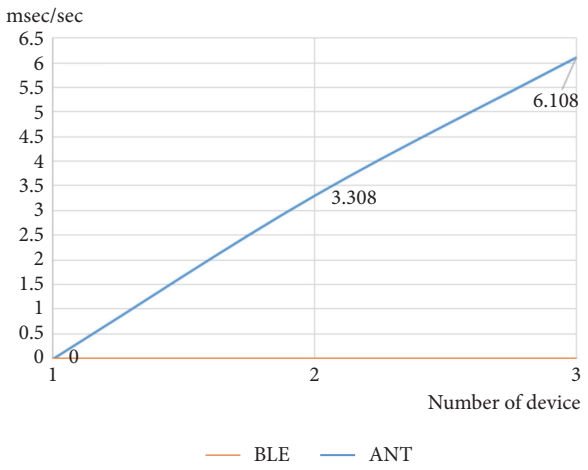

Figure 19: Difference of latency per time (msec/sec).

As shown in Figure 19, when the Bluetooth SMART protocol is used, the difference in the order value increases with time. As the number of devices increases, the cumulative delay time that is accumulated increases with time. In the case of three devices, we can see that the delay is 6.108 msec/sec. On the other hand, when the ANT protocol is used, it can be confirmed that no cumulative signal delay due to queuing occurs.

When the PPG signal was transmitted every 40 ms for 5 minutes, the error rate is 3.26% in ANT communication and 1.74% in Bluetooth SMART. The proposed TDMA method has a relatively small difference of error rate as compared with CSMA/CD-based Bluetooth communication.

7. Conclusions

In this study, based on wireless TDMA communication, wearable devices form self-organization to construct a body area network and transmit data based on a synchronization signal. To form a cluster, the central device periodically transmits a synchronization message to the periphery. At this time, the wearable device within the range receives this message and transmits a response message that includes the device information to the central device side.

Based on this response, the devices form one organization, and the organization is divided by the network key.

Each wearable device learns the biosignal of the worn portion on the connected central device side and delivers it to the allocated time slot.

The central device separately checks the timing of each device through scheduling, generates a separate buffer, stores the biometric data of the corresponding period, and confirms it with an SD card or an external device.

To verify this scenario, we propose a method to transmit the PPG signal over six channels through the ANT protocol (based on TDMA), using three wearable devices and one central device. To do this, we used the CSMA/CD-based protocol and Bluetooth SMART to transmit the same size data. Experimental results show that the average data loss-rate is 2.36%. As the traffic increases, Bluetooth SMART confirms that the signal is transmitted without synchronization. In ANT communication, however, it is confirmed that the data is transmitted in the state in which the synchronization is performed, and the period of the PPG signal is matched.

The number of channels that can be connected in the future is limited, and slot collision may occur due to communication delay. Therefore, it is necessary to study more about how to overcome this problem, and it is necessary to study the process of analyzing biopsy data collected through multiple connections.

Data Availability

The data used to support the findings of this study are available from the corresponding author upon request.

Conflicts of Interest

The authors declare that there are no conflicts of interest regarding the publication of this paper.

Acknowledgments

This research was supported by Basic Science Research Program through the National Research Foundation of Korea (NRF) funded by the Ministry of Education (NRF-2018R1A6A1A03025109).

References

[1] E. Jovanov, A. Milenkovic, C. Otto, and P. C. de Groen, "A wireless body area network of intelligent motion sensors for computer assisted physical rehabilitation," *Journal of Neuro Engineering and Rehabilitation*, vol. 2, no. 1, p. 1, 2005.

[2] J. Jung, K. Ha et al., "Wireless body area network in a ubiquitous healthcare system for physiological signal monitoring and health consulting," *International Journal of Signal Processing, Image Processing and Pattern Recognition*, vol. 1, no. 1, pp. 47–54, 2008.

[3] S. Marinkovic, C. Spagnol, and E. Popovici, "Energy-efficient TDMA-based MAC protocol for wireless body area networks," in *Proceedings of the 3rd International Conference on Sensor Technologies and Applications (SENSORCOMM '09)*, pp. 604–609, IEEE, Athens, Greece, June 2009.

[4] D. Benhaddou, M. Balakrishnan, and X. Yuan, "Remote healthcare monitoring system architecture using sensor networks," in *Proceedings of the 2008 IEEE Region 5 Conference*, pp. 1–6, April 2008.

[5] J. Y. Khan and M. R. Yuce, "Wireless body area network (WBAN) for medical applications," in *Proceedings of the New Developments in Biomedical Engineering*, 2010.

[6] H. Alemdar and C. Ersoy, "Wireless sensor networks for healthcare: a survey," *Computer Networks*, vol. 54, no. 15, pp. 2688–2710, 2010.

[7] N. Sheriff, "Time Synchronization in ANT Wireless Low Power Sensor Network," 2011.

[8] R. Pan, D. Chua, J. S. Pathmasuntharam, and Y. P. Xu, "A WBAN based cableless ECG acquisition system," in *Proceedings of the 2014 36th Annual International Conference of the IEEE Engineering in Medicine and Biology Society, EMBC '14*, pp. 910–913, August 2014.

[9] M. A. Hussain, N. Alam, S. Ullah, N. Ullah, and K. S. Kwak, "TDMA based directional MAC for WBAN," in *Proceedings of the 6th International Conference on Networked Computing, INC '10*, pp. 1–5, 2010.

[10] R. H. Kim, P. S. Kim, and J. G. Kim, "An effect of delay reduced MAC protocol for WBAN based medical signal monitoring," in *Proceedings of the IEEE Pacific Rim Conference on Communications, Computers and Signal Processing, PACRIM 2015*, pp. 434–437, August 2015.

Hindawi
Wireless Communications and Mobile Computing
Volume 2018, Article ID 1780904, 12 pages
https://doi.org/10.1155/2018/1780904

Research Article

Smart Care Beds for Elderly Patients with Impaired Mobility

Youn-Sik Hong

Department of Computer Science and Engineering, Incheon National University, Incheon 406-772, Republic of Korea

Correspondence should be addressed to Youn-Sik Hong; yshong@inu.ac.kr

Received 19 February 2018; Accepted 29 July 2018; Published 12 August 2018

Academic Editor: Seyed M. Buhari

Most accidents occurring at medical institutions treating elderly patients with mobility impairment are bedsores and fall accidents. One of the reasons for this high rate of accidents is the lack of nursing personnel. In order to aid caregivers in nursing elderly patients who are not able to move about freely, in this paper, we propose a design and implementation of a smart bed. In this bed, several pressure sensors are deployed underneath the mattress cover to consider both peoples' standard physical characteristics and the specific body parts where bedsores commonly occur. To manage the pressure ulcer area and to prevent falls, the body area is divided into three vertical areas and three horizontal areas. Each microcontroller unit manages pressure-sensing information in one of the body regions divided horizontally. In this study, a real-time pressure-sensing algorithm is presented that is capable of deciding on the possibilities of bedsores and falling accidents by considering both the intensity and the duration of pressure of specific body parts. Our experimental results demonstrate that a prototype smart bed works well for several human models of various heights and weights.

1. Introduction

In recent years, South Korea has faced the challenge of the rapidly aging society. Therefore, the problem of the elderly patients' care becomes crucial. In addition, an increasing number of specialized medical institutions for the elderly and senior care centers (called sanatoria) have been established. However, the rapid growth of the industry related to the elderly care and the establishment of relevant institutions encounters many problems, including, among others, the lack of appropriate administration.

If an elderly individual is in the same position for too long, whether in bed or a wheelchair, the friction between the skin and the surface may stop the blood flow, causing the pressure area to receive less oxygen and thus causing the cells to die in that area. This is how bedsores will develop [1]. Pressure ulcers in elderly individuals can cause significant morbidity and mortality and are a major economic burden to the healthcare system [2].

Recent surveys [3] have estimated a huge expenditure on direct medical cost for domestic accidents (in the USA, more than US $19 billion for nonfatal falls in subjects >65 years of age; in the UK, US $1.9 billion for emergency services and hospitalization, while an Australian study reported a national healthcare cost for elderly falls of US $66.1 million). Interestingly, two-thirds of the overall medical costs are due to falls requiring hospitalization [3]. Falls are by far the leading cause of injuries among the elderly [4]. One out of every 3 seniors aged 65 and older experiences a fall each year. Falls are the leading cause of both nonfatal and fatal injuries among seniors, and 20 to 30 percent suffer moderate to severe injuries that can cause disability or increase the risk of death. From a healthcare perspective, elderly falls are a major clinical issue in terms of frequency, disability, institutionalization, and overall mortality, with an outgrowing socioeconomic burden [5].

The occurrences of bedsores and fall accidents among the elderly patients are typical problems, accounting for over 80% in such medical institutions [6]. The Ministry of Health and Welfare of Korea has introduced operational regulations for medical institutions and, using these regulations, the latter measure the risk of falls and pressure ulcers. Nevertheless, the number of occurrences of bedsores and fall accidents is still growing. The main reason behind this tendency is the lack of trained personnel.

Internet of Things (IoT) revolution is redesigning modern healthcare with promising technological, economic, and social prospects [7]. Enabled by the global connectivity of the IoT, all the healthcare information (logistics, diagnosis, therapy, recovery, medication, management, finance, and even daily activity) can be collected, managed, and utilized more efficiently [8]. Among the panoply of applications enabled by the IoT, smart and connected healthcare is a particularly important one. Networked sensors, either worn on the body or embedded in our living environments, make possible the gathering of rich information indicative of physical and mental health [9]. By the current technology status, wearable health management systems [10] provide low-cost solutions for ubiquitous, all-day, unobtrusive personal health monitoring and are expected to enable early detection and better treatment of various medical conditions as well as disease prevention and better understanding and self-management of chronic diseases. In addition, RFID technology is to provide part of the IoT physical layer for the personal healthcare in smart environments through low-cost, energy-autonomous, and disposable sensors [11].

In this paper, we have implemented an IoT-based smart bed system designed to aid caregivers to nurse elderly patients with mobility impairments. The primary goal of the smart bed system is to prevent bedsores and/or falling accidents from the bed.

For that purpose, two types of pressure sensors (*strip* and *square* type) were used to sense pressures in the specific body positions depending on sensing purposes. We used sensors regarding both the average body size by age (with reference to the Korea Agency for Technology and Standards (KATS)) and the frequent location of bedsores. Besides, the entire sensing area of a patient's body was divided into three subareas and each of them was monitored by a distinct module operating independently for fault tolerant purposes. In addition, we also introduced the pressure-sensing algorithm that accurately detects the pressure intensity and the duration of the pressure. A short version of this paper has been published elsewhere [12].

The remainder of this paper is organized as follows. Section 2 summarizes related work. In Section 3, we describe the overall architecture and detailed operations of a smart bed system. In Section 4, the experimental results used to validate the proposed method are presented. Finally, conclusions are drawn in Section 5.

2. Related Works

The work in [13] proposed a computer vision-based fall detection system for monitoring an elderly person in a home care application. It suffers from occlusion since subjects can sometimes be behind a sofa or furniture while being monitored [14]. Gasparrini et al. [15] developed a fall detection system using a Microsoft Kinect depth sensor. It uses two sensors, an infrared projector and an infrared sensor, to generate a 3D map of the scene [15]. The use of a 3D map allows differentiating between obstructions and the subject. It can detect a fall-down accident through the analysis of a patient's gestures. The fall-down prevention device [16] is similar to the approach of Gasparrini et al. [15]. The drawback of the above approaches is the increase in computing complexity and cost. In addition, these methods do not prevent the occurrence of bedsores.

Providing accurate and opportune information on people's activities and behavior is one of the most important tasks in pervasive computing. Lara et al. [17] survey the state of the art in human activity recognition based on wearable sensors [17]. Ozcan et al. [18] present a fall detection system using wearable cameras. Since the camera is worn by the subject, monitoring is not limited to confined areas and extends wherever the subject may go including indoors and outdoors. When a fall occurs, edge orientations in a frame vary drastically and extremely fast, as a result of this subsequent frames get blurred [14].

Another work [19] is a system of unobtrusively recognizing actions and promoting physical activities and a smart mat used for the same purpose. A mat sensor is constituted by a FSR (*force sensing resistor)* sensor, a load cell, and a piezoelectric sensor. In addition, an ultrasonic sensor, an infrared sensor, and a thermal sensor are attached outside to monitor the behavior information of a patient lying on the mat. However, since the mats require the use of numerous sensors, their application in senior care centers is too complex and expensive. Furthermore, this patent may be more problematic to apply due to its complicated structure. Among other reasons, power consumption is increased, and the mobility of the bed is not free, as the external power source must be connected. Maintenance is also difficult. However, this patent is advantageous to grasp the behavior of a person to be protected from various sensors, although there appear to be restrictions in terms of commercialization.

BodiTrak Smart Bed [20] uses its own elastic and breathable pressure-sensing fabric. As one lies on it, the system continuously monitors one's body position and pressure distribution and automatically adjusts the bed's air support for maximum comfort. It is a system that keeps pressure distribution balanced for comfortable sleep. There is similarity with the method to be proposed in this paper in terms of utilizing the pressure distribution, but both the purpose of application and the application technique are quite different.

Adaptive sleep thinking system [21] has five independent zones adjusting to relieve pressure and improve sleep quality. This system is functionally similar to [20]. The difference between these two systems is that the system [20] divides the pressure generating part of the body into five zones and independently controls each of the five zones.

MAP system [22] involves a special electronic sheet placed over a mattress that has thousands of sensors that detect the pressure distribution of the patient's body over the bed. It is very similar to our proposed method. However, our proposed system uses 1/20 times fewer sensors than MAP. In addition, depending on the upper body and lower body, different types of sensors are deployed efficiently considering the incidence of bedsores. Notice that the incidences of bedsores are relatively low in the areas with frequent movements such as legs.

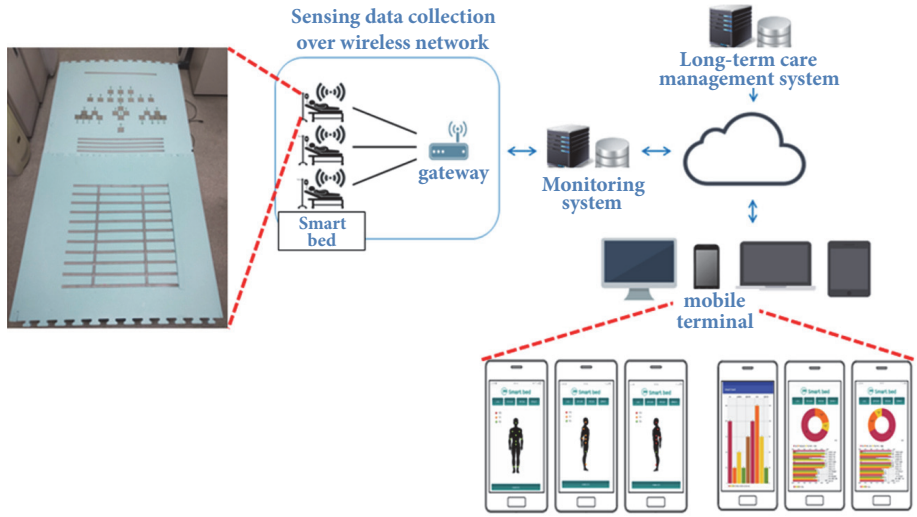

Figure 1: The H/W diagram of a smart bed system.

3. The Smart Bed System

3.1. System Overview. The primary purpose of the proposed smart bed system is to assist caregivers in nursing elderly patients who are not able to move about freely. With a smart bed, several pressure sensors installed under the mattress cover measure pressure intensity due to the weight of the patient lying on the bed. A smart bed can provide the information about pressure intensity of the points or areas of the patient's body. With this information, we know the patient's posture, that is, the supine position or lateral position, and the duration of pressure in a particular body position. This knowledge can help caregivers in terms of preventing the appearance of bedsores and/or falling accidents from the bed.

One of the most important functions of the smart bed system is that it can easily find the specific points of the patient. Based on the average body size by age (with reference to the KATS), a smart bed system is able to recognize the known points where bedsores frequently occur, that is, *occiput, scapula, superfine projections, elbow, iliac crest, sacrum, pubic bone*, *the Achilles tendon, heel*, etc. [23]. Figure 1 shows the block diagram of the smart bed system.

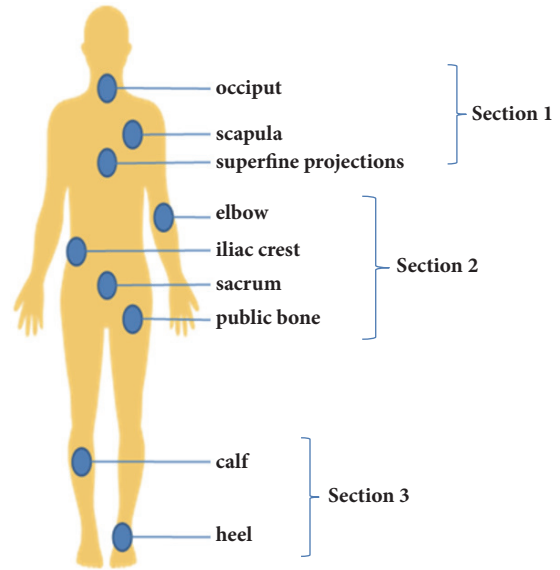

Figure 2: The three distinct sections and the positions of the frequent occurrence of bedsore.

3.2. Design of a Smart Bed System. Our smart bed meets the standard requirements of 1,895cm x 850cm, which are the dimensions of a bed for medical purposes. The entire body area of a patient is divided into three distinct sections (see Figure 2). This classification has been performed based on pressure intensity and the location of the frequent occurrence of bedsores. The points marked as dots in each section have a similar pressure intensity and they are close to the known position of bedsores.

The first section corresponds to the upper body. It consists of the head, with the three dots, namely, occiput, scapula, and superfine projections, respectively. The second section consists of arms and buttocks, with the following four dots: elbow, iliac crest, sacrum, and pubic bone. The third section consists of legs, with two dots for calf and heel (see Figure 2).

In order to collect the data on pressure intensity sent from the sensors, a microcontroller unit (MCU) is allocated in each section. It has been implemented with Arduino MEGA-2560. Since each MCU operates independently, the smart bed system performs its own work, even though one or two MCUs have some troubles or stopped accidentally.

As shown in Figure 1, the *gateway* to the monitoring system is implemented with the Raspberry PI board. It has an ATmega644 CPU and operates on the Linux operating system. The gateway communicates with three distinct MCUs via the *Master-Slave* mode [24]. Each MCU periodically transmits the pressure data to the gateway through wireless communication using Wireless LAN (WLAN). The gateway

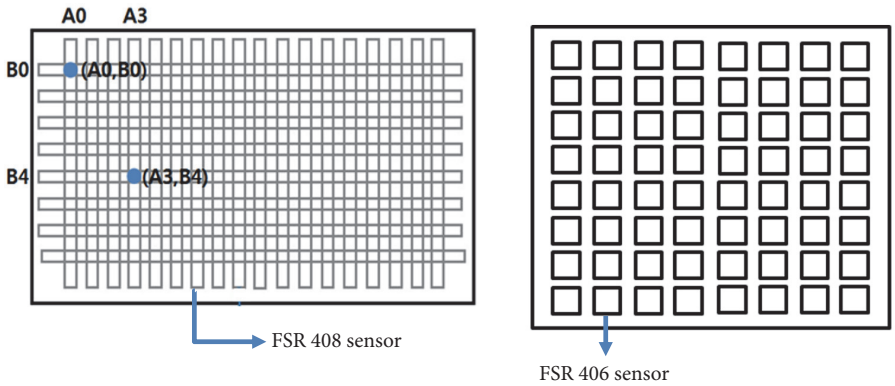

Figure 3: Deployment of FSR-406 and FSR-408 sensors.

converts these raw data into the corresponding formatted data and then stores them in the local database.

These data will be sent to the long-term care management system (LCMS) and then be stored in a permanent database. Finally, they will be used as persistent data for the LCMS. In the case of a high possibility of a bedsore attack or a falling accident from a bed, an alarm message will be sent to the caregiver's smart device immediately via the Google FCM (*Firebase Cloud Messaging*) server.

3.3. Deployment of Two Types of Sensors. The pressure sensor needs to be arranged according to the average body size of each age group. In particular, if the pressure of a specific body part is to be measured, the body part dimensions for each age group should be reflected in the sensor placement process. We have deployed sensors regarding both the average body size by age, as based on the KATS, and the position of the frequent occurrence of bedsores. Doing so will make it possible to detect pressure of body positions with various body dimensions.

Our design goal for sensor deployment is to use the minimum number of sensors to detect pressure of all possible body positions. Depending on the body part, there are areas that require precise measurement of pressure and others that do not. For example, instead of measuring the pressure of a specific part of the *head* and the *lower body*, it is only necessary to measure whether or not the pressure is generated. On the other hand, the *upper* body needs to measure the pressure closely around a specific position where the pressure *ulcer* frequently occurs. In this situation, we will use two kinds of sensors: FSR-408 and FSR-406 [25]. These sensors are chosen in terms of cost effectiveness and ease of implementation. According to the data sheet [25], this force sensitivity is optimized for use in human touch control of electronic devices such as automotive electronics, medical systems, and industrial and robotics applications. The FSR-408 sensor (*strip*-type) is used to detect whether a pressure has been generated. On the other hand, the FSR-406 sensor (*square* type) is used to precisely measure the pressure of a specific area. The dimensions of FSR-408 and FSR-406 are 610mm x 5mm and 38mm x 38mm, respectively. The pressure range for the above two sensors is $0.1 \sim 10.2^2$N (Newton).

Both FSR-406 and FSR-408 are two-wire devices with a resistance that depends on the applied force. The measuring resistor output voltage increases with the increasing force.

The FSR-408 pressure sensor can detect the pressure of a wide area with relatively smaller numbers. It knows only the strength of the pressure, whereas it does not know the exact position of the issued pressure. To use FSR-408 sensors, they are deployed in a grid pattern (see the left part of Figure 3).

Note that, as shown in Figure 4, they are used to detect pressures of patient head, legs, and hips. The vertical spacing between the sensors for detecting pressure of hips is 20~30mm, whereas the vertical spacing for legs is 50mm. To expect the position of issued pressure, two FSR sensors are necessary. For example, assume that two sensors, A0 and B0, in the left part of Figure 3 detect pressures simultaneously. Then, the intersection point (A0, B0) marked as a dot will be expected as the position of pressure issued. Another intersection point (A3, B4) will be the same as in the previous example.

To detect pressure of the upper body, FSR-406 sensors are deployed in a dot pattern (see the right part of Figure 3). FSR-406 sensor does know the exact position of the issued pressure. They have been deployed by 190mm distance away from the FSR-408 sensors deployed in the back of the patient head (called *occipital area sensors*) to detect the pressure of the shoulder portion. Note that the exact dimensions are determined by using the Korean standard body dimensions from KATS. For example, this distance is measured for Koreans to amount to 190.223mm~220.44mm. FSR-406 sensors are also deployed to detect pressure of both superfine projections (*spine*) and elbow positions.

For the actual implementation (see the left part of Figure 5), a total of 45 sensors are used: 18 FSR-408 sensors and 27 FSR-406 sensors. The FSR-406 sensor and the FRS-408 sensor are priced at $10 and $25, respectively. The cost of implementing the entire system is only one-fifth of the cost of competing systems. With this implementation, 22 positions of the frequent occurrence of bedsore can be detected: 10 positions for the supine posture and 12 positions for the lateral posture. Such implementation is designed for elderly patients whose height is within the range of 150~180cm.

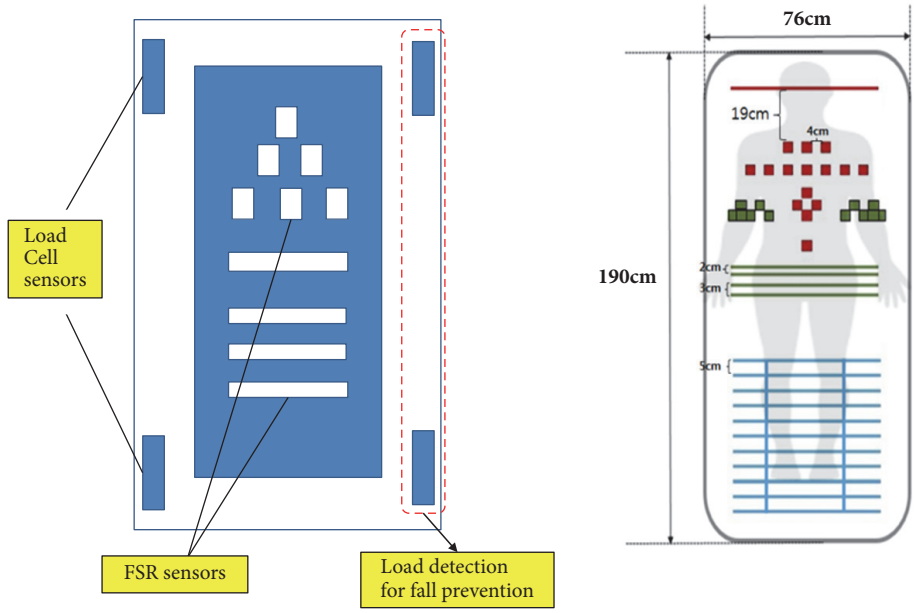

Figure 4: The placements of load-cell sensors and FSR sensors (left) and of the two types of sensors using a grid pattern and a dot pattern (right).

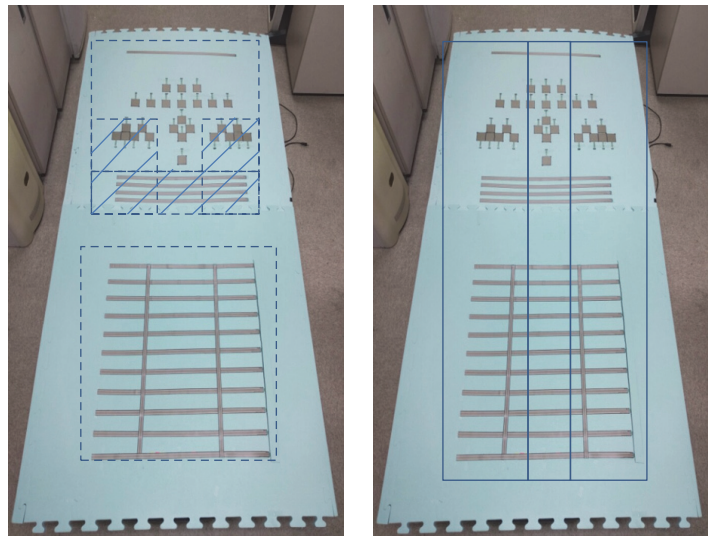

Figure 5: The 3 horizontal subsets of sensors (left) and the 3 vertical subsets of sensors (right).

3.4. Sensing Algorithm for Fall Risk Assessment and Pressure Ulcer Occurrence Warning. As shown in the left part of Figure 4, four load cells for detecting the load are placed on the edge of the bed. They can determine whether the patient is in bed and measure the patient's weight if the patient is lying down properly. In Figure 4, the dot-type (FSR-406) sensor and the strip-type (FSR-408) sensor arrangement are shown on the right. Note that the dimensions of the main parts are also shown.

The set of FSR sensors can be divided into three groups according to the sensing purpose, as shown in Figure 5, either vertically or horizontally. The left side of Figure 5 divides the FSR sensors horizontally into three subsets to measure the pressure of the major body parts. Three MCUs process the pressure information of the sensors of each subset divided in the horizontal direction. Each sensor subset in the horizontal direction is used to monitor whether the pressure at the frequent occurrence of bedsore has been maintained for a certain period of time.

As shown on the right part of Figure 5, the FSR sensors are arranged vertically in three groups: *left*, *center*, and *right*. Depending on how many sensors of one subset, as compared to the other two subsets, sense pressure, we can expect the patient's posture in the bed and thus generate the warning message against a falling accident. If over 80% of the sensors of one of the groups except for the sensors of the central group

At the initial, set the measurement cycle T_0 to 60 seconds:
While (true) **do**
  $\Delta T = 0$;
  The system detects the patient's body position every T_t second;
  If $N_t^{left} < 5\%$ **and** $N_t^{right} < 5\%$ **and** $N_t^{center} < 5\%$ **then**
    The patient has gone out of the bed; $T_t = \infty$; // *The system will halt.*
  Else If $N_t^{left} \geq 80\%$ **and** $N_t^{center} < 20\%$ **and** $N_t^{right} < 20\%$ **then**
    Send the *alarm* immediately to the caregiver's smart device;
    If $T_t/2 < 5$ **then** $\Delta T = 5$; **Else** $\Delta T = T_t/2$; // *The min. cycle is set to 5 seconds.*
  Else If $50\% \leq N_t^{left} < 80\%$ **then**
    If $N_t^{left} - N_{t-1}^{left} > 10\%$ **then**
      Send the *warning* message to the caregiver's smart device;
      $\Delta T = T_t/6$; $N_{t-1}^{left} = N_t^{left}$;
    Else $\Delta T = T_t/12$;
  Else If $N_t^{left} < 50\%$ **and** $N_t^{right} < 50\%$ **then**
    If $T_t + 60 \leq 300$ **then** $T_t = T_t + 60$; $\Delta T = 0$; // *The max. cycle is set to 5 minutes.*
    Else $T_t = 300$; $\Delta T = 0$;
  // *end of if*
  $T_t = T_t - \Delta T$;
// *end of while*;

Algorithm 1: The sensing algorithm for fall risk assessment.

sense the pressure and, at the same time, less than 20% of the sensors of the remaining group sense the pressure, it can be decided to be one of the following two case: either the patient lying on the bed is in danger of falling or s/he is coming down from the bed. In any case, the caregiver will be immediately notified that the patient needs protection.

The system detects the patient's position every 1 minute. However, as the possibility of fall accident increases, the measurement period will be shortened to 30 seconds or less. In Algorithm 1, we present a sensing algorithm for the fall risk assessment.

Let N_t^{left} be the percentage of sensors of the left vertical group which sense pressure at time t. Similarly N_t^{right} and N_t^{center} are the percentage of sensors of the right vertical group which sense pressure and the percentage of sensors of the center vertical group which sense pressure at time t, respectively. Note that, for simplicity, Algorithm 1 describes only the detection of fall accident that occurs in the left end of the bed. In this case we assume that the safety guard on the right side of the bed is raised so that the patient cannot fall down to the right.

As the ratio of the pressure sensed by one group of sensor increases, the measurement cycle T starts to shorten. If the percentage of sensors of the left group sensing pressure increases by over 10% after T interval, the next cycle T will be decreased by half of the current cycle.

After a fall risk warning, if the pressure is no longer measured anywhere on the bed, it is decided that the patient is no longer in bed. It is judged that a fall has occurred or the patient has gone out of bed and moved to another place.

To prevent ulcer occurrence, perform a field test to determine the patient's posture (supine, repose, left position, right position, half position, etc.) according to the pressure pattern applied to the bed. In addition, when a patient lies in the bed, the height of a patient is calculated using the distance between the back head sensor and the farthest distance sensor based on the sensor located at the heels of the patient. In this way, the body part with frequent pressure ulcers is sought. Assume that the background data (gender, age, height, and weight) for the patient are given. A sensing algorithm for pressure ulcer occurrence warning is shown in Figure 6.

Finally, the system implements the following features:

(1) Visualizing and displaying the duration of pressing for each body part.

(2) The graph shows the current status and daily and weekly cumulative status of the patient.

(3) If the same site is continuously pressed for longer than 30 minutes, a warning message will be generated.

4. Experiments

4.1. The Detection Rate of the Pressures of the FSR Sensors. In this experiment, we examine whether the FSR sensors accurately detect pressure. This is because the smart bed system can accurately determine the patient's posture according to whether the pressure is properly detected. If the value sensed by a FSR sensor is below the reference value (i.e., *threshold*), it cannot be used for a determination of lying posture. In general, a FSR sensor can detect the value above the threshold if a patient lying in the bed maintains a constant posture for a certain period.

The pressure range of a FSR sensor is 0~1,023. The threshold used in this experiment is 150, where it was determined empirically. In addition, the detection rate of the pressures of the FSR sensors has been obtained when the patient was lying in the same position for more than one minute (see Figure 7). The values shown in Table 1 are the

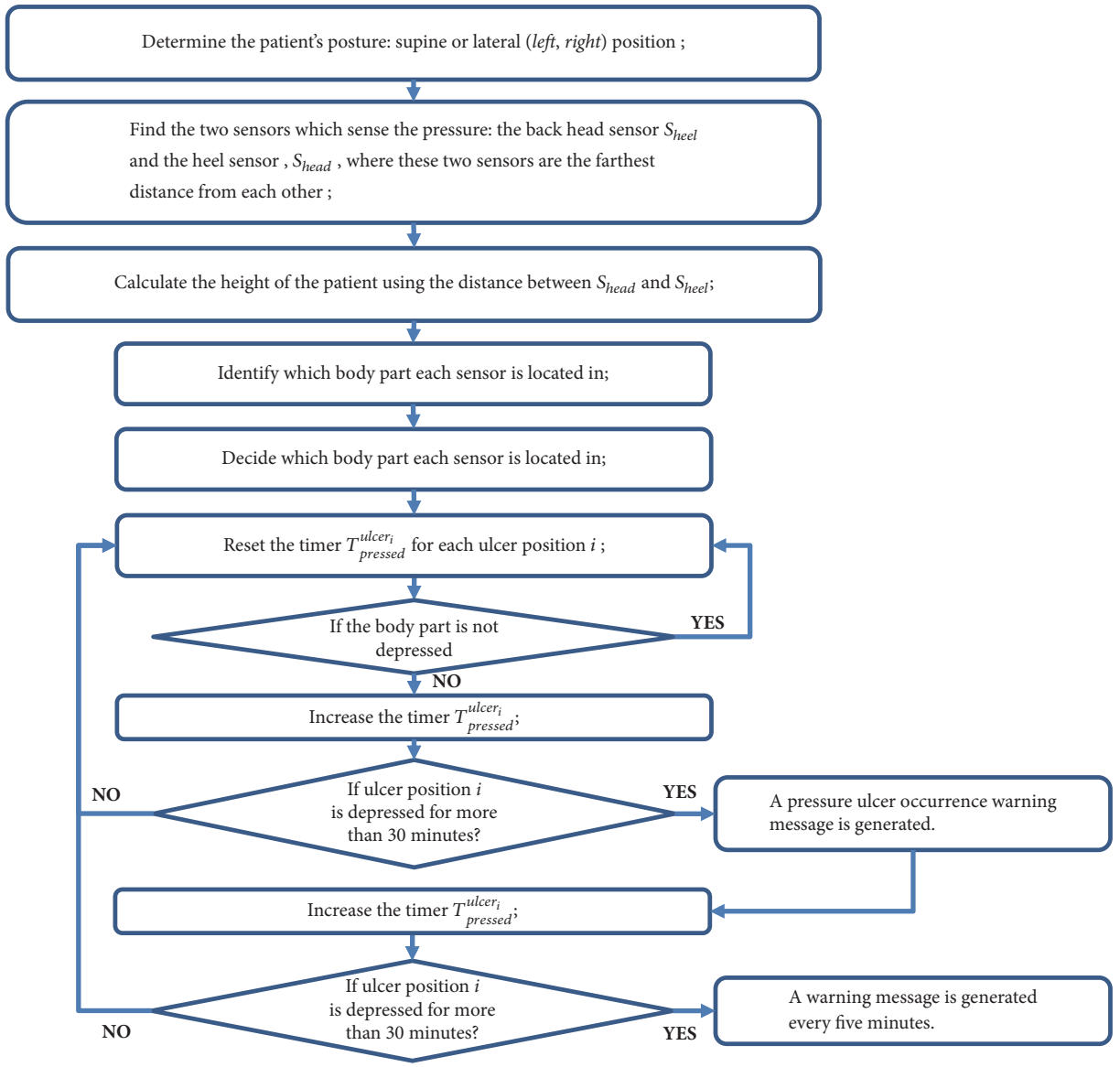

Figure 6: The sensing algorithm for pressure ulcer occurrence warning.

Figure 7: Measurement of the detection rate of the pressures with respect to the lying posture.

number of FSR sensors whose values were measured above the threshold. The measurements were repeated 20 times for each posture. The detection rate when lying down in normal posture (a.k.a. *supine* posture) was higher than the left or right lateral posture.

4.2. The Recognition Rate of the Lying Posture. This is an experiment to evaluate the performance of the algorithm to determine what posture the patient is lying on using the pressure values sensed by the FSR sensors. Notice that the smart bed system can determine the posture when the patient

Table 1: The detection rate with respect to the lying posture.

lying posture	total no of sensors	min. no of sensors	max. no of sensors	average no of sensors
right lateral	26	23	26	24.55
left lateral	26	23	26	24.49
supine	27	24	27	25.48

Table 2: The recognition rate with respect to the threshold.

threshold	no of tests	successful recognition	recognition rate (%)
50	112	85	75.9
150	128	104	81.3
300	134	117	87.3

supine posture | left lateral posture

Figure 8: Experiments for recognizing a patient's posture based on the pressures measured.

is lying in the same position for more than one minute. This delay considers all the delays due to the processing delay, the propagation delay over wireless, and the database processing delay. Experiments were conducted on elderly people in the elderly care facilities (see Figure 8).

As shown in Table 2, for this experiment, three threshold values were used: 50, 150, and 300. As the threshold value becomes greater, the rate of discriminating correct posture increases. *Head*, *shoulder*, and *hip* are the body parts where their pressure values are higher than those of the other parts. The larger the threshold value, the more accurate the main body parts can be measured. If head, shoulder, and hip are recognized as straight lines based on the pressure value, the patient can be judged to be lying in the supine posture. To make such a decision, it is necessary to accurately measure the pressure values corresponding to the body part.

One of the reasons for not recognizing the patient's posture is that when lying down the bed the behavior patterns and the lying postures are different for each patient. This type of the recognition error due to different behavior patterns for each patient can be effectively reduced through data accumulation and analysis. Another reason is that the patient's body size varies. When installing the system, we can reduce the rate of recognition error by adjusting the parameters to match the patient's body size. The values in Table 2 are the results of the experiments without these adjustments.

4.3. The Communication Delay over Wireless. The pressure values sensed by the FSR sensors are transmitted to the Arduino board (*Arduino Mega-2560*) as explained earlier in Section 3.2. It can communicate with the Raspberry PI board via serial communication at 9,600bps baud rate. Then it periodically transmits the stored pressure values to the Raspberry PI. Finally, the Raspberry PI wirelessly transmits them to the remote server through IEEE 802.11n WLAN. Notice that the payload data size used in the experiment is 256 Kbytes.

Experiments assume a single-hop wireless transmission from the Raspberry PI to the server. We measured the time it takes for the values detected by all the FSR sensors to reach the server. This value is used as a basis for estimating the transmission time of an SMS message when an emergency such as a fall accident or a high occurrence of a pressure ulcer happens.

As summarized in Table 3 and also shown in Figure 9, the wireless transmission delay is less than 2.5ms. Based on this value, it is possible to estimate the minimum period required to store the pressures values in the remote database system. In other words, the minimum interval of the data transmission for the smart bed system can be obtained. Since

Table 3: The statistics of the communication delay over WLAN.

No of tests	142
average delay	1.616 [ms]
minimum delay	1.238 [ms]
maximum delay	2.435 [ms]

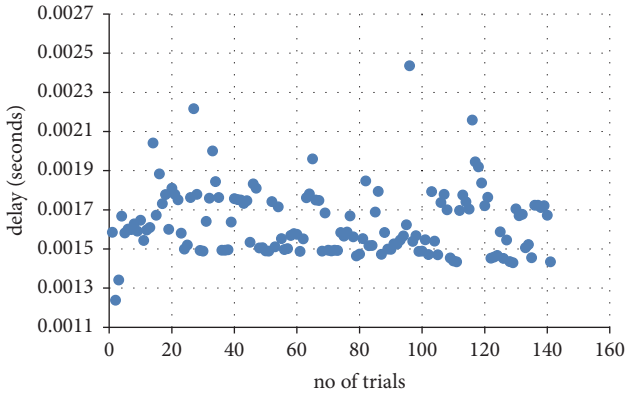

Figure 9: The distribution of the communication delays over WLAN.

the processing delay is less than 1ms, the minimum period becomes 3.5ms. Since these experiments were conducted in the laboratory where there is little traffic in WLAN, it may increase in more realistic environments.

However, it is not necessary to transmit the pressure values in a shorter period less than 1 minute unless there is a risk of fall accidents or occurrence of pressure ulcers. As the transmission period becomes shorter, the number of records inserted into the database increases rapidly. Therefore, it is necessary to adjust the transmission period appropriately. The transmission cycle seems to be appropriate in 3 to 5 minutes in a normal situation.

4.4. The Delay of Transmitting SMS to the Registered User. We used Google FCM, a cross platform messaging solution, to implement emergency text messaging. Performance was measured at maximum payload 4KB including dummy data. The mobile application for users is implemented on the Android platform. The number of mobile terminals to be transferred at the same time was limited to one registered terminal to protect patient information. User authentication uses the sender ID, and the message lifetime is set to only one day. Normally, the message lifetime is set to 2,419,200 seconds (i.e., 28 days). We measured message transmission time and message reception time, respectively.

As shown in the left of Figure 10, we assumed that the high possibility of falling accidents occurs and then the smart bed system sends emergency text message to the registered caregiver. The average delay is 0.74 seconds and the maximum delay is 2.64 seconds, as summarized in Table 4. This is because the variation of the delay is influenced by network traffic at the time of transmission and reception. In the performance evaluation, the measurement was made on one registered terminal, but the maximum delay was within 5 seconds even when the message was transmitted to two terminals at the same time.

Table 4: The statistics of the delays of transmitting text message to the one registered user.

No of tests	142
average delay	0.737 [s]
minimum delay	1. 096 [s]
maximum delay	2. 643 [s]

Table 5: The processing time with respect to the size of D-zone.

type	no of sensors	processing time [ms] (avg.)
min. D-zone	10	0.115
medium D-zone	17	0.268
max. D-zone	24	0.412

4.5. Detection of Falling Accident. We applied the prototype smart bed to two groups of patients: elderly patients who can hardly move and elderly patients with dementia who can move a little. In the case of the former group, little change in the pressure sensor value over time was observed. However, pressure changes occurred frequently in the latter group of patients. Specifically, in this group, it took at least 2.7 minutes (on average) from the time when the *left* (or *right*) pressure ratio of the bed reached 80% to the time when the patient came down from the bed. The fastest alarm cycle was set to 5 seconds, indicating that the caregiver had sufficient time to recognize the alarm and then come back to the patient. Note that, in the experiment, the caregiver was assumed to be on the same floor as the patient. Besides, the caregiver was assumed to be within the 100-meter reach from the patient.

It is not easy to analyze the relationship between detection time and prevention of falls. This is because it is hard to find out what an elderly patient will do on one side of the bed. Therefore, the proposed method only determines whether the patient's position is located one side of the bed as shown in Figure 5. It focuses on informing a caregiver as soon as possible when the patient's position reaches a dangerous zone (called *D-zone*), such as a corner of the bed, so that she (he) can identify the situation.

Experiments were conducted to investigate the effect of the size of D-zone on detection time. This is because limiting the search space can be effective for reducing detection time to prevent fall if a patient moves to one side of the bed. For the purpose of the experiment, the 3 types of D-zone are defined as shown in Figure 11. The minimum D-zone has only 10 sensors, while the maximum D-zone has 24 sensors.

Depending on the D-zone size, the processing time may vary, summarized as Table 5, but the total elapsed time heavily depends on the time it takes to send the text message to the caregiver.

1ms (*processing cycle*) + 2.435ms (*delay over wireless*) + 2.643s (*delay of transmitting SMS*) < 2.7s.

We set the minimum detect cycle to 5 seconds, but it can be shortened to 3 seconds.

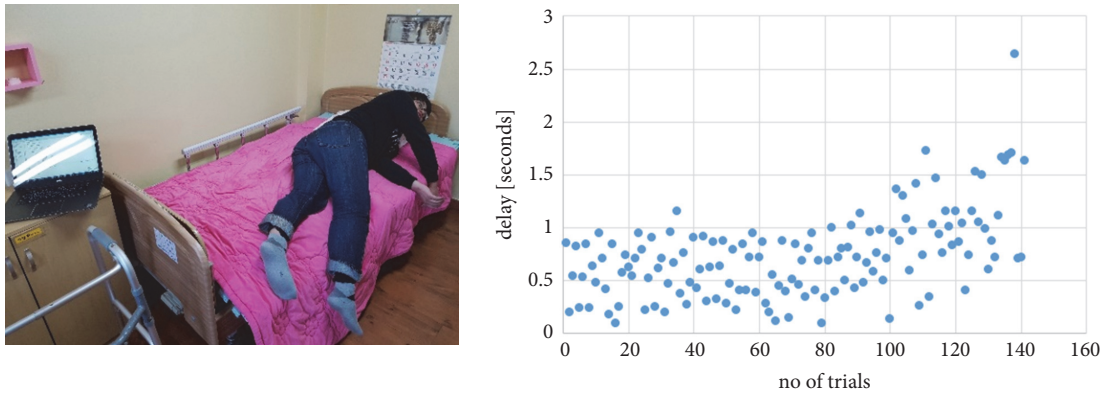

Figure 10: The experimental setup (*left*) and the distribution of the delays (*right*).

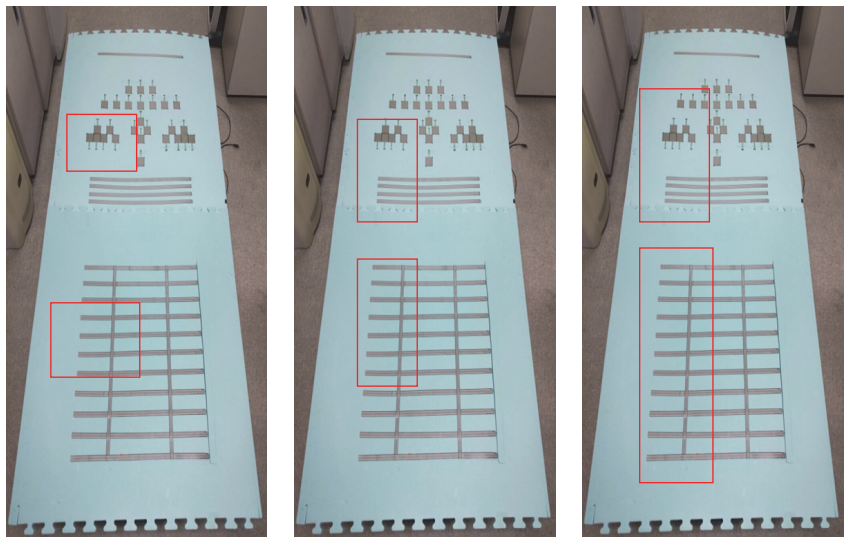

(a) The minimum D-zone (b) The medium D-zone (c) The maximum D-zone

Figure 11: Analysis of detection time with respect to D-zone setting.

4.6. Detection of Bedsores. If a patient is the supine position, his (her) height can be estimated by using the distance between the occipital area sensors and the sensors that are deployed farthest from the occipital area sensors. Based on the average body size from the KATS, we know which sensors are sensed which position of a patient. It is important, because, according to KATS, bedsores frequently occur in specific locations.

In order to prevent bedsore attacks, caregivers should change the patient's posture at least every 2 hours [26]. Whenever the pressure of the specific position continues for longer than 60 minutes, the smart bed system gives caregivers warning messages. When the pressure continues for 90 minutes, it sends an alarm to the caregiver's smart device to change the patient's posture as soon as possible.

Figure 7 shows the duration time with respect to the patient posture. The green, orange, and red dots indicate the duration time of 30, 60, and 90 minutes, respectively. As shown in Figure 12, our smart bed system can identify three types of patient posture: supine, lateral left, and lateral right. Figure 13 shows the patient's posture and accumulated pressure daily.

4.7. Guarantee of Comfort Sleep. The commercialized model is similar to the electric plate as shown in Figure 14. The controllers such as Raspberry PI boards will be placed on the side of the mattress. The survey results showed that more than 93% of users did not feel uncomfortable when lying down because of the smart mattress. To guarantee more comfort sleep, it is necessary to consider the material of smart mattress, which is beyond the scope of this paper.

5. Conclusions

Our smart bed prototype system can sense pressure occurring on the entire body of a patient with mobility impairment at a regular interval through an efficient deployment of sensors, while using a smaller number of sensors. In addition, the

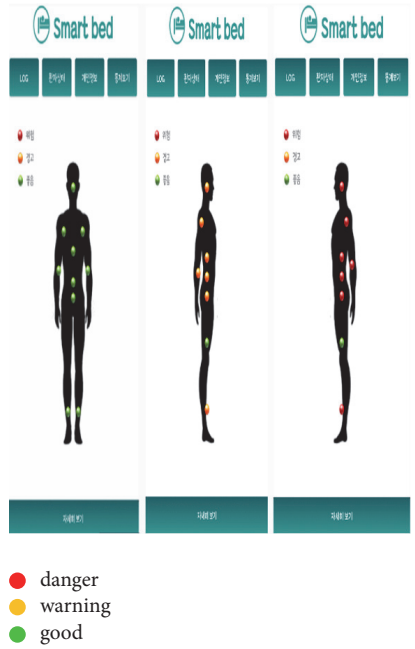

Figure 12: Visualization of the duration time of pressure with respect to the supine position (left) and the lateral position (center, right).

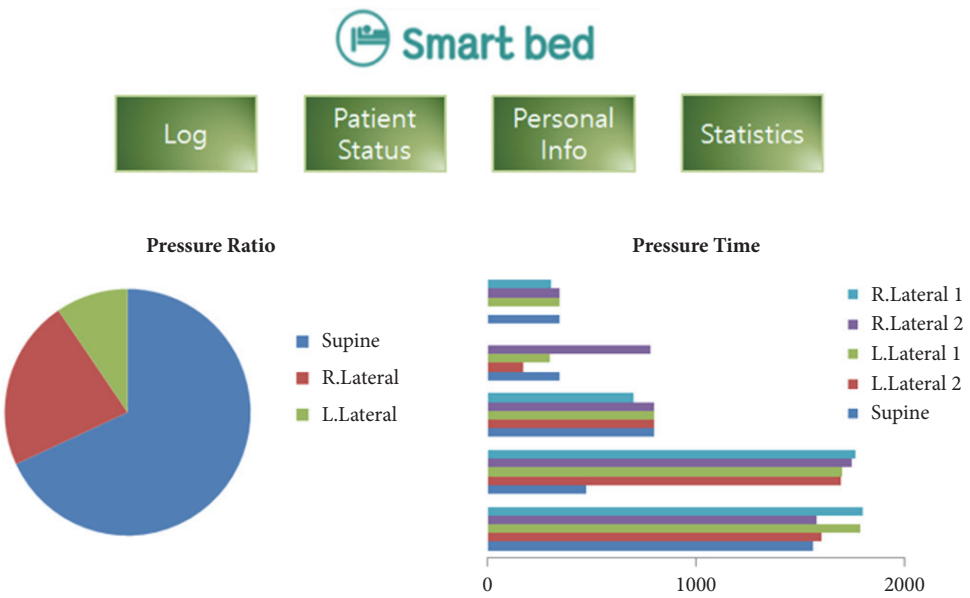

Supine : left heel, buttocks, left elbow, right wing bone, head
Left lateral : heel, buttocks, spine, head
Right lateral : heel, buttocks, spine, head

Figure 13: Patient posture and accumulated pressure daily.

proposed system can detect the position with the highest possibility of bedsore attack by finding the largest accumulated pressure.

The proposed system can also provide the information about the position of the frequent occurrence of bedsore for caregivers depending on the patient's personal characteristics, for example, his (her) height or weight. Thus, it can help caregivers in terms of appropriately nursing their patients. Our system will be the one of the possible solutions to prevent bedsores and/or falling accidents and will be particularly useful in nursing homes and senior care centers.

At present, our smart bed can distinguish only three postures among elderly patients lying on the bed. If a patient is lying in a bent position, it may not be able to properly

Figure 14: The prototype smart mattress (without controllers).

locate the pressure ulcer. Thus, we are currently studying ways to find various postures of patients more effectively. In the future, we will continue to investigate methods to measure the weight of elderly patients with impaired mobility even when they are lying down.

Data Availability

The data are generated at regular interval and stored in our local database system. Thus, all the data are stored in our local database system. These data will be given for proofing the correctness of our approach to the specific interests.

Conflicts of Interest

The author declares that there are no conflicts of interest regarding the publication of this paper.

Acknowledgments

This work is supported by the 2013 Grant of Incheon National University.

References

[1] "Nonstop Pressure," http://www.nursinghomeabuseguide.org/neglect/bed-sores/.

[2] T. Yoshikawa, N. J. Livesley, and A. W. Chow, "Infected pressure ulcers in elderly individuals," *Clinical Infectious Diseases*, vol. 35, no. 11, pp. 1390–1396, 2002.

[3] M. Sartini, M. L. Cristina, A. M. Spagnolo et al., "The epidemiology of domestic injurious falls in a community dwelling elderly population: An outgrowing economic burden," *European Journal of Public Health*, vol. 20, no. 5, pp. 604–606, 2010.

[4] "Fall-Related Injuries," http://www.homecareassistancecincinnati.com/common-elderly-injuries/.

[5] G. D. Velhal, "Domestic accidents among the elderly," *Annals of Tropical Medicine and Public Health*, vol. 5, no. 2, pp. 61-62, 2012.

[6] Y.-O. Hwang, "Geriatric care facilities: recent trends in risk management," *Journal of the Korean Gerontological Society*, vol. 26, no. 3, pp. 505–520, 2006.

[7] S. M. R. Islam, D. Kwak, H. Kabir, M. Hossain, and K. Kwak, "The internet of things for health care: a comprehensive survey," *IEEE Access*, vol. 3, pp. 678–708, 2015.

[8] M. C. Domingo, "An overview of the internet of things for people with disabilities," *Journal of Network and Computer Applications*, vol. 35, no. 2, pp. 584–596, 2012.

[9] S. Amendola, R. Lodato, S. Manzari, C. Occhiuzzi, and G. Marrocco, "RFID technology for IoT-based personal healthcare in smart spaces," *IEEE Internet of Things Journal*, vol. 1, no. 2, pp. 144–152, 2014.

[10] M. Hassanalieragh, A. Page, T. Soyata et al., "Health monitoring and management using internet-of-things (IoT) sensing with cloud-based processing: opportunities and challenges," in *Proceedings of the IEEE International Conference on Services Computing, SCC 2015*, pp. 285–292, IEEE, July 2015.

[11] A. Pantelopoulos and N. G. Bourbakis, "A survey on wearable sensor-based systems for health monitoring and prognosis," *IEEE Transactions on Systems, Man, and Cybernetics, Part C: Applications and Reviews*, vol. 40, no. 1, pp. 1–12, 2010.

[12] W. Jung and Y. Hong, "A Design and Implementation of a Smart Bed for Elderly Patients," *International Journal of Elderly Welfare Promotion and Management*, vol. 1, no. 1, pp. 1–6, 2017.

[13] M. Yu, A. Rhuma, S. M. Naqvi, L. Wang, and J. Chambers, "A posture recognition-based fall detection system for monitoring an elderly person in a smart home environment," *IEEE Transactions on Information Technology in Biomedicine*, vol. 16, no. 6, pp. 1274–1286, 2012.

[14] Y. S. Delahoz and M. A. Labrador, "Survey on fall detection and fall prevention using wearable and external sensors," *Sensors*, vol. 14, no. 10, pp. 19806–19842, 2014.

[15] S. Gasparrini, E. Cippitelli, S. Spinsante, and E. Gambi, "A depth-based fall detection system using a kinect sensor," *Sensors*, vol. 14, no. 2, pp. 2756–2775, 2014.

[16] Kei-Myung University R&DB Foundation, Fall-down prevent device, Patent No. 10-2013-0021614, 2014.8. 29 (registration date).

[17] Ó. D. Lara and M. A. Labrador, "A survey on human activity recognition using wearable sensors," *IEEE Communications Surveys & Tutorials*, vol. 15, no. 3, pp. 1192–1209, 2013.

[18] K. Ozcan, A. K. Mahabalagiri, M. Casares, and S. Velipasalar, "Automatic fall detection and activity classification by a wearable embedded smart camera," *IEEE Journal on Emerging and Selected Topics in Circuits and Systems*, vol. 3, no. 2, pp. 125–136, 2013.

[19] HIMS Co. Ltd, System of unobtrusively recognizing actions and promoting physical activities and smart mat for the same purpose, Patent No. 10-2013-0024409, 2014. 4. 28 (registration date).

[20] "Smart Bed," http://boditrak.com/products/smartbeds.php.

[21] "Adaptive Sleep Thinking," http://www.elementsofrest.com/the-rest-bed/rest-technology.

[22] "Mattress Sensing MAP System," https://www.medgadget.com/2013/07/mattress-sensing-map-system-prevents-pressure-ulcers.html.

[23] "Symptoms of Pressure Ulcers," http://www.nhs.uk/Conditions/Pressure-ulcers/Pages/Symptoms.aspx.

[24] "Arduino Forum," http://forum.arduino.cc/index.php.

[25] "FSR-408 and FSR-406," https://cdn-shop.adafruit.com/datasheets/FSR400Series_PD.pdf.

[26] E.-S. Kwon, *Study on the knowledge of bedsores care of a hospital nurse, recognition and execution*, Hanyang University Graduate School of Public Administration, 2005.

Hindawi
Wireless Communications and Mobile Computing
Volume 2018, Article ID 4607464, 11 pages
https://doi.org/10.1155/2018/4607464

Research Article

Double Cache Approach with Wireless Technology for Preserving User Privacy

Adnan A. Abi Sen,[1] **Fathy B. Eassa**,[1] **Mohammad Yamin**,[2] **and Kamal Jambi**[1]

[1]*College of Computer Science and Information Technology, King Abdulaziz University, Jeddah 21589, Saudi Arabia*
[2]*Department of MIS, Faculty of Economics and Administration, King Abdulaziz University, Jeddah 21589, Saudi Arabia*

Correspondence should be addressed to Adnan A. Abi Sen; adnanmnm@hotmail.com

Received 23 February 2018; Revised 4 May 2018; Accepted 7 June 2018; Published 1 August 2018

Academic Editor: Milos Stojmenovic

Several methods use cache for decreasing the number of connections to protect privacy of user data and improve performance in Location Based Services (LBS). Many of these methods require users to trust other users or third parties, which could be servers. An intruder could be disguised as a user or a third party. In this article, we propose a new method, known as "Double Cache Approach", which uses a pair of caches to reduce the vulnerability of trust between users or third party and offers a vast improvement in privacy and security of user data in healthcare and other applications that use LBS. This approach divides the area into many cells and manages the cooperation among users within two caches at the access point with wireless communication. To demonstrate the superiority, we also provide simulation results of user queries, comparing the proposed method with those using only one cache. We believe that our approach would solve the trust problem optimally, achieve a comprehensive protection for users' data, and enhance the privacy and security levels.

1. Introduction

Healthcare is one of the critical domains [1] where Internet of Things (IoT) has enhanced its quality and usability [2, 3] with smart phones or wearable devices like RFID tags. Most of the healthcare applications use Location Based Services (LBS) for searching points or places of interest like hospitals, health centres, and pharmacies with the help of GPS technology [4–6]. This technology plays a significant role in medical emergencies, healthcare applications, and establishing contacts in other domains [7, 8]. However, the use of LBS services entails significant risks of breach of user's privacy and security [9, 10]. The attacker may be able to determine the location and track and build profile and pattern of the user's movements [11, 12]. The attackers can also gain user's personal and sensitive information like their whereabouts at a specific time, job, health conditions, financial and social status, and religion, political, and ethical inclinations [13–15], which could limit future use of e-healthcare systems [16–18]. A server provider can also breach the privacy, consequences of which could be quite serious [19, 20].

Many methods and techniques exist to protect privacy in application and services of IoT but none of them can ensure total protection. Before embarking on these methods, let us discuss the standard format of queries that are launched from clients to LBS server. As shown in Figure 1, there are three components in a query, namely, ID, Location, and Query-Type. Existing approaches are designed to defend privacy from an outer attacker, server provider, and all other types of attacks [21] by protecting one or more components. The methods or approaches for privacy of data in LBS, as in [22], may be grouped into eight classes, namely,

(i) Trusted Third Party (TTP) (also known as Cloaking area & K-anonymity);

(ii) Obfuscation and Land-marking;

(iii) Mix Zone, Private Information;

(iv) Retrieval (PIR) and Encryption;

(v) Dummies;

(vi) Cooperation between Peers;

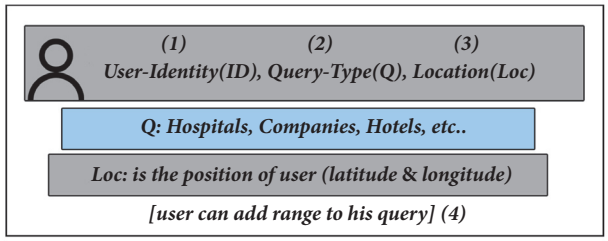

Figure 1: Query format in LBS.

(vii) Caching;

(viii) Hybrid.

Each one of them has one or more kind of limitations and consolidated open problems [21–25], which are described below.

(1) How to deal with Anonymizer or TTP without having trust?

(2) How to generate high-efficiency dummies?

(3) How to establish reliability between users and reputation of peers?

(4) Can the cache hit ratio be improved to achieve more privacy?

(5) Can the overhead computation be relaxed in the PIR approach?

In this paper we shall resolve first four problems by proposing the following:

(1) An approach, known as Double Cache, for protecting privacy in the applications of LBS from different attacks in all fields including the healthcare;

(2) A new method for generating smart dummies with high performance;

(3) A new technique for managing cache and enhancing performance;

(4) A solution for the trust issue between peers.

2. Literature Review

With the emergence of the IoT paradigm, enhancement and developments of services have taken place in several domains. In particular, healthcare has been a major beneficiary. Healthcare is now benefited by sophisticated applications and tools such as wearable sensors, which can

(i) Monitor patients and senior citizens continuously;

(ii) Help people with breathing problems to find less polluted routes;

(iii) Help in statistical or data mining processing;

(iv) Determine the likelihood of spreading a contagious viruses and diseases in specific areas

(v) Frequently update donor locations;

(vi) Help in emergencies and ambulance services;

(vii) Assist drones in transporting medical supplies to obscure locations;

(viii) Track and monitor activities of infants or children and subsequently report any associated emergencies to their parents or guardians [1, 26, 27].

Since most of these services use mobile LBS, requiring wireless connections, privacy can easily be violated by server providers through revealing the locations, movements pattern, habits, and behaviours of the people they serve [25, 28, 29].

Use of cache for preserving privacy is a relatively new approach and hence only a small number of researchers have discussed it so far. Most of classical approaches like collaboration, dummy, and K-Anonymity have used additional storage; however they have suffered from many limitations including uncertainty, overhead on user's device, disconnecting, and trust [30]. Concept of a TTP-Free class was introduced which did not need any trust with LBS server or any third party. Instead, it relied upon collaboration between users and peers to preserve privacy; however the issue of trust between peers still needed a resolution [31]. In pursuit of a resolution of trust issue, some researchers have proposed an idea of exchanging some information about previously visited area among peers to create a robust cloak area, which paved the way to consider storing some information on the client side [32]. The method in [23] used cache in TTP to store answers of some queries of users for the purpose of using them in future. It increased the privacy and performance level but resulted in decreasing the number of connections to server. This approach posed the challenges of cache management processes like data freshness, query selection, data consistency, cache hit\miss ratio, and estimation of required area to cache.

In the K-Anonymity approach, TTP would send the queries of K-Users to LBS server and store the answers for future queries [33]. This is an effective approach to protect privacy, although the cost of computation and connection turns out to be high. Use of cache was suggested to overcome this but as we know cache would require its management. To overcome the limitations of K-Anonymity, some more complex methods were suggested [34]. There are other techniques where cache is used as an aid tool in the cooperation systems to enhance the privacy and decrease the overhead on connections to LBS server [35]. In [25], mobile cache is used for saving results of the queries which can be used as answers for user queries.

Another approach known as "Mobi-Cache" is based on two ideas. The first one is an algorithm for dummies selection (DSA) in addition to an enhancing method (en-DSA) based on the Entropy of each cell (ratio of queries raised from each cell), used for optimizing the benefit of these dummies for new queries. The second idea proposed is using the cache at the access point available in each cell or specific area to store the answers of queries and dummies [36]. By having description and more details of DSA and en-DSA algorithms for careful generation, the dummies can be used or requested in the future as they achieve increased privacy and performance. The main idea is to divide the area into

many cells (equal sizes) and then calculate the Entropy metric for each one through the number of queries that are launched from it. After that, the dummies would be selected from the cells that have similar value to increase LBS server's uncertainty and use the dummies' answers in the future [37].

In the subsequent research, focus was on usage of cache, which was also divided the area into many cells, pointing each to an access point. This approach relaxed the overhead problem of dummy approach and that of the need for trusted parties [38]. In [39], Long Statistical Attack (LSA) and Regional Statistical attack (RSA) were proposed. As an enhancement of this approach, two new techniques were introduced. The first of them suggested dividing cells into four levels of privacy and changing size of each one to be bigger or smaller to achieve the required Entropy Value, and the second proposed using multinames (M-Name) for each user instead of single name (S-Name) [5]. It divided previous approaches to three classes according to the trust, namely, TTP based, Semi TTP, and Free TTP, and suggested a protocol for dealing between peers lacking trust, by hiding precise location to create a suitable cloaking area.

Collaboration between peers to obfuscate their locations into cloak area with K-users has led to more research [40], which supported continuous queries, as opposed to a snapshot, by way of using the cache. In [41], a new technique of cooperation between users by exchanging queries between themselves before sending them to a server in the Private Information Retrieval (PIR) systems was proposed to hide the identity of each one and retrieve the data from the server without revealing it. Although it enhanced the users' privacy in LBS server, it also relied upon the trust among peers in addition to overhead of using encryption.

Authors in [23] have created an integration between the cache technique and another one for exchanging queries among each pair of users to provide a solution of some problems and challenges. This includes the overhead in generating dummies and the need to trust in third party (TP) and the cache hit ratio, but at the cost of trusting another peer. Throughout this article, this approach will be referred to as P2PCache, which provided a new method to manage cache and the freshness issue of cache. A research survey of protection strategies and attack models is discussed in [42], which has outlined the following research topics in the privacy domain:

(1) Using semantics of data or locations to enhance the privacy;

(2) Preserving privacy for the location of data collection;

(3) Using an efficient indexing technique to relax the high cost;

(4) Creating a generic framework to address all privacy elements.

In view of the forging discussion, we have the following open problems in privacy domain:

(1) How to create a trusted party;

(2) How to optimize the cost of connections and overhead in some techniques;

(3) How to efficiently manage cache, freshness, and enhance the hit-ratio;

(4) How to effectively manage connections and collaboration among peers.

In this paper, as follows, we have provided solution for these problems.

3. Proposed Method

The major issues of user privacy are in the existing methods being centred around the trust and cache management.

3.1. Trust Management Issues. As mentioned earlier, ensuring trust between users and third party (server) is an open problem. The "trust" can be classified as follows:

(i) Trust with a service provider: it is regarded as the biggest threat because the service providers have all information about the users. Many techniques, as discussed before, had tried to address this issue but the problem was far from being resolved.

(ii) Trust with third party: this is known as anonymizer and used to avoid the trust with LBS server by hiding the identity of users, obfuscation their locations, generating dummy users, managing cloaking area, or helping peers to create a protected area. But this ended up shifting the problem from LBS server to another server and so did not produce an effective solution.

(iii) Trust with peers: in this case, users cooperate with each other to protect themselves. This technique as provided in [23] is superior though it still has its own issues. On one hand, the threat may still come from peers and on the other hand the management of cache is a complex procedure.

3.2. Cache Management Issues. As we discussed before, the cache was utilized to store some results of user's queries for answering future queries. In addition, it used so-called freshness technique to refresh the stored results. However, the freshness technique suffers from the following drawbacks:

(i) Sometimes the cache may not be utilized at all and so it will be cleared;

(ii) Using refresh process would affect system performance;

(iii) No distinction exists between queries that are submitted repeatedly and the ones which are submitted once only, which would adversely affect the efficiency of cache itself;

(iv) Filling cache by generated dummies would affect the cache hit-ratio adversely.

To overcome these anomalies, we propose a new technique, known as Double Cache Approach (DCA), which uses a pair of caches and replaced the freshness technique with a proposed one.

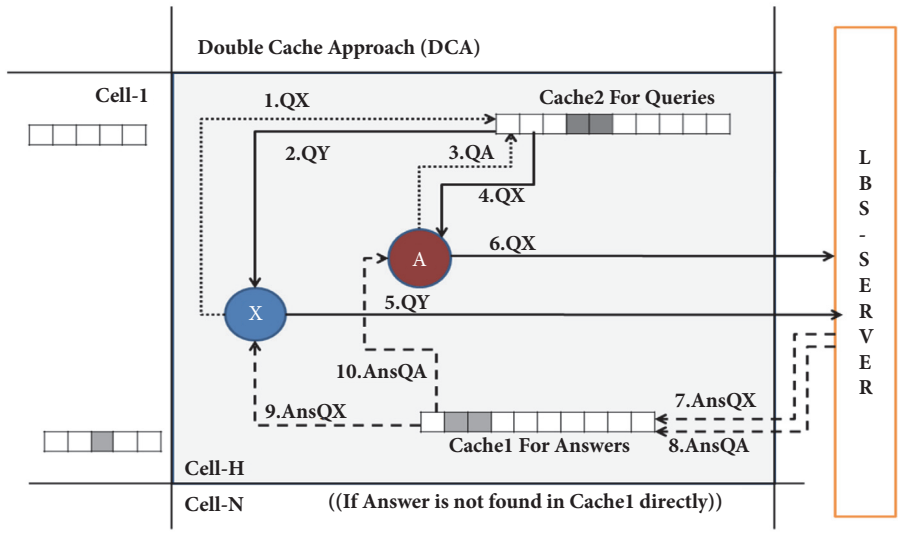

Figure 2: First scenario double cache approach.

3.3. Double Cache Approach (DCA). Initially the use of cache in privacy domain was to reduce the number of connections to LBS server, which was considered to be the biggest threat for users. In doing so, the privacy level was enhanced and so was the performance. However, this did not solve any of the open problems in the LBS system.

Before providing the details of the proposed DCA, we explain it by means of a simple example. Suppose a client or user A wants to choose a less polluted walkway without revealing their identity and the chosen walkway. For example, the query Q_A of A would be sent to another user B, who would submit it to LBS server. Consequently, server receives wrong information about B, but A would receive right answer for Q_A. To hide the information of A from B, a pair of cache would be used. This process can be repeated by A with other users. We shall call this method as the Double Cache Approach (DCA) and demonstrate the capabilities of that DCA to protect the patient location from malicious SP without effecting the quality of services. It should be noted the other known methods as those discussed in [43–46] cannot protect the privacy of A from B or SP. In reality, DCA can be seen as an enhancement of the P2PCache and removes the following anomalies of [23]:

(a) Lack of trust between peers, regarded as an open problem.

(b) Self-management for communication between peers affecting performance.

In DCA, we have a pair of caches, namely, $Cache_1$ *and* $Cache_2$, for addressing the trust issue between peers themselves and achieving new benefits. We shall use $Cache_1$ for collecting previous answers and $Cache_2$ for swapping queries between peers and managing the cooperation among them.

3.3.1. First Scenario ($Cache_2$ with First-In-First-Out). Suppose a user A wants to submit a query Q_A to LBS server. Before doing so, A should search for an answer of the query in $Cache_1$. If an answer was not found, Q_A should be swapped with Q_X, a query from some other user X in $Cache_2$, and then send Q_X to LBS. It is unlikely to find Cache2 empty but in case it was, user would submit just a dummy query to LBS server and store the query in Cache2. When an answer of Q_X was received, A would store it and look for an answer of Q_A in $Cache_1$. In the same manner X can swap Q_X with a query Q_Y of another user Y. This process is demonstrated in Figure 2.

3.3.2. Second Scenario (Cache2 with Priority). Unlike the previous case, user A can directly submit query Q_A to $Cache_2$, and wait for an answer in $Cache_1$. However, this may cause a considerable delay in getting an answer. To increase the priority of query resolution, A should submit one or (preferably) more queries of other users to LBS server. This method is shown in Figure 3. Let us calculate priority for query position in $Cache_2$. For example, let NQC be the number of current queries in the $Cache_2$, UQC the number of queries which user U has stored in $Cache_2$, and UQL number of queries which U has submitted to LBS server. So

$$Priority = \frac{\text{UQL}}{\text{UQC} + 1 + \text{NQC}} \tag{1}$$

$$Position_{in\_Cache} = \lfloor NQC - Priority * NQc \rfloor \tag{2}$$

The idea behind this second scenario is to increase the level of cooperation among peers for mutual benefit through saving of power consumption for users with limited battery/bandwidth. This situation does not arise in the first scenario, which forces users to connect LBS server. In contrast, the second scenario allows users with more resources to get more than one query from the cache and direct them to the LBS server. Users with low battery would place their queries in the cache and not connect to server.

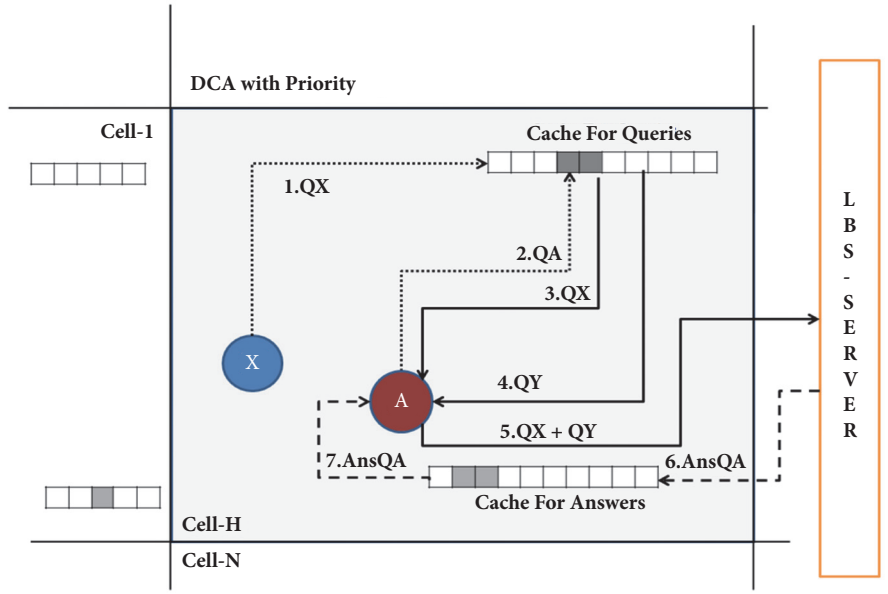

Figure 3: Second scenario double cache approach.

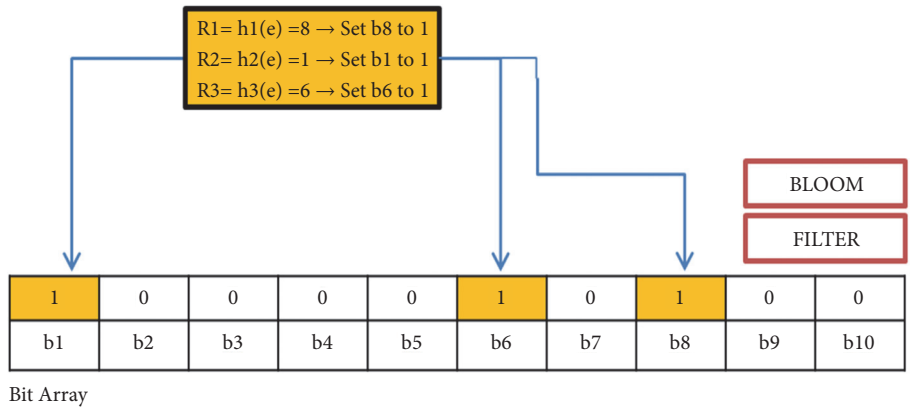

Figure 4: Hashing filter (Bloom).

According to waiting issue:

UQC = 1 often, because user usually needs answer for one query in the same time and cell.

If UQL = 1, it would revert to the first scenario.

If UQL > 1, that means the frequency of outing of queries to LBS server would outnumber the incoming quires to cache ⟶ NQC will tend to 1, eliminating need for any waiting.

If UQL=0, the query will be at the position NQC, which is the last of position in the cache. In this situation, user might wait until another user gets more than one query from cache.

Therefore, the waiting would occur only rarely, and if it did, it would be in the case when none of the other users would have taken more than one query from the cache, which is not realistic in the LBS system because all users would want to send more dummies to the LBS server. Moreover, if user was patient, they could easily take a query from the cache and send it to the LBS server to return to first scenario. Note that both scenarios are starvation-free.

3.4. Proposed Cache Management Technique. The DCA regards cache as a special queue and eradicates previous drawbacks by exploiting its size. It will hence store answers in Cache_1 and if Cache_1 was full, the oldest answer (Min ID) would be removed and the new answer would be added and Max ID would be incremented by 1. However, if answer already existed in Cache_1, then only ID of answer would be changed to MaxID+1. We have also used Bloom filter (Figure 4) (Hashing Technique) to increase the efficiency of cache and decrease the response time, especially in the miss-hit cases, where it would directly find out if the required answer for specific query was removed from cache or not determined by (O(I)), where O in [38] is the number of

Input: Query (q) of User A **Output**: Answers of q
// Search-Function
if (q ∈ Query in $Cache_1$) then
    q_{ID} = (Max_{ID} in $Cache_1$) + 1
    Return q_{ANS}
end
else
    Insert (q in $Cache_2$)
    Get first q~ of $Cache_2$ // Unknown User
    Insert $q\sim_{ANS}$ to $Cache_1$ with Max_{ID}
    Query with Min_{ID} in the $Cache_1$ will be deleted.
end
Recall Search-Function
End Function

Algorithm 1

elements in cache. Bloom filter directly gets an answer for O(I), if the element existed in cache or not before I search.

3.5. Algorithm of Cache Management. See Algorithm 1.

3.6. Benefits of DCA. Use of additional cache to handle query swapping among peers, with a new technique for managing caches, resolves the issue of trust between peers and enhances performance of the whole system without having to generate dummies. DCA facilitates superior collaboration among peers, unlike that in [23], where the user had to search and contact a peer directly. In particular:

(i) answers of queries would be kept in $Cache_1$ permanently without having to refresh them;

(ii) DCA would utilize the whole size of $Cache_1$;

(iii) no dummy queries would be stored in the $Cache_1$;

(iv) user would not need to trust other peers;

(v) query swapping would improve the performance and the cache hit-ratio, in addition to increasing the level of privacy by feeding LBS with misleading information about users.

3.7. Mathematical Proof for Superiority of DCA. We divide the area for N different cells and assume that q_i is the probability of the number of queries produced from the cell i, so

$$\sum qi = 1: \quad i = 1 \text{ to } N \tag{3}$$

If user sends k queries to server, one of them real and others (k-1) dummies, then

$$Pi = \frac{qi}{(\sum qi)}: \quad i = 1 \text{ to } k \tag{4}$$

where Pi denotes the probability of qi being a real query from k ones which will be (1/k) only if the whole queries have same priority.

If H is the Cache hit ratio, then

$$H = \frac{(\text{queries answered by cache})}{(\text{queries answered by cache} + \text{queries sent to server})} \tag{5}$$

The privacy level, according to Entropy metrics (E), lies in [0, 1], where E = 0 means that a server knows the user's query, and E = 1 means it does not. Then

$$E = \sum_{i=1}^{k} (pi.\log_2 (pi)) \tag{6}$$

Earlier methods have tried to increase E [38] and added k-1 dummies to the real query before sending it to server to make E larger. In case of the method of [23], E would attain maximum value of 1 for server, because query would not be sent by the user. However, the E value peers will be zero because when swapping user sends his real query to other peer so Pi = 1 thereby would be zero, which is a drawback in [23]. DCA has solved this issue by avoiding the direct dealing between peers and so E = 1, both for server and peers. This would achieve more privacy in addition to better performance. Note that the privacy and performance can be increased in two ways, namely, if H or E becomes larger.

4. Threats Models and Security/Privacy Analysis of DCA

Service providers, who can access, manipulate, and reveal user data from LBS, can be classified as active attackers, whereas the other users who only eavesdrop, may be known as passive attackers. Here we discuss the effectiveness of DCA in dealing with these kinds of attackers in the following scenarios:

(i) Semantic context: attacker has personal information like age, work history, etc. of the user. In DCA a user is not required to send personal information and exchange their query with random and this kind of threat is eliminated.

(ii) Trajectory infers: tracing user. DCA solves this problem as the user would be in a different location, which the attacker cannot trace.

(iii) Historical (temporal) attack: it happens when attacker accesses and analyses a lot of user queries. In DCA, this would not happen because a user would always submit other user's query to LBS.

(iv) Inversion attack: this happens when the attacker knows user's algorithm or technique of protection. In DCA, again this would not happen because, even the attacker knows the used technique, they would not know the real query of the user.

Other types of attacks relate to skills and knowledge of attackers about different kinds of information of cells, as follows:

(i) Diversity level: kinds of people of interest (POIs).

(ii) Closeness level (uniformity): cells have been adjacent to each other.

(iii) Congestion: number of users are close to be the same in each cell.

(iv) Location homogeneity: all POIs in the cell have same location (healthy buildings).

(v) Knowledge about the map: an attacker may be skilled to determine the type of area or crop some parts of it to make the area smaller to detect more accurate information about user's location.

In DCA, the possibilities of these can be diminished by having unequal sizes of cells. In addition, we propose that the users should change their alias when they enter a new cell.

4.1. Matrices. Here we discuss and compare privacy and performance metrics of other approaches [5, 35, 42, 47] with DCA.

4.1.1. Privacy Metrics. Many of these metrics are used to measure the system efficiency and compare between approaches. Here we discuss only the critical ones.

K-Anonymity. It refers to number of dummies which are sent to LBS server with real queries. If the number of dummies, k, equals to nine, the user would send ten queries to server (the user should keep the value of k to the minimum). We know that

$$\text{K-Anonymity} = \frac{1}{(1 + k)} \tag{7}$$

Entropy (E). It is the most important measure which refers to privacy level and quantifies the anonymity and the amount of data that LBS server has from each user. The user should aim to have it close to 1. As in (6), it is defined as

$$E = \sum pi * \log_2 (pi) \tag{8}$$

Ubiquity (U). It refers to user's existence at each point in the cell to deny attackers to detect identity. It is easily achieved in DCA because of query swapping mechanism. Actually, U is used to measure the movements of users and probability of their existent in a specific location in a cell and is defined as

$$U = 2^E \tag{9}$$

Uncertainty/Estimate Error (EE). This metric is related to the server to measure the amount of error in trying to determine the position of users. In DCA, EE will be maximum because server provider would not have any clue of the user location (only false information). It is defined as

$$EE = (E)\ 100\% \tag{10}$$

The Entropy of Privacy is related to the amount of right information in the LBS server about user A. Therefore, if the amount of right information in LBS server equals 0, that means the Entropy will be maximum (E = 1) and it leads to maximum uncertainty (EE = 100%).

4.1.2. Performance Metrics. The performance is dependent on factors like number of dummies, algorithm of generating dummies or obfuscation, encryption, cache management, number of queries sent to LBS server, and cost. In DCA, cache concept, smart dummies, and cooperation are used, to measure the performance as follows.

Cache Hit-Ratio (CHR). We use cache hit ratio to measure the percentage of the queries answered by the cache, which depends on the number of connections to LBS server and is defined as

$$\text{CHR} = \frac{(\text{number of queries answered by C1})}{(\text{total number of queries})} \tag{11}$$

Response Time (RT). It is related to the requested time of all operations in the system. It is defined as

$$RT = 2 * ST + PT \tag{12}$$

where ST is the time of sending and returning a query and PT is the processing time.

5. Simulation and Results

This section contains simulation of implementation of main features of DCA that draws a comparison with P2PCache [23] and other methods, namely, Enhanced-CaDSA, Enhanced-DLS, and MoCrowd [36, 38]. For this, we have used MATLAB 2015. We propose to divide the area into 100×100 cells with 10,000 virtual users. Out of the par of caches, first ($cache_1$) was dedicated for saving the answers of queries with POI included in cells with wireless connections and the second ($cache_2$) to store queries and manage the swapping among peers and by avoiding direct cooperation.

As mentioned earlier, the format of any query in LBS applications is {⟨Latitude, Longitude⟩, POI/TYPE, USER-ID} where POI represent the type of user's query. Enhanced approach changed the location part to cell-number and added time-stamp instead of USER-ID for cache freshness

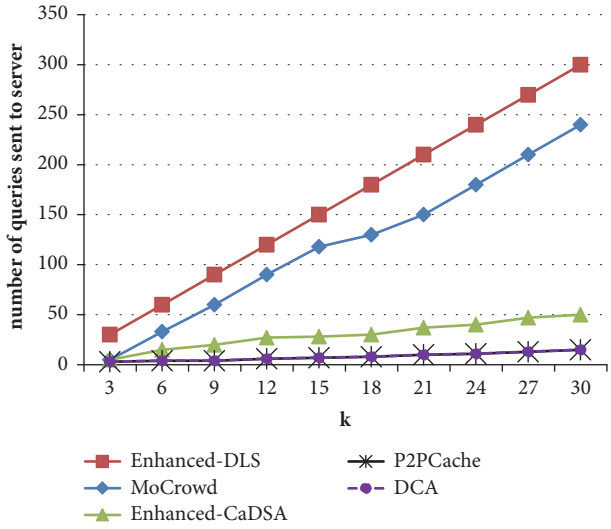

Figure 5: Cost communication with LBS server.

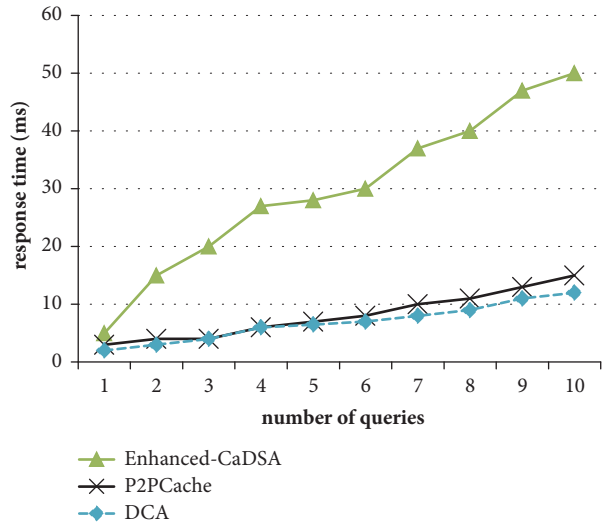

Figure 6: Response time.

operation. Therefore, each query needed less than 1 KB of the cache and after 4 hours the storage cost was 53.7 KB [38]. Consequently, the total size of cache in each cell was 100 KB, which was sufficient. The count of POIs from Google-API for New-York city was around 250,000, requiring 250 MB storage. Finally, either 3G or 4G Wi-Fi connection in the smart cities environment or in specific areas and infrastructure would be adequate.

In DCA, same query format was used as in P2PCache but removed the part of the USER-ID and Time-Stamp {⟨Latitude, Longitude⟩, POI} to make it cost less. However, we added another cache ($cache_2$) to facilitate query swapping.

We now provide examples to prove our claim of supremacy of DCA over earlier available methods. Note that the connection between peers would rely on the mobile app and Wi-Fi, despite having $Cache_2$.

5.1. Cost Communication. It is a measure of the number of connections in LBS server and amount of data on the link, which in our approach, as shown in Figure 5, has better performance than any other methods described in [38]. Notice that DCA and P2PCache have used the minimum and same number of queries sent to LBS server; however the difference lies in the management of cooperation between peers.

5.2. Response Time. DCA overcame the anomalies of P2PCache [23] and Enhanced-CaDSA discussed in [38], and, with the help of Bloom filter, saved time in case of miss-hit in the $cache_2$. Furthermore, the swapping technique did not need searching for or direct dealing with peers, resulting in improvement of performance and enhancement of privacy, as can be seen in Figure 6.

5.3. Cache Hit Ratio. This metric can be improved by storing the queries in $Cache_2$, which may later be requested by other users. As shown in Figure 7, DCA and P2PCache achieved

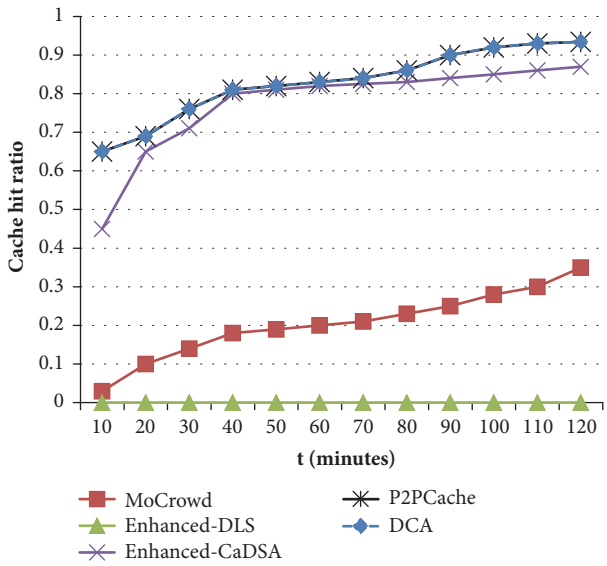

Figure 7: Cache hit-ratio.

the best result because we submitted real queries in $Cache_2$ instead of dummies and better management of cache as explained earlier.

5.4. Privacy Metric (Entropy). Other methods, as in [38], have used dummies (k = 10, 20 or 30) along with the real query to send to LBS to increase the privacy and to maximize this metric. However, it would reduce performance and cache hit-ratio. In DCA, user would just send only one query and the same would be done by the other user, resulting in enhancing the performance and cache hit ration, in addition to maximizing Entropy Value to 1 as shown in Figure 8.

5.5. Amount of Data Collected by the LBS Server. Like Entropy, it relates to the amount of information that the server can obtain for each user. When k increases, the ratio

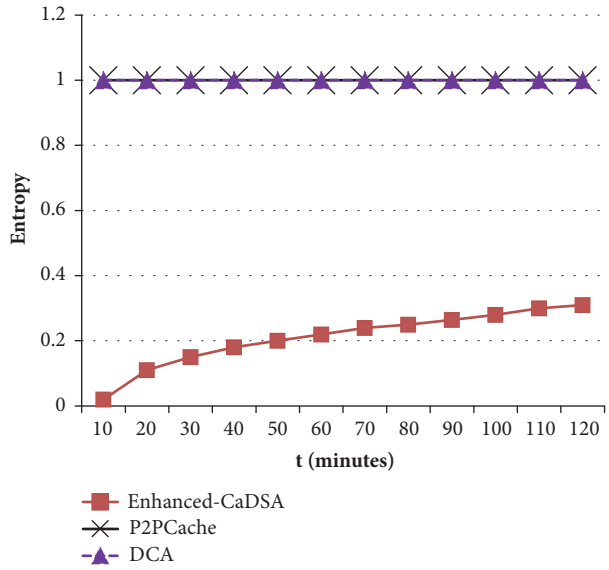

Figure 8: Entropy metrics.

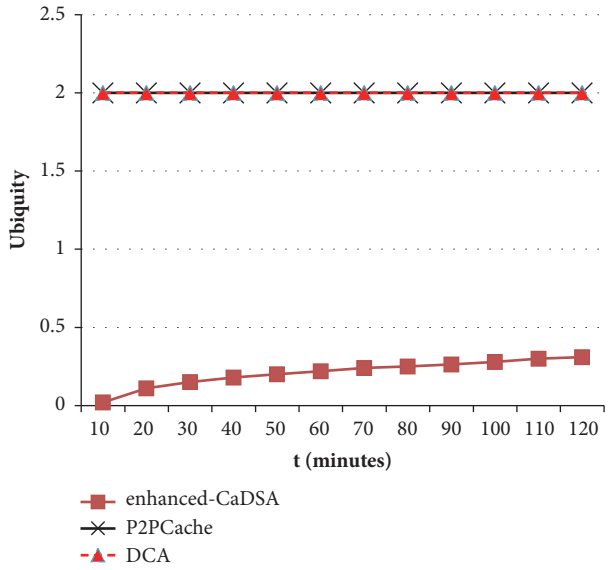

Figure 9: Ubiquity metrics.

would decrease because the server cannot distinguish the actual query from dummies. Thus, DCA would perform better than other approaches because the number of queries is only one, information obtained by server is zero, and so is the ratio.

$$\text{Information Ratio in LBS Server} = \left(\frac{\text{Number of Actual Queries}}{1} + K\right) \quad (13)$$

5.6. Amount of Data Collected by the LBS Server. It refers to degree of spread of a user in a cell and so if it increases, so does privacy because LBS server would not be able to determine the real location of user. Ubiquity (Figure 9) in

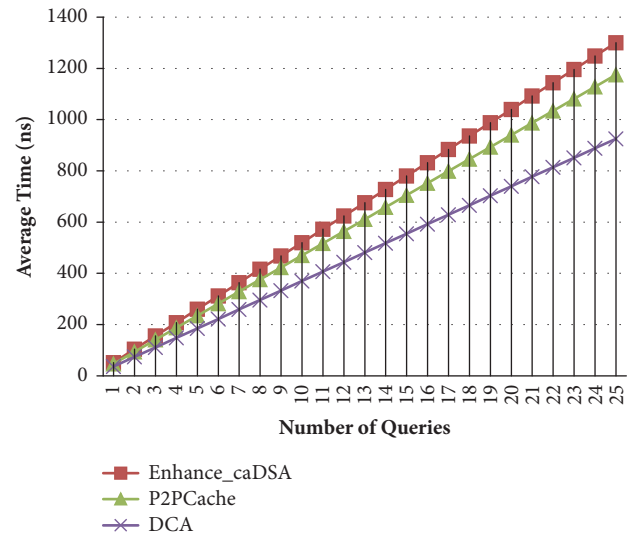

Figure 10: Search performance of cache.

DCA is the best as compared with other methods because it has best Entropy and the swapping technique in $Cache_2$, which amounts to better spread of data in the whole cell.

5.7. Performance of Searching in Cache. As we discussed before, the Enhanced-CaDSA approach [38] uses freshness-time method to manage the content of cache and refresh the time-stamp of the remaining duration of each query in the cache. In the case of DCA, we achieve better results by updating the position of higher order queries and removing the least requested ones in $Cache_1$. In the simulation shown in Figure 10, we have used the hit-ratio, Tc-hit, the response time in the hit case, TC-mis, the response time in the missed case, Tl, the response time from LBS server, Ct, and the response time of collaboration among peers. Using Bloom filter, we get TC-mis ≈ 0, and, for $Cache_2$, we get Ct ≈ 0. Also Avg_enhance = Tc-hit $*$ H + (1-H) (Tl+Tc-miss), Avg_Previous = Tc-hit $*$ H + (1-H)(Tl) + Ct, and Avg_DoubleC = Tc-hit $*$ H + (1-H)(Tl)

5.8. Comparing between Cache Management Methods. In earlier methods of freshness [38], for each stored query time, there are N write operations on cache, where N is the count of current stored queries in cache. When N is changed, so is the ratio of management time. In the hit case of cache, there is just one read operation, and in the miss case there are N read operations. In the miss case of DCA, there is just one read operation, and in the hit case there is one write and one read operation. There is no dealing with freshness here; instead, after each hit or miss, there is one write operation to change the order of selected query. From Figure 11, we can note that the time of management will be static in DCA, whereas it would increase adversely with increase in the time period of frequency freshness.

5.9. Limitations. For performance, trust, and privacy, DCA approach would be better. However, there are some drawbacks:

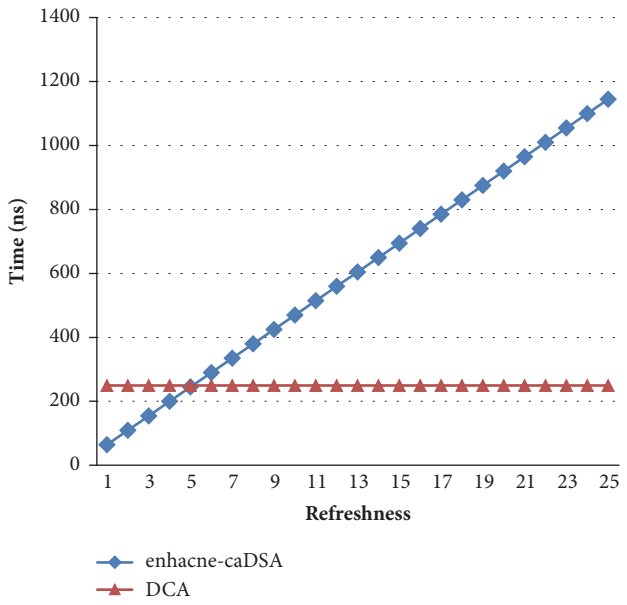

Figure 11: Cache management.

(a) Cost of distribution of the caches by dividing at the access points cells in the physical environment would be higher. Therefore, we have proposed that this issue should be dealt with smart city, which the governments or significantly large organisations can afford by investing the resources required.

(b) Cache needs to be protected from eavesdropper or hacker.

(c) DCA would work well with LBS but there are other privacy issues in healthcare domain which we shall address in future.

6. Conclusions

In this paper, we proposed DCA as a novel approach for preserving privacy and security in LBS of IoT applications in general and the medical field in particular. It is the first technique which uses the idea of two caches, addresses the trust among peers, and manages the relations between them in wireless environment. Simulation results have shown overcoming superiority of this approach over previously known ones dealing with the privacy, cost of communication, and performance.

Data Availability

The data used to support the findings of this study are available from the corresponding author upon request.

Conflicts of Interest

The authors declare that they have no conflicts of interest.

References

[1] H. Chen, A. Nicogossian, S. Olsson et al., "Electronic health," *International journal of telemedicine and applications*, vol. 2009, Article ID 308710, 2 pages, 2009.

[2] C. Stingl and D. Slamanig, "Health records and the cloud computing paradigm from a privacy perspective," *Journal of Healthcare Engineering*, vol. 2, no. 4, pp. 487–508, 2011.

[3] Q. Huang, L. Wang, and Y. Yang, "Secure and Privacy-Preserving Data Sharing and Collaboration in Mobile Healthcare Social Networks of Smart Cities," *Security and Communication Networks*, vol. 2017, Article ID 6426495, 12 pages, 2017.

[4] W. Sun, C. Chen, B. Zheng, C. Chen, and P. Liu, "An air index for spatial query processing in road networks," *IEEE Transactions on Knowledge and Data Engineering*, vol. 27, no. 2, pp. 382–395, 2015.

[5] M. Wernke, P. Skvortsov, F. Dürr, and K. Rothermel, "A classification of location privacy attacks and approaches," *Personal and Ubiquitous Computing*, vol. 18, no. 1, pp. 163–175, 2014.

[6] D. Gavalas, P. Nicopolitidis, A. Kameas et al., "Smart Cities: Recent Trends, Methodologies, and Applications," *Wireless Communications and Mobile Computing*, vol. 2017, Article ID 7090963, 2017.

[7] S. Guan, Y. Zhang, and Y. Ji, "Privacy-preserving health data collection for preschool children," *Computational and mathematical methods in medicine*, vol. 2013, Article ID 501607, 5 pages, 2013.

[8] S. I. Konomi and C. S. Nam, "Supporting collaborative privacy-observant information sharing using RFID-tagged objects," *Advances in Human-Computer Interaction*, vol. 2009, 5 pages, 2009.

[9] R. S. Zuberi and S. N. Ahmad, "Secure mix-zones for privacy protection of road network location based services users," *Journal of Computer Networks and Communications*, vol. 2016, Article ID 3821593, 8 pages, 2016.

[10] J. Wang and Z. Wang, "A survey on personal data cloud," *The Scientific World Journal*, vol. 2014, Article ID 969150, 13 pages, 2014.

[11] Y. Liang, Z. Cai, Q. Han, and Y. Li, "Location privacy leakage through sensory data," *Security and Communication Networks*, vol. 2017, Article ID 7576307, 12 pages, 2017.

[12] M. Zhou, X. Li, and L. Liao, "On preventing location attacks for urban vehicular networks," *Mobile Information Systems*, vol. 2016, Article ID 5850670, 13 pages, 2016.

[13] M. S. Alrahal, M. U. Ashraf, and A. Abesen, "AES-Route Server Model for Location based Services in," in *Proceedings of the AES-Route Server Model for Location based Services in Road Networks. International Journal Of Advanced Computer Science And Applications*, vol. 8, pp. 361–368, 2017.

[14] A. Ukil, S. Bandyopadhyay, and A. Pal, "IoT-privacy: To be private or not to be private," in *Proceedings of the In Communications Workshops (INFOCOM WKSHPS, '14)*, pp. 123-124, 2014.

[15] L. Da Xu, W. He, and S. Li, "Internet of things in industries: A survey," *IEEE Transactions on industrial informatics*, vol. 10, no. 4, pp. 2233–2243, 2014.

[16] A. B. Labrique, G. D. Kirk, R. P. Westergaard, and M. W. Merritt, "Ethical issues in mHealth research involving persons living with HIV/AIDS and substance abuse," *AIDS research and treatment*, vol. 2013, Article ID 189645, 6 pages, 2013.

[17] A. Fragopoulos, J. Gialelis, and D. Serpanos, "Security framework for pervasive healthcare architectures utilizing," *International journal of telemedicine and applications*, vol. 2009, Article ID 461560, 9 pages, 2009.

[18] J. M. Shin, "Secure Remote Health Monitoring with Unreliable Mobile Devices," *Journal of Biomedicine and Biotechnology*, vol. 2012, Article ID 546021, 5 pages, 2012.

[19] J. Bou Abdo, T. Bourgeau, J. Demerjian, and H. Chaouchi, "Extended privacy in crowdsourced location-based services using mobile cloud computing," *Mobile Information Systems*, vol. 2016, Article ID 7867206, 13 pages, 2016.

[20] J. Zhong, W. Wu, C. Cao, and W. Feng, "A Variable Weight Privacy-Preserving Algorithm for the Mobile Crowd Sensing Network," *Journal of Electrical and Computer Engineering*, vol. 2017, Article ID 3053202, 7 pages, 2017.

[21] B. Kang, J. Wang, and D. Shao, "Attack on Privacy-Preserving Public Auditing Schemes for Cloud Storage," *Problems in Engineering*, Article ID 8062182, 6 pages, 2017.

[22] A. A. A. Sen, F. A. Eassa, K. Jambi, and M. Yamin, "Preserving privacy in internet of things: a survey," *International Journal of Information Technology*, pp. 1–12, 2018.

[23] M. Yamin and A. A. A. Sen, "Improving Privacy and Security of User Data in Location Based Services," *International Journal of Ambient Computing and Intelligence (IJACI)*, vol. 9, no. 1, pp. 19–42, 2018.

[24] O. Vernesan, P. Friess, G. Woysch et al., *Europes IoT strategic research agenda, 2012., The Internet of Things*, UK, Halifax, 2012.

[25] A. AbiSen, F. Albouraey, and K. A. Jambi, "A Survey of FOG Computing: Properties, Roles and Challenges," *Computing for Sustainable Global Development (BVICAM)*.

[26] I. Y. Jung, G. J. Jang, and S. J. Kang, "Secure eHealth-care service on self-organizing software platform," *Mathematical Problems in Engineering*, vol. 2014, Article ID 350876, 9 pages, 2014.

[27] Z. Lin, X. Xiao, Y. Sun, Y. Zhang, and Y. Ma, "A Privacy-Preserving Intelligent Medical Diagnosis System Based on Oblivious Keyword Search," *Mathematical Problems in Engineering*, vol. 2017, Article ID 8632183, 7 pages, 2017.

[28] L. Sun, M. Yamin, C. Mushi, K. Liu, M. Alsaigh, and F. Chen, "Information analytics for healthcare service discovery," *Journal of healthcare engineering*, vol. 5, no. 4, pp. 457–478, 2014.

[29] A. A. Sen, F. Eassa, K. Jambi et al., "Preserving privacy in internet of things: a survey," *International Journal of Information*, vol. 10, no. 2, pp. 189–200, 2018.

[30] M. Mokbel and C. Chow, "Challenges in Preserving Location Privacy in Peer-to-Peer Environments," in *Proceedings of the Seventh International Conference on Web-Age Information Management Workshops*, pp. 1-1, Hong Kong, China, June 2006.

[31] A. Solanas, J. Domingo-Ferrer, and A. Martínez-Ballesté, "Location privacy in location-based services: Beyond TTP-based schemes," in *Proceedings of the 1st International Workshop on Privacy in Location-Based Applications, PiLBA 2008*, pp. 12–23, Spain, October 2008.

[32] D. Miorandi, S. Sicari, F. de Pellegrini, and I. Chlamtac, "Internet of things: vision, applications and research challenges," *Ad Hoc Networks*, vol. 10, no. 7, pp. 1497–1516, 2012.

[33] Y. Chen, J. Bao, W. Ku, and J. Huang, "Cache Management Techniques for Privacy Preserving Location-based Services," in *Proceedings of the Ninth International Conference on Mobile Data Management Workshops, MDMW*, pp. 88–96, Beijing, China, April 2008.

[34] J. Cacheclock Meyerowitz and R. Roy Choudhury, "Hiding stars with fireworks: location privacy through camouflage," in *Proceedings of the In Proceedings of the 15th annual international conference on Mobile computing and networking*, pp. 345–356, 2009.

[35] K. G. Shin, X. Ju, Z. Chen, and X. Hu, "Privacy protection for users of location-based services," *Wireless Communications*, vol. 19, no. 1, 2012.

[36] X. Zhu, H. Chi, B. Niu, W. Zhang, Z. Li, and H. Li, "Mobicache, When k-anonymity meets cache," in *Proceedings of the Global Communications Conference (GLOBECOM, '13)*, pp. 820–825, 2013.

[37] B. Niu, Q. Li, X. Zhu, G. Cao, and H. Li, "Achieving k-anonymity in privacy-aware location-based services," in *Proceedings of the Proceedings IEEE*, pp. 754–762, 2014.

[38] B. Niu, Q. Li, X. Zhu, G. Cao, and H. Li, "Enhancing privacy through caching in location-based services," in *Proceedings of the IEEE Conference Computer Communications (INFOCOM '15)*, pp. 1017–1025, 2015.

[39] Y. Sun, M. Chen, L. Hu, Y. Qian, and M. M. Hassan, "ASA, Against statistical attacks for privacy-aware users in Location Based," *Service. Generation Computer Systems*, vol. 70, pp. 48–58, 2017.

[40] C. Ma, L. Zhang, S. Yang, and X. Zheng, "Hiding Yourself Behind Collaborative Users When Using Continuous Location-Based Services. of Circuits," *Systems and Computers*, vol. 26, no. 07, Article ID 1750119, p. 10, 2017.

[41] J. Domingo-Ferrer, M. Bras-Amorós, Q. Wu, and J. Manjón, "User-private information retrieval based on a peer-to-peer community," *Knowledge Engineering*, vol. 68, no. 11, pp. 1237–1252, 2009.

[42] P. Jagwani and S. Kaushik, "Privacy in Location Based Services: Protection Strategies, Attack Models and Open Challenges," in *Proceedings of the International Conference on Information Science and Applications*, pp. 12–21, Singapore, 2017.

[43] Y. L. Chen, B. C. Cheng, H. L. Chen et al., "A privacy-preserved analytical method for eHealth database with minimized information loss," *BioMed Research International*, Article ID 521267, 9 pages, 2012.

[44] S. S. Kim, Y. H. Lee, J. M. Kim, D. S. Seo, G. H. Kim, and Y. S. Shin, "Privacy protection for personal health device communication and healthcare building applications," *Journal of Applied Mathematics*, vol. 2014, Article ID 462453, 5 pages, 2014.

[45] P. Zhang, M. Durresi, and A. Durresi, "Enhanced Internet Mobility and Privacy Using Public Cloud," *Mobile Information Systems*, vol. 2017, Article ID 4725858, 11 pages, 2017.

[46] J. Qu, G. Zhang, and Z. Fang, "Prophet: A Context-Aware Location Privacy-Preserving Scheme in Location Sharing Service," *Discrete Dynamics in Nature and Society*, vol. 2017, 7 pages, 2017.

[47] M. S. Alrahhal, M. Khemakhem, and K. Jambi, "A survey on privacy of location-based services: classification, inference attacks, and challenges," *Journal of Theoretical and Applied Information Technology*, vol. 95, no. 24, 2017.

Hindawi
Wireless Communications and Mobile Computing
Volume 2018, Article ID 7361597, 15 pages
https://doi.org/10.1155/2018/7361597

Research Article

Managing Crowds with Wireless and Mobile Technologies

Mohammad Yamin,[1] **Abdullah M. Basahel**,[1] **and Adnan A. Abi Sen**[2]

[1]*Department of MIS, Faculty of Economics and Administration, King Abdulaziz University, Jeddah 21589, Saudi Arabia*
[2]*College of Computer Science and Information Technology, King Abdulaziz University, Jeddah 21589, Saudi Arabia*

Correspondence should be addressed to Mohammad Yamin; myamin@kau.edu.sa

Received 23 February 2018; Revised 28 May 2018; Accepted 9 July 2018; Published 1 August 2018

Academic Editor: Simone Morosi

Thousands of people have lost their lives in stampedes and other crowd related disasters in recent years. Most of these fatalities seem to have been caused by poor control and management of crowds, which is discussed in this article. An efficient and effective crowd management system must also have a plan to deal with the ongoing threat of terrorism and outbreak of various kinds of communicable diseases. In this article, we present a framework of a Crowd Control and Health Management System specially designed to prevent and manage stampedes and other disasters. The system has two subsystems; one for dealing with the management of stampedes and other disasters and the other with healthcare management. As part of the proposed system, an algorithm for an early detection of stampedes, with proof and simulation of implementation, is provided. As part of the healthcare management subsystem, we integrate several mobile applications and develop four of them dealing with relief issues, blood donations, complaints and alerts, and utilizing mobile phones as a sensor device. Our system makes use of various kinds of wireless, mobile, and other technologies and tools including Fog Computing, Smart Phones, Smart Digital Street, IP-Cameras, Radio Frequency Identification (RFID), Voice Alarm, Light Alarm, and Global Positioning System (GPS). We compare merits and effectiveness of RFID and Wireless Sensor Networks (WSNs), as well as those of Cloud and Fog with a view of using them as part of the proposed framework. We also discuss applications of our systems in real-life cases of Hajj, an annual pilgrimage of millions of people to Mecca, and Kumbh Mela, a periodic gathering of tens of millions of people in India, both of which have accounted for the majority of fatalities in stampedes and other disasters.

1. Introduction

During 1980-2015, more than twelve thousand people have lost their lives because of stampedes [1–3]. Crowd managers worldwide seem not to have learned from past experiences, particularly regarding significant crowd events; otherwise the death toll (more than seven thousand) during the first sixteen years of this century would not be more than that in the whole of the last century. The root causes of stampedes are overcrowding and mismanagement and, therefore, some would argue that this colossal loss of lives could have been minimized by better control and management.

An increased growth in and spread of highly contagious viruses and diseases have been witnessed in recent years. Of these viruses and diseases are EBOLA [4], HIV Aids [5], Swine Influenza H1N1 and H1N2 [6], various strands of flu [7], Severe Acute Respiratory Syndrome (SARS) [8], and Middle Eastern Respiratory Syndrome (MERS) [9]. They have occurred mainly in Africa and the Middle East, but also in some other parts of the world. Treatment of these afflictions is a very challenging job [10]. The spread of these diseases in crowds could be catastrophic; and so, the crowd management must take adequate measures to prevent their spread and have treatment plans in place.

Some crowded events attract people from hundreds of different cultural and linguistic backgrounds, which create significant communication challenges for management to deal with. Large crowds would also witness medical and other life-threatening emergencies. As expected, some participants in large crowds go missing for different reasons. Tracking their way back through a dense crowd, especially in a foreign land, with significant communication and transportation problems, could be a very daunting task for them. It is the

Table 1: Communication protocols of WSNs/RFID.

Protocol	Range	Devices/Nodes	Power Consumption & Cost	Bandwidth
Wi-Fi IEEE-802.11 WLAN (2,3,4G)	30 m	128 devices	More power and cost	10-100 Mb/s
Bluetooth-802.15.1 WPAN	10 m	8 devices	Less power and cost	1 Mb/s
ZigBee-802.15.4 Low Power	10-70 m	65000 nodes	Lowest power and cost	250 kb/s

responsibility of the crowd administration to manage these kinds of emergencies and issues.

Many parts of the globe are now facing the menace of terrorism [11]. Crowded places have greater likelihood of being subjected to terrorist attacks as observed by the history of previous attacks. Possibilities of terrorist strikes must be taken into consideration seriously and the management should have adequate plans and measures to minimize this threat and deal with the aftermath in case the terrorists do succeed.

The aim of this article is to propose a framework for Crowd Control and Health Management System (CCHMS). The CCHMS will have two subsystems, namely, Disaster Control and Management System (DCMS), aimed at reducing the risk of stampedes and other disasters, and Healthcare Management System (HMS), to ensure safety and wellbeing of the people in crowds.

We shall describe various layers of DCMS and provide the following:

(a) An algorithm for an early detection of an ensuing stampede. We shall also provide the proof of the algorithm as well as its implementation by simulation.

(b) Analysis of various kinds of wireless connectivity, sensors, mobile tools and technologies, and their integration and usage in the system.

(c) A comparison of WSN versus RFID and Fog versus Cloud and their role in the system.

As part of HMS, we shall present the following:

(d) A design of mobile applications, which includes the most critical subsystems dealing with medical issues and emergencies, terror attacks, and other disasters.

(e) Implementation of four mobile applications in (d) for Android and iOS. These include (i) relief issues, (ii) blood donor, (iii) complaints and alerts, and (iv) turning mobile phones to WSNs and active RFID tags.

We shall also analyse the usefulness and effectiveness of CCHMS in real cases of Hajj [12–15] and Kumbh Mela [15–17]. In the next section, we shall briefly describe different kinds of crowds and examine the role of various technologies and tools used in CCHMS.

2. Literature Review

Crowds which we witness time to time differ in many ways. A crowd would usually belong to an event, which may be regular or otherwise. Events like Hajj, Kumbh Mela, and Arbaeen [33] are regular and generally predictable, whereas irregular events are usually unpredictable in nature and size and the crowd within them can build up spontaneously. Examples of these are funeral processions, protest or celebration marches, election rallies, sporting events, and musical concerts. Prediction of the size and nature of the irregular and spontaneous crowds is very difficult due to many uncertainties surrounding them. To illustrate, it was not anticipated that the funeral of South Indian politician, Annadurai, in 1969, would gather fifteen million people.

Table 2 shows properties of WSNs/RFID Protocols (WSNs can be IP-based and non-IP) [18–26].

Management of regular events might seem easier but the reality is quite opposite as most of the stampedes have occurred during Hajj and Kumbh Mela. However, technologies like RFID, WSNs, Cloud, and Fog can be used to manage a regular crowd, which may not be feasible in cases of irregular and spontaneous crowds.

2.1. Radio Frequency Identification (RFID) and Wireless Sensor Networks. Radio Frequency Identification (RFID) [19] technology and tools, which are already being used for tracking the movements of people, vehicles, goods etc., can help to manage some of the problems of crowding. The RFID chips, usually in the form of tags, can be linked to a Wireless Sensor Network (WSN) [34, 35], cellular (3G/4G) network, or GPS [36]. Choosing one of these networks would depend on the terrain where RFID chips are deployed or the path they traverse. If deployed in urban areas, density of buildings, width of streets, congestion, and other related issues would have to be taken into consideration. A Wireless Sensor Network (WSN) is a cluster of a large number of sensors, each of them tasked to monitor and detect physical events such as light, heat, pressure, pollution, and RFID tags. Being wireless, they are more flexible in deployment and have larger scalability. Using a WSN for accessing signals from RFID tags is quite effective and provides very accurate longitudinal and latitudinal coordinates. However, their installation and deployment can be costly as well as hazardous in places with limitations. Efficient tracking with a Cellular Network would require many repeaters to ensure access in all areas of RFID tags. For details, see [37].

It is well known that GPS does not efficiently function in tunnels and densely built up locations [38]. Likewise, some of the RFID tags may not be detected in very dense crowds, and the local sensor network may not be deployed in places with a lack of space. Despite limitations, these technologies have revolutionised tracking and obtaining information from obscure places. These technologies have also created a launching pad for the Internet of Things (IoT) and hence paved the way for abundant applications [39]. Table 1 provides a comparison between WSNs and RFID.

2.2. Fog and Cloud Computing. Fog is a model for computing, introduced by CISCO in 2012 to reduce or eliminate some limitations of Cloud Computing. Fog can be defined as an

Table 2: Comparison between RFID and WSN.

Factor	WSN	RFID
Main goal	Monitor and sense environment [18].	Detection location and Identity [19].
Tasks	Collect, Process, Transfer, and Store [20]	Usually reflects RF signal transmitted from Reader for identification of location of the attached object [21].
Element	(i) Sink aggregates the information from sensor nodes. (ii) Sensor node with sensing, Computing, and communicating elements [21].	(i) Tag (Passive/Active) stores the unique serial number, and it provides memory for some additional info. Passive tag is used only for reading info by a Reader. Active tag supports two ways communications with higher signal strength and can store some information, but it is costly. (ii) Reader can read or write data on Tag and pass it to the host. Capable to send messages to an individual tag or broadcast to all tags within range. (iii) Host Computer analyses data [22].
Range	Can't support long range of communication, so it uses multihub to reach the Sink Node and increase the range [21].	Usually small Range of communication, where Passive Tag (2-3 meters), Active Tag (100-200 meters), but it is costly relative to its abilities [22].
Application	Applications in many fields including Safety and Wellbeing, Healthcare, Smart-Grid, Environment [23].	The main applications are Tracing, Security & Access Control, Healthcare, Crowding, Clothes stores, etc. [22].
Protocol of connection	Wireless connections: Wi-Fi 802.11WLAN but is High on power, Bluetooth 802.15.1 WPAN, ZIGBEE 802.15.4 Low Power WPAN [24].	RFID Protocols (Air-Interface) (IOS-x), LF, UHF, NFC, etc. [25].
Communication and Connection	Multi-hop to increase strength of signal, and WSNs can link to each other (Ad hoc) [24].	Single-hub and there isn't communication between RFIDs [21].
Mobility	Usually Static	Usually Mobile
Programmability	Supported	No Support
Deployment	Random or Fixed	Attached to or embedded in objects
Power and energy	Battery for sensors, and power supply for Sink Node [20].	No need of battery for Passive Tag, but powered-battery is needed for Active Tag, and power supply for Reader. [26].
Usability	Car, phone, clothes, electronic devices, etc.	Card, bracelet, phone, car, etc.
Limitation	Range, Architecture, Massively heterogeneous, Real-Time Apps, Privacy & Security, etc. [23].	Power, Communications, Cost of Active Type, Security & Privacy, etc. [21]

extension of Cloud to the edge of a network with smaller memory and processing power—it can be any device with an ability to do some computing and storage. Therefore, unlike Clouds, Fog is close to the end-user and supports the distributed computing model. More information about Fog is available in [40, 41]. Here we provide a comparison between Fog and Cloud.

(1) Fog can be any device with the ability to compute and cache data in addition to network, whereas Cloud is a set of servers.

(2) Fog supports time-sensitive applications like the ones dealing with emergencies, where usage of Fog reduces latency, increases response speed, and decreases traffic on the links, which are difficult to achieve with Clouds.

(3) The Fog Node is close to the end-user, which makes it suitable for filtering and processing data before sending it to the Cloud, resulting in a reduction of the overhead processing on the Cloud as well as traffic on the links and network. Fog can process images and detect features and then send these features instead of images to the Cloud. The use of Clouds is to store entire data and apply big-data applications to explore unknown associations within the data.

(4) Fog may also implement some access restrictions on data before sending it to Cloud, which increases the security, especially for IoT objects not having enough memory and processing power to perform similar tasks.

(5) Fog can be used as smart traffic to support mobility apps and manage crowds better than Cloud.

(6) Fog increases the availability service as compared to Cloud, which is very beneficial in crowd management.

(7) Fog nodes can be spread intensely to completely cover any area (like the areas of intense crowding in Hajj

Table 3: Tools and technologies for CCHMS.

Name	Usages in our System
WSNs	Monitor and sense important indicators about environment based on some conditions like the level of oxygen, pressure, pollution, heat, which are very important managing health and crowd conditions.
RFID Tags	Detection of location and identity of objects in local area, which is critical in calculating the count of participants in specific area, as well as for searching objects in the crowd.
Drones	Observe crowd vertically from overhead positions in all directions. Additionally, we can use them to promptly deliver some material and medical supplies in areas where ground transportation is not feasible [27, 28].
Airships	Deploy them if GPS, Cellular network and Internet Connection do not work from ground [29].
IP Cameras	Take photo frames for headcount of segments of a crowd and then send them for processor as an input for our stampede detection algorithm included in this article [30].
Smart phone and devices	Use them instead of WSN, RFID or Alarm where Cellular/Wi-Fi connection is available. Also, use them for other applications provided in the article [31].
Digital Street	Turn venerable areas into a screen of LEDs to make it a tool for alerting and controlling crowds [32].
GPS	For finding global location of objects and tracking
FOG	Caching and expediting processing of the data generated by various tools and devices included in this table. If were to use cloud instead, there would be latency in communicating, transferring data, and decision-making. Latency in a sensitive system like ours can lead to the system failure.
Cloud	Storing and processing historical data into a data warehouse for the purpose of data mining and big data analytics.

or Kumbh Mela). In other words, Fog supports the distributed model of computing better than a Cloud.

(8) Unlike Clouds, a Fog Node has limited resources, and hence the need for Clouds persists.

(9) Fog supports awareness location, which is not achievable in Clouds.

(10) Users can have full control on Fog, whereas in Clouds there are three different control models, namely, SaaS, PaaS, and IaaS.

To make the best use of the Fog technology, the crowded area needs to be divided into many cells, each containing Fog to enable connection to all objects in the given cell. In this way, Fog can calculate the number of participants (usually with tags) in its cell and manage them by facilitating specific services. Fog's node in each area will feed the aggregate of the result of processing of data in a given cell to the Core Fog, which could also perform some operations before sending the data to the Cloud. Data in the Cloud can be mined and/or big-data analysis can be performed. In case of an emergency, Fog can directly take decisions without latency [42, 43].

3. Merit and Integration of Technologies for the Proposed System

Many of the sensors, wireless devices, and new technologies available today are helping to manage many businesses and real-life operations. Table 3 explains the usefulness of the technologies, which we use in our systems [31].

In Figure 1, we have integrated some of the tools and technologies mentioned in Table 3 into a Fog architecture, which forms an integral and important part of our proposed Crowd Control and Management System. We have divided the crowd-assembly area to a number of cells, each of them with many IP-cameras, RFID, WSN, and Smart Devices for collecting data. Then the data would be processed locally in the Fog Node, which would be available in each cell to make a decision without latency. The results from Fogs would then be sent to a Core Fog Node for rigorous processing and organizing. Finally, all data would be stored in a data warehouse in the Cloud for mining and analysis [44].

4. Algorithm for Stampede Detection

Here we provide an algorithm based on image processing for detecting and preventing stampedes. This is an integral part of the proposed system. A stampede occurs when many people simultaneously lose grip under their feet, which usually happens when a sizable body of a crowd stops moving while the others keep on moving towards them. To stop its occurrence, crowd monitoring technology or field observers should identify abnormal crowd behaviour as soon as it is noticed. We focus on detecting the likelihood of a stampede due to a sudden change in the number of heads in a segment of a crowd and provide an algorithm for that purpose. There are already many methods/approaches to calculate

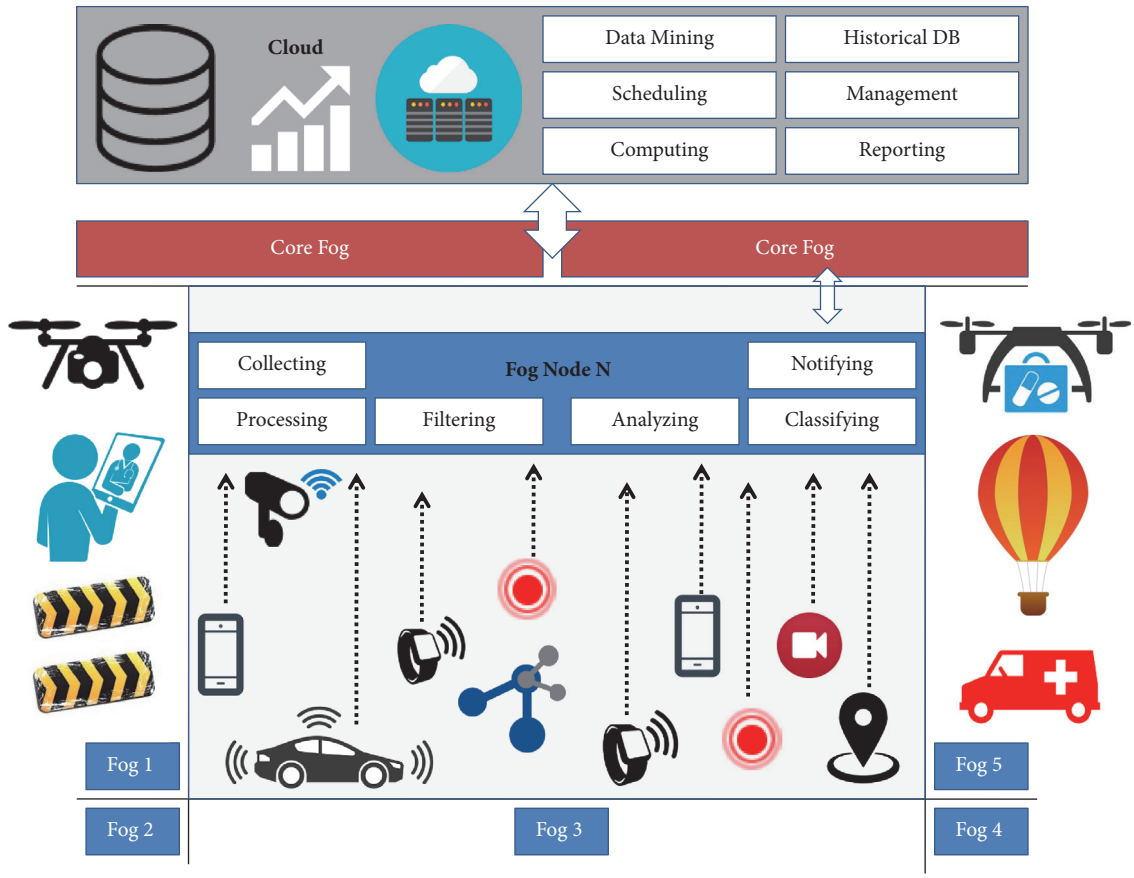

Figure 1: Integration the technologies in the proposed system.

the number of heads in an image; some of them are listed below.

(i) Rely only on the number of objects in the image [45, 46].

(ii) Rely on the colour and number of objects as in Viola Jones Algorithm [47].

(iii) Rely on motion to separate the background from objects and then estimate the number of objects according to the number of pixels. Here gradient orientation can be used, block matching, or histogram orientation and colour distribution [48, 49].

(iv) Rely on the edge detection or skeleton (Thinning) and then number of pixels [47].

(v) Detect the deviation and then use clustering, regression, training techniques as neural network to estimate the number [50, 51].

(vi) Rely on texture feature to estimate the density [48].

(vii) Convert the image from special domain to frequency domain by many transformation functions (HAAR, DCT, DFT, HOUGH, HOG, SIFT, SVM, GABOR, EIGEN, etc.), and then apply estimate or training to find the number of objects [52, 53].

4.1. Proposed Algorithm for Stampede Detection (ASD). Proposed algorithm (ASD) relies on integration among the number of objects, edge detection, and Hough transformation to insure higher reliability when sending notification to human observer to take suitable decision and action promptly. ASD processes images to find the number of heads; the images are continually transmitted by the IP-Camera to Fog, which saves them and records the number of heads in the cache. The process is repeated to find and record the number of heads in successive images, which are compared. If the deference in the number of head-count exceeds the threshold, the observer would be notified. As a result, security personnel on the ground would be alerted to either make the crowd thinner or break into different sections and zones. While the crowd was in motion, the number of participants could be reduced by cropping a crowd-rectangle from the middle. Other ways of crowd downsizing could also be employed.

4.2. Steps of ASD for Finding Number of Heads. As mentioned before, here we provide steps to find the number of heads.

(1) X = imread(Image.png'); // Read Image

(2) X1=rgb2gray(X); // Convert Image to Gray

(3) Threshold_Head_Size=1800; //Can be changed according to the camera position and far.

(4) X2=edge(X1,'canny',0.3); // Edge Detection

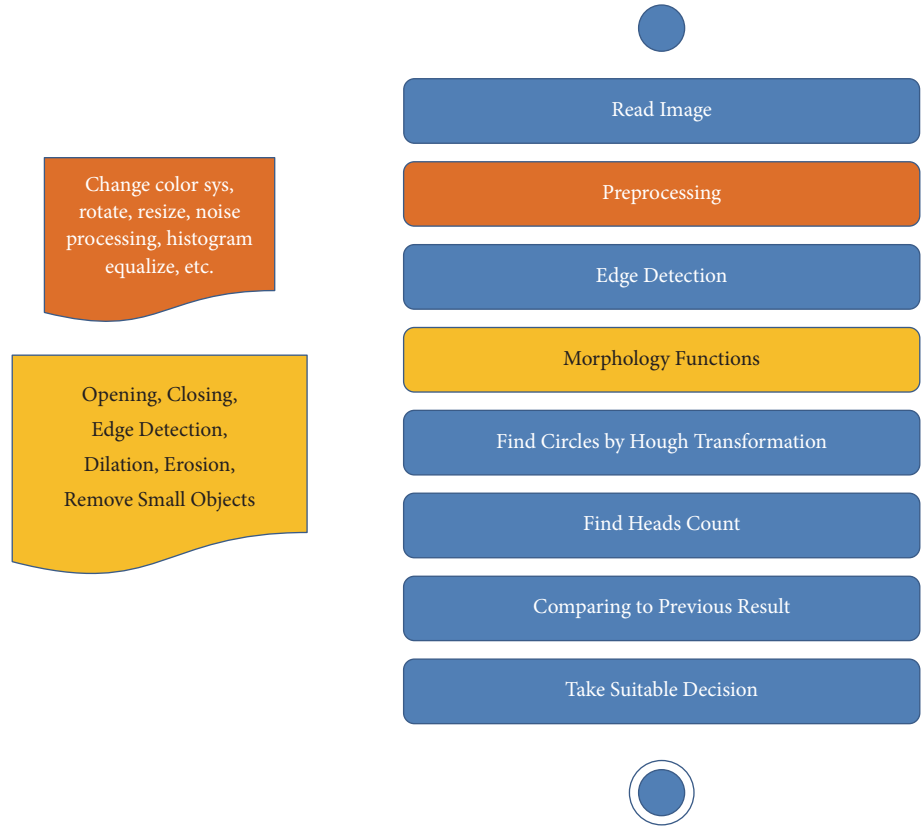

Figure 2: Flow diagram of ASD.

(5) X3=bwmorph(x2,'close',1); // Morphology Processing

(6) X4=1-x3; // Reverse Colour

(7) X5=bwmorph(X4,'open',inf); // Morphology Processing to separate the objects (heads)

(8) X6 = bwareaopen(X5,Threshold); // Remove objects with size lesser than the threshold

(9) // Find Circles Functions and its Attributes

(10) [centers, radii] =

imfindcircles(X1,[Min Max], 'ObjectPolarity', 'bright', 'Sensitivity', 0.95, 'EdgeThreshold',0.1, 'Method', 'TwoStage');

// 'Min & Max' would determine the radius of the head according to camera position.

// 'Object Polarity' can be dark or bright according to light condition

// If 'Sensitivity' value lies in [0 1]; if it was smaller, the sensitivity would be lesser.

// If 'EdgeThreshold' value lies in [0 1], it would determine the degree of difference among object boundaries.

// 'Method' can be Two-Stage (Hough Transformation) of Phase-Code (Atherton)

(11) H = VISCIRCLES (centres, radii); // This is for drawing circles

(12) Count=size(centers,1); // This is to find head-count

(13) Title (num2str(count));// This is to print the head-count

(14) Calculate the "Deference" between current 'Count' and previous frame 'P-Count'

(15) If 'Deference' > Threshold ⟶ send alert.

(16) Save last 'Count'

(17) Repeat all steps.

4.3. Flow Diagram for ASD. Figure 2 shows a flow diagram of ASD

It is worth mentioning that the proposed system does not rely on ASD alone. There are other inbuilt mechanisms to detect stampedes, which will be discussed in the next section.

5. Proposed Crowd Control and Health Management System

Crowd management is a highly critical operation as it is linked to the safety of human beings. An oversized crowd could be very difficult to manage. Technology can play a significant and crucial role in controlling and managing crowds and, in particular, alerting about an ensuing stampede. Here we present a framework for Crowd Control and Health Management System (CCHMS), which has two subsystems: Disaster Control and Management System (DCMS) and

Healthcare Management System (HMS). As part of DCMS, we propose a number of ways and techniques for predicting a stampede and other disasters before they occur. For HMS, we propose integrated mobile applications with a number of modules for dealing with health issues in crowds. Our techniques in CCHMS rely on coordination and integration of different technologies and tools including Cloud Computing, Fog Computing, Smart Phone Application, Smart Digital Street, RFID, WSNs, GPS, IP-Cameras, Sound Alarm, and Flasher/Light Alarm. Integration of these technologies would enhance efficiency, reliability, and success in providing life-saving applications [54].

5.1. Disaster Control and Management System (DCMS). In order to manage crowds successfully, cooperation and education among all stakeholders are highly desirable. In particular, participants must obey the signals and commands; otherwise, the system would not attain its desired goals. Another factor critical to a stampede (or another disaster) aversion is the response time. Here we provide a detailed description of layers of DCMS.

5.1.1. Overview of DCMS. We divide areas and places of crowd build-ups into a number of cells and distribute crowd data from the sensor networks continuously to many computing (Fog) nodes, enabling each of them for speed processing and decision taking. Each set of Fog nodes is connected to the core of the Fogs to control the integration and cooperation between them and to ensure data processing before relaying the information to Cloud, where an extensive data analysis for the detection of new knowledge is performed. The new knowledge will be very beneficial for the prediction of future health and crowd cases and preparing advance solutions to deal with the aftermath of a disaster if it occurs.

5.1.2. Layer 1: Collecting/Sensing Data. Described below are different types of tools for collecting data in each cell of the crowded area.

(i) Attach RFID-Passive (low-cost) tags (cards/bracelets) to the body parts (wrist, waist) of individuals of the crowd for determining their whereabouts and the size of the crowd in each and any moment of time. Tag Readers can be in the Fog Node, or many Readers can be distributed in the cell and the Host will be in the Fog. The Identity can be used to get more details and information about each individual from the Cloud based central database. In situations where GPS and Cellular network do not work, airships may be used. In cases where other methods of reading RFID and WSNs are not usable, drones [27] may be effective to use.

(ii) Deploy different purpose WSNs in each cell for sensing parameters, conditions, and situation, namely, for example, pollution, temperature, and pressure sensors, which provide important information about environment of cell and play a vital role in alerting about a potential danger of a disaster. Moreover, the data sensed by them can be stored and analysed for future purposes.

(iii) Use IP-Cameras to take high-resolution images of the crowd in each cell and then process these images in Fog to detect the likelihood of any accident or some other disaster without latency or delay. In addition, it would lighten up the size of data transferred on links and the data storage in the Cloud because Fog nodes would only send the features of each image instead of their parts. The stampede detection algorithm, provided in the next section, would rely on matching the features of new images with previously stored features. Extensive data processing on Cloud can enhance and increase the accuracy of features of each case. We can also use images to analyse the mood and emotions of the people. In case of apparent signs of sickness or distress, remedial action can be taken [55].

(iv) Use Mobile Applications (Android and IOS), which should be installed on participant Smart Phones to enable them to notify the management by a simple click about any eminent danger on the location and time of their being there. In this manner, each participant would act as a sensor.

(v) Collect information from social media like Twitter, which is considered as one of the fastest ports for news nowadays. However, because of the size, the management would need to perform big-data analytics for processing social media data or environment to expedite the notification of information as quickly as possible [56].

5.1.3. Layer 2: Take Decision. DCMS uses Fog Computing nodes to improve the efficiency of processing to meet the critical requirement of the system and analyses the collected data without latency. In addition, it uses Core Fog for the organization and integration of the cells and so makes them more flexible and faster in dealing with emergency situations.

5.1.4. Layer 3: Notify Crowd. We propose a number of tools (hardware/software) for notifying and alerting the participants, whose details are as follows:

(i) Create Digital Streets in the areas prone to disasters, which are considered very important for controlling and notifying crowds in critical situations, which no one has used so far. If an alarming situation was detected, Fog would send an alert to Smart Streets to light up the ground by red colour as a result of which the participants would sense the danger and stop moving any further. Moreover, Digital Street can guide to a safer way of movement in the same way as in the case of aeroplanes directing passengers in their movement.

(ii) Participant Smart Phones would be registered and used to send alerts from the management.

(iii) Voice/Light Alarm, Announcement, and other traditional methods, if deemed safer, can be used to notify and guide the crowd.

(iv) Drones can be used to send some urgent medical supplies to an event, which may have access problems by other means.

(v) An E-health services application made for Android/iOS can be used to guide participants to take safety precautions and to provide general guidance.

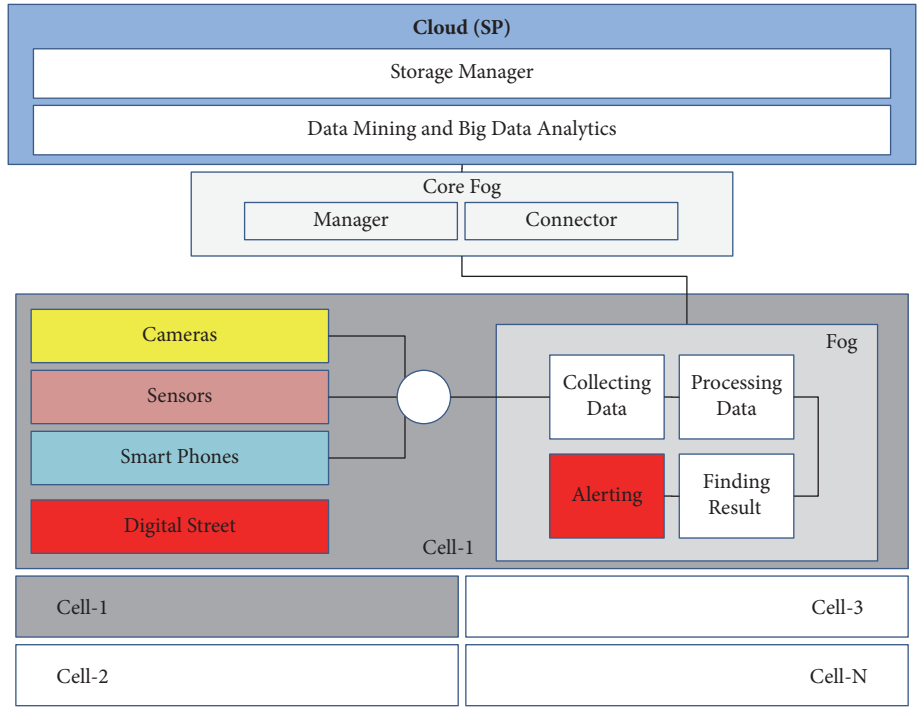

Figure 3: Architecture of DCMS.

5.1.5. Layer 4: Cloud Computing. Data received from sensors and other management tools can be collected, stored, cleaned, refined, and analysed. All of this can take place on the Cloud (data center), where deep processing and mining can detect new relationships of data to provide comprehensive knowledge for future management of the same or similar events to minimize the chances of disasters.

Figure 3 provides a framework of DCMS. As discussed earlier, the success of this or any other system would depend on the cooperation between participants and management. In particular, participants must promptly act on alerts and notifications and follow the instructions.

We are aware that the proposed system may at times encroach into participants' privacy. We endeavour to return to the issue of preservation of privacy in the future.

5.2. Proposed Healthcare Management System (HMS). The health and wellbeing of people in crowds should not be compromised. Management should use a comprehensively developed healthcare system, which makes use of the best available technology. Regular and recurring crowded events must capture and store medical information about their participants. If people with contagious viruses and diseases are allowed to participate, they must be isolated and properly managed. Here, we provide a design of HMS, a comprehensive health management system, built on several mobile application subsystems. Figure 4 exhibits a screen of mobile apps of this system, as they would appear on the mobile devices of the participants. The mobile apps can also be exhibited as icons to help those with reading difficulties. The system can also be multilingual [57, 58]. A brief description of various subsystems or mobile applications follows.

(i) **Poison System**: this mobile application aims to tell participants about the presence of poisons in artefacts, alert about issues or conditions that can spread poisons, and guidelines to avoid situations of contamination.

(ii) **Drug System**: it is a search engine to suggest general-purpose drugs and their usage and to list forbidden and unsafe drugs with their side effects.

(iii) **Food System**: it provides beneficial information about unhealthy foods; especially the ones that can quickly become contaminated in crowding and environment conditions.

(iv) **Survey System**: this will send a questionnaire every day to find people with illnesses and to direct them to follow a course of action.

(v) **Relief System**: This system would empower participants to provide First Aid in the case of an emergency. The system will have videos on key aspects of healthcare, which can be played at times of need until the medical relief arrives.

(vi) **E-File System**: this is for users to record some indicators about their health, such as heart rate, pressure, and sugar, to help the government to capture real statistical health data to enhance and improve the level of services.

(vii) **Advices System**: this system can frequently provide health advice and tips to the participants.

(viii) **Medical Appointment System**: this system would enable patients to make online booking for appointment with a health center.

Figure 4: Proposed application and services for crowd control and management system.

(ix) **Question (Consultation) System**: this system enables users to ask for electronic consultations from physicians with selected specialists.

(x) **Monitor System**: this system uses GPS and Location Based Servers for tracking old and weak persons in order to take fast action.

(xi) **Health Centers**: this system helps users to search for the nearest health centers or pharmacies by name, location, and other details, in conjunction with Google maps.

(xii) **Paths System**: this system provides information about the paths that have less traffic and less pollution for some participants with conditions of breathing and other issues. In reality, Google maps and GPS cannot scan all areas of some crowded events.

(xiii) **Blood Donation System**: this system will send a request for blood donations and would enable participants to opt for it. The donors can provide personal details including the blood group and their locations. Based on the details, the system can organize blood collection and can call them to any position by one click.

(xiv) **Autism System**: this system provides videos and beneficial links for families that have a child with autism, in addition to providing some specialised mobile games for this group of children.

(xv) **Drone System**: this system would be used for keeping an account of drones used for supplying medical supplies to obscure locations.

(xvi) **Alerts**: This system would send alerts and notifications to participants to manage their movement and behaviours.

(xvii) **Terrorist**: This system is included in the Alerts App to get or send notification about any terror case, to protect people and request police assistance.

6. Implementation and Results

Here we shall present the results of implementations of various constituents of CCHMS.

6.1. DCMS Implementation and Results. In Figure 5, we provide results of ASD applied to a virtual image, with five successive frames. We have numbered these frames F(1-3), F(2-4), F(3-5), F(4-6), and F(5-End). After counting heads in each frame, we did not find any significant difference.

Next, we apply the same method on real frames and obtain the same head-count as shown in Figure 6. In Figure 7, we depict the results of successive steps of ASD, first on a picture without making any change to it and then that on the same picture after making some manual alteration. A remarkable difference can be seen in the results. Figure 8 demonstrates the accuracy of the head-count by ASD, applied on real and virtual images. We notice that the accuracy of head-count by ASD was more than 94% in most of the cases.

6.2. Superiority of ASD. In order to obtain better results, we combine elements of some of the existing approaches in ASD. Description of the function of four of these approaches

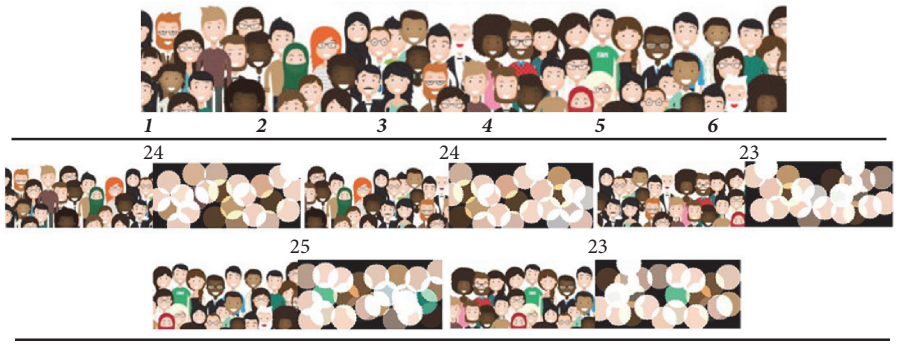

Figure 5: Head-count in frames of a virtual image.

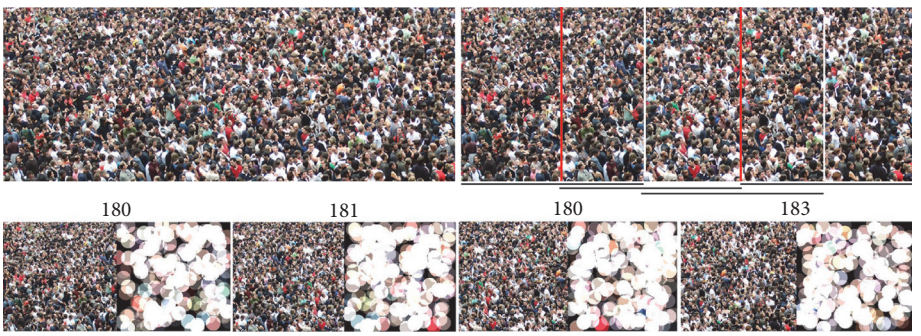

Figure 6: Head-count in frames of a real image.

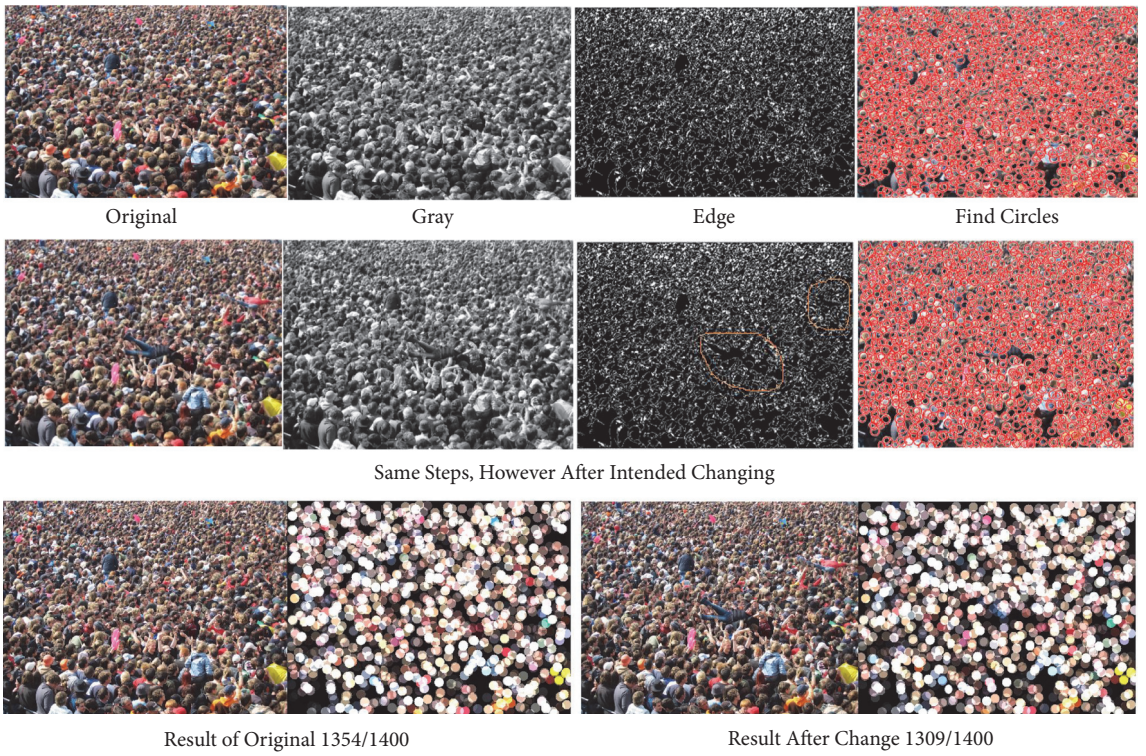

Figure 7: Head-count in frames of unaltered and altered images.

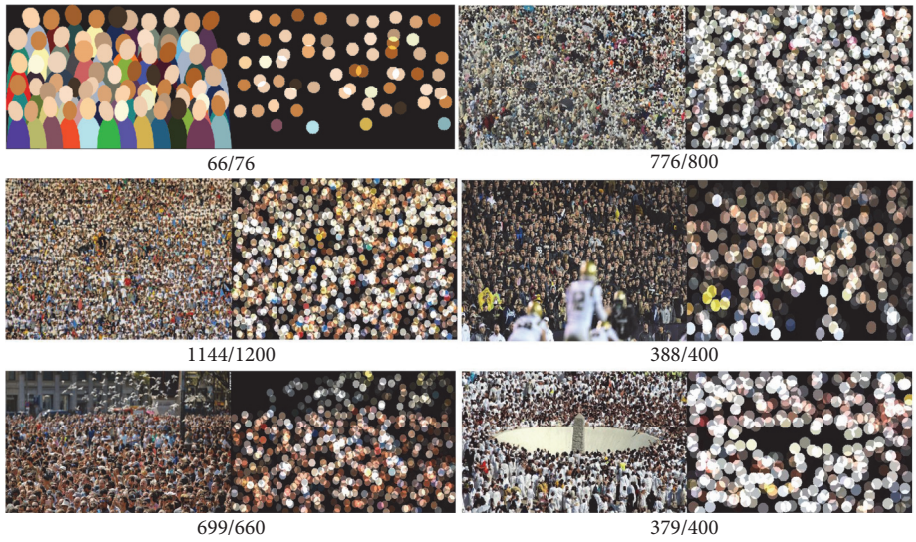

Figure 8: Accuracy of head-count in ASD.

Table 4: Accuracy of headcount approaches.

ASD (Finding Cycle)	Number of Objects (Using Morphology)	Fourier & Estimation	SHIF & Estimation	Motion & Separate background	Cluster & Estimation
94%	85%	60%	70%	92%	93%

follows. The first of these approaches, to be identified as "Number of Objects," depends on the count of objects. This approach uses morphology to separate the objects and converts them into black and white images. Then morphology filters separate the objects and find their sum by dividing the size of each object on the threshold [45–47]. Another approach uses transformation filters like "Fourier & Estimation" or "SHIF & Estimation." Once a transformation filter is applied, the image is converted into a frequency image. In the frequency image, white pixels are used to estimate the number of heads in the new frequency image [48]. The third approach, known as "Motion & Separate Background" uses an earlier approach, like Number of Objects, to enhance the result by isolating the background of the image from real and moving objects [49]. Finally, an approach known as Cluster & Estimation divides the image into many sections and then estimates the count of objects in each section with different factors of density [50]. Table 4 and Figure 9 provide simulation results of ASD compared with the four approaches that have been described.

Superiority of ASD is evident from its implementation on virtual and real images. Moreover, ASD, unlike other approaches, relies on the difference of head counts between successive frames of images to determine abnormal crowd behaviour. The importance of head-count difference can be understood by the following example. Suppose ASD gives an inaccurate count C1 for a frame F1, the head-count C2 in the next frame F2 would approximately be the same. Thus, the difference between C1 and C2 would be negligible and hence would not affect the overall result unless a sudden unusual event occurs. If an unusual event does occur, the difference between C1 and C2 will be significant, and the difference between C2 and C3 of another frame F3 would also be significant.

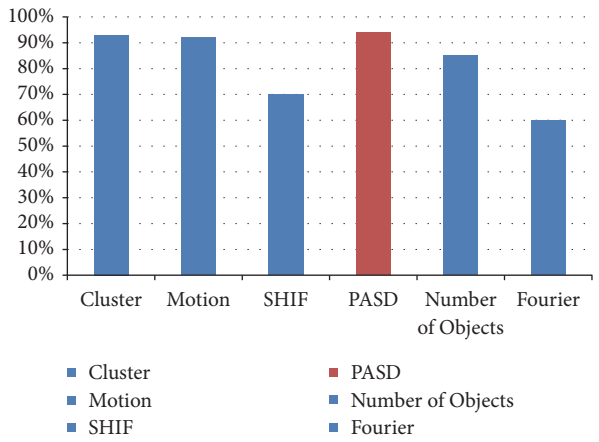

Figure 9: Accuracy comparison.

6.3. Implementation and Results of HMS. Here we provide implementation of four applications (subsystems) of HMS, namely, emergency, blood donor, complaints and alerts, and turning mobile phone to act as a sensor device. Figure 10 depicts an interface of these applications on the mobile device, and Figure 11 shows the server and admin side of these applications.

7. Applications of CCHMS in Real-Life Cases

Here we provide some cases where CCHMS can be successfully used.

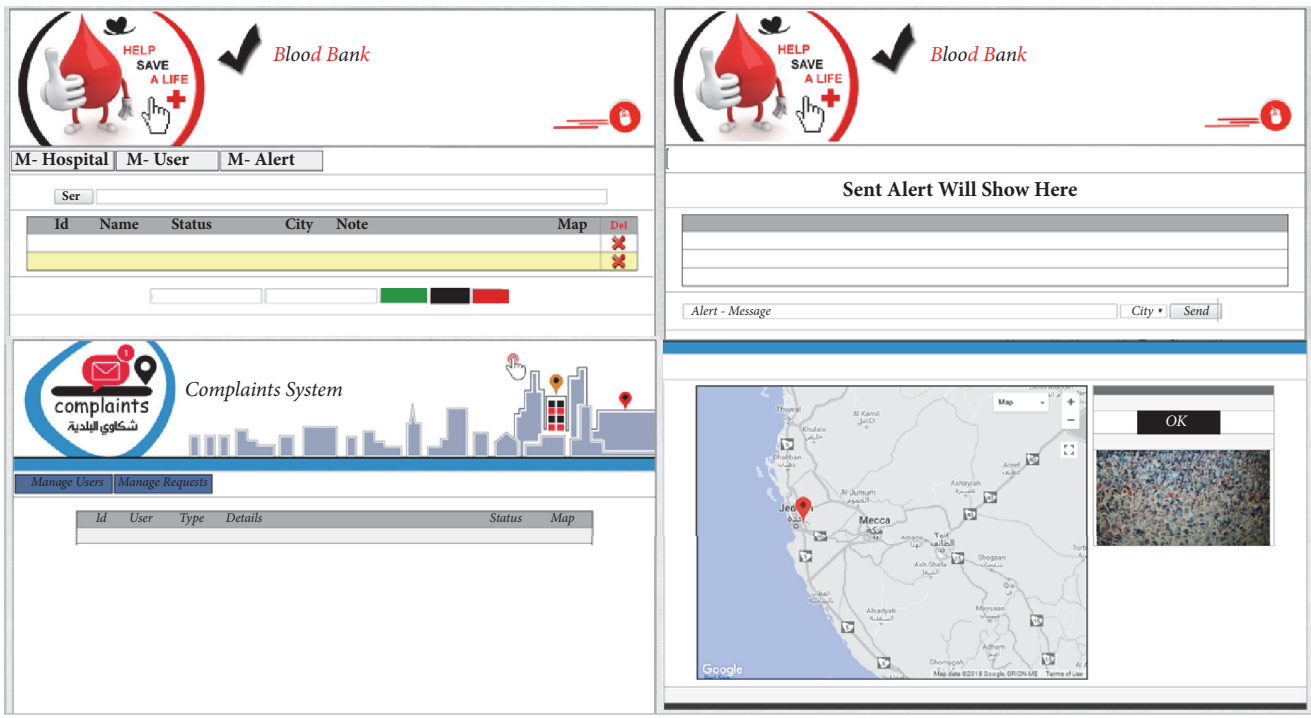

Figure 10: Mobile apps interface.

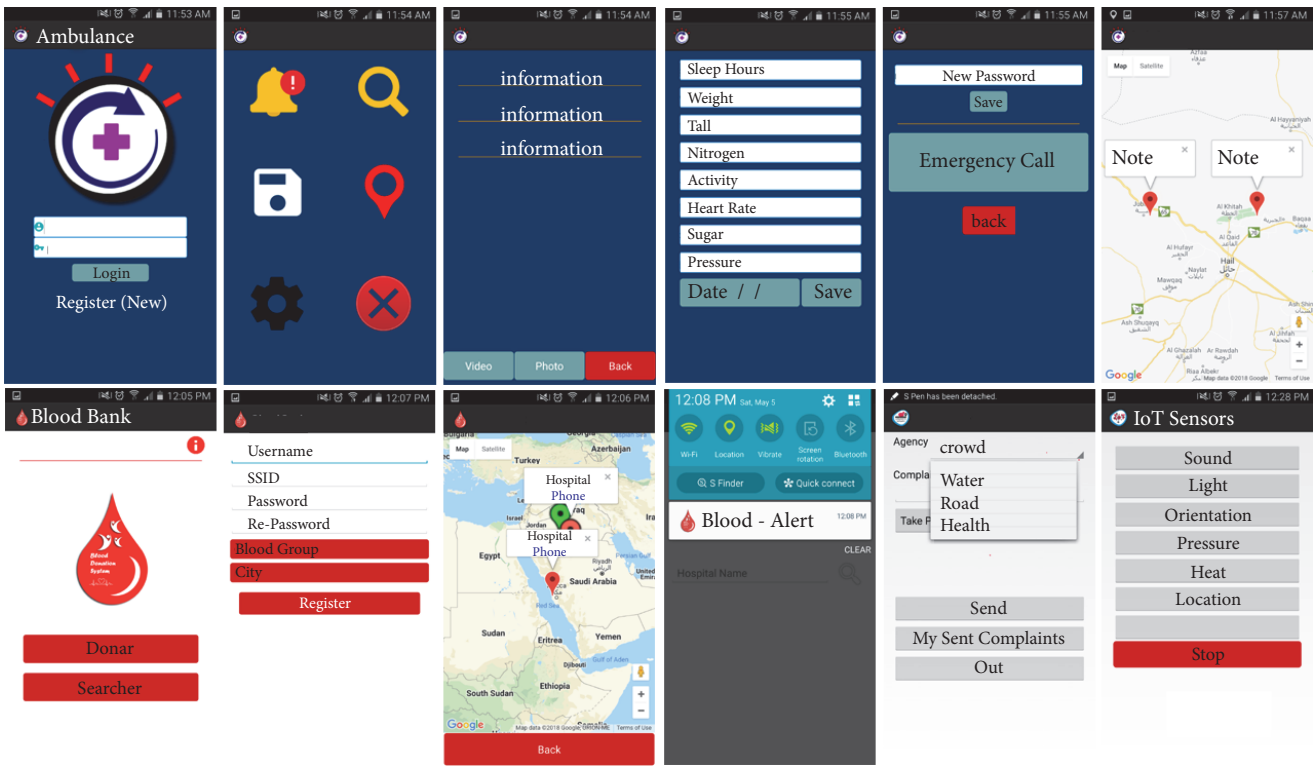

Figure 11: Admin view of mobile applications.

7.1. The Case of Hajj. Hajj [12–15, 59] is an annual pilgrimage in which more than two million people from different parts of the world travel to Mecca in Saudi Arabia. For several days, the pilgrims are required to travel en masse to different places of the Hajj precinct with very tight schedules. These movements in the past have witnessed several stampedes, resulting in thousands of deaths. In order to perform Hajj, participants must furnish personal and medical information months before the journey. This allows Hajj management to capture data of pilgrims. Hajj is a perfect case for using CCHMS as places of gathering of pilgrims and disaster-prone areas are well known, which can be conveniently divided into cells. A critical requirement of Step (2) for attaching RFID tags to the pilgrim bodies can be easily achieved, where Fog Node can read data from the RFID. In some places wireless sensor networks can be installed whereas in other places GPS can be used. Different purpose WSNs can be easily deployed in the majority of areas with an expectation of open spaces of intense crowding. As the mobile devices would have been registered in the central database, pilgrims would be able to access Hajj Mobile Apps easily.

Creation of Digital Streets in selected walkways, as in Step (3), can be achieved easily. As for Step (4), sensors' data with that of the pilgrims can be stored in a Cloud for mining and analysing. Hajj is a perfect case for using healthcare applications of HMS. Pilgrims can download these apps on their mobile devices.

7.2. The Case of Kumbh Mela. Kumbh Mela [12, 17] takes place every three years in one of the four Indian cities, namely, Allahabad, Haridwar, Ujjan, and Nasik, all situated along one or the other river. It attracts several millions of participants over a period of eight weeks. Unlike Hajj, the pilgrims mostly come from India and do not require prior permission, and hence there is no mechanism for collecting personal data of the pilgrims. Therefore, layers of CCHMS dependent on personal data, like those requiring medical and communication media, will not work. However, many other tasks and applications, including stampede detection algorithm, would work. If the crowding of the Kumbh Mela is to be properly managed, the management should introduce a mechanism for data collection.

7.3. Case of Irregular Crowds. There is no way of collecting personal data of participants of irregular and spontaneous crowds. As in the case of Kumbh Mela, CCHMS will be applicable in all those areas that do not require personal data.

8. Conclusions, Suggestions, Limitations, and Future Research

The framework within the CCHMS takes into account the nature of crowding and has built-in mechanisms to deal with them with the help of sensor and mobile technology. When applying CCHMS in real crowds, it is expected that the system would require some minor operational changes and adjustments. We believe that CCHMS can be adapted to manage crowded events around the globe. Analysis of stampedes in the last fifteen years reveals that the crowds in some of those events were neither contained nor controlled. Personal experience of the authors of this article affirms that participants generally lack education and training of the usage of facilities and proper performance of various functions of the event. It is suggested that event participants must be provided with adequate education and training with simulations. Out of bounds crowds are very difficult to manage and hence it is the responsibility of the relevant authorities to limit the size of the crowd. Providing adequate facilities for managing crowded events would be very helpful in reducing the chances of disasters.

Going forwards, we would like to conduct a proof of concept for the layers in CCHMS while utilizing the required technology. This is however a difficult undertaking as most of the crowded events are organized and managed by the state. It is not feasible to access data or test and validate our algorithm for detecting and preventing stampedes from occurring, as it would require a lot of resources, permissions, and cooperation from various stakeholders of the event. For example, organization and management of Hajj involves interior, Hajj, foreign, and health ministries, as well as other historical stakeholders of the Kingdom of Saudi Arabia. The authors are making efforts to propose CCHMS to the stakeholders of the Hajj management for the purpose of adapting and implementing it in a phased manner.

If in the future we gain access to data for Hajj or other crowded event/s, we would trial the proposed Mobile Applications of HMS. If the access to Hajj data was granted, we would mine historical data which we believe would be very beneficial in organizing and managing future events. Our future research would also focus on privacy of security of participants' data and prevention and management of terror attacks as part of CCHMS.

Data Availability

There is no data used to support this study.

Conflicts of Interest

The authors declare that they have no conflicts of interest.

References

[1] M. R. L. M. de Almeida, *Human Stampedes: A Scoping Review*, Department of Public Health Science, Karolinska Institutet, 2016.

[2] L. Soomaroo and V. Murray, "Disasters at Mass Gatherings: Lessons from History," *PLoS Currents*, 2012.

[3] K. M. Ngai, F. M. Burkle Jr., A. Hsu, and E. B. Hsu, "Human stampedes: A systematic review of historical and peer-reviewed sources," *Disaster Medicine and Public Health Preparedness*, vol. 3, no. 4, pp. 191–195, 2009.

[4] J. R. Spengler, E. D. Ervin, J. S. Towner, P. E. Rollin, and S. T. Nichol, "Perspectives on west africa ebola virus disease outbreak, 2013–2016," *Emerging Infectious Diseases*, vol. 22, no. 6, pp. 956–963, 2016.

[5] S. E. Rutstein, J. Ananworanich, S. Fidler et al., "Clinical and public health implications of acute and early HIV detection and

treatment: a scoping review," *Journal of the International AIDS Society*, vol. 20, no. 1, p. 21579, 2017.

[6] O. Rajoura, R. Roy, P. Agarwal, and A. Kannan, "A study of the swine flu (H1N1) epidemic among health care providers of a medical college hospital of Delhi," *Indian Journal of Community Medicine*, vol. 36, no. 3, pp. 187–190, 2011.

[7] S. Ghebrehewet, P. Macpherson, and A. Ho, "Influenza," *BMJ*, vol. 355, Article ID i6258, 2016.

[8] M. D. Christian, S. M. Poutanen, M. R. Loutfy, M. P. Muller, and D. E. Low, "Severe acute respiratory syndrome," *Clinical Infectious Diseases*, vol. 38, no. 10, pp. 1420–1427, 2004.

[9] H. A. Mohd, J. A. Al-Tawfiq, and Z. A. Memish, "Middle East Respiratory Syndrome Coronavirus (MERS-CoV) origin and animal reservoir," *Virology Journal*, vol. 13, no. 1, 2016.

[10] S. J. Rajakaruna, W. Liu, Y. Ding, and G. Cao, "Strategy and technology to prevent hospital-acquired infections: Lessons from SARS, Ebola, and MERS in Asia and West Africa," *Military Medical Research*, vol. 4, no. 1, 2017.

[11] T. Sandler, "The analytical study of terrorism," *Journal of Peace Research*, vol. 51, no. 2, pp. 257–271, 2014.

[12] Y. Mohammad and Y. Ades, "Crowd Management with RFID & Wireless Technologies," in *Proceedings of the First International Conference on Networks & Communications, IEEE Computer Society*, Washington, DC, USA, 2009.

[13] D. Clingingsmith, A. I. Khwaja, and M. Kremer, "Estimating the impact of the Hajj: Religion and tolerance in Islam's global gathering," *The Quarterly Journal of Economics*, vol. 124, no. 3, pp. 1133–1170, 2009.

[14] M. Yamin, "Secure and Healthy Hajj Management: A Technological Overview," *American Academic & Scholarly Research Journal*, vol. 7, no. 3, pp. 195–202, 2015.

[15] M. Yamin, M. Mohammadian, X. Huang, and D. Sharma, "Health Management in Crowded Events: Hajj and Kumbh," *BIJIT - BVICAM's International Journal of Information Technology*, vol. 7, no. 1, pp. 791–794, 2015.

[16] T. Khanna, J. Leaning, J. Macombe et al., *Kumbh Mela: Mapping the Ephemeral Mega City*, Harward University, South Asia Institute, Hatje Cantz, 2015.

[17] S. David and N. Roy, "Public health perspectives from the biggest human mass gathering on earth: Kumbh Mela, India," *International Journal of Infectious Diseases*, vol. 47, pp. 42–45, 2016.

[18] M. Yamin, X. Huang, and D. Sharma, "Wireless Sensor Technology and Crowd Management," *Journal of Cooperation among University, Research and Industrial Enterprises*, vol. 2, no. 1, 2009.

[19] V. Rajaraman, "Radio frequency identification," *Resonance (Indian Academy of Sciences)*, vol. 22, no. 6, pp. 549–575, 2017.

[20] N. Sabor, S. Sasaki, M. Abo-Zahhad, and S. M. Ahmed, "A comprehensive survey on hierarchical-based routing protocols for mobile wireless sensor networks: Review, taxonomy, and future directions," *Wireless Communications and Mobile Computing*, vol. 2017, 2017.

[21] Z. Chen, A. Liu, Z. Li, Y.-J. Choi, H. Sekiya, and J. Li, "Energy-Efficient Broadcasting Scheme for Smart Industrial Wireless Sensor Networks," *Mobile Information Systems*, vol. 2017, Article ID 7538190, 17 pages, 2017.

[22] A. Khattab, Z. Jeddi, E. Amini, and M. Bayoumi, "Introduction to RFID," in *RFID Security*, Analog Circuits and Signal Processing, pp. 3–26, Springer International Publishing, Cham, 2017.

[23] J. Lee, B. Shah, G. Pau, J. Prieto, and K.-I. Kim, "Real-Time Communication in Wireless Sensor Networks," *Wireless Communications and Mobile Computing*, vol. 2018, Article ID 9612631, 2 pages, 2018.

[24] S. Khan, J. Lloret, H. Song, and Q. Du, "QoS Based Cooperative Communications and Security Mechanisms for Ad Hoc Sensor Networks," *Journal of Sensors*, vol. 2017, Article ID 9768421, 2 pages, 2017.

[25] X. Chen, A. Liu, Z. Wei, L. Ukkonen, and J. Virkki, "Experimental Study on Strain Reliability of Embroidered Passive UHF RFID Textile Tag Antennas and Interconnections," *Journal of Engineering*, vol. 2017, Article ID 8493405, 7 pages, 2017.

[26] J. Zhang, G. Tian, A. Marindra, A. Sunny, and A. Zhao, "A review of passive RFID tag antenna-based sensors and systems for structural health monitoring applications," *Sensors*, vol. 17, no. 2, article 265, 2017.

[27] E. Vattapparamban, I. Güvenç, A. I. Yurekli, K. Akkaya, and S. Uluağaç, "Drones for smart cities: Issues in cybersecurity, privacy, and public safety," in *Proceedings of the 12th IEEE International Wireless Communications and Mobile Computing Conference, IWCMC '16*, pp. 216–221, Cyprus, September 2016.

[28] H. Kong, F. Biocca, T. Lee, K. Park, and J. Rhee, "Effects of Human Connection through Social Drones and Perceived Safety," *Advances in Human Computer Interaction*, vol. 2018, Article ID 9280581, 5 pages, 2018.

[29] P. Sun, X. Wang, and W. Xie, "Centrifugal Blower of Stratospheric Airship," *IEEE Access*, vol. 6, pp. 10520–10529, 2018.

[30] B. Cusack and Z. Tian, "Evaluating IP surveillance camera vulnerabilities," in *Proceedings of the 15th Australian Information Security Management Conference*, C. Valli, Ed., pp. 25–32, Edith Cowan University, Perth, Western Australia, 2017.

[31] S. H. Chang and Z. R. Chen, "Protecting Mobile Crowd Sensing against Sybil Attacks Using Cloud Based Trust Management System," *Mobile Information Systems*, vol. 2016, Article ID 6506341, 10 pages, 2016.

[32] R. Fujdiak, P. Mlynek, J. Misurec, and J. Slacik, "Simulation of intelligent public light system in smart city," in *Progress in Electromagnetics Research Symposium-Spring (PIERS)*, pp. 2515–2519.

[33] U. S. M. Husein, "A phenomenological study of Arbaeen foot pilgrimage in Iraq," *Tourism Management Perspectives*, vol. 26, pp. 9–19, 2018.

[34] A. Kumar, H. Y. Shwe, K. J. Wong, and P. H. Chong, "Location-Based Routing Protocols for Wireless Sensor Networks: A Survey," *Journal of Wireless Sensor Network*, vol. 09, no. 01, pp. 25–72, 2017.

[35] A. Abuarqoub, M. Hammoudeh, B. Adebisi, S. Jabbar, A. Bounceur, and H. Al-Bashar, "Dynamic clustering and management of mobile wireless sensor networks," *Computer Networks*, vol. 117, pp. 62–75, 2017.

[36] O. O. FAGBOHUN, "Comparative studies on 3G,4G and 5G wireless technology," *IOSR Journal of Electronics and Communication Engineering*, vol. 9, no. 2, pp. 133–139, 2014.

[37] A. Das, P. Dash, and B. K. Mishra, "An Innovation Model for Smart Traffic Management System Using Internet of Things (IoT)," in *Cognitive Computing for Big Data Systems Over IoT*, vol. 14 of *Lecture Notes on Data Engineering and Communications Technologies*, pp. 355–370, Springer International Publishing, Cham, 2018.

[38] X. Hu, S. An, and J. Wang, "Taxi Drivers Operation Behavior and Passengers Demand Analysis Based on GPS Data," *Journal*

of Advanced Transportation, vol. 2018, Article ID 6197549, 11 pages, 2018.

[39] U. K. Vishwakarma and R. N. Shukla, "WSN and RFID: Diffrences and Integration," *International Journal of Advanced Research in Electronics and Communication Engineering (IJARECE)*, vol. 2, no. 9, pp. 778–780, 2013.

[40] Y. Fan, Q. Zhu, and Y. Liu, "Cloud/Fog Computing System Architecture and Key Technologies for South-North Water Transfer Project Safety," *Wireless Communications and Mobile Computing*, 2018.

[41] P. Mach and Z. Becvar, "Mobile Edge Computing: A Survey on Architecture and Computation Offloading," *IEEE Communications Surveys & Tutorials*, vol. 19, no. 3, pp. 1628–1656, 2017.

[42] A. V. Dastjerdi, H. Gupta, R. N. Calheiros, S. K. Ghosh, and R. Buyya, "Fog computing: Principles, architectures, and applications," https://arxiv.org/abs/1601.02752.

[43] R. Roman, J. Lopez, and M. Mambo, "Mobile edge computing, Fog et al.: A survey and analysis of security threats and challenges," *Future Generation Computer Systems*, vol. 78, no. 2, pp. 680–698, 2016.

[44] A. Manzoor, "RFID in Health Care-Building Smart Hospitals for Quality Healthcare," in *Health Care Delivery and Clinical Science: Concepts, Methodologies, Tools, and Applications*, pp. 839–867, IGI Global, 2018.

[45] J. Yoshida, Y. Fujino, and T. Sugiyama, "Image processing for capturing motions of crowd and its application to pedestrian-induced lateral vibration of a footbridge," *Shock and Vibration*, vol. 14, no. 4, pp. 251–260, 2007.

[46] R. C. Gonzalez, *Digital image processing*, Pearson, 4th edition, 2016.

[47] V. Dhinakaran and S. M. Sakthivel, *FPGA based System for crowd analysis using Computer vision algorithm*, 2013.

[48] B. Krausz and C. Bauckhage, "Automatic detection of dangerous motion behavior in human crowds," in *Proceedings of the 8th IEEE International Conference on Advanced Video and Signal Based Surveillance, AVSS '11*, pp. 224–229, Austria, September 2011.

[49] S. D. Khan, G. Vizzari, S. Bandini, and S. Basalamah, "Detecting dominant motion flows and people counting in high density crowds," *Journal of WSCG*, vol. 22, no. 1, pp. 21–30, 2014.

[50] M. Li, Z. Zhang, K. Huang, and T. Tan, "Estimating the number of people in crowded scenes by mid based foreground segmentation and head-shoulder detection in Pattern Recognition," in *Proceedings of the 19th International Conference (ICPR '08)*, pp. 1–4, 2008.

[51] Y. Zhang, F. Chang, N. Li, H. Liu, and Z. Gai, "Modified AlexNet for Dense Crowd Counting," *DEStech Transactions on Computer Science and Engineering*, 2017.

[52] S.-F. Lin, J.-Y. Chen, and H.-X. Chao, "Estimation of number of people in crowded scenes using perspective transformation," *IEEE Transactions on Systems, Man and Cybernetics, Part A: Systems and Humans*, vol. 31, no. 6, pp. 645–654, 2001.

[53] H. Idrees, I. Saleemi, C. Seibert, and M. Shah, "Multi-source Multi-scale Counting in Extremely Dense Crowd Images," in *Proceedings of the IEEE Conference on Computer Vision and Pattern Recognition (CVPR '13)*, pp. 2547–2554, Portland, OR, USA, June 2013.

[54] L. Catarinucci, D. de Donno, L. Mainetti et al., "An IoT-aware architecture for smart healthcare systems," *IEEE Internet of Things Journal*, vol. 2, no. 6, pp. 515–526, 2015.

[55] K. Guan, M. Shao, and S. Wu, "A Remote Health Monitoring System for the Elderly Based on Smart Home Gateway," *Journal of healthcare engineering*, vol. 2017, Article ID 5843504, 9 pages, 2017.

[56] A. Soliman, K. Soltani, J. Yin, A. Padmanabhan, and S. Wang, "Social sensing of urban land use based on analysis of Twitter users' mobility patterns," *PLoS ONE*, vol. 12, no. 7, p. e0181657, 2017.

[57] J. Xiao, H. Li, X. Wang, and S. Yuan, "Traffic Peak Period Detection from an Image Processing View," *Journal of Advanced Transportation*, vol. 2018, Article ID 2097932, 9 pages, 2018.

[58] N. B. Bahadure, A. K. Ray, and H. P. Thethi, "Image analysis for MRI based brain tumor detection and feature extraction using biologically inspired BWT and SVM," *International Journal of Biomedical Imaging*, vol. 2017, Article ID 9749108, 12 pages, 2017.

[59] E. A. Khan and M. K. Shambour, "An analytical study of mobile applications for Hajj and Umrah services," *Applied Computing and Informatics*, vol. 14, no. 1, pp. 37–47, 2018.

Hindawi
Wireless Communications and Mobile Computing
Volume 2018, Article ID 7841026, 11 pages
https://doi.org/10.1155/2018/7841026

Research Article

A Novel Emergency Healthcare System for Elderly Community in Outdoor Environment

Hui-Ru Cao and Choujun Zhan

Nanfang College of Sun Yat-sen University, Guangzhou 510970, China

Correspondence should be addressed to Hui-Ru Cao; xiaocao0924@163.com

Received 15 January 2018; Revised 20 May 2018; Accepted 8 July 2018; Published 22 July 2018

Academic Editor: Heng Qi

By exploiting the advanced information and communication technologies, the current community healthcare systems provide digital healthcare services. However, the current healthcare framework for senior citizen in outdoor environment faces new challenges. The traditional healthcare systems are not efficient, and they do not comprise user-friendly devices and interfaces suitable for the elderly in outdoor environment. Hence, in this work, we develop an outdoor healthcare system for community senior citizens based on unmanned aerial vehicle (UAV) and Internet of things (IoT). Our system includes physical devices, wireless and wired networks, cloud and data center, and smart terminals. Further, the analysis of the proposed healthcare architecture is presented from the perspective of different layers, and an algorithm on UAV for creating high-speed communication channel and delivering medicine is provided. In addition, the healthcare UAV, related devices, and friendly APPs are designed. The proposed framework is evaluated by comparison with the current healthcare architecture. The emulating and experimental results show that our proposed system can provide a high-quality wireless communication link even at large communication distances, and in real testbed our proposal can reduce the response time by about 20% in comparison with the current methods.

1. Introduction

With the increase of life expectancy in many countries, the continuously growing aging trends bring a dramatic increase in the elderly population [1]. Specifically, most of the developing countries are facing a serious aging problem, and more and more senior citizens suffer from the acute conditions such as blood pressure, heart disease, and fall-related injuries [2]. On the other hand, in most developing countries, most of the younger generation move to big cities for work, and this leads to a large number of old people living alone without family. This has become a common phenomenon in many developing countries, especially in China [3]. If a senior citizen suffers from an acute disease or injury, especially in outdoor environment, he/she must be treated immediately. Hence, it is essential to develop economical, convenient, and scalable communal healthcare systems, which can effectively reduce the response time of outdoor healthcare services and support the elderly community.

Providing an effective health system for senior citizens is significant, especially for those suffering from acute conditions. Therefore, increasing researchers focus on the topic and propose a great deal of valuable works. The research works in [4–8] focused on improving the healthcare systems using technological advances. The presented architectures for the communal healthcare systems are developed by introducing advanced digital technologies such as robot technology, cloud computing, wireless communication, and IoT, into the design framework [9, 10]. These new technologies have contributed immensely to improving the existing healthcare system and providing effective health services [11, 12]. However, the existing healthcare frameworks are still not sufficient for providing an efficient service to the senior citizen community. The existing healthcare frameworks show slow first aid response time for the acute diseases or fall-related injuries of elderly due to the environment, non-user-friendly devices, traffic situations, and other obstacles. The three most important aspects of the senior citizen community healthcare system are as follows: (1) a fast response time for the first aid; it is known that if a senior citizen suffer from acute disease, the health system must respond within limited time; (2) an effective communication equipment and communication

scheme; communication system is the basement for the new health framework, as effective communication equipment and scheme can promote the efficiency of whole system; (3) a set of user-friendly devices and user terminals. Lack of friendly terminal and devices is harmful for the efficiency and first aid response times. These new requirements bring new challenges for developing a healthcare system suitable for the elderly in outdoor environment, especially for response time and an effective communication system. Unfortunately, the traditional healthcare system cannot provide a fast access, efficient means, and valid communications system, which makes it difficult to meet the new requirements of the elderly healthcare system.

With the development of advanced technologies, such as smart robots, UAV, and wireless communication, it is possible to develop a new healthcare system to meet the demands of providing an efficient healthcare for elderly people in an outdoor environment. As discussed above, the existing healthcare systems are facing more challenges and cannot meet the requirements of providing highly efficient service and user-friendly devices and interface for the elderly community in outdoor environment. Hence, in this work, we propose a new outdoor healthcare system for senior citizens community by introducing the UAV and IoT. Moreover, we analyze the proposed healthcare architecture from the point of view of four layers: devices, communication, cloud, and terminal interface. Then, the proposed system is emulated in the terms of first aid response time and data communication delay in a simulation. A prototype is implemented using the designed healthcare UAV, user-friendly devices, and a related APP. Further, we build an experimental testbed and perform the experiment in a campus environment. The experimental results show that our proposed system can reduce the response time and provide a high-quality communications link. We believe that our work will shed light on outdoor healthcare system for senior citizens and accelerate the implementation of UAV and IoT-based healthcare services.

The rest of this paper is organized as follows. We present a summary of related works in Section 2. In Section 3, we introduce the system architecture and design of our proposed healthcare system for the elderly in outdoor environment and proposed an algorithm for health emergent event. We present the analysis of the proposed system and simulation and experimental results in Sections 4 and 5. Finally, conclusions of this work are given in Section 6.

2. Related Work

Combining advanced technologies to develop a smart healthcare system is an efficient method for providing an improved healthcare for the public, especially for senior citizens in modern society. These advanced technologies and systems enhance the performance of the healthcare services significantly. In this section, we review some of the related works of recent advances in emergency care technologies and healthcare systems.

2.1. Emergency Care Technologies. In [13], the authors integrated the RFID technology, ZigBee technology, and long-range wireless communication to build an emergency care system. Similarly, a global system for mobile (GSM) based smart wearable system with different sensors is developed in [14]. The developed device is capable of detecting sudden fall situations, cardiac abnormalities, and hyper/hypotension. In [15], Robson et al. proposed a tool called intelligent detection of arrhythmic heartbeats on electrocardiograms (IDAH-ECG). The IDAH-ECG tool collects data from an electrocardiograph to analyze and classify the data to detect patterns of arrhythmic beats in the ECG signal. In [16], the authors developed a location and emergency monitoring system for providing emergency care to the elderly. In [17], for predicting ambulance arrival time in an emergency situation, a linear regression model based on the information of weather, patient characteristics, lights and sirens, daylight, and rush-hour intervals is developed, and it was implemented as a Google maps web application.

From the perspective of application level, the novel technologies for emergency care could be divided into three categories: communication, data analysis, and data mining. However, the existing works related to emergency care technologies mainly focused on the healthcare service from a prediction aspect, which suffers from two undesirable drawbacks: real-time care deficiency and lack of emotional care. By incorporating UAV, IoT, and video technology, our proposed system can overcome these drawbacks.

2.2. Healthcare System. With the development of the information and communication technologies, such as wireless networks, cloud computing, data mining, and IoT, healthcare systems have made a great progress. In [18], a novel healthcare system architecture is proposed. The proposed architecture includes three components: collaborative data collection via wearable devices, enhanced sentiment analysis and forecasting models, and controllable affective interactions. In [18], a healthcare system based on cloud computing and robotics is developed, and it comprises wireless body area networks, a robot, a software system, and cloud platform. Further, in order to improve the practicability of multimedia transmission in the healthcare system, the authors in [19] proposed a novel scheme to deliver real-time video through an improved UDP-based protocol. In [20], a cyber-physical system for patient-centric healthcare applications and services, called Health-CPS, is proposed. The Health-CPS system is built based on cloud computing and big-data analytics technologies. In [21] a new system based on IoT-aware smart architecture is developed for automatic monitoring and tracking of patients, personnel, and biomedical devices within hospitals and nursing institutes. In [22], the authors proposed a new healthcare system based on second-generation RFID systems characterized by the introduction of encoding rules that are dynamically stored in RFID tags.

From the described summary of the existing healthcare systems, it can be understood that various healthcare systems and devices are developed for accurately sensing and collecting data related to physical and mental health of users. However, there are several drawbacks for the existing healthcare systems. Firstly, the current healthcare system and the corresponding research mainly focus on a common

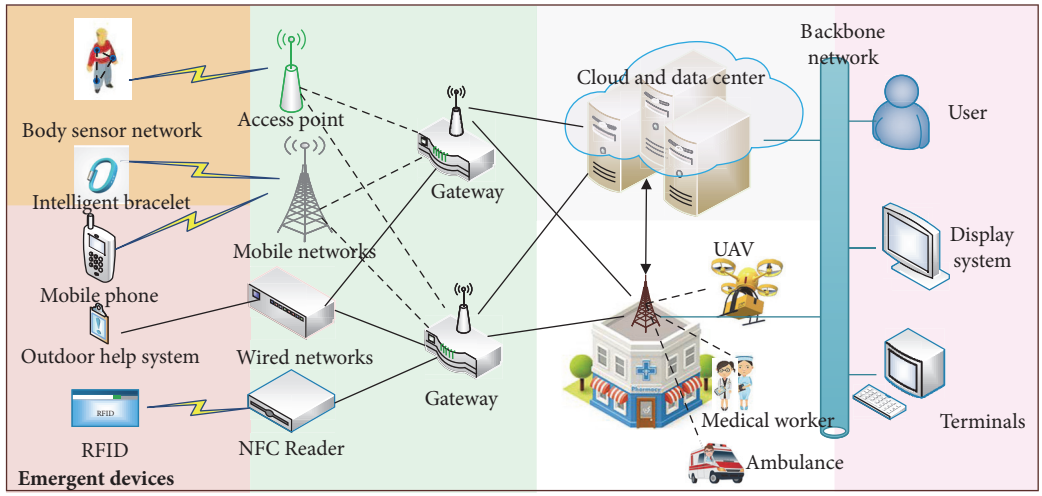

Figure 1: Architecture of network for senior citizen community in outdoor environment.

system for everyone and lack specific concrete applications, especially for senior citizen community outdoors. Moreover, the existing research studies assume that the users move in a limited range or at home. Obviously, this assumption is one of the limiting factors. In addition, for a healthcare system, it is important to have an efficient and real-time corresponding medical emergency subsystem, particularly for the users in emergency situations in outdoor environment. Nevertheless, the current emergency healthcare system is influenced by the position of hospital or medical center, buildings, and traffic situation. Hence, in this work, we focus on UAV and IoT- based emergency healthcare system for senior citizen community in outdoor environment.

3. System Architecture

In our work, UAV and IoT will play a significant role in the proposed healthcare system for outdoor environment. For facilitating the discussion and analysis of the framework, we divide the architecture of the outdoor healthcare system into four layers: the multiple model physical layer, networks layer, cloud layer, and the smart terminals (including UAV and medical workers) layer. The data communication links the four layers from the physical layer to the terminals. In the proposed system, the healthcare UAV plays a bridging role for information delivering during senior citizens and cloud sever; meanwhile UAV deliver the medicine, bandages, and emergency supplies. Therefore, in this section, after a brief description of the proposed healthcare system, the healthcare UAV subsystem is discussed.

3.1. Framework of the Proposed System. In the proposed system, all of the status data should be gathered by the sensor nodes and the outdoor system. Next, the data is transmitted to the cloud and data center. Meanwhile, the analyzed data can be sent to the smart terminals (e.g., doctors, users, smart phones, and other smart devices). It can be seen that the information exchange plays a significant role in our proposed healthcare system; i.e., the communication network supports the whole architecture. As shown in Figure 1, the information exchange system could be divided into data gathering layer, communication layer, cloud and data center, and smart terminals (including UAV and medical workers).

(1) Multimodel Data Gathering Layer. The data gathering layer determines the types of data that need to be collected by various devices in the system. The data gathering devices could be divided into two types, namely, forecasting and emergency devices. The body sensor nodes, the intelligent bracelet, environment sensors, and other sensors form the forecasting devices. The forecasting devices mainly gather the data for the general case and forecast the health condition of the users. The emergency devices are responsible for the emergency situations such as heart attack, hypertension, and other acute diseases. The emergency devices include the mobile phone, the outdoor help system node, RFID cards, and other smart devices.

(2) Communication Layer. This layer is responsible for communication between the cloud and smart devices, hospital system, and the users. The communication layer uploads and delivers the sensing data, control commands, and other information. In the proposed system, the communication media platform uses both the wired and wireless communication technologies. The wired network mainly deals with the static nodes such as outdoor help system, real-time data transfer, and situations with large amounts of data transfer. For the mobile entities (such as the ambulance, UAV, medical workers, and users), wireless communication technologies such as Bluetooth, ZigBee, Wi-Fi, LTE, and NFC are used in the system.

(3) Cloud and Data Center. The cloud and data center perform computing to match the users' requirements and store massive amount of information. Moreover, the cloud and data center act as the processing module for all the networks. In an emergency situation, the cloud and data

center create the list of the key medicines and rescue devices, by comparing the current information and the stored medical history records of a patient. The Hadoop software is used for storing massive amount of user data. After data mining and analysis, the results are delivered to users, nearby hospital, medical workers, and other smart terminals based on the priority of the message.

(4) Smart Terminals. The smart terminals are used to display the related information and key data using messages, web pages, or other application. This interface could provide an intuitional, effective, personal, and visual result for the elderly community and medical workers. The smart terminals can be the mobile phone, the intelligent bracelet, and the display system. For example, with the application software installed on the smart phone, the user could check the monitoring status of health conditions such as heart-rate, blood pressure, and environment data. When real-time information is issued from data server, the reminders will be driven by sound and video.

3.2. Problem Formulation and First Aid Strategies Based on UAV. In our system, two types of data traffic are considered: (1) general data, where all of the data are delivered in normal situation; namely, the elders are not in emergency; (2), emergent data, where the data are delivered in emergent situation, that is, the elders being in a critical situation.

Assume that there are n senior citizens randomly distributed in A (L, W), where L and W are are length and width of A. Let (x_i, y_i) be the position of the i-th senior citizen. For the system model, given that a senior citizen (we use current node i which stands for the senior citizen) is falling into the emergent situation at the time t_0 and the first aid at time t_{arrived}. So, the first aid response time T is

$$T = t_{arrived} - t_0 \tag{1}$$

Let the coordinate of medical center be (x_0, y_0) and (x_e, y_e) be the position of emergent event. Let l denote the length of path for ambulance from (x_0, y_0) to (x_e, y_e). So, the direct length of medical center and emergent event site l_{d} can be described as follows:

$$l_d = \sqrt{(x_0 - x_e)^2 + (y_0 - y_e)^2}. \tag{2}$$

To better understand the solution to a problem, establish the relationship between l (real path length) and l_d, shown in the following:

$$l = (1 + \gamma) l_d \tag{3}$$

where γ is path length increase coefficient and the value of γ depends on different method for the emergent situation. So, the first aid response time T is formulated as follows:

$$T = t_{recieve\_RQ} + t_{arrived\_AM} + t_{data\_process} \tag{4}$$

where $t_{recieve\_RQ}$ is the communication delay for the emergency request information (ERI) arriving to medical center. $t_{arrived\_AM}$ denotes the time of the ambulance arriving at the emergent site; $t_{data\_process}$ is the data processing for dealing with the healthcare emergent event. Moreover, in the communication network, $t_{recieve\_RQ}$ can be descripted as

$$t_{recieve\_RQ} = \sum_{j=1}^{k} \left(\frac{Q}{V_{C,j}} + t_{wait,j} \right) \tag{5}$$

where Q is the data size of ERI and $V_{c,j}$ and $t_{wait,j}$ are communication rate and unload communication task time of the j-th relay node. For easy understanding, let $V_{c,j}$ and $t_{wait,j}$ have the same value; namely, $V_{c,j} = V_c$, $t_{wait,j} = t_{wait}$. So, (5) can be reduced to

$$t_{recieve\_RQ} = k \left(\frac{Q}{V_C} + t_{wait} \right) \tag{6}$$

Let V_m be the speed of ambulance. It is known that there is a relationship between real path length (l) and ambulance moving speed (V_m), as shown in the following:

$$t_{arrived\_AM} = \frac{l}{V_m}. \tag{7}$$

So, formulation (4) can simplify into

$$T = k \left(\frac{Q}{V_C} + t_{wait} \right) + \frac{l}{V_m}. \tag{8}$$

As discussed above, in the emergent situation, we hope to get the minimum response time (MRT). So, the problem of MRT can be formulated as (9):

$$\min \quad T \tag{9}$$

$$\text{s.t.} \quad l \geq l_d \tag{10}$$

$$V_m \leq V_{m,\max} \tag{11}$$

$$0 \leq \gamma \leq \gamma_{\max} \tag{12}$$

$$Q > 0 \tag{13}$$

$$(x_0, y_0), (x_e, y_e) \in A \tag{14}$$

$$t_{wait} > 0, \; V_c > 0 \tag{15}$$

where formulations (10), (11), (12), (13), (14), and (15) are the constraints of length of medical center and emergent event site, and ambulance moving speed, path length increase coefficient, data size of ERI, position of emergent event, communication rate, and unload communication task time, respectively.

On the grounds of the processing of dealing with the healthcare emergent event and the above discussion, problem (9) can be decoupled into the following three subproblems, as being formulation as

$$\min T = \min \left(t_{recieve\_RQ} + t_{arrived\_AM} + t_{data\_process} \right) \tag{16}$$

According to formulations (6) and (7), the optimal problem (9) can be further simplified into (17)

$$\begin{aligned} \min T = {} & \min (k) \left(\frac{Q}{V_C} + t_{wait} \right) + \frac{\min (l)}{V_m} \\ & + \min \left(t_{data\_process} \right) \end{aligned} \tag{17}$$

Require: $Q, V_c, t_{wait}, V_m, \alpha, \beta, P_{r,\min}$
Ensure: ***HEA_FLAG***
(1) $HEA\_FLAG \longleftarrow 0, ERI\_flag[n] \longleftarrow 0$
(2) **for** $i = 1{:}n$ *do*
Read ERI_flag$[i]$
(3) **if** $ERI\_flag = 1$ & $HEA\_FLAG = 0$
(4) Read the *ERI*
(5) Acquire the position of emergent event $(x_{e,i}, y_{e,i})$
(6) $l_d \longleftarrow \sqrt{(x_0 - x_{e,i})^2 + (y_0 - y_{e,i})^2}$
(7) $P_t(i) \longleftarrow P_{r,\min} + \alpha + 10\beta \lg(l_d)$
(8) Create the direct wireless communication between (x_0, y_0) and $(x_{e,i}, y_{e,i})$.
(9) Cloud and data center analysis the information
(10) Healthcare cloud server give the key medicines and rescue devices for the i-th patient
(11) Ambulance UAV carrying the key medicine and rescue devices directly to the emergency location
(12) **end if**
(13) **if** UAV arrived at the site $(x_{e,i}, y_{e,i})$
(14) Create the high-speed communication channel
(15) Download data from Current Node (i, D)
(16) **end if**
(17) $HEA\_FLAG \longleftarrow 1$
(18) **End for**
(19) **Return** *HEA_FLAG*

Algorithm 1: First aid in emergent situation based on UAV.

In other words, for getting the first aid response time T, we can reduce the relay number of k and decrease the real path length l. Furthermore, in wireless mobile network, the receiving power P_r must satisfy the following inequality:

$$P_r = P_t - \alpha - 10\beta \lg(R) \geq P_{r,\min} \tag{18}$$

where P_t is transmitting power; R is the wireless communication radius; α and β are the attenuation at reference distance and the path loss exponent, respectively; $P_{r,\min}$ is the minimum receiving power for wireless communication. For solving the first subproblem ($\min(k)$), we can create the direct wireless communication between (x_0, y_0) and (x_e, y_e).

So, for acquiring the minimum data exchanging time, we can turn the first subproblem into searching the minimum transmitting power.

$$\min P_t = P_{r,\min} + \alpha + 10\beta \lg(l_d) \tag{19}$$

According to the above analysis, we propose a novel strategy for dealing with the health emergent event. For dealing with problem (9) with constraints of (10)-(15), we proposed the new healthcare system by using UAV, IoT, and cloud server. The strategy is shown in Algorithm 1.

Our proposed algorithm is explained as follows. When a senior citizen is in an emergency condition, he/she and the finder could send the request ($ERI\_flag[i]$) for help by using the outdoor help network terminal, intelligent bracelet, and other smart terminals (shown using the red line in Figure 2). Once the network receives the emergency request information, it creates a real-time wireless channel to deliver the information. By comparing the current information and the recorded history, the cloud and data center can give information regarding list of the key medicines and rescue devices for the patient. The hospital data center drives the ambulance UAV carrying the key medicine and rescue devices directly to the emergency location $(x_{e,i}, y_{e,i})$. Meanwhile, the cloud and data center inform the nearest medical workers and doctors requesting assistance at the site. When the UAV arrives at the emergency location, the wireless link will establish a connection with the hospital center, medical workers, and doctors. Meanwhile, the related emotional music will play, and the video phone will be linked, according the specific situation. Then, the finder and the nearest medical worker could give a medical care.

As shown in Algorithm 1, when UAV arrived at site, UAV will create the high-speed wireless channel for delivering video or other key data. Our proposal can reduce the data processing time by adopting cloud server f. Let V_c be the wireless communication rate and D be the volume of delivering data. So, we can get the communication delay, as shown in

$$T_{communication\_delay} = \theta \frac{D}{V_c} \tag{20}$$

where θ is the average number of hops for delivering data D. It is easily known that in our proposal we use UAV to create two hops for finishing the data transmitting.

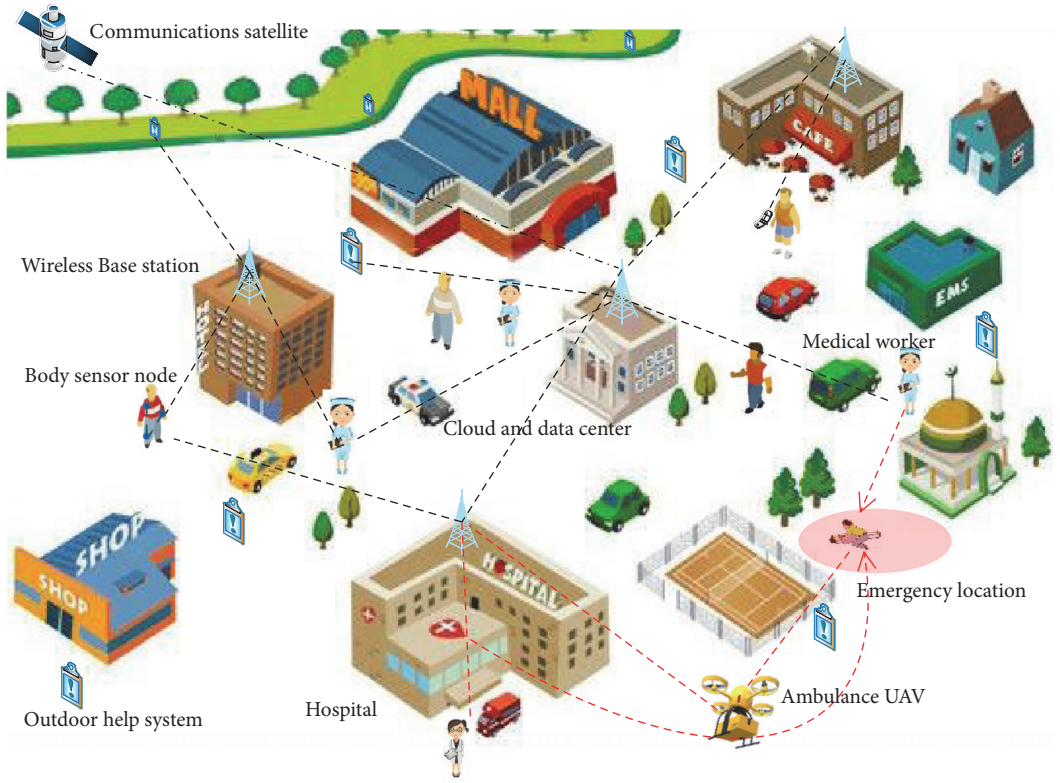

Figure 2: The outdoor healthcare system for elderly community. The red line shows the emergency situation case.

Table 1: Simulation parameters.

Parameters	values	Parameters	values
(x, y)	(0,0)	α	-30
γ_{HSUAV}	0	β	2
$t_{data\_process}(HSUAV)$	10 s	$t_{data\_process}(RTME)$	10 s
$t_{data\_process}(SMHS)$	100 s	θ_{RTME},θ_{SMHS}	2, 4
Q	1Mb	$P_{r,\min}$	-100 dBm
t_{wait}	1 ms	r_{TMHC}	1~2
θ_{HSUAV}	1	l_d	100~1000 m
Vc	1Mb/s	Vm	2 m/s
D	100Mb~1000Mb	R	*50 m*

4. Performance Evaluation

In this section, we will evaluate the performance of the proposed healthcare architecture and algorithm by comparing with traditional method in terms of first aid response time and communication delay.

The strategies are simulated in related software. Without loss of generality, we assume that the healthcare center is at the origin of coordinate system (namely, $(x, y) = (0, 0)$). The distance between emergent healthcare event position and origin of coordinate system will increase for evaluating the performance index. For easy reading, we use HSUAV which stands for our proposed method and RTME and SMHS which stand for the healthcare method in [23] and [24], respectively. In the simulation setup, let speed of the ambulance vehicle of HSUAV, RTME, and SMHS be 2 m/s. The details of the remaining parameters are listed in Table 1.

The simulation results of *first aid response time* and *communication delay* in different healthcare frameworks are given in Figure 3. The first aid response time total time consumption is the best standard metric for different architecture. It is known that, with increase of l_d, the first aid response time T of the three strategies will be added, as shown in Figure 3(a). However, HSUAV will use less time than RTME and SMHS. When $l_d = 1000$ m, HSUAV can reduce by 30 % and 48 % first aid response time comparing with RTME and SMHS. In other words, in our proposal framework, we can get a higher efficiency for healthcare emergent event.

Similar performance results of *communication delay* can be observed in Figure 3(b). In general, communication delay

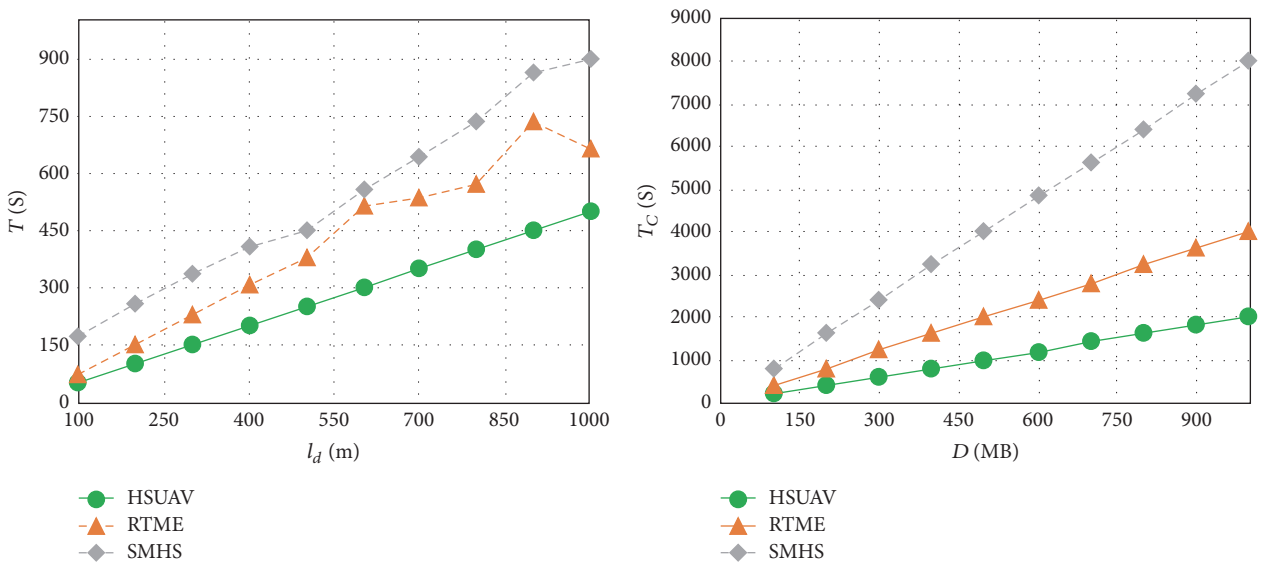

(a) First aid response times

(b) Communication delay in different loads

FIGURE 3: First aid response times and communication delays in different ways.

of HSUAV, RTME, and SMHS will increase with the rising of transmission data volume. The results in Figure 3(b) indicate that HSUAV has the smaller average time consumption for data delivering. In short, our proposed method outperforms the traditional framework in terms of first aid response time and communication delay.

5. Experiment Testbed

5.1. Healthcare UAV Subsystem. The ambulance UAV is used in the platform for reducing the response time. The UAV could directly fly to the emergency site, without being affected by the traffic situation. In order to implement the UAV system, dual-microprogrammed control units (MCUs) are used, as shown in Figure 4. Using PWM (Pulse Width Modulating, PWM), the MCU controls the motor, and propellers. At the same time, air velocity (MS-5611), working current, and voltage could be monitored by corresponding sensors. Further, using the universal asynchronous receiver/transmitter (UART) and serial peripheral interface (SPI), the UAV MCU configures and controls the GPS and wireless communication module for remote controlling (433 MHz DTU).

The sub-MCU connects the UAV MCU using the I2C interface. The sub-MCU accesses the loudspeaker, camera, SD card, ambient light, and environment sensors for the corresponding information. When the UAV flies to the emergency site, the main MCU sends a signal from the site and then the sub-MCU begins to work. At first, the sub-MCU establishes the wireless communication links with the hospital data center and the doctor. Next, some emotional music and conversations will be sent by the program processed in the sub-MCU. Further, the sensing data, images, videos, voice, and other key parameters will be sent to the data center and other related devices.

On the one hand, the sub-MCU could receive the emergency commands from the wireless module. When an emergency command is received by the hospital data sever, after being equipped with corresponding medicine and based on the patient information, the sub-MCU sends the GPS position data to the main UAV MCU. The main UAV MCU will fly to the emergency site. On the other hand, when the UAV arrives at the site, it could transmit the real-time video to hospital, ambulance, and medical workers. Meanwhile, the UAV can play music and sound to alleviate psychological pressure. In some special situations, the doctor could give assisted help by the remote video communication from the hospital. It is important to note that the wireless communication link can be supported by outdoor help system network, Wi-Fi, or LTE.

5.2. Implementation of Prototype. In this section, we briefly introduce an effective UAV and IoT-based healthcare service prototype developed for testing in a smart campus use case scenario as shown in Figure 5. This prototype system includes serval smart devices, such as cloud data center, wireless nodes, and display screen. Meanwhile, a four-axis UAV is used as the ambulance UAV. The UAV is equipped with different sensor nodes and devices, such as GPS, wireless modules, and different kinds of sensors. The main UAV MCU is equipped with an 8-bit ATMEGA2560-16AU microcontroller unit with AVR architecture, a 256 KB RAM memory, and a CPU with 16 MHz speed. The sub-MCU board is used for supporting the functions described above. In our ambulance UAV, for reducing the energy consumption, a 32-bit ST STM32F427VIT6 microcontroller unit with ARM Cortex-M4 architecture, a 2048 KB of flash memory, a 256 KB RAM memory, and a CPU with 168 MHz speed are used. Wireless communication capabilities are provided by the IEEE 802.15.4 TI (CC2530) chip with the working frequency

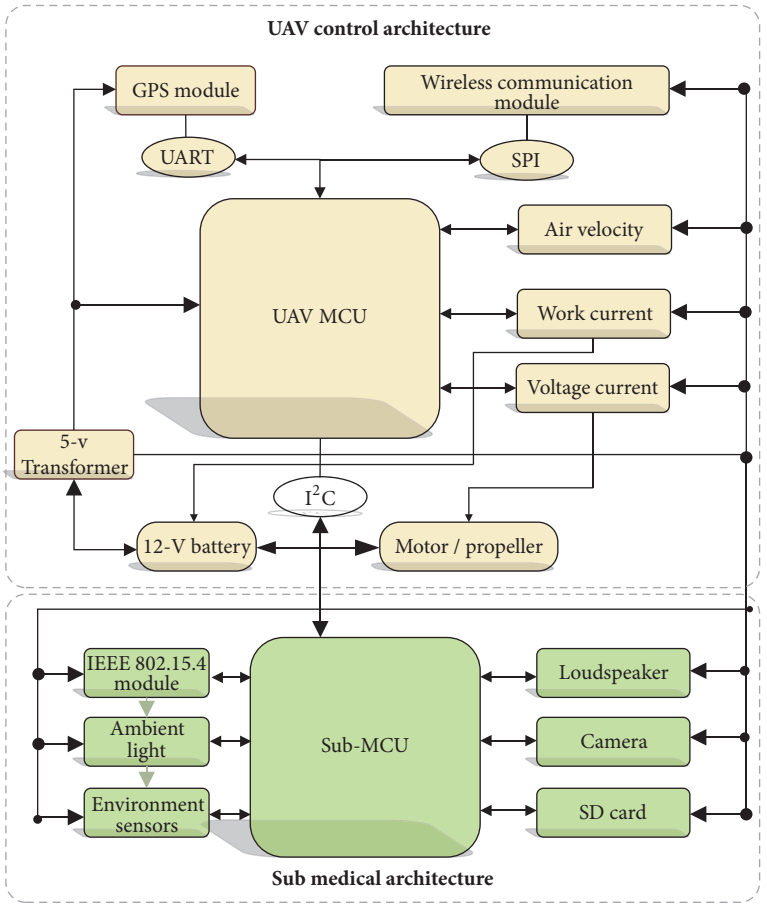

Figure 4: The UAV system hardware architecture.

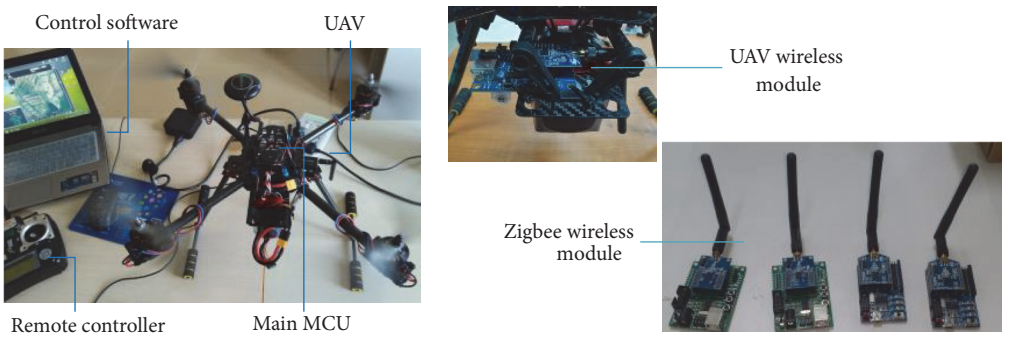

(a) Ambulance UAV (b) The prototype system

Figure 5: The platform and ambulance UAV.

of 2.4 GHz. Hence, a simple ZigBee network is established on the campus.

The smart terminal software is developed based on the android development kit with the android operating system with version 4.5. The emergency situation information and the collected sensory data can be displayed on smart phone by the corresponding application. Figure 6 shows the environmental data and body physiological data captured by various sensors in a visualization chart. Figure 6 shows a set of screenshots of the medical application used on the phone, the application has the option to display GPS position, emergency message, heart-rate, and blood pressure information. Figure 6(a) shows main page of the user terminal, and it includes various parameters such body temperature, heart-rate, location, and environmental data. The histogram of averaging humidity per minute is also displayed as shown in Figure 6(b). Furthermore, the body temperature illustration is shown in Figure 6(c).

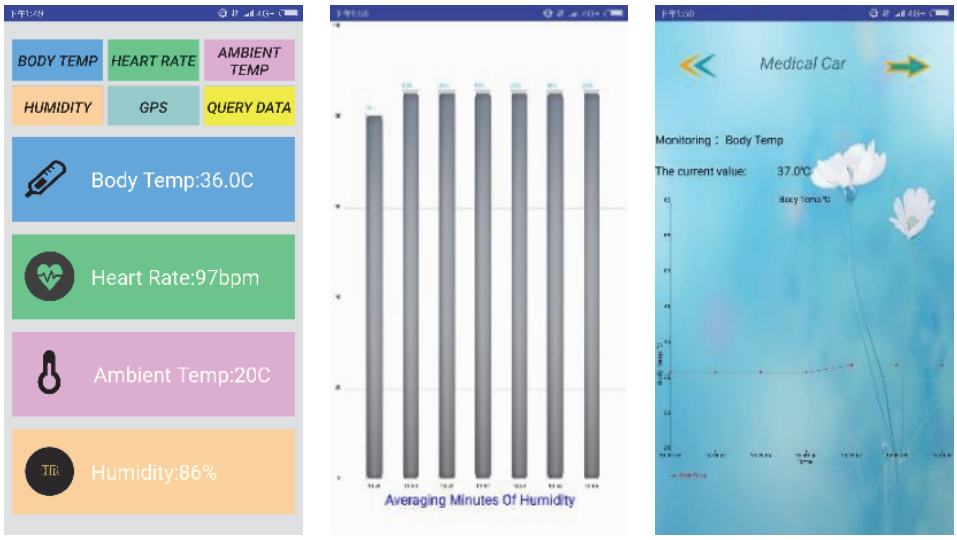

(a) (b) (c)

Figure 6: Screenshots of the medical app on the smart phone.

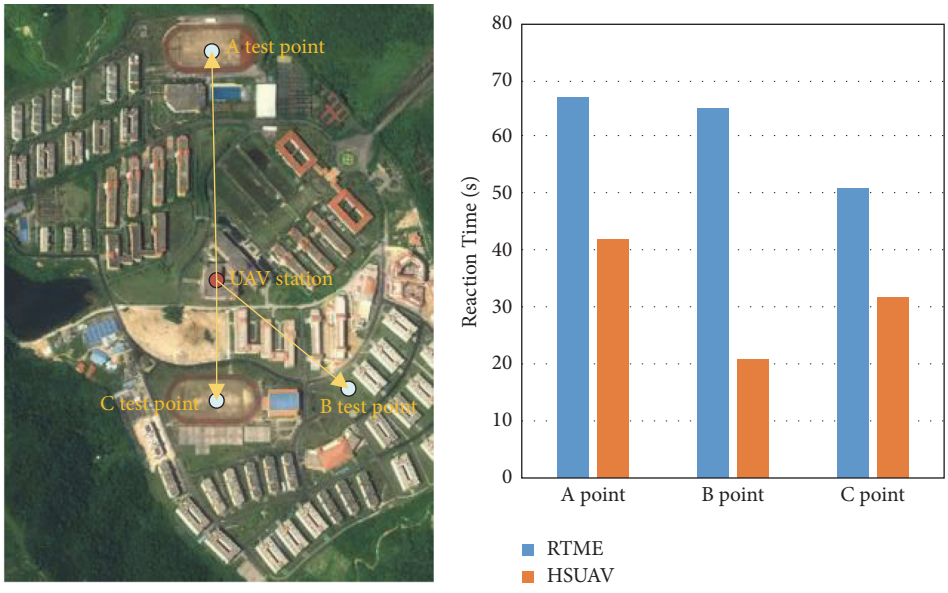

(a) The diagram of experiment location (b) The result of RT for different schemes

Figure 7: Comparison of reaction time for different systems.

5.3. Experiment Results and Analysis

First Aid Reaction Time. For assessing the reaction time performance of our proposed healthcare system, a comparison between the proposed system and other traditional architectures is carried out in our campus. We assumed that the UAV and the traditional medical ambulance have the same speed of 36 Km/h. We choose three different distance points as the emergency sites as shown in Figure 7(a). Figure 7(b) illustrates the comparison result. From the figure, our proposed system can reduce the response time by 20%. Our proposed system has a fast reaction time compared to RTME. Results show that the proposed system outperforms the traditional architectures, which can be easily affected by building, traffic, and road network. However, the UAV could fly directly to destination without any obstacles.

6. Conclusion

In this paper, we considered the outdoor healthcare system for senior citizens in emergency situations. For reducing the response time in case of an emergency situation, a healthcare system based on UAV and IoT is designed. The proposed system can provide real-time help to the senior citizens in

outdoor emergency situations with the help of the UAV. Moreover, it can also deliver the emergency information using the communication networks and assist specialist or medical workers. The proposed system includes four functions: sensing, communication, data processing, and medical aid. Since we used a UAV in the system, the proposed system is a closed loop system. Moreover, we discussed the communication architecture of the proposed system from the perspective different layers. Finally, a testbed for the outdoor healthcare system has been presented and functional validation and performance validation are presented. The experimental results show that the proposed system outperforms the traditional emergency care system architectures. Simulation and experimental results show that the proposed system outperforms the current architectures, which can be easily affected by building, traffic and road network. However, the UAV could fly directly to destination without any obstacles.

Data Availability

The simulation results data and experimental data can be accessed from the website, https://pan.baidu.com/s/1HVw1xZ2VLrpoLW6W8tuskw, or acquired from the corresponding author upon request.

Ethical Approval

All procedures performed in studies involving human participants were in accordance with the ethical standards of the institutional and/or national research committee and with the 1964 Helsinki declaration and its later amendments or comparable ethical standards.

Consent

Informed consent was obtained from all individual participants included in the study.

Conflicts of Interest

The authors declare that they have no conflicts of interest.

Acknowledgments

This work is supported by the Youth Innovation Project of Important Program for College of Guangdong Province with no. 2015KQNCX228 and Guangzhou Science and Technology Program (no. 201804010427). This work was also partly supported by the colleagues in the Department of Electronic Communication & Software Engineering Nanfang College of Sun Yat-sen University and School of Information Science and Technology, South China Agricultural University.

References

[1] W. C. Mann, "The aging population and its needs," *IEEE Pervasive Computing*, vol. 3, no. 2, pp. 12–14, 2004.

[2] H. M. Holmes, M. S. Beck, and J. H. Rowe, "Geriatrics: Year in review," *Journal of Geriatric Oncology*, vol. 7, no. 5, pp. 404–408, 2016.

[3] Y. Li, S. Wang, J. Li et al., "A survey of physicians who care for older persons in Southwest China," *Journal of Nutrition Health Aging*, vol. 17, no. 2, pp. 192–195, 2013.

[4] P. A. Laplante, M. Kassab, N. L. Laplante, and J. M. Voas, "Building Caring Healthcare Systems in the Internet of Things," *IEEE Systems Journal*, pp. 1–8, 2017.

[5] L. Wan, G. Han, L. Shu, and N. Feng, "The critical patients localization algorithm using sparse representation for mixed signals in emergency healthcare system," *IEEE Systems Journal*, vol. 12, no. 1, pp. 52–63, 2015.

[6] B. P. Zeigler, "Discrete Event System Specification Framework for Self-Improving Healthcare Service Systems," *IEEE Systems Journal*, vol. 12, no. 1, pp. 196–207, 2018.

[7] Y. Ma, Y. Wang, J. Yang, Y. Miao, and W. Li, "Big Health Application System based on Health Internet of Things and Big Data," *IEEE Access*, vol. 5, pp. 7885–7897, 2017.

[8] A. Srivastava, N. Sankar K., B. Chatterjee et al., "Bio-WiTel: A Low-Power Integrated Wireless Telemetry System for Healthcare Applications in 401–406 MHz Band of MedRadio Spectrum," *IEEE Journal of Biomedical and Health Informatics*, vol. 22, no. 2, pp. 483–494, 2018.

[9] M. M. Baig, H. GholamHosseini, and M. J. Connolly, "Mobile healthcare applications: system design review, critical issues and challenges," *Australasian Physical & Engineering Sciences in Medicine*, vol. 38, no. 1, pp. 23–38, 2015.

[10] J. Wan, C. Zou, S. Ullah, C.-F. Lai, M. Zhou, and X. Wang, "Cloud-Enabled wireless body area networks for pervasive healthcare," *IEEE Network*, vol. 27, no. 5, pp. 56–61, 2013.

[11] H. Qi, M. Stojmenovic, K. Li, Z. Li, and W. Qu, "A low transmission overhead framework of mobile visual search based on vocabulary decomposition," *IEEE Transactions on Multimedia*, vol. 16, no. 7, pp. 1963–1972, 2014.

[12] Y. Sang, H. Qi, K. Li, Y. Jin, D. Yan, and S. Gao, "An effective discretization method for disposing high-dimensional data," *Information Sciences*, vol. 270, pp. 73–91, 2014.

[13] H. Shieh, C. Huang, F. Lyu, Z. Zhang, and T. Zheng, "An Emergency Care System Using RFID and Zigbee Techniques," in *Proceedings of the 2016 International Symposium on Computer, Consumer and Control (IS3C)*, pp. 65–68, Xi'an, China, July 2016.

[14] S. Tewary, S. Chakraborty, J. Majumdar et al., "A novel approach towards designing a wearable Smart Health Monitoring System measuring the vital parameters and emergency situations in real-time and providing the necessary medical care through telemedicine," in *Proceedings of the IEEE Students' Conference on Electrical, Electronics and Computer Science, SCEECS 2016*, pp. 1–8, Bhopal, India, March 2016.

[15] R. Pequeno, N. Carvalho, K. Galdino et al., "A Portable System to Support Electrocardiography in Emergency Care," in *Proceedings of the 2015 IEEE 28th International Symposium on Computer-Based Medical Systems (CBMS)*, pp. 256-257, Sao Carlos, Brazil, June 2015.

[16] C. Park and J. Kim, "A location and emergency monitoring system for elder care using ZigBee," in *Proceedings of the 2011 7th International Conference on Mobile Ad-hoc and Sensor Networks, MSN 2011*, pp. 367–369, China, December 2011.

[17] R. J. Fleischman, M. Lundquist, J. Jui, C. D. Newgard, and C. Warden, "Predicting ambulance time of arrival to the

emergency department using global positioning system and Google maps," *Prehospital Emergency Care*, vol. 17, no. 4, pp. 458–465, 2013.

[18] M. Chen, Y. Zhang, Y. Li, M. M. Hassan, and A. Alamri, "AIWAC: affective interaction through wearable computing and cloud technology," *IEEE Wireless Communications Magazine*, vol. 22, no. 1, pp. 20–27, 2015.

[19] Y. Ma, Y. Zhang, J. Wan, D. Zhang, and N. Pan, "Robot and cloud-assisted multi-modal healthcare system," *Cluster Computing*, vol. 18, no. 3, pp. 1295–1306, 2015.

[20] Y. Zhang, M. Qiu, C.-W. Tsai, M. M. Hassan, and A. Alamri, "Health-CPS: Healthcare cyber-physical system assisted by cloud and big data," *IEEE Systems Journal*, vol. 11, no. 1, pp. 88–95, 2015.

[21] L. Catarinucci, D. de Donno, L. Mainetti et al., "An IoT-aware architecture for smart healthcare systems," *IEEE Internet of Things Journal*, vol. 2, no. 6, pp. 515–526, 2015.

[22] M. Chen, S. Gonzalez, V. Leung, Q. Zhang, and M. Li, "A 2G-RFID-based e-healthcare system," *IEEE Wireless Communications Magazine*, vol. 17, no. 1, pp. 37–43, 2010.

[23] M. M. Rathore, A. Ahmad, A. Paul, J. Wan, and D. Zhang, "Real-time Medical Emergency Response System: Exploiting IoT and Big Data for Public Health," *Journal of Medical Systems*, vol. 40, no. 12, article no. 283, 2016.

[24] Y. Ren, R. Werner, N. Pazzi, and A. Boukerche, "Monitoring patients via a secure and mobile healthcare system," *IEEE Wireless Communications Magazine*, vol. 17, no. 1, pp. 59–65, 2010.

Hindawi
Wireless Communications and Mobile Computing
Volume 2018, Article ID 8180296, 14 pages
https://doi.org/10.1155/2018/8180296

Research Article

Data Fusion in Ubiquitous Sports Training: Methodology and Application

Krzysztof Brzostowski and Piotr Szwach

Faculty of Computer Science and Management, Wroclaw University of Science and Technology, Wybrzeze Wyspianskiego 27, 50-370 Wroclaw, Poland

Correspondence should be addressed to Krzysztof Brzostowski; krzysztof.brzostowski@pwr.edu.pl

Received 26 January 2018; Revised 7 May 2018; Accepted 27 May 2018; Published 20 June 2018

Academic Editor: Milos Stojmenovic

We present a data fusion-based methodology for supporting the sports training. Training sessions are planned by coach on the basis of the analyzed data obtained during each training session. The data are usually acquired from various sensors attached to the athlete (e.g., accelerometers or gyroscopes). One of the techniques dedicated to processing the data originatnig from different sources is data fusion. The data fusion in sports training provides new procedures to acquire, to process, and to analyze the sports training related data. To verify the effectiveness of the data fusion methodology, we design a system to analyze training sessions of a tennis player. The main functionalities of the system are the tennis strokes detection and the classification based on data gathered from the wrist-worn sensor. The detection and the classification of tennis strokes can reduce the time a coach spends in analyzing the trainees' data. Recreational players for self-learning may also use these functionalities. In the proposed approach, we used Mel-Frequency Cepstrum Coefficients, determined from the accelerometer data, to build the feature vector. The data are gathered from amateur and professional athletes. We tested the quality of the designed feature vector for two different classification methods, that is, k-Nearest Neighbors and Logistic Regression. We evaluate the classifiers by applying two tests: 10-fold cross-validation and leave-one-out techniques. Our results demonstrate that data fusion-based approach can be used effectively to analyze athlete's activities during the training.

1. Introduction

The need for sports achievements motivates research laboratories and sports clubs to search for more efficient training methods. New ways in the enhancement of the training methods have emerged together with the development of mobile technologies. Over the last decade, the results of research on applying mobile technologies into sports training have been encouraging. The sensors such as accelerometers, gyroscopes, or GPS receivers are the most helpful parts of various applications used by coaches and athletes. These sensors enable monitoring, for example, the type, the duration, and the intensity of athletes' sports activities. It is useful for both the trainers and the trainees to improve the effectiveness of sports training. On one hand, the trainers can send helpful and timely feedback to the athlete, reinforcing the link between research and coaching practice. On the other hand, the monitoring of the athletes' sports activities supports better training performance of the athletes.

The sports training is a complex task in which the knowledge from fields related to anatomy, biomechanics, physiology, psychology, and didactics is needed [1]. One of the purposes of sports training is to achieve maximal performance from an athlete or the team. Trainer and well-prepared training sessions should help either the athlete or the team to gain the maximal performance repeatedly before each competition. The well-prepared training sessions should improve injuries prevention of the athlete or even help in rehabilitation of injured trainee [2].

There are types of sports training [3]: physical, technical, tactical, and psychological. The physical training pursues improving the motor abilities of an athlete. Regarding physical variables to be monitored, we should mention acceleration, endurance, speed, force, flexibility, and fatigue

index [1, 4]. The technical training aims at acquiring and mastering the sports skills. Among the technical variables, there are the proper execution of movements, repetition of sequential movements, correct posture during movement execution, and starting time [4, 5]. The tactical training is related to the studies of different strategies in the sports discipline. The psychological training is oriented towards improving the athlete's personality.

Typically, the sports training is composed of planning, monitoring, and analyzing. The planning of the training sessions takes into account the specific needs and conditions of the athlete, that is, information on athlete's sports performance, shape, mental preparation, skills, predispositions, abilities, and limitations. Obviously, planning the training session is a complex task, since it needs to take into account the long-term objective and depends on various external factors, that is, temperature or nutrition.

The monitoring of sports training is the process of data collection during the sports session. Recent advances in wearable technologies allow continuously monitoring the athlete discreetly and without obstructing the comfort during training sessions. The modern wearable sensors can capture motion-related parameters, useful for supporting athletes' sports activities. The standard devices for the athletes' motion-capture are the inertial sensors, that is, accelerometers and gyroscopes, as well as magnetometers [4, 6]. These sensors are gaining more and more popularity, and various applications are relying on these sensors in sports training [7–9]. The other example of sensors applied to support the athletes' sports sessions is video cameras. Unfortunately, the mobility of the systems composed of video cameras is limited. Moreover, the computational costs of the analysis of captured data are very high.

Once the data are collected, the next phase of the sports training is the data analysis. The data analysis is the crucial step in the sports training and must be performed efficiently. The reason is that, during each training session, the massive amount of data produced by various sensors could be gathered. The problem is the efficient processing of the vast volume of data acquired from different sources at the different level of complexity. It is clear that the up-to-date information on physiological (i.e., sports performance and shape) and technical (i.e., skills) preparation of the athlete has a significant influence on the further training process and its outcomes. Thus, there is a need for developing the methods to fuse such data.

Some authors [10] suggest that one of the techniques designed to process a large volume of data originating from different sources is data fusion. The data fusion technique combines the data acquired from multiple sources (a) to improve the accuracy and robustness of the outcomes, (b) to create meaningfully new information that cannot be obtained from the sources separately, and (c) to provide a complete picture of the investigated object or process. The data fusion results, in the more complex analysis, help to improve the decision-making process. We present how the trainers and trainees may benefit from the fusion of the data originating from different sources during training sessions.

This paper aims to demonstrate the data fusion methods in the context of sports training. We present self-developed system for detection and classification of the tennis strokes (serve, backhand, and forehand) based on the accelerometer's data gathered from the wrist-worn sensor. The proposed approach can reduce the time of data analysis and help the coaches to quickly retrieve the critical elements of an athlete's training session. It also provides insights into tennis players for improving their strokes technique and overall performance. The proposed system can also be used by recreational players for self-learning. Applying the wrist-worn sensor eliminates the need for expensive setup for the sensing data.

The main contribution of the work is the algorithm for tennis strokes detection and recognition based on Mel-Frequency Cepstrum Coefficients as the feature generator. We test the performance of two classifiers: k-Nearest Neighbors and Logistic Regression. To investigate the proposed approach, we also collected 1794 samples of tennis strokes from 15 amateur players and 621 samples from 8 professional players.

The paper is organized as follows. In the first part, we present an overview of data fusion techniques and algorithms and the example applications in sports training. In the second part, to provide a broader view, we present and discuss original research result obtained from applying data fusion to support sports training of tennis player. In the end, the results are discussed, and the conclusions are given.

2. Related Works

The monitoring of sports training can be considered as a part of the human activity recognition (HAR). There are two main approaches to solve the HAR problems, that is, by applying external or wearable sensors [11, 12]. The external sensors-based methods can be used only in the predefined locations, whereas in the wearable sensor-based approaches, the devices are attached to the users' bodies.

The camera-based systems (e.g., BTS Bioengineering, OptiTrack, Vicon) are the typical example of the motion-capture systems composed of external sensors. Unfortunately, most of such systems are expensive, and they can be employed only in a laboratory setting. The alternative to the camera-based tracking systems, that is, wearable sensor-based systems, has become increasingly popular. The application of wearable sensors in human motion analysis aids in overcoming the main drawback of camera-based tracking systems, that is, the lack of mobility.

The basic example of a system capable of processing motion data is composed of the accelerometer or the gyroscope. There are numerous commercial products supporting the tracking of the physical activities of athletes. For example, Adidas and Nike provide the devices for running activities [13, 14]. The accelerometer can also be used in the technical training of tennis player [9, 15–17]. Ahmadi at el. introduce the IMU sensor-based approach to the skill assessment and acquisition. The results show that it is possible to apply the accelerometer data for assessing the skill level of the tennis player. However, the authors point out that this approach has

some limitations related to the measurement range and the sampling frequency of the accelerometer.

Another example of one-sensor systems is presented in [7]. The authors propose an approach to recognize the swimming strokes and to count their number. In the study, two different sensor placements were tested: one was attached to the wrist and the second one to the upper back of the subject. Data acquired from the accelerometer are fused by QDA classifier (Quadratic Discriminant Analysis). It is reported that the classification accuracy of the approach is 96.7% (breast-stroke), 96.1% (freestyle), 97.1% (back-stroke), and 89.8% (turn) for the data gathered from the upper back-worn sensor. The classification accuracy for the wrist-worn sensors is significantly lower.

Tracking the sports activities can be also based on two, three, or more sensors. There are some commercial devices dedicated to supporting athletes' training. For example, for tennis players, the wrist-worn wearable devices by Indiegogo [18] and Babolat [19] are offered. The first company offered *Pivot*, the wireless motion-capture system designed for tennis players. The system composed of triaxial accelerometers, triaxial gyroscopes, and triaxial magnetometers can track footwork, body position, elbow bend, and knee bend. On the contrary, Babolat delivers a smart wristband to track training of the tennis player. It is mainly designed to track tennis strokes.

There are also some papers that study the applications of data fusion to support sports training [20–23]. For example, Connaghan et al. [21] consider the problem of monitoring the technical training of tennis players. In the proposed system, the data are acquired from single wearable IMU sensor (Inertial Measurement Unit) composed of the triaxial accelerometer, the triaxial gyroscope, and the triaxial magnetometer. The sensing device was attached to the player's forearm. In order to fuse the measurement data, the authors used the Naive-Bayes classifier. The classifier was trained using data gathered from seven players. The classification accuracy of detection and classification depends on the source of data. For example, fusing data from the accelerometer and the gyroscope improves the overall accuracy of classification up to 82.5%. On the contrary, the fusion of the data from both the accelerometer and the magnetometer enhances the performance up to 86% and from the gyroscope and the magnetometer up to 88%. Applying data fusion for data acquired from the accelerometer, the gyroscope, and the magnetometer improves the overall performance up to 90%.

In paper [24], the other example of a fusion-based approach supporting sports training is considered. The authors proposed an approach to golf swing classification relying on measurement data from the triaxial accelerometer and the triaxial gyroscope. The gathered data are fused by deep convolutional neural network (deep CNN). The results are compared with Support Vector Machine (SVM) classifier. The reported overall accuracy for deep CNN is 95.04% and it is 86.79% from SVN.

As we presented, the measurements acquired from accelerometers, gyroscopes, and magnetometers are sources of essential data in the monitoring of athlete's activities. The fusion of these data with a video signal can improve the overall performance of the motion tracking system. With this new functionality, the trainer can provide corrections and guidance to the trainee. It is worth stressing that adding a video camera to the tracking system limits the mobility of the system. For example, the work in [25] introduces the data fusion-based approach to combine the data acquired from IMU sensor and a video camera. To test the performance of the proposed algorithm, the authors used the system to detect and to classify the tennis strokes. The system was composed of video cameras arranged in the laboratory setting and IMU sensor attached to the player's forearm. The features used to detect and to classify the tennis strokes are generated from video images and IMU sensor. The authors tested two classifiers, that is, k-Nearest Neighbors (K-NN) and Support Vector Machine (SVM). The dataset used to train classifiers consists only of the samples gathered from the professional players. The results show that it is possible to obtain the better detection and classification performance for data originating from multiple sources.

As it is presented in paper [26], inertial sensors can also be fused with other measurement units, for example, the force sensor. The authors applied gathered data to estimate rider trunk pose with the use of Extended Kalman Filter. The performance of the proposed approach is demonstrated through indoor and outdoor riding experiments. In the study, five healthy and experienced bicycle riders (four males and one female) perform both the indoor and the outdoor tests. The results showed the outperformance of the proposed algorithm compared to methods estimating the rider trunk pose without the force sensor. Moreover, the proposed algorithm gives the estimation accuracy comparable with other fusion methods known in the literature.

3. Data Fusion

3.1. Motivation for Data Fusion. The data acquired through wearable sensor-based systems for sports training usually originate from different sources. Thus, building a complete and coherent picture of the athlete based on the gathered data is a challenging problem. Among existent approaches to process multisourced data, we propose a framework based on data fusion. Data fusion offers various methods, techniques, and architectures for building the picture of the object of interest [27].

The system relying on multiple sensors, in which measurements from each sensor are processed separately, suffers several limitations and issues [28, 29]:

(i) *Sensor deprivation*: lost ability to monitor the desired features

(ii) *Limited spatial coverage*: each sensor has a limited area of operation

(iii) *Imprecision*: the precision of sensors' measurements is limited

(iv) *Uncertainty*: it appears when the sensor cannot measure all desired features

Data fusion methods in the multisensory systems introduce some advantages, such as reduction of uncertainty, improvement of the measurement precision, enhancement of

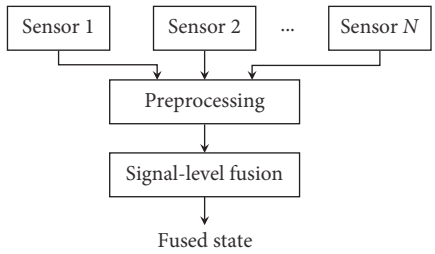

Figure 1: Signal-level fusion (based on [31]).

the signal to noise ratio, and compensation for lacking the features. A significant advantage of fusion methods is their ability to integrate the independent features and prior knowledge. It is essential when the noncommensurate data must be combined. The noncommensurate data originate from the heterogeneous sensors [30]. For example, the data from the accelerometer and the video camera are noncommensurate data.

3.2. Methods for Data Fusion. Levels of abstraction are one of the main concepts of data fusion [10] and they define the stages at which the fusion can take place. In paper [10], the following three categories of levels of abstraction were specified: the signal level, the feature level, and the decision level.

3.2.1. Signal Fusion Algorithms. Fusion at the signal-level fusion is usually used to combine raw signals acquired from different sensors. The signals at this level are commensurate, that is, acquired from sensors measuring directly the same property. For example, the signals from the accelerometer and the gyroscope are commensurate, since they are measuring directly the same property, that is, the kinematic parameters of moving object.

A typical issue at the first level of fusion is the state estimation. The popular method to address this issue is the Kalman Filter (KF). Kalman Filter is the statistical approach to fusing commensurate signals relying on recursively made predictions and updates. One of the most common examples of the Kalman Filter application is the fusion of signals acquired from the accelerometer and the gyroscope to estimate the attitude of the object. The modifications of the KF are Extended Kalman Filter (EKF) and Unscented Kalman Filter (UKF). These extensions of Kalman Filter are usually applied to the nonlinear problems. Another approach applied at the first level of abstraction is particle filtering (PF). The PF algorithm based on Sequential Monte Carlo techniques is estimating the parameters of the conditional probability density function.

The fusion methods at this level allow getting further description of the object which is not possible with the use of the existing sensors. In Figure 1, we show the model of data fusion at signal level.

3.2.2. Feature Fusion Algorithms. Fusion at the second level is used when the sensors provide the noncommensurate data. At this level, we start with determining the feature vector; then we perform the feature fusion. The feature vector is the high-level representation of the object. To construct the feature vector, we have to generate the features set and select the most relevant from the original ones. The suitable features are determined by applying feature selection or feature extraction methods.

The generated features can be grouped as (a) time domain, (b) frequency domain, and (c) time-frequency domain. In the first group, we have the features characterizing the signal (e.g., maximum or minimum of amplitude, zero crossing rate, rise time, etc.), its statistics (e.g., mean, standard deviation, cross-correlation, peak-to-valley, energy, kurtosis, entropy, skew, etc.), and the fractal features. The second group mainly consists of spectral features (e.g., spectral peaks, roll-off, centroid, flux, and energy), Fourier coefficients, power spectral density, and the energy of the signal. For the last group, we have wavelet representation (e.g., Gabor wavelet features), Wigner-Ville distribution-based analysis, and Mel-Frequency Cepstral Coefficients (MFCC) [33].

The number of generated features might be large (e.g., the Fourier coefficients). Thus, it might be necessary to reduce it. We have two approaches to reach the proper amount of features: the feature selection or the feature extraction. The feature selection is applied to select the most appropriate elements from the original set, whereas the feature extraction methods reduce the dimensionality of the initial feature vector. In the context of multisensory systems, the feature-level data fusion is vital due to the communication bandwidth and the energy limitation.

Afterwards, having prepared the feature vector, the next step is the feature fusion. In general, we can divide feature fusion method into two categories: nonparametric and parametric. The classical nonparametric methods are k-NN, SVM, Logistic Regression (LR), and Artificial Neural Networks (ANN).

The main parametric algorithms are Gaussian Mixture Models (GMM) and k-Means methods. In GMM, we perform the feature fusion based on the value of the likelihood function. To train Gaussian Mixture Models, we usually used Expectation Minimization method. The k-Means method is the distance-based approach to unsupervised classification of the observations.

In Figure 2, we present the basic model of feature-level fusion.

3.2.3. Decision Fusion Algorithms. The decision-level fusion is performed at the highest level of abstraction. It is the process of selecting one hypothesis from the set of hypotheses generated at the lower levels. Operations at this level have two main advantages: improving the decision accuracy and saving the bandwidth for systems working in network settings [34]. To enhance the quality of decision, in some cases, it is possible to apply on unique mechanism for incorporating domain-specific knowledge and information [33]. The typical decision-level fusion methods include Bayesian inference, fuzzy logic, and Dempster-Shafer theory.

We present the model of decision fusion in Figure 3.

3.3. General Architecture for Data Fusion-Based Systems. In the section, we introduce the general architecture of the data

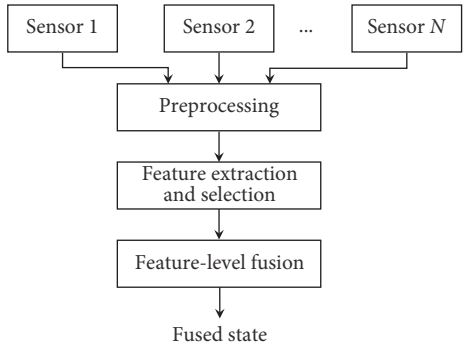

Figure 2: Feature-level fusion (based on [31]).

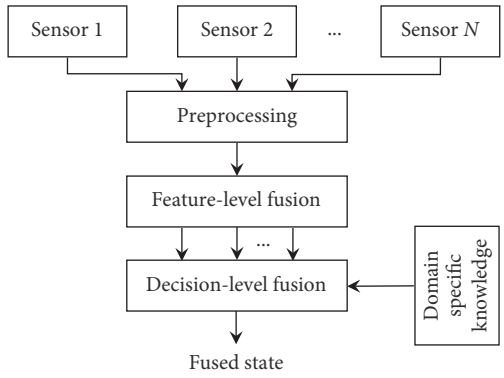

Figure 3: Decision-level fusion (based on [31]).

fusion-based multisensory system (Figure 4). In the proposed architecture, we can distinguish the following tiers:

(i) Data acquisition tier

(ii) Data fusion tier

(iii) Data presentation tier

The first tier is composed of the sensors (e.g., wearable sensors) attached to the human body or near the human body. Then, the sensor data are transferred (e.g., wirelessly) to the computational unit (e.g., smartphone, personal computer, or cloud).

The primary element of the proposed architecture is the second tier. All of the data fusion related computations take place herein. At this tier, the transferred data are processed at the different levels of abstraction using the previously discussed methods. The applied data fusion-based approach allows designing systems well suited to the user's needs.

The last tier is designed for data presentation, that is, visualizing (e.g., charts and plots) and reporting (e.g., tables) results. In general, the tier allows interaction between the user and the system.

The general architecture of data fusion-based system can be applied in problems related to industry, environmental monitoring, medicine, or sports [35]. One of the well-known problems in industrial communities is the condition-based maintenance. In paper [36], the authors consider the problem of engine fault diagnosis. The approach is also applied in robotics, for example, in navigation [37], localization and mapping [38], and object recognition [39]. Data fusion can also be used in the environmental monitoring. For example, in [40], the environmental data are fused to detect a volcanic earthquake. In [41], gathered data are used to monitor the weather conditions. In medicine, data fusion is mainly used in the analysis of medical images for location and identification of tumors, abnormalities, and disease. In paper [42], data fusion is used for the brain diagnosis, in [43], the data fusion-based algorithm is applied to the breast cancer diagnosis, and in [44], an approach to recognize the anatomical brain object is proposed.

In Figure 5, we present the data fusion in the context of the sports training. At the first stage, the sports training is planned by taking into account the current sports performance, shape, mental preparation, skills, predispositions, abilities, and limitations of the athlete. Then, the training session is monitored, and some data are gathered. The gathered data are analyzed at the third stage by applying data fusion methods. The first level of data fusion is used to obtain the athlete's parameters that cannot be measured directly. One of the examples is the estimation of the trainee's body orientation on the basis of the data from the accelerometer and the gyroscope [26]. Another example is the estimation of the walking speed of the athlete [45, 46]. The walking speed can be estimated by fusing data from the accelerometer and the gyroscope and by applying the numerical integration. The second-level data fusion can be used to support sports training in case of noncommensurate data. At this level, it is possible to detect and to classify specific sports discipline movements, for example, strokes for tennis or swimming or the swing motion in golf. The last level of data fusion is the least known in the sports training. However, in paper [47], the authors showed that applying the data fusion at the third level can improve the overall accuracy of the classification.

Based on the data fusion-based analysis of measurements, the adaptation of the sports training is performed (Figure 5). The adaptation of the sports training can be completed automatically or semiautomatically. In the second case, the coach is supporting the adjustment of the sports training. It can be seen that the fusion-based training process has an iterative nature.

4. Materials and Methods

4.1. Data Collection and Experimental Setup. In this paper, we apply data fusion methods to monitor the sports training. The proposed approach is validated experimentally on data collected during the sessions of tennis training.

To test the proposed approach, we develop the system to acquire and to process the measurement data. The system is connected with the wrist-worn *Pebble Watch* motion sensor (Figure 6). *The Pebble Watch* can measure the acceleration (from the three-axis accelerometer) and the strength of magnetic field (from the three-axis magnetometer). The sensor can measure the acceleration up to ±4 [G] with sampling frequency of 10 Hz, 25 Hz, 50 Hz, and 100 Hz.

Accelerometers measure the change of velocity over time in a three-dimensional space. The measured acceleration signals are composed of gravitational and body motion

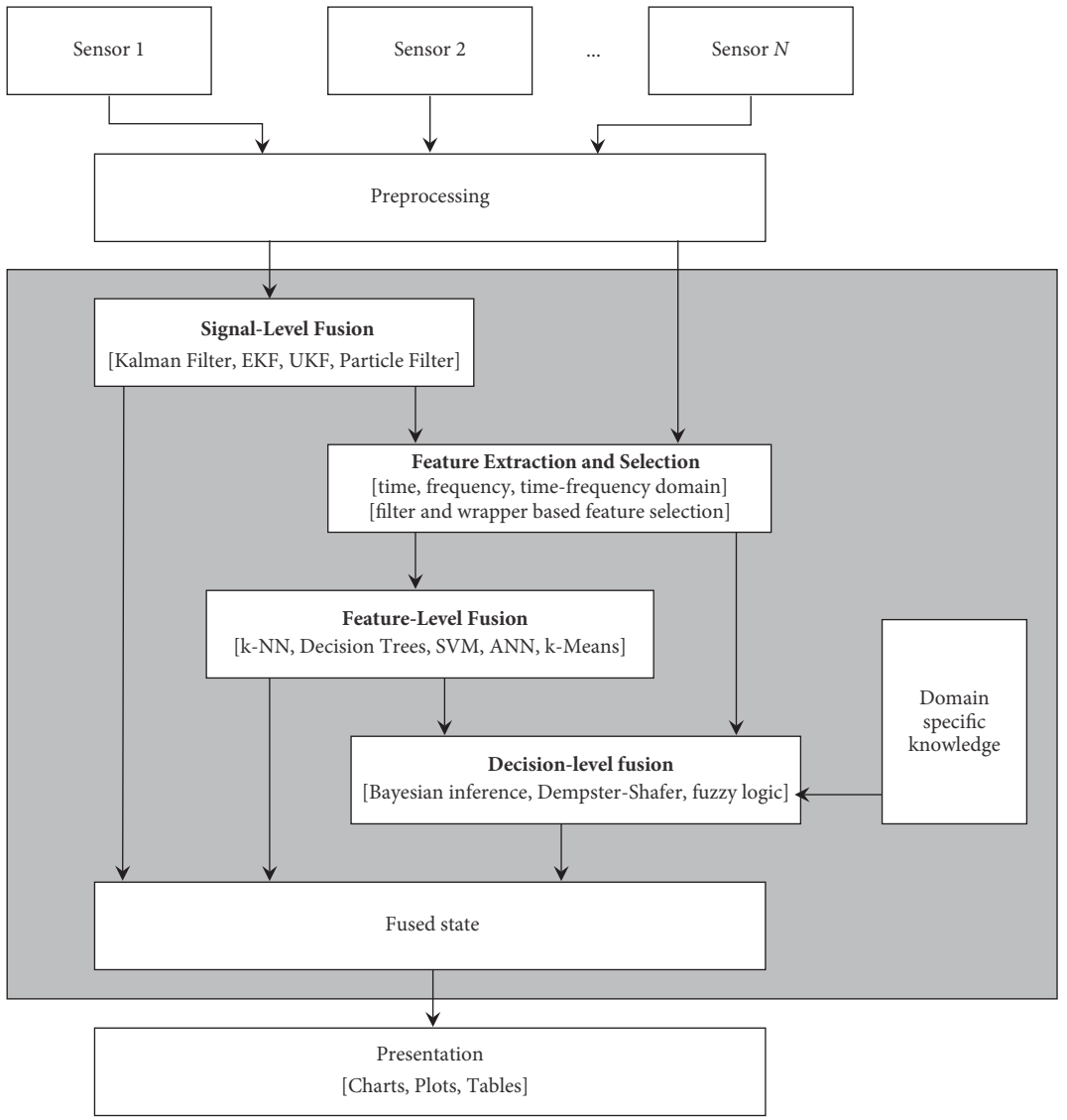

Figure 4: The architecture of data fusion-based multisensory system (based on [32]).

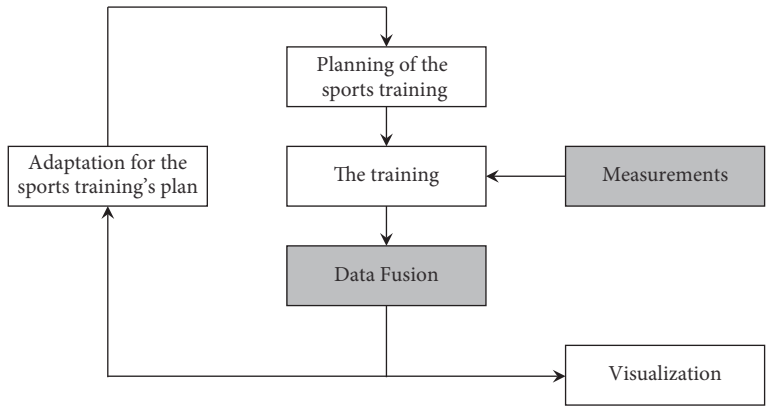

Figure 5: Data fusion in the context of sports training.

Figure 6: *The Pebble Watch* sensor used during experiments.

Figure 7: The self-developed system for storing data on the mobile device.

components. Data gathered from accelerometers attached to the human body can be used to recognize various human activities. The type of action recognized based on measurements depends on the sensor placement. Typical places of sensor attachment are upper limbs (the arm and the forearm), lower limbs (e.g., the ankle and the thigh), and lumbar [4].

The self-developed system has two main parts: the data acquisition subsystem and the analysis and inference subsystem. The data acquisition subsystem consists of two components: the first one transfers data from *the Pebble Watch* sensor, and the second one stores data on the mobile device (Figure 7). The system helps in recording data from each participant, profiling and managing the participants, and browsing the history of stored samples.

The tennis players' activity was measured on the indoor tennis court. We acquired measurement data from each participant after warming-up; that is, the players were instructed to perform several serves, forehand, and backhand strokes. Each participant used wrist-worn sensor, *the Pebble Watch*, to measure the acceleration in three axes. The data are transferred wirelessly to the system (Figure 7).

Participants were divided into two groups: the amateurs and the professionals. The first group consisted of 12 male and 3 female amateur tennis players. The second group consisted of 6 male and 2 female professional tennis players. The participants were asked to perform the following tennis strokes: forehand, backhand, and serve. In Table 2, we summarized the number of samples of each tennis stroke

Table 1: The number of samples of tennis strokes from the amateur and the professional players.

Skill level	Number of participants	Number of samples
Amateur	15	1794
Professional	8	621

Table 2: The number of the samples gathered during the tennis training.

Type of tennis stroke	Amateurs	Professionals
	Number of samples	
Forehand	961	271
Backhand	491	257
Serve	342	93

from the amateur and the professional players. We present the number of acquired samples in Table 1.

The samples of the acceleration measurements for the selected tennis strokes are shown in Figure 8. In Figure 9, we illustrate the sequence of movements for serve stroke.

4.2. Methods. In this section, we present a data fusion-based approach for monitoring the training of a tennis player. The proposed algorithm detects and classifies the tennis strokes based on the data gathered during training sessions. It is based on the general architecture of the system introduced in Figure 4. In Figure 10, we specify the main steps of the proposed approach: the preprocessing, the feature generation and extraction, and the classification. In the preprocessing step, we remove unwanted components of high-frequency noise; that is, the raw signals captured from the accelerometer were passed through a low-pass filter. In presented approach, we applied the Simple Moving Average (SMA) algorithm. SMA is a fast and simple algorithm to remove unwanted high-frequency components from the measurement signals.

When the preprocessing is completed, the next step in our approach is the feature extraction. We propose a method for feature extraction based on Discrete Fourier Transform (DFT) and Mel-Frequency Cepstral Coefficients, since the designed system should not allow heavy computations. Originally, MFCC were applied in speech recognition [48] but this method has also been successfully applied in the image recognition [49], the emotion recognition [50], and the eye movement identification [51]. The MFCC-based features have some advantages: ability to represent the signal in a compact form, low cost of determination, and high accuracy of classification for the basic classifiers [51].

4.2.1. Mel-Frequency Cepstral Coefficients. The section presents the MFCC-based feature extraction algorithm for the acceleration signal. We denote measurements from the acceleration as $a(n), n = 1, 2, \ldots, N$. N corresponds to the number of the samples.

Initially, the first phase of MFCC algorithm is the pre-emphasis for the compensation of rapid decaying spectrum of speech. Because the frequency of the acceleration signal

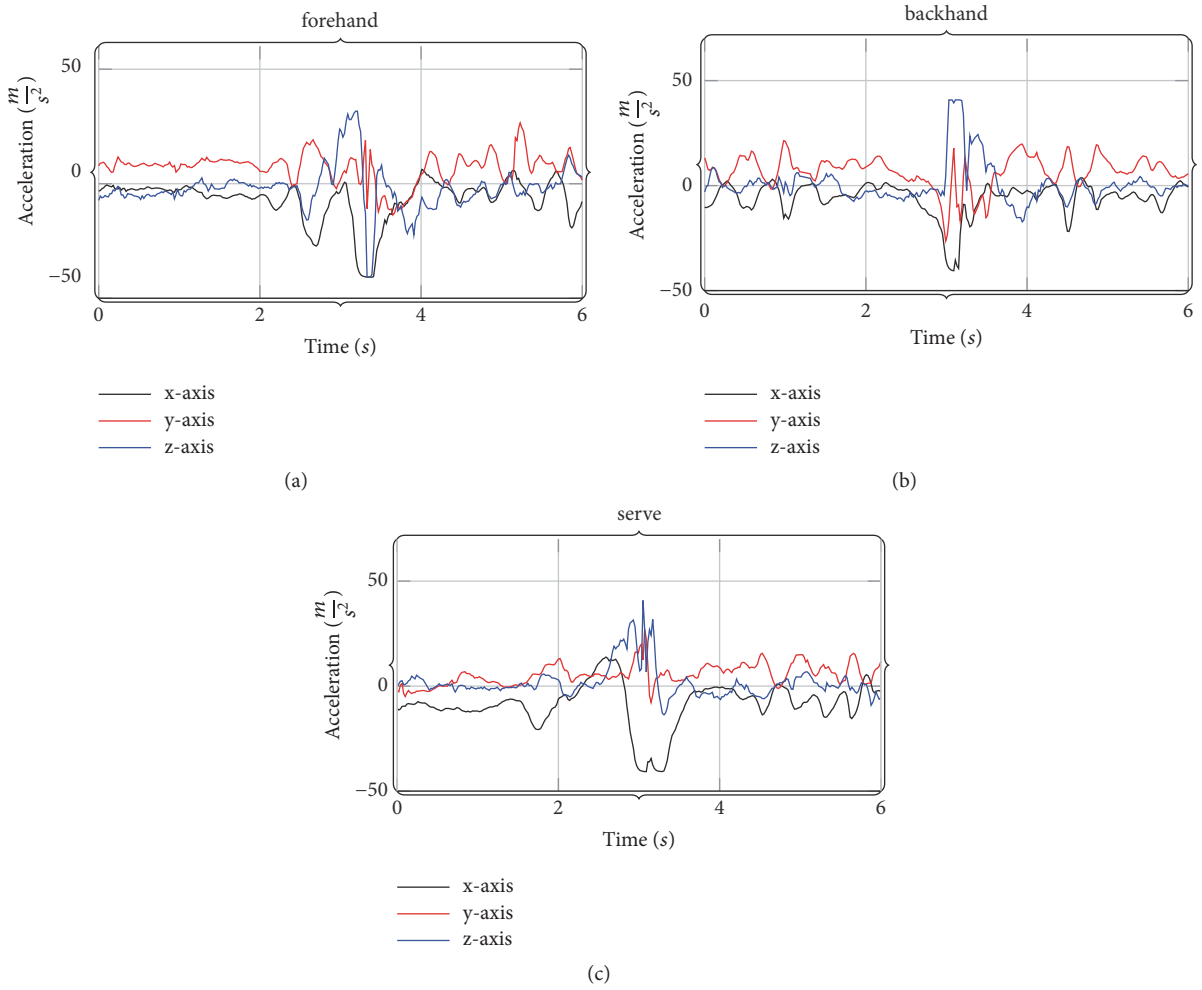

Figure 8: The acceleration measurements for selected tennis strokes: forehand, backhand, and serve.

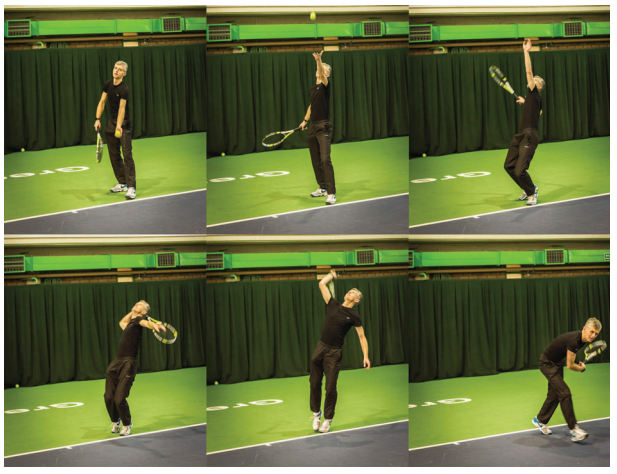

Figure 9: The sequence of movement for serve stroke.

is smaller compared to the speech signal, this step is not necessary for our approach [52].

In the next step, we transform the acceleration signal from the time domain to the frequency domain by applying Discrete Fourier Transform:

$$A(k) = \sum_{n=0}^{N_w-1} a(n)\, w(n) \exp\left(\frac{-j2\pi kn}{N_w}\right), \quad 0 \le k \le N_w \tag{1}$$

where N_w is the size of the frame and $w(n)$ is the *Hamming* function calculated from [53]:

$$w(n) = 0.54 - 0.46 \cos\left(\frac{\pi n}{N_w}\right), \quad 0 \le n \le N_w \tag{2}$$

Then, we can determine the energy spectrum from the following formula:

$$s(q) = \ln\left(\sum_{k=0}^{Q-1} |A(k)|^2 H_q(k)\right) \tag{3}$$

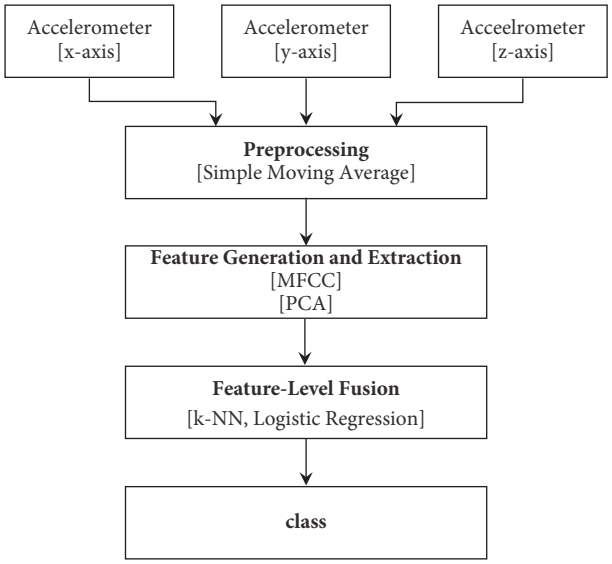

Figure 10: Flow diagram of the system to classify the tennis strokes.

where Q is the number of the filters and $H_q(k)$ is the triangular filter bank:

$$H_q(k) = \begin{cases} 0 & \text{if } k < k_{b_{q-1}} \\ \dfrac{k - k_{b_{q-1}}}{k_{b_q} - k_{b_{q-1}}} & \text{if } k_{b_{q-1}} \le k < k_{b_q} \\ \dfrac{k_{b_{q+1}} - k}{k_{b_{q+1}} - k_{b_q}} & \text{if } k_{b_q} \le k < k_{b_{q+1}} \\ 0 & \text{if } k_{b_q} \ge k_{b_{q+1}} \end{cases} \quad (4)$$

where k_{b_q} are the boundary points of the filters.

Then, we determine the mapping between the real frequency scale (in Hz) and the perceived frequency scale (in Mels) by

$$Mel(f) = 2595 \log\left(1 + \frac{f}{700}\right) \quad (5)$$

Finally, we apply a Discrete Cosine Transform (DCT) to the natural logarithm of the Mel spectrum, obtaining the Mel-Frequency Cepstral Coefficients:

$$c(i) = \sum_{q=0}^{Q-1} s(q) \cos\left(\frac{\pi i}{2Q}(2q+1)\right) \quad (6)$$

Flow diagram for the MFCC-based feature extraction is shown in Figure 11.

4.2.2. Feature Extraction. As the dimension of the MFCC related features generated from the acceleration data becomes very high, we applied Principal Component Analysis (PCA) in this regard (Figure 10). PCA is a linear technique to project data onto an orthogonal lower-dimensional space so that the variance of the projected data is maximized [54]. Thus, we

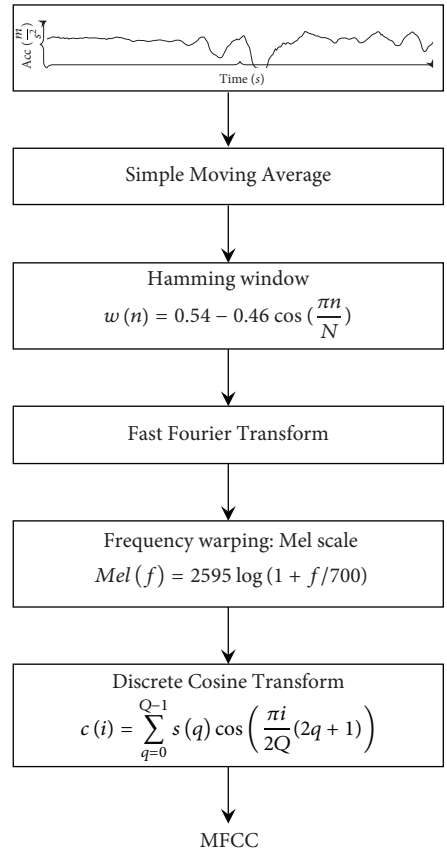

Figure 11: Flow diagram for MFCC calculation.

adopt the PCA algorithm to reduce the dimensions of high-dimensional features.

Suppose that we have dataset $\mathscr{A} = [a(1), a(2), \ldots, a(N)]^T$, where $a(n) \in \mathbb{R}^L$, L is the dimension of a data point, and N is the length of measurement sequence. We determine the covariance matrix from

$$S = \frac{1}{N} \sum_{n=1}^{N} (a(n) - \overline{a})(a(n) - \overline{a})^T \quad (7)$$

where

$$\overline{a} = \frac{1}{N} \sum_{n=1}^{N} a(n) \quad (8)$$

Since S is real and symmetric, we can diagonalize the matrix

$$\Lambda = USU^T \quad (9)$$

where U is a real and unitary matrix. The diagonal elements of Λ are the eigenvalues of S, and the columns of U are the eigenvectors of S. We sort the eigenvalues from the large one to the small one, and $\{u_1, u_2, \ldots, u_D\}$ are the corresponding eigenvectors. A data point $a(n)$ is projected onto eigenvector u_d by

$$z_d(n) = u_d^T (a(n) - \overline{a}) \quad (10)$$

The eigenvector u_1 with the largest eigenvalue is called the principal component. The vector provides the best direction of data projection. Similarly, the set of eigenvectors $\{u_1, u_2, \ldots, u_D\}$ is used to transform the L-dimensional space to the D-dimensional space. More details on the PCA method can be found, for example, in [54].

4.2.3. Classification. In the presented approach, we applied two different classifiers to fuse features, that is, k-Nearest Neighbors and Logistic Regression algorithms. In our studies, we decided to compare k-NN with LR, since the first method does not need a training process, while the second one requires training. Also the chosen methods have relatively low computational costs [54–57].

k-NN is a nonparametric distance-based supervised classifier. This method is efficient and easy to implement. The classifier is based on the closest training examples in the feature space [54] and has the form

$$pr\left(y \mid a, \mathscr{D}, R\right) = \frac{1}{R} \sum_{i \in N_R(a,\mathscr{D})} \mathbb{I}\left(y_i\right) \tag{11}$$

where $\mathscr{D}$ denotes training set of N examples, R corresponds to the number of the nearest points, $N_R(a, \mathscr{D})$ is the set of indices of R nearest points of a in training set $\mathscr{D}$, and $\mathbb{I}(z)$ is the indicator function.

$$\mathbb{I}\left(y\right) = \begin{cases} 1 & \text{if } y \text{ is true} \\ 0 & \text{if } y \text{ is false} \end{cases} \tag{12}$$

LR is a generalization of the linear regression algorithm [58]. In this case, the linear combination of inputs is passed through a sigmoid function, and the Gaussian distribution is replaced by the Bernoulli distribution [58]. The general formula for Logistic Regression is as follows:

$$pr\left(y \mid a, h\right) = Ber\left(y \mid sigm\left(h^T a\right)\right) \tag{13}$$

where $Ber(\cdot)$ stands for Bernoulli distribution, h denotes the weights, and $sigm(\cdot)$ is the sigmoid function.

We employ the training process for the sigmoid activation function. To this end, we optimize the following cost function:

$$\begin{aligned} Q\left(h\right) = -\frac{1}{N} \sum_{n=1}^{N} \Big(& y\left(n\right) \log sigm\left(h^T a\left(n\right)\right) \\ & + \left(1 - y\left(n\right)\right) \log\left(1 - sigm\left(h^T a\left(n\right)\right)\right)\Big) \end{aligned} \tag{14}$$

where N is the number of training examples, $x(n)$ is the training sample, and $y(n)$ is the corresponding correct label. We determine the parameters of LR by applying the Gradient Descent optimization approach. More details on learning algorithm for Logistic Regression can be found, for example, in [58].

5. Experimental Results and Discussion

The proposed algorithm is evaluated on data gathered during the tennis training sessions. The dataset contains the labeled three-axis acceleration measurements captured for serve, backhand, and forehand strokes using the wrist-worn sensor, *the Pebble Watch* (Section 4.1).

In the performance analysis of the proposed approach, we applied both 10-fold cross-validation and leave-one-out methods. The cross-validation-based evaluation technique means that the data from each participant is used in training and testing stages. The leave-one-out technique aims to prove the performance of the algorithm for the new user. In our experiments, we applied one of the versions of this approach, that is, *user-independent*. In this case, data provided by the test user is evaluated based on the training data acquired from the other participants.

To measure the performance of the proposed approach, we applied the accuracy metric. It is the standard metric to summarize the overall performance of the classifier. The accuracy metric is defined as follows.

$$Accuracy = \frac{\text{correct predictions}}{\text{total predictions}} \tag{15}$$

where *correct predictions* correspond to the number of correct predictions and *total predictions* are the total number of predictions.

In this study, the features are generated by the MFCC-based features generator, while PCA was applied as the method to reduce their number. We evaluate the performance of the proposed fusion-based approach for two classifiers: k-NN and Logistic Regression.

In the next subsections, we study the effects of the feature vector size, the window size, and the MFCC-based features vector on the performance of the proposed approach. We also analyze the performance of the proposed algorithm applying the cross-validation and leave-one-out techniques.

5.1. The Effect of Different Number of Features. In this section, we study the impact of a different number of features on the classification performance. To this end, we used the PCA method to extract the proper number of features from the set of MFCC-related features. The extracted features were tested on two classifiers, that is, k-NN and Logistic Regression. In Figure 12, we present the classification performance of the classifiers for different sizes of the features vector.

Figure 12 shows the best classification accuracy of k-NN for the vector size equal to 25 features. Meanwhile for the Logistic Regression-based classifier, we obtain the best performance for a size of feature vector equal to 50.

5.2. The Effect of Window Size. In this section, we discuss the role of the window size in the classification task for both k-NN and Logistic Regression-based approaches. As is shown in Figure 13, when we increase the window size, we also improve the classification performance of k-NN and Logistic Regression classifiers. The optimal window sizes are similar for both methods, and they are equal to 80 samples. When we increase the size of the window, the classification performance decreases.

5.3. The Effect of MFCC-Based Features. In Figure 14, we present the example of MFCC-based features obtained from

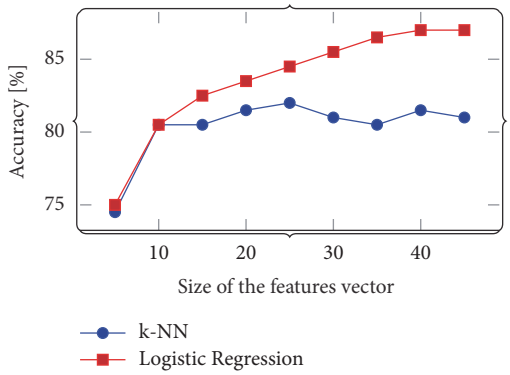

Figure 12: The classification accuracy against the various numbers of features.

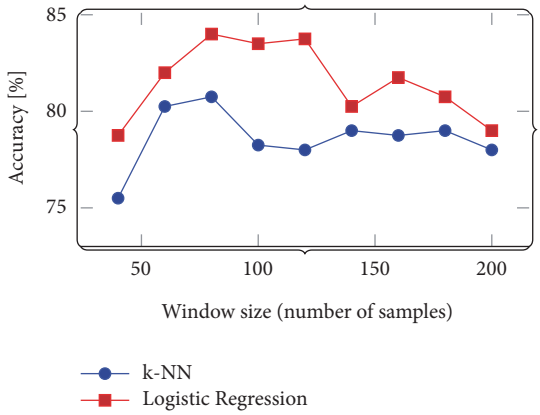

Figure 13: The classification accuracy against the different window sizes.

the acceleration signal acquired from the serve stroke. The section shows the results from the analysis of the effects of MFCC coefficients. In Figure 15, we compare the classification performance of k-NN and Logistic Regression-based methods against the different size of the frame in Discrete Fourier Transform. The optimal size of the frame for k-NN equals 40 samples. Meanwhile for Logistic Regression, we found the optimal size of frame to be equal to 80 samples. It can be seen that further increasing of the frame size for both k-NN and Logistic Regression decreases the classification performance. In our research, we applied optimal size of the frame for the proposed classifiers.

In Figure 16, we present the results of analysis on how the number of filters in MFCC-based generator changes the classification performance. An optimal number of filters for the k-NN method equals 16. The optimal number of filters for Logistic Regression is also equal to 16.

5.4. Analysis Using Cross-Validation. In this section, we assess the predictive performance of the proposed approach. To this end, we applied cross-validation technique. To create the training set and the test set, we applied 10-fold cross-validation procedure. In this study, a 10-fold cross-validation procedure was used to generate the training set and the test set. The training set is used to train k-NN and Logistic Regression algorithms. In the test step, the obtained classes were compared to the true classes in order to measure the classifiers' performance. The performance analysis was tested separately for the two datasets. The first dataset contains the measurements gathered during a tennis training of amateur players. The second dataset is based on the data acquired from the professional players.

In Table 3, we compare the results of performance analysis for both k-NN and Logistic Regression methods. As it is shown, we obtain better results for Logistic Regression with the data acquired from amateur players during training sessions. The k-NN method had the better performance for the dataset collected from the professional players.

5.5. Analysis Using Leave-One-Out. In this section, we analyze the performance of the proposed approach to predict the tennis strokes based on the new data acquired from a new player. In order to evaluate k-NN and Logistic Regression classifiers, we applied the *leave-one-out* evaluation [59]. In Table 4, we present the results obtained based on the data from amateur and professional players. Similarly, Logistic Regression-based classifier obtains better results for amateur players, whereas the k-NN method obtains better results for the professional participants.

6. Conclusions

This work proposed the data fusion-based approach to support the sports training of tennis players. The proposed solution is based on the features determined in the frequency domain. We prepared the datasets for three tennis strokes: backhand, forehand, and serve. The data was divided into two subsets: the first one contained the measurements from amateur players, and the second one comprised the data provided by professional players.

We evaluated two different classification methods: k-NN and Logistic Regression. In 10-fold cross-validation test, the Logistic Regression-based classifier provided better results for the datasets containing the measurements gathered from amateur players and for the collection of data acquired from all participants. The k-NN algorithm achieves better results for the data provided by professional players. We obtain similar results in the leave-one-out evaluation test. Based on our studies, we recommend using the k-NN algorithm to classify the data gathered from professional players and the Logistic Regression method for data acquired from amateur players.

The accuracy of the used classifiers is high, particularly for dataset containing measurements gathered from professional players; however, it is possible to improve the presented results. One of the methods that we plan to use in further works is the Naive-Bayes classifier. Another direction of the future works relates to adding the third level of data fusion. The decision-level data fusion can improve the overall accuracy of the detection and classification algorithm.

The presented data fusion-based algorithm is a useful tool for both the trainer and the trainee. On one hand, it can help the trainer to analyze not only the effects of the specific

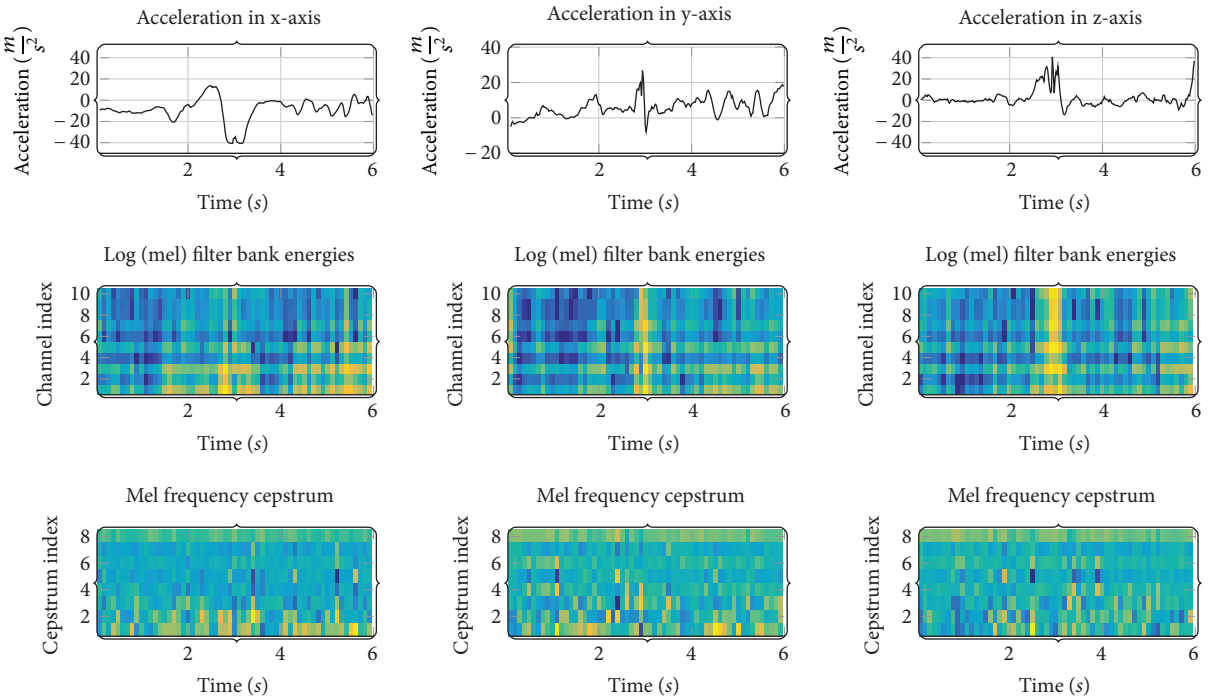

FIGURE 14: The MFCC coefficients of the acceleration measured for the serve stroke.

TABLE 3: The results of classification for k-NN and Logistic Regression algorithms in 10-fold cross-validation evaluation.

Classification method	Amateurs	Professionals	Amateurs and professionals
		Accuracy [%]	
k-NN	79.65 ± 11.36	91.33 ± 10.56	82.22 ± 11.30
Logistic Regression	85.55 ± 8.24	88.44 ± 11.12	87.99 ± 8.48

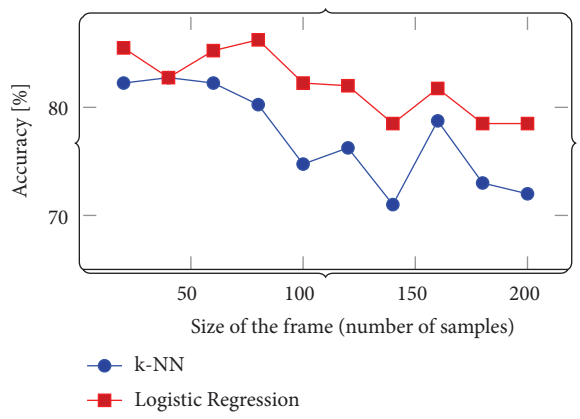

FIGURE 15: The classification accuracy against the different sizes of frame (parameter N_w) in DFT.

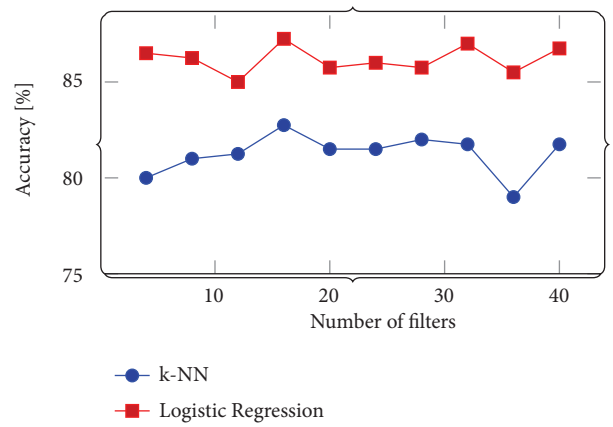

FIGURE 16: The classification accuracy against the different number of filters (parameter Q).

training session but also the trends in a sequence of training sessions. On the other hand, it can be used by the trainee in self-training, for example, to count tennis strokes during each training session. In summary, the data fusion in sports training provides new procedures to process and to analyze the sports training data.

In the future work, we will add more tennis strokes, which can be detected and classified by the proposed method. We

Table 4: The results of classification for k-NN and Logistic Regression algorithms in leave-one-out evaluation.

Classification method	Amateurs	Professionals	Amateurs and professionals
		Accuracy [%]	
k-NN	81.96 ± 10.54	92.22 ± 12.22	82.16 ± 9.79
Logistic Regression	85.12 ± 5.16	88.66 ± 12.37	87.16 ± 6.86

also plan new algorithms extending the systems' functionalities that support the analysis of the tennis strokes.

Data Availability

The dataset used in the research can be downloaded from https://www.ii.pwr.edu.pl/~krzysztof.brzostowski/files/Tenis_dataset.zip.

Conflicts of Interest

The authors declare that they have no conflicts of interest.

References

[1] J. Fister, K. Ljubič, P. N. Suganthan, M. z. Perc, and I. Fister, "Computational intelligence in sports: challenges and opportunities within a new research domain," *Applied Mathematics and Computation*, vol. 262, pp. 178–186, 2015.

[2] D. F. Whelan, M. A. O'Reilly, T. E. Ward, E. Delahunt, and B. Caulfield, "Technology in rehabilitation: Evaluating the single leg squat exercise with wearable inertial measurement units," *Methods of Information in Medicine*, vol. 56, no. 2, pp. 88–94, 2017.

[3] D. Zahradnik and P. Korvas, *The Introduction into Sports Training*, Masaryk University, Brno, Czech Republic, 2012.

[4] J. J. A. Mendes, M. E. Vieira, M. B. Pires, and S. L. Stevan, "Sensor fusion and smart sensor in sports and biomedical applications," *Sensors*, vol. 16, no. 10, 2016.

[5] F. R. Al-Osaimi, "A novel multi-purpose matching representation of local 3D surfaces: a rotationally invariant, efficient, and highly discriminative approach with an adjustable sensitivity," *IEEE Transactions on Image Processing*, vol. 25, no. 2, pp. 658–672, 2016.

[6] A. Ahmadi, E. Mitchell, C. Richter et al., "Toward automatic activity classification and movement assessment during a sports training session," *IEEE Internet of Things Journal*, vol. 2, no. 1, pp. 23–32, 2015.

[7] P. Siirtola, P. Laurinen, J. Roning, and H. Kinnunen, "Efficient accelerometer-based swimming exercise tracking," in *Proceedings of the IEEE Symposium on Computational Intelligence and Data Mining (CIDM '11)*, pp. 156–161, 2011.

[8] R. Burchfield and S. Venkatesan, "A framework for golf training using low-cost inertial sensors," in *Proceedings of the 2010 International Conference on Body Sensor Networks, BSN 2010*, pp. 267–272, sgp, June 2010.

[9] A. Ahmadi, D. Rowlands, and D. A. James, "Towards a wearable device for skill assessment and skill acquisition of a tennis player during the first serve," *Sports Engineering*, vol. 2, no. 3-4, pp. 129–136, 2010.

[10] D. L. Hall and J. Llinas, "An introduction to multisensor data fusion," *Proceedings of the IEEE*, vol. 85, no. 1, pp. 6–23, 1997.

[11] Ó. D. Lara and M. A. Labrador, "A survey on human activity recognition using wearable sensors," *IEEE Communications Surveys & Tutorials*, vol. 15, no. 3, pp. 1192–1209, 2013.

[12] M. Munoz-Organero and A. Lotfi, "Human movement recognition based on the stochastic characterisation of acceleration data," *Sensors*, vol. 16, no. 9, 2016.

[13] Adidas. Micoach, April 2018.

[14] Nike. Nike+, April 2018.

[15] Y. Iijima, K. Watanabe, K. Kobayashi, and Y. Kurihara, "Measurement and analysis of tennis swing motion using 3D gyro sensor," in *Proceedings of the SICE Annual Conference*, pp. 274–277, 2010.

[16] A. Ahmadi, D. D. Rowlands, and D. A. James, "Investigating the translational and rotational motion of the swing using accelerometers for athlete skill assessment," in *Proceedings of the 2006 5th IEEE Conference on Sensors*, pp. 980–983, kor, October 2006.

[17] A. Ahmadi, D. D. Rowlands, and D. A. James, "Development of inertial and novel marker-based techniques and analysis for upper arm rotational velocity measurements in tennis," *Sports Engineering*, vol. 12, no. 4, pp. 179–188, 2010.

[18] Indiegogo. Pivot, April 2018.

[19] Babolatplay. Babolat pop, April 2018.

[20] M. Sharma, R. Srivastava, A. Anand, D. Prakash, and L. Kaligounder, "Wearable motion sensor based phasic analysis of tennis serve for performance feedback," in *Proceedings of the IEEE International Conference on Acoustics, Speech, and Signal Processing (ICASSP '17)*, pp. 5945–5949, 2017.

[21] D. Connaghan, P. Kelly, N. E. O'Connor, M. Gaffney, M. Walsh, and C. O'Mathuna, "Multi-sensor classification of tennis strokes," in *Proceedings of the IEEE Sensors*, pp. 1437–1440, 2011.

[22] W. Pei, J. Wang, X. Xu, Z. Wu, and X. Du, "An embedded 6-axis sensor based recognition for tennis stroke," in *Proceedings of the 2017 IEEE International Conference on Consumer Electronics (ICCE '17)*, pp. 55–58, January 2017.

[23] M. Kos, J. Ženko, D. Vlaj, and I. Kramberger, "Tennis stroke detection and classification using miniature wearable IMU device," in *Proceedings of the 23rd International Conference on Systems, Signals and Image Processing, IWSSIP 2016*, pp. 1–4, 2016.

[24] L. Jiao, H. Wu, R. Bie, A. Umek, and A. Kos, "Multi-sensor Golf Swing Classification Using Deep CNN," *Procedia Computer Science*, vol. 129, pp. 59–65, 2018.

[25] C. Ó. Conaire, D. Connaghan, P. Kelly, N. E. O'Connor, M. Gaffney, and J. Buckley, "Combining inertial and visual sensing for human action recognition in tennis," in *Proceedings of the first ACM international workshop on Analysis and retrieval of tracked events and motion in imagery streams*, pp. 51–56, 2010.

[26] Y. Zhang, K. Chen, and J. Yi, "Rider trunk and bicycle pose estimation with fusion of force/inertial sensors," *IEEE Transactions on Biomedical Engineering*, vol. 60, no. 9, pp. 2541–2551, 2013.

[27] B. Khaleghi, A. Khamis, and F. Karray, "Multisensor data fusion," *Algorithms and Architectural Design to Applications*, 15 pages, 2015.

[28] R. Gravina, P. Alinia, H. Ghasemzadeh, and G. Fortino, "Multi-sensor fusion in body sensor networks: State-of-the-art and research challenges," *Information Fusion*, vol. 35, pp. 1339–1351, 2017.

[29] W. Elmenreich, *An Introduction to Sensor Fusion*, Vienna University of Technology, Austria, 2002.

[30] l. Wald, *Data Fusion: Definitions And Architectures: Fusion of Images of Different Spatial Resolutions*, Presses des MINES, 2002.

[31] J. Llinas, D. L Hall, and M. E Liggins, *Handbook of Multisensor Data Fusion: Theory and Practice*, CRC Press, 2009.

[32] R. C. King, E. Villeneuve, R. J. White, R. S. Sherratt, W. Holderbaum, and W. S. Harwin, "Application of data fusion techniques and technologies for wearable health monitoring," *Medical Engineering & Physics*, vol. 42, pp. 1–12, 2017.

[33] G. Z. Yang and M. Yacoub, *Body Sensor Networks*, Springer, 2006.

[34] A. K. Chowdhury, D. Tjondronegoro, V. Chandran, and S. G. Trost, "Physical Activity Recognition Using Posterior-Adapted Class-Based Fusion of Multiaccelerometer Data," *IEEE Journal of Biomedical and Health Informatics*, vol. 22, no. 3, pp. 678–685, 2018.

[35] M. Liggins, D. Hall, and J. Llinas, *Handbook of Multisensor Data Fusion: Theory And Practice*, CRC press, 2017.

[36] O. Basir and X. H. Yuan, "Engine fault diagnosis based on multi-sensor information fusion using Dempster-Shafer evidence theory," *Information Fusion*, vol. 8, no. 4, pp. 379–386, 2007.

[37] M. Kam, X. Zhu, and P. Kalata, "Sensor fusion for mobile robot navigation," *Proceedings of the IEEE*, vol. 85, no. 1, pp. 108–119, 1997.

[38] J. Kelly and G. S. Sukhatme, "Visual-inertial sensor fusion: Localization, mapping and sensor-to-sensor Self-calibration," *International Journal of Robotics Research*, vol. 30, no. 1, pp. 56–79, 2011.

[39] K. Bernardin, K. Ogawara, K. Ikeuchi, and R. Dillmann, "A sensor fusion approach for recognizing continuous human grasping sequences using hidden Markov models," *IEEE Transactions on Robotics*, vol. 21, no. 1, pp. 47–57, 2005.

[40] R. Tan, G. Xing, J. Chen, W. Song, and R. Huang, "Fusion-based volcanic earthquake detection and timing in wireless sensor networks," *ACM Transactions on Sensor Networks*, vol. 9, no. 2, pp. 1–25, 2013.

[41] L. Snidaro, R. Niu, P. K. Varshney, and G. L. Foresti, "Automatic camera selection and fusion for outdoor surveillance under changing weather conditions," in *Proceedings of the IEEE Conference on Advanced Video and Signal Based Surveillance (AVSS '03)*, pp. 364–369, 2003.

[42] G. K. Matsopoulos, S. Marshall, and J. N. H. Brunt, "Multiresolution morphological fusion of MR and CT images of the human brain," *IEE Proceedings Vision, Image and Signal Processing*, vol. 141, no. 3, pp. 137–142, 1994.

[43] M. Raza, I. Gondal, D. Green, and R. L. Coppel, "Classifier fusion to predict breast cancer tumors based on microarray gene expression data," in *Proceedings of the International Conference on Knowledge-Based and Intelligent Information and Engineering Systems*, pp. 866–874, Springe.

[44] H. Li, R. Deklerck, B. De Cuyper, E. Nyssen, J. Cornelis, and A. Hermanus, "Object Recognition in Brain CT-Scans: Knowledge-Based Fusion of Data from Multiple Feature Extractors," *IEEE Transactions on Medical Imaging*, vol. 14, no. 2, pp. 212–229, 1995.

[45] K. Brzostowski, "Novel approach to human walking speed enhancement based on drift estimation," *Biomedical Signal Processing and Control*, vol. 42, pp. 18–29, 2018.

[46] K. Brzostowski, "Toward the Unaided Estimation of Human Walking Speed Based on Sparse Modeling," *IEEE Transactions on Instrumentation and Measurement*, vol. 67, no. 6, pp. 1389–1398, 2018.

[47] W. Zhang and Z. Zhang, "Belief function based decision fusion for decentralized target classification in wireless sensor networks," *Sensors*, vol. 15, no. 8, pp. 20524–20540, 2015.

[48] T. Fukada, K. Tokuda, T. Kobayashi, and S. Imai, "An adaptive algorithm for mel-cepstral analysis of speech," in *Proceedings of the 1992 International Conference on Acoustics, Speech, and Signal Processing (ICASSP '92)*, vol. 1, pp. 137–140, 1992.

[49] M. M. M. Fahmy, "Palmprint recognition based on Mel frequency Cepstral coefficients feature extraction," *Ain Shams Engineering Journal*, vol. 1, no. 1, pp. 39–47, 2010.

[50] N. Sato and Y. Obuchi, "Emotion recognition using mel-frequency cepstral coefficients," *Information and Media Technologies*, vol. 2, no. 3, pp. 835–848, 2007.

[51] N. V. Cuong, V. Dinh, and L. S. T. Ho, "Mel-frequency cepstral coefficients for eye movement identification," in *Proceedings of the IEEE 24th International Conference on Tools with Artificial Intelligence (ICTAI '12)*, vol. 1, pp. 253–260, 2012.

[52] R. San-Segundo, J. M. Montero, R. Barra-Chicote, F. Fernández, and J. M. Pardo, "Feature extraction from smartphone inertial signals for human activity segmentation," *Signal Processing*, vol. 120, pp. 359–372, 2016.

[53] L. D. Enochson and K. R. Otnes, "Programming and analysis for digital time series data," DTIC Document, 1968.

[54] R. O. Duda, P. E. Hart, and D. G. Stork, *Pattern Classification*, John Wiley & Sons, 2012.

[55] S. Dreiseitl and L. Ohno-Machado, "Logistic regression and artificial neural network classification models: a methodology review," *Journal of Biomedical Informatics*, vol. 35, no. 5-6, pp. 352–359, 2002.

[56] C. M. Bishop, *Pattern Recognition and Machine Learning*, Springer, New York, NY, USA, 2006.

[57] T.-S. Lim, W.-Y. Loh, and Y.-S. Shih, "Comparison of prediction accuracy, complexity, and training time of thirty-three old and new classification algorithms," *Machine Learning*, vol. 40, no. 3, pp. 203–228, 2000.

[58] K. P Murphy, *Machine Learning: A Probabilistic Perspective*, MIT press, 2012.

[59] R. Kohavi, "A study of cross-validation and bootstrap for accuracy estimation and model selection," in *Proceedings of the 14th International Joint Conference on Artificial Intelligence (IJCAI '95)*, vol. 14, pp. 1137–1145, Montreal, Canada, August 1995.

Hindawi
Wireless Communications and Mobile Computing
Volume 2018, Article ID 8430626, 5 pages
https://doi.org/10.1155/2018/8430626

Research Article

Compact Microstrip Lowpass Filter with Low Insertion Loss for UWB Medical Applications

Mohammed A. Aseeri, Meshaal A. Alyahya, Hatim A. Bukhari, and Hussein N. Shaman

National Centre for Sensors and Defense Systems Technologies (NCSDST), King Abdulaziz City for Science and Technology (KACST), Riyadh 11442, Saudi Arabia

Correspondence should be addressed to Mohammed A. Aseeri; masseri@kacst.edu.sa

Received 21 February 2018; Accepted 13 May 2018; Published 6 June 2018

Academic Editor: Seyed M. Buhari

A microstrip lowpass filter based on transmission line elements for UWB medical applications is proposed in this paper. The filter is constructed of two symmetric shunt open-circuited stubs and three series unit elements. The filter is designed to exhibit an elliptic function response with equal ripple in the passband and the rejection band. A prototype is successfully designed, fabricated, and measured, where a good agreement is attained. The filter shows a high filtering selectivity and an ultra-wide stopband up to 20 GHz with an attenuation level of more than 20-dB. The filter is compact and has a low insertion loss and an ultra-wideband (UWB) rejection which makes it attractive for many technologies such as UWB medical applications.

1. Introduction

Ultra-wideband (UWB) technology has several features which makes it suitable for the application of medical monitoring such as penetrating through obstacles, high precision ranging at the centimeter level, low electromagnetic radiation, and low processing energy consumed. These monitoring applications could be patient motion monitoring, wireless vital signs monitoring of human body, and the medicine storage monitoring. One of the primary passive components of the UWB systems is lowpass filter which is necessary for blocking unwanted signals and suppressing spurious harmonics.

Lowpass planer filters with sharp roll-off, wide stopband, compact circuit size, and low insertion loss are in high demand in modern wireless communication systems and military radar receiver systems for blocking unwanted signals and suppressing spurious harmonics. A general common microstrip structure of lowpass filter is using high and low impedance (stepped-impedance) transmission lines which is known as stepped-impedance lowpass filter [1]. This type of filter has simple design methodology but it exhibits a poor skirt selectivity and a very low attenuation level at the rejection band. In order to improve the filter performance at the stopband, the low-impedance line can be replaced with a quarter guided wavelength open-circuited stub [2]. The open-circuited stub shorts can out the transmission at the resonant frequency and therefore a wider rejection band with a transmission zero can be obtained. Alternatively, a longitudinal slot can be implemented in the ground plane of a stepped-impedance filter to enhance its performance [3]. Due to the slow-wave effect of the slot-back microstrip line, the filter can exhibit a wider stopband and a sharper cut-off compared with the conventional filter. Other techniques can also be used to enhance the performance of the stepped-impedance filters such as stepped-impendence hairpin resonators [4, 5], folded stepped-impedance resonators [6], defected ground-plane structures (DGS) slot [7–12], and interdigital or semicircle defected ground-plane structures (DGS) [13, 14]. In addition, various methods and structure have been developed to enhance the performance of microstrip lowpass filters such as using circular-shaped patches and open stubs [15], rat-race directional couplers [16], stepped-impedance spiral resonator [17], combination of DGSs and a transformed radial stub (TRS) [18], T-shaped microstrip resonator cells [19], and coupled-line stub-loaded hairpin unit [20] and triangular and radial patch resonators [21].

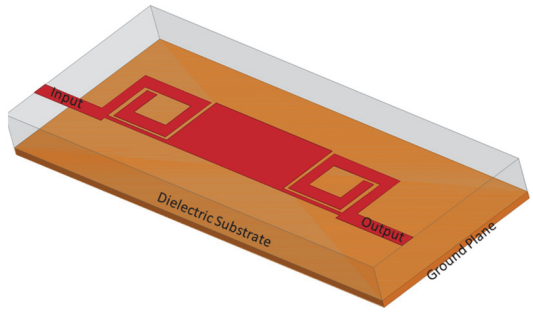

Figure 1: 3D view of the proposed microstrip lowpass filter.

Lowpass filter can also be designed using distributed elements such as open-circuited stubs and unit elements [2]. This type of filter has spurious harmonics and therefore, it requires more elements to enhance its performance. Alternatively, a cross-coupling can be introduced between the input/output feed lines to allow the filter to exhibit additional transmission zeros at the rejection band [22]. This proposed filter can be used in many technologies such as UWB medical applications [23].

A compact lowpass filter with an elliptic function response and a very wide rejection band is introduced in this paper. The filter is constructed of three series unit elements and two shunt open-circuited stubs. The filter is designed to provide an equal ripple in the passband and the rejection band. It is designed to have a passband with a sharp selectivity and an ultra-wide stopband. The proposed designed is implemented on a microstrip substrate and fabricated using printed-circuited-board (PCB). The filter design, analysis, and measurement results are demonstrated in detail.

2. Filter Design

The 3-dimensional view of the microstrip design of the proposed filter is shown in Figure 1 and Figure 2 illustrates its transmission line equivalent circuit model. The filter is comprised of two symmetric shunt open-circuited stubs, with a characteristic impedance of Z_s, separated by three series unit elements or connecting lines with characteristic impedances of Z_1 and Z_2. The open-circuited stub has an electrical length of θ_s while the electrical lengths of the unit elements are described by θ_1 and θ_2.

The $ABCD$ matrix (M_t) of the equivalent circuit model can be written as

$$M_t = \begin{bmatrix} A_t & B_t \\ C_t & D_t \end{bmatrix} = M_s M_1 M_2 M_1 M_s, \quad (1)$$

where M_s is the $ABCD$ matrix of the open-circuited stub and M_n is the $ABCD$ matrix for the unit elements (for $n = 1, 2$) which can be defined by

$$M_s = \begin{bmatrix} 1 & 0 \\ \dfrac{j \tan \theta_s}{Z_s} & 1 \end{bmatrix}$$

Table 1: Circuit parameters for the proposed filter at 4.0 GHz.

Parameter	Z_o	Z_s	Z_1	Z_2	θ_s	θ_1	θ_2
Value	50 Ω	96 Ω	170 Ω	20.2 Ω	90°	30°	60°

$$M_n = \begin{bmatrix} \cos \theta_n & jZ_n \sin \theta_n \\ \dfrac{j \sin \theta_n}{Z_n} & \cos \theta_n \end{bmatrix} \quad (2)$$

For a feed line impedance of Z_o, the insertion loss (S_{21}) and return loss (S_{11}) responses can be computed as follows:

$$S_{21} = \frac{2\left(A_t D_t - B_t C_t\right)}{A_t + B_t/Z_o + C_t Z_o + D_t}$$
$$S_{11} = \frac{A_t + B_t/Z_o - C_t Z_o - D_t}{A_t + B_t/Z_o + C_t Z_o + D_t} \quad (3)$$

In general, a transmission line filter with quarter-wavelength elements ($\theta_s = \theta_1 = \theta_2 = \lambda/4$ at f_o) has all of its transmission zeros at a single frequency, e.g., midstopband frequency (f_o). Therefore, it requires more elements to enhance the selectivity and to increase the bandwidth of the rejection band. Alternatively, the circuit elements are designed to have different or unequal electrical lengths to allow the filter to exhibit three transmission zeros inside the rejection band, at $f_o/3$, f_o, and $5f_o/3$. In this case, the electrical lengths are chosen to be $\theta_s = 3\theta_1 = 2\theta_2$ at the midstopband (f_o). In order to show the performance of this new structure, the filter is designed to have a cut-off frequency at about 3.0 GHz. The filter is also designed to have a return loss of more than 24-dB within the desired passband and an insertion loss of more than 20-dB over the whole rejection band. Furthermore, the filter is designed to generate three transmission zeros at the rejection band at 4.0 GHz, 12 GHz, and 20 GHz. In order to achieve this, the circuit model is optimized based on the above formulations and the calculated parameters are displayed in Table 1. The calculated magnitude response, of the circuit model using the parameters values in Table 1, is demonstrated in Figure 3. As can be noticed, the filter exhibits three transmission zeros which are widely separated from each other providing a very ultra-wide rejection band with high selectivity. These transmission zeros are generated by the two open-circuited stubs. This is because the length of each open-circuited stub (θ_s) is a quarter-wavelength at 4.0 GHz and therefore, its fundamental resonant frequency is generated at 4.0 GHz and it has spurious resonant frequencies occur at odd multiples of the fundamental one. Hence, the first and second spurious resonant frequencies are located at 12 GHz and 20 GHz as shown in Figure 4. Since the first three resonant frequencies of the open-circuited stubs are located inside the rejection band, the filter exhibits vey wide stopband. The filter exhibits an equal ripple for the return loss at the passband and for the insertion loss at the rejection band. Furthermore, addition, the first resonant frequency of the stub is located close to the cut-off frequency of the lowpass filter leading to a sharp rate of cut-off.

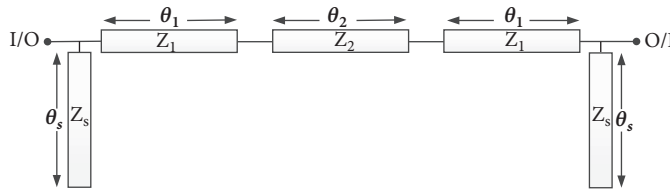

Figure 2: Equivalent circuit model of proposed lowpass filter.

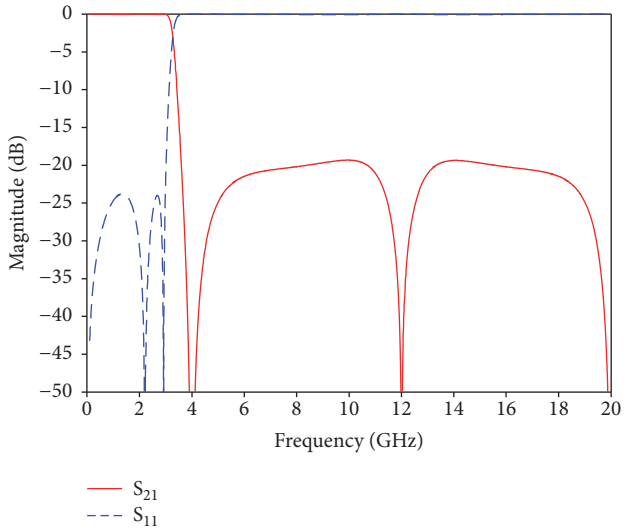

Figure 3: Calculated performance of the circuit model in Figure 2 with the parameters values in Table 1.

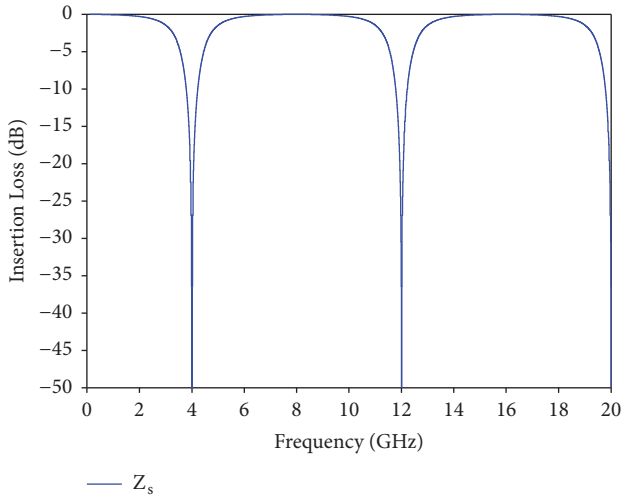

Figure 4: Calculated insertion loss of the open-circuited stub connected to 50 Ohm line.

3. Microstrip Design and Experiment Results

The proposed filter design is constructed on a RT Duroid 5880 substrate with $\varepsilon r = 2.2$ and thickness 0.254 mm and the microstrip layout is demonstrated in Figure 5. Based on the microstrip design equations in [2] with a slight tuning,

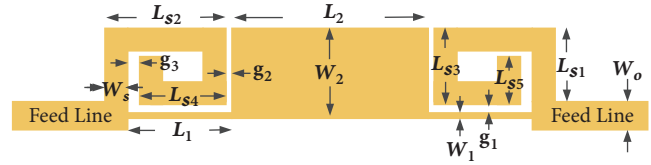

Figure 5: Microstrip layout of the proposed filter.

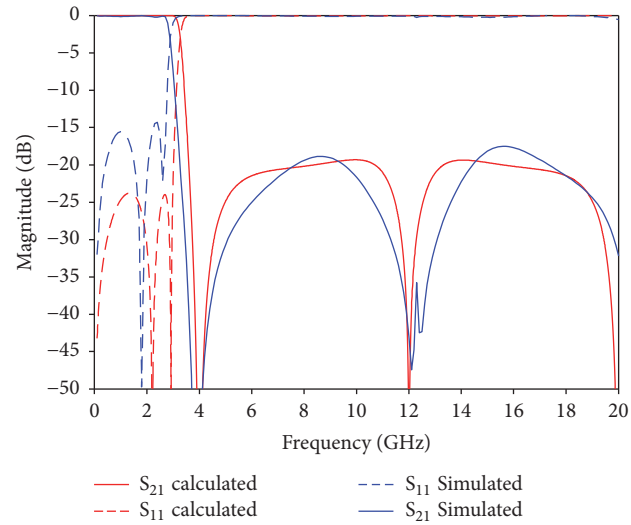

Figure 6: Calculated and simulated responses of the proposed filter.

the parameters of the microstrip layout are as follows: $W_o = 0.75$ mm, $W_s = 0.7$ mm, $W_1 = 0.05$ mm, $W_2 = 3.4$ mm, $L_{s1} = 3.0$ mm, $L_{s2} = 4.65$ mm, $L_{s3} = 3.15$ mm, $L_{s4} = 3.65$ mm, $L_{s5} = 2.3$ mm, $L_1 = 4.2$ mm, $L_2 = 8.2$ mm, $g_1 = g_2 = 0.25$ mm, and $g_3 = 0.3$ mm. The open-circuited stubs are folded in a rectangular spiral shape to reduce the filter size. The distance g_2 is optimized to have no effect on the filter performance. The microstrip layout is simulated using a commercially available tool [24] and the simulated performance is compared with the calculated results as depicted in Figure 6. Good agreement between the theoretical and simulated responses is obtained. However, there is a slight difference between the simulated and the theoretical passband. The microstrip layout can be further tuned to reduce the effect of discontinuity and to obtain a better agreement. A prototype of this filter is successfully fabricated and measured and Figure 7 shows a photograph of the fabricated filter. The fabricated filter is very small with an overall size of about 18.0 mm by 3.75 mm. The measured

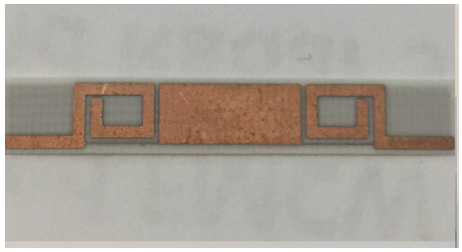

Figure 7: Photograph of fabricated filter.

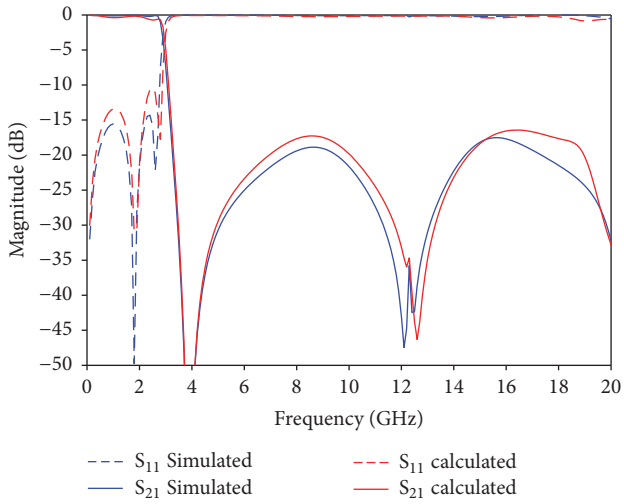

Figure 8: Simulated and measured insertion and return losses of the fabricated filter.

performance of the prototype is compared with the simulated results and demonstrated in Figure 8. The experimental filter shows excellent results with an insertion loss of about 0.4 dB at the passband centre frequency. It also exhibits an ultra-wide rejection band up to 20 GHz with three transmission zeros and an attenuation level of more than 20-dB. The filter shows an equal ripple for the return loss at the passband and for the insertion loss at the stopband. A performance comparison between published works and proposed filter is demonstrated in Table 2. It can be noticed that the proposed filter shows wider stopband bandwidth.

4. Conclusion

In this paper, a microstrip lowpass filter based on transmission line elements is proposed. The filter has been constructed of three series unit elements between two symmetric shunt open-circuited stubs. The filter has been designed to have a cut-off frequency at about 3.0 GHz. In order to allow the filter to exhibit an equal ripple in both passband and rejection band, the open-circuited stub has been designed to have its first three resonant frequencies inside the stopband. A prototype has been successfully designed, fabricated, and measured, where excellent agreement between the expected and measured performances is obtained. The filter exhibits a quasielliptic function response leading to a high filtering selectivity and an extended stopband up to 20 GHz with an attenuation level of more than 20-dB. Due to the small size, low insertion loss, and wide rejection band, the proposed filter looks attractive for making it attractive for many technologies such as UWB medical applications.

Table 2: Performance comparisons between published works and proposed filter.

Ref	Relative stopband bandwidth	Rejection level (dB)	Up to
[3]	0.92	20	6.8 GHz
[4]	1.54	14	17 GHz
[5]	1.52	10	12 GHz
[7]	0.85	15	5 GHz
[8]	1.45	20	20 GHz
[9]	1.07	10	10 GHz
[11]	0.58	15	10 GHz
[12]	1.2	30	10 GHz
[13]	1.36	10	16 GHz
[16]	1.42	10	6 GHz
[17]	1.14	15	11 GHz
[18]	1.2	10	20 GHz
[19]	1.2	10	8 GHz
[20]	1.407	20	4.5 GHz
[21]	1.3	20	19 GHz
[22]	0.8	30	5 GHz
This work	*1.5*	*20*	*20 GHz*

Data Availability

The data used to support the findings of this study are available from the corresponding author upon request.

Conflicts of Interest

The authors declare that they have no conflicts of interest.

Acknowledgments

This work is sponsored by King Abdulaziz City for Science and Technology (KACST).

References

[1] G. L. Matthaei, L. Young, and E. M. T. Jones, *Microwave Filters, Impedance-Matching Network, and Coupling Structures*, Artech House, Norwood, Mass, USA, 1980.

[2] J. Hong and M. J. Lancaster, *Microstrip Filters for RF/Microwave Applications*, John Wiley & Sons, New York, NY, USA, 2001.

[3] S. Y. Huang and Y. H. Lee, "Compact stepped-impedance low-pass filter with a slot-back microstrip line," *Microwave and Optical Technology Letters*, vol. 50, no. 4, pp. 1058–1061, 2008.

[4] F. Zhang, S. Liu, P. Zhao, M. Du, X. Zhang, and J. Xu, "Compact ultra-wide stopband lowpass filter using transformed

stepped impedance hairpin resonator," in *Proceedings of the 2017 IEEE International Symposium on Antennas and Propagation & USNC/URSI National Radio Science Meeting*, pp. 2227-2228, 2017.

[5] M. H. Yang and J. Xu, "Design of compact, broad-stopband lowpass filter using modified stepped impedance hairpin resonators," *IEEE Electronics Letters*, vol. 44, no. 20, pp. 1198–1200, 2008.

[6] S. Pinel, R. Bairavasubramanian, J. Laskar, and J. Papapolymerou, "Compact planar and vialess composite low-pass filters using folded stepped-impedance resonator on liquid-crystal-polymer substrate," *IEEE Transactions on Microwave Theory and Techniques*, vol. 53, no. 5, pp. 1707–1712, 2005.

[7] A. B. Abdel-Rahman, A. K. Verma, A. Boutejdar, and A. S. Omar, "Control of bandstop response of Hi-Lo microstrip low-pass filter using slot in ground plane," *IEEE Transactions on Microwave Theory and Techniques*, vol. 52, no. 3, pp. 1008–1013, 2004.

[8] S. Sen and T. Moyra, "Design of a Chebyshev stripline based lowpass filter using open stubs and Defected Ground Structure (DGS)," in *Proceedings of the 2016 IEEE International Conference on Wireless Communications, Signal Processing and Networking, WiSPNET 2016*, pp. 936–939, Chennai, India, March 2016.

[9] D. Ahn, J. Park, C. Kim, J. Kim, Y. Qian, and T. Itoh, "A design of the low-pass filter using the novel microstrip defected ground structure," *IEEE Transactions on Microwave Theory and Techniques*, vol. 49, no. 1, pp. 86–93, 2001.

[10] T. Kim and C. Seo, "A novel photonic bandgap structure for low-pass filter of wide stopband," *IEEE Microwave and Guided Wave Letters*, vol. 10, no. 1, pp. 13–15, 2000.

[11] H. Fu and Y. Yu, "A novel lowpass filter based on multistage defected ground structure," in *Proceedings of the 16th IEEE International Conference on Ubiquitous Wireless Broadband, ICUWB 2016*, Nanjing, China, October 2016.

[12] L.-H. Hsieh and K. Chang, "Compact elliptic-function low-pass filters using microstrip stepped-impedance hairpin resonators," *IEEE Transactions on Microwave Theory and Techniques*, vol. 51, no. 1, pp. 193–199, 2003.

[13] F. Wei, L. Chen, X.-W. Shi, Q.-L. Huang, and X.-H. Wang, "Compact lowpass filter with wide stop-band using coupled-line hairpin unit," *IEEE Electronics Letters*, vol. 46, no. 1, pp. 88–90, 2010.

[14] A. Balalem, A. R. Ali, J. Machac, and A. Omar, "Quasi-elliptic microstrip low-pass filters using an interdigital DGS slot," *IEEE Microwave and Wireless Components Letters*, vol. 17, no. 8, pp. 586–588, 2007.

[15] G. Karimi, A. Lalbakhsh, and H. Siahkamari, "Design of sharp roll-off lowpass filter with ultra wide stopband," *IEEE Microwave and Wireless Components Letters*, vol. 23, no. 6, pp. 303–305, 2013.

[16] R. Gómez-García, M.-A. Sánchez-Soriano, M. Sánchez-Renedo, G. Torregrosa-Penalva, and E. Bronchalo, "Extended-stopband microstrip lowpass filter using rat-race directional couplers," *IEEE Electronics Letters*, vol. 49, no. 4, pp. 281-282, 2013.

[17] S. Majidifar, S. V. Makki, A. Ahmadi, and S. Alirezaee, "Compact microstrip lowpass filter using stepped impedance spiral resonator," in *Proceedings of the 2012 4th International Conference on Computational Intelligence and Communication Networks (CICN)*, pp. 23–26, Mathura, Uttar Pradesh, India, November 2012.

[18] S. Xu, K. Ma, F. Meng, and K. S. Yeo, "DGS embedded transformed radial stub for ultra-wide stopband lowpass filter," *IEEE Electronics Letters*, vol. 48, no. 23, pp. 1473–1475, 2012.

[19] K. Zhao, L. Li, and Y. Wang, "A Novel lowpass filter using three corner-cutting T-shaped compact microstrip resonator cells," in *Proceedings of the 2012 Spring Congress on Engineering and Technology (S-CET)*, pp. 1–3, Xi'an, China, May 2012.

[20] V. K. Velidi and S. Sanyal, "Sharp roll-off lowpass filter with wide stopband using stub-loaded coupled-line hairpin unit," *IEEE Microwave and Wireless Components Letters*, vol. 21, no. 6, pp. 301–303, 2011.

[21] M. Hayati, S. Naderi, and F. Jafari, "Compact microstrip lowpass filter with sharp roll-off using radial resonator," *IEEE Electronics Letters*, vol. 50, no. 10, pp. 761-762, 2014.

[22] H. Shaman and J.-S. Hong, "Wideband bandstop filter with cross-coupling," *IEEE Transactions on Microwave Theory and Techniques*, vol. 55, no. 8, pp. 1780–1785, 2007.

[23] E. Pancera, "Medical applications of the ultra wideband technology," in *Proceedings of the 6th Loughborough Antennas and Propagation Conference, LAPC 2010*, pp. 52–56, Loughborough, UK, November 2010.

[24] Sonnet Software Inc., EM User's Manual, Ver. 12, NY 2005.

Hindawi
Wireless Communications and Mobile Computing
Volume 2018, Article ID 1013234, 12 pages
https://doi.org/10.1155/2018/1013234

Research Article

A Novel Technique for Speech Recognition and Visualization Based Mobile Application to Support Two-Way Communication between Deaf-Mute and Normal Peoples

Kanwal Yousaf[1], **Zahid Mehmood**[1], **Tanzila Saba**[2], **Amjad Rehman**[3], **Muhammad Rashid**[4], **Muhammad Altaf**[5] and **Zhang Shuguang**[6]

[1]*Department of Software Engineering, University of Engineering and Technology, Taxila 47050, Pakistan*
[2]*College of Computer and Information Sciences, Prince Sultan University, Riyadh 11586, Saudi Arabia*
[3]*College of Computer and Information Systems, Al-Yamamah University, Riyadh 11512, Saudi Arabia*
[4]*Department of Computer Engineering, Umm Al-Qura University, Makkah 21421, Saudi Arabia*
[5]*Department of Mathematics, University of Engineering and Technology, Taxila 47050, Pakistan*
[6]*Department of Statistics and Finance, University of Science and Technology of China, Hefei 23026, China*

Correspondence should be addressed to Kanwal Yousaf; kanwal.yousaf@uettaxila.edu.pk

Received 15 January 2018; Accepted 17 April 2018; Published 24 May 2018

Academic Editor: Seyed M. Buhari

Mobile technology is very fast growing and incredible, yet there are not much technology development and improvement for Deaf-mute peoples. Existing mobile applications use sign language as the only option for communication with them. Before our article, no such application (app) that uses the disrupted speech of Deaf-mutes for the purpose of social connectivity exists in the mobile market. The proposed application, named as vocalizer to mute (V2M), uses automatic speech recognition (ASR) methodology to recognize the speech of Deaf-mute and convert it into a recognizable form of speech for a normal person. In this work mel frequency cepstral coefficients (MFCC) based features are extracted for each training and testing sample of Deaf-mute speech. The hidden Markov model toolkit (HTK) is used for the process of speech recognition. The application is also integrated with a 3D avatar for providing visualization support. The avatar is responsible for performing the sign language on behalf of a person with no awareness of Deaf-mute culture. The prototype application was piloted in social welfare institute for Deaf-mute children. Participants were 15 children aged between 7 and 13 years. The experimental results show the accuracy of the proposed application as 97.9%. The quantitative and qualitative analysis of results also revealed that face-to-face socialization of Deaf-mute is improved by the intervention of mobile technology. The participants also suggested that the proposed mobile application can act as a voice for them and they can socialize with friends and family by using this app.

1. Introduction

Historically the term *deaf-mute* referred to the person who was either deaf using sign language as a source of communication or both deaf and unable to speak. This term continues to be used to refer to the person who is deaf but has some degree of speaking ability [1]. In deaf community, the word *deaf* is spelled in two separate ways. The small "d" deaf represents a person's level of hearing through audiology and being not associated with the other members of the deaf community whereas the capital "D" Deaf indicates the culturally Deaf people who use sign language for communication [2].

According to world federation of the deaf (WFD) over 5% of the world's population (≈360 million people) has disabling hearing loss including 328 million adults and 32 million children [3]. The degree of hearing loss is categorized into mild, moderate, severe, or profound levels [4]. Hearing loss of a person has a direct impact on his/her speech and language development. People with severe or profound hearing loss have higher voice handicap index (VHI) scores than those who suffer from mild hearing loss [5]. A person with mild hearing loss has less problems in speech development as he/she might not be able to hear certain sounds and the speech clarity is not affected that much. A person with severe or profound hearing

loss can have a severe problem in speech development and usually relies on sign language as a source of communication.

Deaf people face many irritations and frustrations that limit their ability to do everyday tasks. Research indicated [6] that Deaf people, especially Deaf children, have high rates of behavioral and emotional issues in relation to different methods of communication. Most people with such disabilities become introverts and resist social connectivity and face-to-face socialization. The inability to speak with family and friends can cause low self-esteem and may result in social isolation of Deaf person. It is not only that they lack social interactions but communication is also a major barrier to Deaf-mute healthcare [7]. In such conditions, it becomes difficult for the caretaker to interact with the deaf person.

Different medical treatments are available for the deaf community in order to get rid of their deafness but the cost of these treatments are expensive [8]. A report of world health organization (WHO) 2017 [9] states that there are different types of costs associated with hearing loss, which are as follows: (1) direct costs: they include the cost associated with hearing loss incurred by healthcare systems; some other types of direct costs include the education support for such children; (2) indirect costs: they include the loss of productivity and usually refer to the cost of individual being unable to contribute to the economy; and (3) intangible costs: they refer to the stigma experienced by the families that are experiencing the hearing loss. This report concludes that unaddressed hearing loss poses substantial costs to the healthcare system and to the economy as a whole.

Many communication channels are available, through which Deaf-mute people can deliver their messages, e.g., notes, helper pages, sign language, books with letters, lip reading, and gestures. Despite these channels, there are many problems which are encountered by Deaf-mutes and normal people during communication. The problem is not confined only to a Deaf-mute person who is unable to hear or speak, but another problem is lack of awareness of Deaf culture by normal people. Majority of hearing people have either no/little knowledge or experience of sign language [10]. There are also more than 300 sign languages and it is hard for a normal person to understand and become used to these languages [11]. The above-mentioned problems can be solved by involving the assistive technology as it can be used as an interpreter for converting the sign languages into text or speech for better communication between the Deaf community and hearing individuals [12]. Other technologies such as speech technologies can assist in different ways to help people with hearing loss by improving their autonomy [13]. A common example of speech technology is speech recognition, also termed as automatic speech recognition (ASR). It is the process of converting the speech signal into sequences of words with the help of an algorithm [14]. The ASR process comprises three steps, i.e., (1) feature extraction, (2) acoustic model generation, and (3) recognition phase [15, 16]. For feature extraction, MFCC is the most commonly used technique [17, 18]. The success of MFCC makes it the standard choice in the state-of-the-art speech recognizers such as HTK [19].

The main purpose of this research paper is to use a mobile-based assistive technology for providing a simple and cost-effective solution for Deaf-mute with little or complete speech development. The proposed system used HTK based speech recognizer to identify the speech of Deaf-mute and provide a communication platform for them. The next two sections explain the related work and proposed methodology of our system. Section 4 states the experimental setup and results of the proposed system.

2. Related Work

The Deaf community is not a monolithic group; it has a diversity of groups which are as follows [20, 21]:

(1) Hard-of-hearing people: they are neither fully deaf nor fully hearing, also known as culturally marginal people [22]. They can obtain some useful linguistic information from speech.

(2) Culturally deaf people: they might belong to deaf families and use sign language as the primary source of communication. Their voice (speech clarity) may be disrupted.

(3) Congenital or prelingual deaf people: they are deaf by birth or become deaf before they learn to talk and are not affiliated with Deaf culture. They might or might not use sign language based communication.

(4) Orally educated or postlingual deaf people: they have been deafened in their childhood but developed the speaking skills.

(5) Late-deafened adults: they have had the opportunity to adjust their communication techniques as their progressive hearing losses.

Each group of a Deaf community has a different degree of hearing loss and use a different source of communication. Table 1 illustrates the details of Deaf community groups with their degree of hearing loss and source of communication with others.

Hearing loss or deafness has a direct impact on communication, educational achievements, or social interactions [23]. Lack of knowledge about Deaf culture is documented in society as well as in healthcare environment [24]. Kuenburg et al. also indicated that there are significant challenges in communication among healthcare professionals and Deaf people [25]. Improvement in healthcare access among Deaf people is possible by providing the sign language supported visual communication and implementation of communication technologies for healthcare professionals. Some of the implemented technology-based approaches for facilitating Deaf-mutes with easy-to-use services are as follows.

2.1. Sensor-Based Technology Approach. Sensors based assistance can be used for solving the social problems of Deaf-mute by bridging the communication gap. Sharma et al. used wearable sensor gloves for detecting the hand gestures of sign language [26]. In this system, flex sensors were used to record the sign language and to sense the environment. The hand gesture of a person activates glove, and flex sensors on glove convert those gestures into electrical signals. The signals

Table 1: Mapping of Deaf community groups with a degree of hearing loss and communication source [3, 20, 21].

Deaf Community Groups	Degree of Hearing Loss	Communication Source
Hard-of-Hearing People	Mild to Severe	Speech/Sign Language
Culturally Deaf People	Profound	Sign Language
Congenital or Pre-lingual Deaf People	Profound	Sign Language
Orally Educated or Post-lingual Deaf People	Severe to Profound	Speech/Sign Language
Late-Deafened Adults	Moderate to Profound	Speech/Sign Language

are then matched from the database and converted into corresponding speech and displayed on LCD. The cost-effective sensor-based communication device [27] was also suggested for Deaf-mute people to communicate with the doctor. This experiment used a 32-bit microcontroller, LCD to display the input/output, and a processing unit. The LCD displays different hand sign language based pictures to the user. The user selects relevant pictures to describe the illness symptoms. These pictures then convert into patterns and pair with words to make sentences. Vijayalakshmi and Aarthi used flex sensors on the glove for gesture recognition [28]. The system was developed to recognize the words of American Sign Language (ASL). The text output obtained from sensor-based system is converted into speech by using the popular speech synthesis technique of hidden Markov model (HMM). The HMM-based-text-to-speech synthesizer (HTS) was attached to the system for converting the text obtained from hand gestures of people into speech. The HTS system involved training phase for extraction of spectral and excitation parameters from the collected speech data and was modeled by context-dependent HMMs. The synthesis phase of HTS system was used for the construction of HMM sequence by concatenating context-dependent HMMs. Similarly, Arif et al. used five flex sensors on a glove to translate ASL gestures for Deaf-mute into the visual and audio output on LCD [29].

2.2. Vision-Based Technology Approach. Many vision-based technology interventions are used to recognize the sign languages of Deaf people. For example, Soltani et al. developed a gesture-based game for Deaf-mutes by using Microsoft Kinect which recognizes the gesture command and converts it into text so that they can enjoy the interactive environment [7]. Voice for the mute (VOM) system was developed to take input in the form of fingerspelling and convert into corresponding speech [30]. The images of fingerspelling signs are retrieved from the camera. After performing noise removal and image processing, the fingerspelling signs are matched from the trained dataset. Processed signs are linked to appropriate text and convert this text into required speech. Nagori and Malode [31] proposed the communication platform by extracting images from the video and converting these images into corresponding speech. Sood and Mishra [32] presented the system that takes images of sign language as input and displays speech as output. The features used in vision-based approaches for speech processing are also used in different object recognition based applications [33–39].

2.3. Smartphone-Based Technology Approach. Smartphone technology plays a vital role in helping the people with impairments to get themselves interacted socially and to overcome their communication barriers. Smartphone technology approach is more portable and effective as compared to sensor or vision technology. Many of the new smartphones are furnished with advanced sensors, high processors, and high-resolution cameras [40]. A real-time emergency assistant "iHelp" [41] was proposed for Deaf-mute people where they can report any kind of emergency situation. The current location of the user is accessed through built-in GPS system in a smartphone. The information about the emergency situation is sent to the management through SMS and then passed on to the closest suitable rescue units, and hence the user can get rescue through the use of iHelp. MonoVoix [42] is an Android application that also acts as a sign language interpreter. It captures the signs from a mobile phone camera and then converts them into corresponding speech. Ear Hear [43] is an Android application for Deaf-mute people. It uses sign language to communicate with normal people. The speech-to-sign and sign-to-speech technology are used. For a hearing person to interact with Deaf-mute, the text-to-speech (TTS) technology inputs the speech signal, and a corresponding sign language video is played against that input through which the mute can easily understand. Bragg et al. [44] proposed a sound detector. The app is used to detect the red alert sounds and alert the deaf-mute person by vibrating and showing a popup notification.

3. Proposed Methodology

Nowadays many technology devices such as smartphone-enabled devices prefer speech interfaces over visual ones. The research [49] highlighted that off-the-shelf speech recognition system cannot be used to detect the speech of deaf or hearing loss people as these systems contain a higher ratio of word error rate. This research recommended using human-based computations to recognize the deaf speech and using text-to-speech functionality for speech generation. In this regard, we proposed and developed an Android based application named as vocalizer to mute (V2M). The proposed application acts as an interpreter and encourages two-way communication between Deaf-mute and normal person. We refer to normal person as the one who has no hearing or vocal impairment or disability. The main features of the proposed application are listed below.

3.1. Normal to Deaf-Mute Person Communication. This module takes text or spoken message of a normal person as an input and outputs a 3D avatar that performs sign language for a Deaf-mute person. ASL based animations of an avatar

are stored in a central database of application. Each animation file is given 2–5 tags. The steps of normal to Deaf-mute person communication are as follows:

(1) The application takes text/speech of normal person as an input.

(2) The application converts the speech message of a normal person into text by using the Google Cloud Speech Application Program Interface (API) as this API detects normal speech better compared to Deaf persons' speech.

(3) The application matches the text to any of the tags associated with an animation file and displays the avatar performing corresponding sign for Deaf-mute.

3.2. Deaf-Mute to Normal Person Communication. Not everyone has knowledge of sign language so the proposed application uses disrupted speech of a Deaf-mute person. This disrupted form of speech is converted into recognizable speech format by using speech recognition system. HMM-based speech recognition is a growing technology as evidenced by the rapidly increasing commercial deployment. The performance of HMM-based speech recognition has already reached a level that can support viable applications [50]. For this purpose, HTK [51] is used for developing speech recognition system as this toolkit is primarily designed for building HMM-based speech recognition systems.

3.2.1. Speech Recognition System Using HTK. ASR system is implemented by using HTK version 3.4.1. The speech recognition process in HTK follows four steps to obtain the recognized speech of Deaf-mute. The steps are training corpus preparation, feature extraction, acoustic model generation, and recognition as illustrated in Figure 1.

(a) Training Corpus Preparation. The training corpus consists of recordings of speech samples obtained from Deaf-mute in .wav format. The corpus contains spoken English alphabets (A–Z), English digits (0 to 9), and 15 common sentences used in daily routine life, i.e., good morning, hello, good luck, thank you, etc. The utterance of one participant is separated from the others due to the variance in speech clarity among Deaf-mute people. The training utterances of each participant are labeled to simple text file (.lab). This file is used in acoustic model generation phase of the system.

(b) Acoustic Analysis. The purpose of the acoustic analysis is to convert the speech sample (.wav) into a format which is suitable for the recognition process. The proposed application used MFCC approach for acoustic analysis. MFCC is the feature extraction technique in speech recognition [52]. Main advantages of using MFCC are (1) low complexity and (2) better performance with high accuracy in recognition [53]. The overall working of MFCC is illustrated in Figure 2 [19].

The features of each step of MFCC are listed below.

(1) Pre-Emphasis. The first step of MFCC feature extraction is done by passing the speech signal through a filter. The pre-emphasis filter is the first-order high-pass filter. It is responsible for boosting the higher frequencies of a speech signal.

$$x'(n) = x(n) - \alpha x(n-1) \quad 0.9 \le \alpha \le 1.0, \tag{1}$$

where α represents the pre-emphasis coefficient, $x(n)$ is the input speech signal, and $x'(n)$ is the output speech signal with a high-pass filter applied to the input. Pre-emphasis is important because the components of speech with high frequency have small amplitude w.r.t components of speech with low frequency [54]. The silent intervals are also removed in this step by using the logarithmic technique for separating and segmenting speech from noisy background environments [55].

(2) Framing. Framing process is used to split the pre-emphasized speech signal into short segments. The voice signal is represented by N frame samples and the interframe distance or frameshift is M ($M < N$). In the proposed application, the frame sample size (N) = 256 and frameshift (M) = 100. The frame size and frameshift (in milliseconds) are calculated as

$$\begin{aligned} \text{FrameSize (ms)} = f_n = \frac{1}{N * M} = 25.6\,\text{ms}, \\ \text{Frame\_Shift} = 10\,\text{ms}. \end{aligned} \tag{2}$$

(3) Windowing. The speech signal is a nonstationary signal but it is stationary for a very short period of time. The window function is used to analyze the speech signal and extract the stationary portion of a signal. There are two types of windowing:

(i) Rectangular window,

(ii) Hamming window.

Rectangular window cuts the signal abruptly so the proposed application used Hamming window. Hamming window shrinks the values towards zero at the boundaries of the speech signal. The value of Hamming window ($w(n)$) is calculated as

$$w(n) = \begin{cases} 0.54 - 0.46 * \cos\left(\dfrac{2\pi n}{N-1}\right) & 0 \le n \le N-1 \\ 0 & \text{otherwise.} \end{cases} \tag{3}$$

The windowing at time n is calculated by

$$y_t(n) = w(n) * s(n). \tag{4}$$

(4) Discrete Fourier Transform (DFT). The most efficient approach for computing Discrete Fourier Transform is to use Fast Fourier Transform algorithm as it reduces the computation complexity from $\Theta(n^2)$ to $\Theta(n \log n)$. It converts the N discrete samples of speech from the time domain to the frequency domain as calculated by

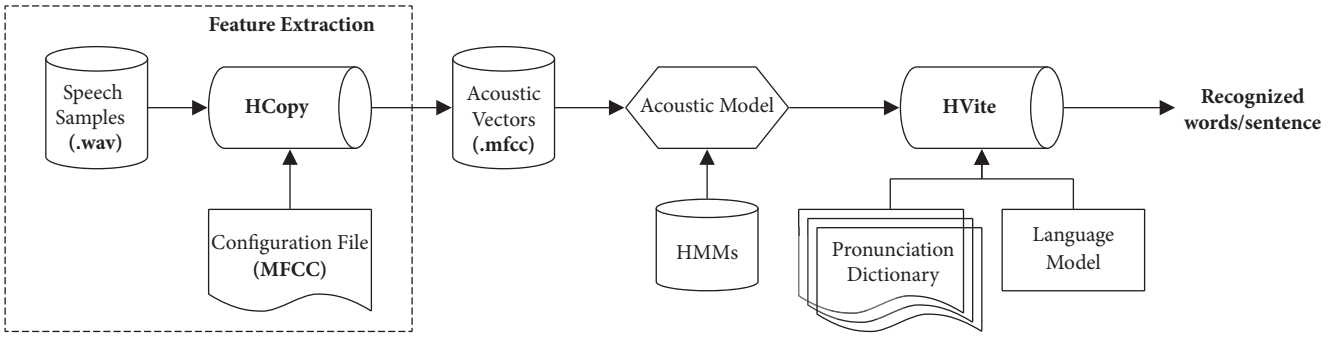

Figure 1: Speech recognition process using MFCC and HTK.

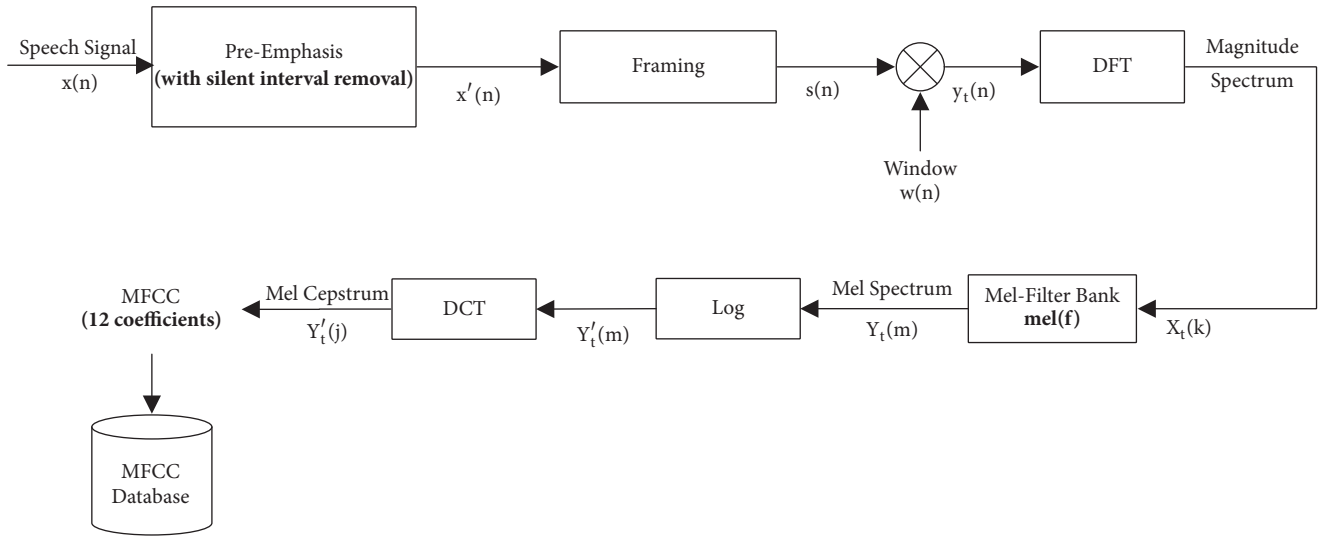

Figure 2: Block diagram of MFCC feature extraction technique.

$$X_t(K) = \sum_{n=1}^{N} s(n) * w(n) * e^{-j2\pi(k/N)n} \quad 1 \le K \le k = \sum_{n=1}^{N} y_t(n) * e^{-j2\pi(k/N)n}, \tag{5}$$

where $X_t(K)$ is the Fourier transform of $y_t(n)$ and k is the length of the DFT.

(5) Mel-Filter Bank Processing. Human ears act as band-pass filters; i.e., they focus on only certain frequency bands and have less sensitivity at higher frequencies (roughly >1000 Hz). A unit of pitch (mel) is defined for separating the perceptually equidistant pair of sounds in pitch into an equal number of mels [56] and it is calculated as

$$Y_t(m) = \text{mel}(f) = 2595 * \log_{10}\left(1 + \frac{f}{700}\right). \tag{6}$$

(6) Log. This step takes the logarithm of each of the mel-spectrum values. As human ear has less sensitivity to the slight difference in amplitude at higher amplitudes as compared to lower amplitudes. Logarithm function makes the frequency estimates less sensitive to the slight difference in input.

(7) Discrete Cosine Transform (DCT). It converts the frequency domain (log mel-spectrum) back to the time domain by using DCT. The result of the conversion is known as mel frequency cepstrum coefficient (MFCC) [57]. We calculated the mel frequency cepstrum by

$$Y'_t(j) = \sum_{m=1}^{M} \log\left(\left|Y_t(m)\right|\right) \cos\left(j(m - 0.5)\frac{\pi}{M}\right), \quad k = 1, \ldots, J. \tag{7}$$

In the proposed methodology, the value of $J = 12$ because a 12-dimensional feature parameter is sufficient to represent the voice feature of a frame [17]. The extraction of cepstrum via DCT results in 12 cepstral coefficients for each frame. These set of coefficients are called acoustic vectors (.mfcc). The acoustic vector (.mfcc) files are used for both the training and

Table 2: Details of a configuration file (config.txt).

Description	Parameters
Input Source File Format ($x(n)$)	SOURCEFORMAT = WAV
Output of Speech Sample	TARGETKIND = MFCC_0
Pre-emphasis Coefficient (α)	PREEMCOEF = 0.97
Frameshift (M)	TARGETRATE = 100000
Window Size	WINDOWSIZE = 250000
Using Hamming Window ($w(n)$)	USEHAMMING = T
No. of Filter Bank Channels (f)	NUMCHANS = 26
No. of the Cepstral Coefficients	NUMCEPS = 12
Save the Output File Compressed	SAVECOMPRESSED = T

testing speech samples. The HTK-HCopy runs for conversion of input speech sample into acoustic vectors. The configuration parameters, used for MFCC feature extraction of the speech sample, are listed in Table 2.

(c) Acoustic Model Generation. It provides a reference acoustic model with which the comparisons are made to recognize the testing utterances. A prototype is used for the initialization of first HMM. This prototype is generated for each word of the Deaf-mute dictionary. The HMM topology comprises 6 active states (observation functions) and two nonemitting states (the initial and the last state with no observation function) which are used for all the HMMs. Single Gaussian observation functions with diagonal matrices are used as observation functions and are described by a mean vector and variance vector in a text description file known as prototype. This predefined prototype file along with acoustic vectors (.mfcc) of training data and associated labels (.lab) is used by the HTK tool HInit for initialization of HMM.

(d) Recognition Phase. HTK provides a Viterbi word recognizer called HVite, and it is used to transcript the sequence of acoustic vectors into a sequence of words. HVite uses the Viterbi algorithm in finding the acoustic vectors as per MFCC model. The testing speech samples are also prepared in the same way of preparing the training corpus. In the testing phase, the speech sample is converted into series of acoustic vectors (.mfcc) using the HTK-HCopy tool. These input acoustic vectors along with HMM list, Deaf-mute pronunciation dictionary, and language model (text labels) are taken as an input by HVite to generate the recognized words.

3.3. Messaging Service for Deaf-Mute and Normal Person. The application also provides messaging feature to both Deaf-mute and normal people. A person can choose between the American Sign Language or English keyboard for sending the messages. The complete flowchart of "V2M" is illustrated in Figure 3.

4. Experimental Results and Discussions

4.1. Experimental Setup. The proposed application V2M required a camera, a mobile phone for the installation of the V2M app, laptop (acting as a server), and an instructor to guide the Deaf-mute student. The complete scenario is shown in Figure 4.

A total of 15 students from Al-Mudassir Special Education Complex Baharwal, Pakistan, participated in this experiment and the participated students were between the ages of 7 and 13 with some speech training in school. The instructor guided all students in using the mobile application. The experiment consisted of two phases.

4.1.1. Speech Testing Phase. In this phase, instructor selected a "register voice" option from a menu of the app and entered a word/sentence or question (label) in a text field of the "register sample" dialog box, for which the training speech samples of participants were taken (see Figure 5(b)). At first, the instructor needed sign language for asking the participants to speak a word/sentence or an answer. The system took 2 to 4 voice samples of each word/sentence. Whenever the participant registered his/her voice, the system acknowledged by a visual support (as in Figure 5(c)). For testing, the researcher asked questions via the V2M app, and it displayed an avatar that performed sign language for a Deaf-mute participant in order to understand the questions (see Figure 5(d)). In response, the participant selected the microphone icon (as shown in Figure 5(e)) to speak his/her answer. The app processed and compared the recorded speech sample with the registered samples. After the comparison, it returned the text and spoke out the answer of the participant (see Figure 5(f)).

4.1.2. Message Activity Phase. The participants took minimal support from an instructor in this phase. They easily composed and sent the messages by selecting sign language keyboard (see Figure 5(g)).

4.2. Qualitative Feedback. Researchers formalized questionnaire survey to evaluate the effectiveness of the Deaf-mute application. The survey comprised 12 questions for participants to answer and the reason for this short-length selection of questions was not to overwhelm Deaf-mute students with longer interviews. Secondly, these students had no experience of using any Deaf-mute based application. The qualitative feedback is summarized into following categories (paraphrased from the feedback forms).

Familiarity with Existing Mobile Apps. All participants have not heard or used any mobile applications which are dedicated to Deaf-mutes.

Ease of Use and Enjoyment. All participants enjoyed using the app. They liked the idea of using an avatar for performing sign language. Out of 15 students, 12 students performed the given tasks quite easily and 3 students have not used or interacted with mobile devices before. Initially, they found this app difficult but it became easier for them after app functions were performed 2-3 times in front of them. Overall they found this app user-friendly and interactive.

Application Interface. Participants liked the interface of the app. They learned the steps of app quite fast and they also

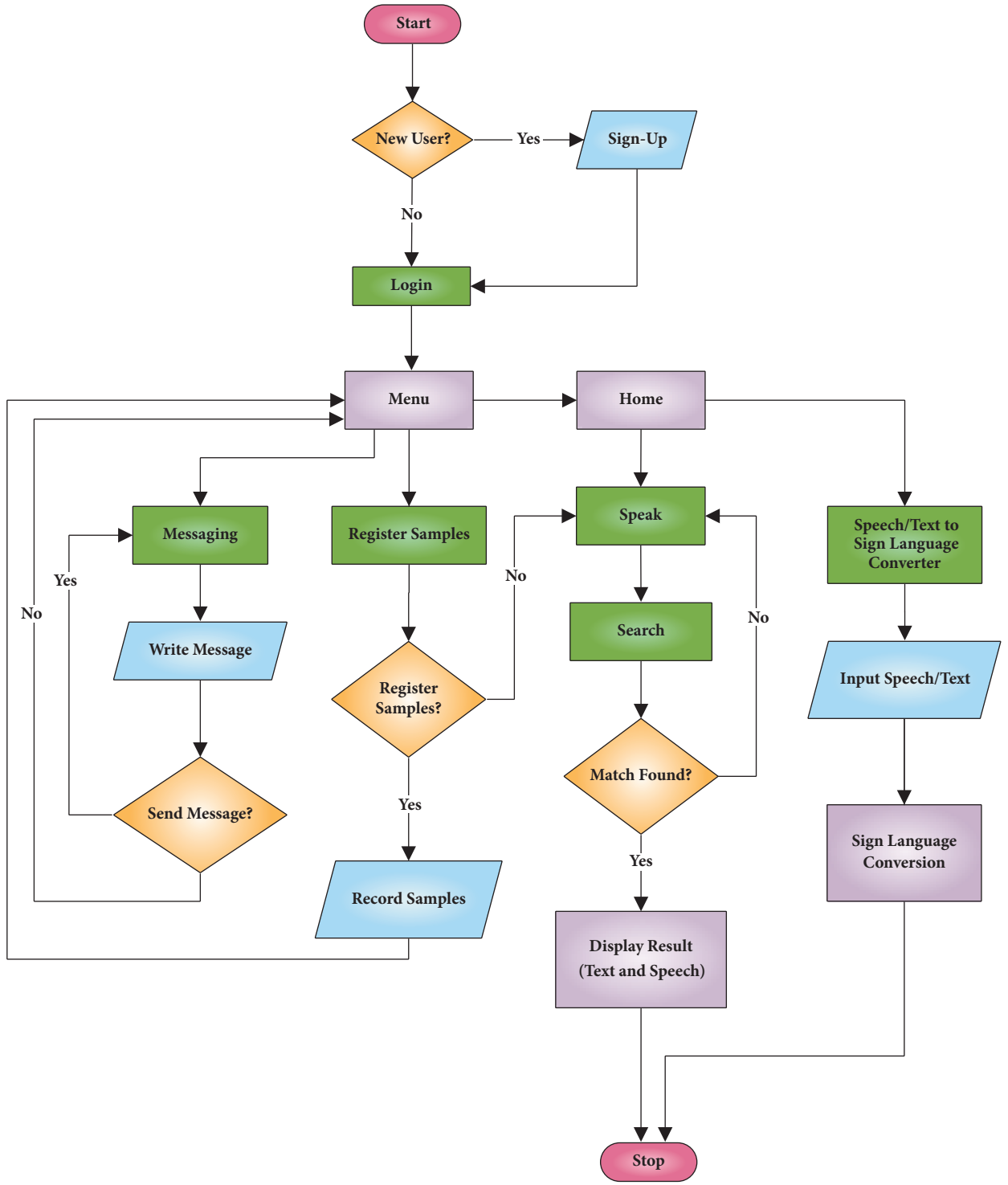

Figure 3: Flowchart of V2M application.

liked the idea of an avatar performing greeting gesture at home screen.

Source of Communication. All participants were using sign language as a primary source of communication. They recommended the intervention of mobile application as a source of communication for them. They acknowledged that the mobile app can be used to convey the message of deaf-mute to a normal person.

4.3. Results and Comparative Analysis. The application training and testing corpus are obtained from the speech samples

Figure 4: Experimental setup: a participant performing registration of speech sample task.

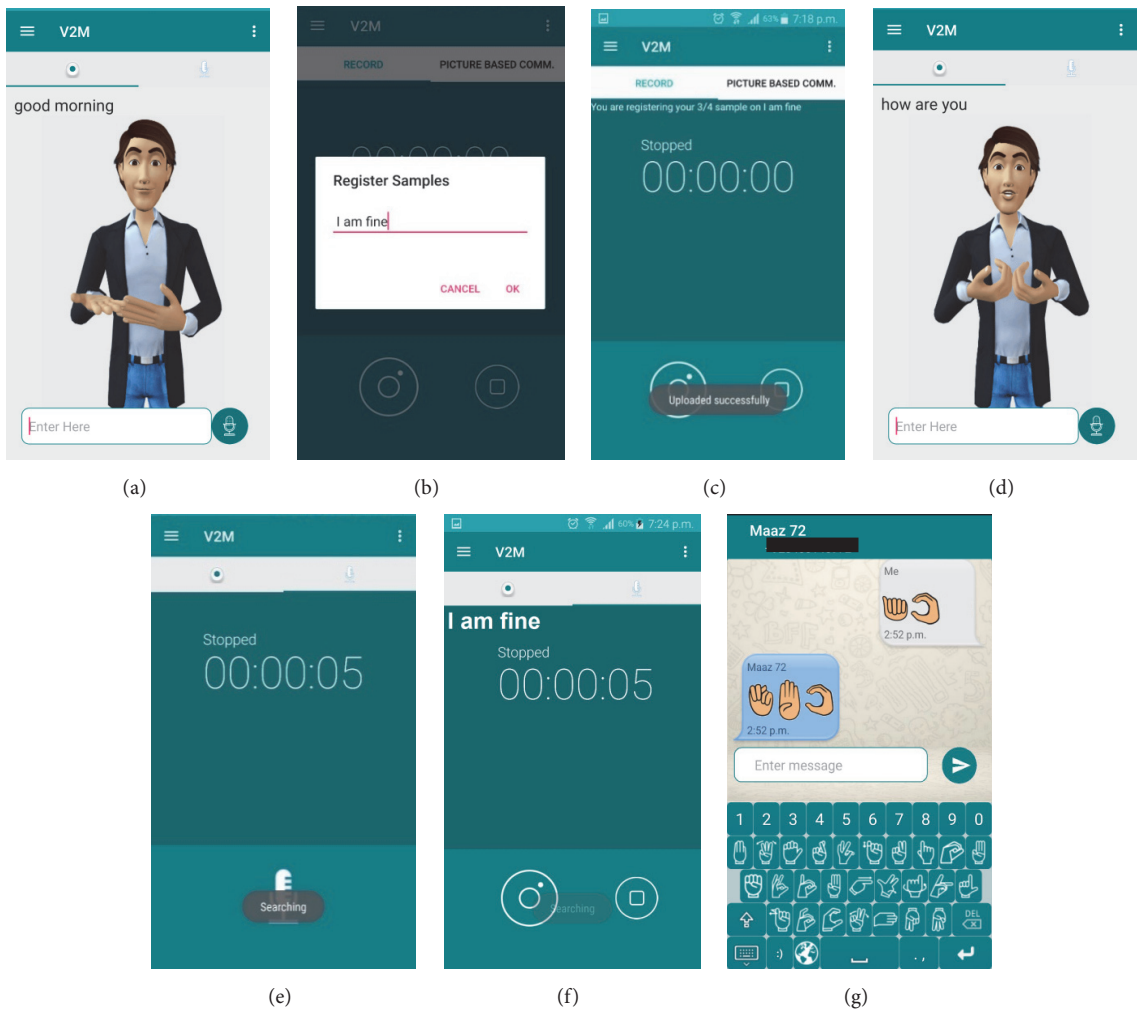

Figure 5: The working of V2M. (a) Avatar greets deaf-mute person. (b) Instructor registers text sample to ask participant for speaking it. (c) Participant recorded his/her speech samples. (d) Avatar asks a question to the Deaf-mute person. (e) Participant recorded his/her answer and app is processing the speech signal. (f) V2M displays and speaks the answer after matching the speech signal. (g) Sign language-based message service.

of Deaf-mutes. Training corpus is comprised of English alphabets (A–Z), English digits (0 to 9), and 15 common sentences used in daily routine life, i.e., good morning, hello, good luck, thank you, etc. All participants uttered each alphabet, digit, and statement 2–4 times. The total training utterances are 2440. The HTK speech recognizer was used in training process and speech recognition. HMM was used at the backend of speech recognizer HTK. For testing, each participant was asked 10 questions to answer. There are a total of 390 testing utterances. The application recorded the answer

(speech sample), processed it, and displayed (text/speech) result for normal person understanding. The accuracy of simulation results of proposed application is calculated by using precision and recall. For the V2M app, the precision is calculated by a fraction of correctly identified speech signals to a total number of speech samples whereas recall is a percentage of the number of relevant results. Precision, recall, and accuracy are calculated by using the following formulas:

$$\begin{aligned}
\text{precision} &= \frac{\text{true positive (tp)}}{\text{true positive (tp)} + \text{false positive (fp)}} \\
\text{recall} &= \frac{\text{true positive (tp)}}{\text{true positive (tp)} + \text{false negative (fn)}} \\
\text{accuracy} &= \frac{\text{true positive (tp)} + \text{true negative (tn)}}{\text{true positive (tp)} + \text{true negative (tn)} + \text{false positive (fp)} + \text{false negative (fn)}}.
\end{aligned} \tag{8}$$

True positive (tp) refers to words that are uttered by the person and detected by the system.

False positive (fp) refers to words not uttered by the person but detected by the system.

False negative (fn) refers to words that are uttered by the person but the system does not detect it.

True negative (tn) refers to everything else.

The experimental results of the proposed methodology in terms of precision, recall, and accuracy parameters are illustrated in Table 3.

It is observed from Table 3 that the number of speech samples has direct impact on precision and recall of the application. Overall average precision is 56.79% and recall is 46.79% when registered sample count in all statements is 2 ($N = 2$) for each participant. However, the average precision is 93.16% and recall is 83.19% for registered sample count 3 ($N = 3$). The average accuracy in terms of precision and recall is above 97% when registered sample count in all statements is 4 ($N = 4$) for each participant. The $F1$-score of best precision and recall is calculated:

$$\begin{aligned}
F1\ \text{score}_{(N=4)} &= 2 * \frac{\text{precision} * \text{recall}}{\text{precision} + \text{recall}} \\
&= 2 * \frac{0.9861 * 0.979}{0.9861 + 0.979} = 0.98.
\end{aligned} \tag{9}$$

Hence it is deducted that the precision of application decreases by taking the limited number of speech samples ($N \leq 2$) of the deaf-mute. The application outperforms when the number of speech samples for each statement is greater than 2 ($2 < N \leq 2$). The speech recognition methodology of proposed application is compared with other speech recognition systems as shown in Table 4.

5. Conclusion

Deaf people face many irritations and frustrations that limit their ability to do everyday tasks. Deaf children have high rates of behavioral and emotional issues in relation to different methods of communication. The main inspiration behind the proposed application is to remove the communication barrier for Deaf-mutes especially children. This app uses the speech or text input of normal person and translates it into sign language via 3D avatar. It provides speech recognition system for the distorted speech of Deaf-mutes. The speech recognition system uses MFCC feature extraction technique to extract the acoustic vectors from speech samples. The HTK toolkit is used to convert these acoustic vectors into recognizable words or sentences by using pronunciation dictionary and language model. The application is able to recognize Deaf-mute speech samples of English alphabets (A–Z), English digits (0 to 9), and 15 common sentences used in daily routine life, i.e., good morning, hello, good luck, thank you, etc. It provides message service for both Deaf-mutes and normal people. Deaf-mutes can use customized sign language keyboard for composing the message. The app also can convert the received sign language message to text for a normal person. The proposed application was also tested on 15 children aged between 7 and 13 years. The accuracy of proposed application is 97.9%. The qualitative feedback of children also highlighted that it is easy for Deaf-mutes to adapt the mobile technology and mobile app can be used to convey their message to a normal person.

Conflicts of Interest

The authors declare that there are no conflicts of interest regarding the publication of this paper.

Acknowledgments

The authors are thankful to Maaz Khalid and Mustabshira Zia for their valuable assistance in this study. The authors also gratefully acknowledge Al-Mudassir Special Education Complex Baharwal, Pakistan, for providing them a platform to test the proposed technique of this article. The authors are appreciative of the hard work and dedication of instructors and children who participated in this study. This work was financially supported by the Machine Learning Research

Table 3: Precision and recall of proposed application with speech samples (N = 2, 3, and 4).

Testing Statement	Speech Samples N = 2			Speech Samples N = 3			Speech Samples N = 4		
	Precision	Recall	Accuracy	Precision	Recall	Accuracy	Precision	Recall	Accuracy
S:1	37.5%	30%	20%	91.6%	78.5%	73.3%	100%	93.3%	93.3%
S:2	62.5%	41.6%	33.3%	85.7%	92.4%	80%	100%	100%	100%
S:3	66.6%	30.7%	26.67%	100%	80%	80%	100%	93.3%	93.3%
S:4	60%	54.54%	40%	100%	86.6%	86.67%	92.8%	100%	100%
S:5	80%	61%	53.3%	92.8%	86.6%	86.67%	100%	100%	100%
S:6	57.1%	33.3%	26.67%	100%	73.3%	73.3%	100%	93.3%	93.3%
S:7	53.8%	77.7%	46.67%	84.6%	84.6%	73.3%	100%	100%	100%
S:8	45.45%	55.5%	33.3%	100%	80%	80%	100%	100%	100%
S:9	30%	37.5%	20%	100%	86.7%	86.67%	100%	100%	100%
S:10	75%	46.1%	40%	76.9%	83.3%	66.67%	93.3%	100%	100%
Average	*56.79%*	*46.79%*	*46.67%*	*93.16%*	*83.19%*	*78.67%*	*98.61%*	*97.9%*	*97.9%*

Table 4: Comparison of proposed methodology with state-of-the-art ASR systems.

ASR Systems	Methodology	Accuracy	
Proposed Methodology (N = 4)	MFCC + HTK (8-state HMM)	97.9%	
MSIAC (Liu et al., 2017) [15]	MFCC + GMM	Experiment 1	89.50%
		Experiment 2	85.92%
TAMEEM V1.0 (Abushariah, 2017) [45]	MFCC + Sphinx 3	92.36%	
Speaker Identification System (Leu and Lin, 2017) [46]	MFCC + GMM	Experiment 1	94.08%
		Experiment 2	84.88%
Telugu Speech Signals (Mannepalli et al., 2016) [47]	MFCC – GMM	92%	
AMAZIGH LANGUAGE (Elouahabi et al., 2016) [48]	MFCC + HTK (6-state HMM)	80%	

Group, Prince Sultan University, Riyadh, Saudi Arabia [RG-CCIS-2017-06-02]. The authors are grateful for this financial support and the equipment provided to make this research successful.

References

[1] W. Tin, Z. Lin, -. Swe, and N. K. Mya, "Deaf mute or Deaf," *Asian Journal of Medical and Biological Research*, vol. 3, no. 1, pp. 10–19, 2017.

[2] I. W. Leigh and J. F. Andrews, *Deaf People and Society: Psychological, Sociological and Educational Perspectives*, Psychology Press, 2016.

[3] WHO, "Deafness and Hearing Loss," *Fact Sheet*, vol. 300, 2017.

[4] J. G. Clark, "Uses and abuses of hearing loss classification," *Asha*, vol. 23, no. 7, pp. 493–500, 1981.

[5] B. H. Jacobson, A. Johnson, C. Grywalski et al., "The Voice Handicap Index (VHI): development and validation," *American Journal of Speech-Language Pathology*, vol. 6, no. 3, pp. 66–70, 1997.

[6] P. Vostanis, M. Hayes, M. Du Feu, and J. Warren, "Detection of behavioural and emotional problems in deaf children and adolescents: Comparison of two rating scales," *Child: Care, Health and Development*, vol. 23, no. 3, pp. 233–246, 1997.

[7] F. Soltani, F. Eskandari, and S. Golestan, "Developing a gesture-based game for deaf/mute people Using microsoft kinect," in *Proceedings of the 2012 6th International Conference on Complex, Intelligent, and Software Intensive Systems, CISIS 2012*, pp. 491–495, July 2012.

[8] D. G. Blazer, S. Domnitz, C. T. Liverman, C. on Accessible, A. H. H. C. for Adults, E. National Academies of Sciences, and Medicine, Hearing Loss: Extent, Impact, and Research Needs. 2016.

[9] WHO, "Global costs of unaddressed hearing loss and cost-effectiveness of interventions: a WHO report, 2017, in Global costs of unaddressed hearing loss and cost-effectiveness of interventions: a WHO report," Tech. Rep., 2017.

[10] T. Humphries, "Of Deaf-mutes, the Strange," in *Deaf World: A Historical Reader and Primary Sourcebook*, 2001.

[11] List of Sign Languages, n.d.

[12] J. Gugenheimer, K. Plaumann, F. Schaub et al., "The impact of assistive technology on communication quality between deaf and hearing individuals," in *Proceedings of the 2017 ACM Conference on Computer Supported Cooperative Work and Social Computing, CSCW 2017*, pp. 669–682, March 2017.

[13] A. Piquard-Kipffer, O. Mella, J. Miranda, D. Jouvet, and L. Orosanu, "Qualitative investigation of the display of speech recognition results for communication with deaf people," in *Proceedings of SLPAT 2015: 6th Workshop on Speech and Language Processing for Assistive Technologies*, pp. 36–41, Dresden, Germany, September 2015.

[14] B. Chigier, "Automatic speech recognition," Google Patents, 1997.

[15] J.-C. Liu, F.-Y. Leu, G.-L. Lin, and H. Susanto, "An MFCC-based text-independent speaker identification system for access control," *Concurrency Computation*, vol. 30, no. 2, Article ID e4255, 2018.

[16] L.-S. Lee, J. Glass, H.-Y. Lee, and C.-A. Chan, "Spoken Content Retrieval - Beyond Cascading Speech Recognition with Text Retrieval," *IEEE Transactions on Audio, Speech and Language Processing*, vol. 23, no. 9, pp. 1389–1420, 2015.

[17] R. Vergin, D. O'Shaughnessy, and A. Farhat, "Generalized mel frequency cepstral coefficients for large-vocabulary speaker-independent continuous-speech recognition," *IEEE Transactions on Audio, Speech and Language Processing*, vol. 7, no. 5, pp. 525–532, 1999.

[18] M. Holmberg, D. Gelbart, and W. Hemmert, "Automatic speech recognition with an adaptation model motivated by auditory processing," *IEEE Transactions on Audio, Speech and Language Processing*, vol. 14, no. 1, pp. 43–49, 2006.

[19] F. S. Al-Anzi and D. AbuZeina, "The Capacity of Mel Frequency Cepstral Coefficients for Speech Recognition," *World Academy of Science, Engineering and Technology, International Journal of Computer, Electrical, Automation, Control and Information Engineering*, vol. 11, no. 10, pp. 1094–1098, 2017.

[20] J. L. Pray and I. K. Jordan, "The deaf community and culture at a crossroads: Issues and challenges," *Journal of Social Work in Disability and Rehabilitation*, vol. 9, no. 2, pp. 168–193, 2010.

[21] S. Barnett, "Communication with deaf and hard-of-hearing people: A guide for medical education," *Academic Medicine: Journal of the Association of American Medical Colleges*, vol. 77, no. 7, pp. 694–700, 2002.

[22] N. Glickman, "Cultural Identity, Deafness, and Mental Health," *Journal of Rehabilitation of the Deaf*, vol. 20, no. 2, pp. 1–10, 1986.

[23] R. E. Perkins-Dock, T. R. Battle, J. M. Edgerton, and J. N. McNeill, "A Survey of Barriers to Employment for Individuals Who Are Deaf," *Journal of the American Deafness & Rehabilitation Association (JADARA)*, vol. 49, no. 2, 2015.

[24] L. Sirch, L. Salvador, and A. Palese, "Communication difficulties experienced by deaf male patients during their in-hospital stay: findings from a qualitative descriptive study," *Scandinavian Journal of Caring Sciences*, vol. 31, no. 2, pp. 368–377, 2017.

[25] A. Kuenburg, P. Fellinger, and J. Fellinger, "Health Care Access Among Deaf People," *Journal of Deaf Studies and Deaf Education*, vol. 21, no. 1, pp. 1–10, 2016.

[26] M. V. Sharma, N. V. Kumar, S. C. Masaguppi, S. Mn, and D. R. Ambika, "Virtual talk for deaf, mute, blind and normal humans," in *Proceedings of the 2013 1st Texas Instruments India Educators' Conference, TIIEC 2013*, pp. 316–320, April 2013.

[27] K. Rojanasaroch and T. Laohapensaeng, "Communication aid device for illness deaf-mute," in *Proceedings of the 12th International Conference on Electrical Engineering/Electronics, Computer, Telecommunications and Information Technology, ECTI-CON 2015*, June 2015.

[28] P. Vijayalakshmi and M. Aarthi, "Sign language to speech conversion," in *Proceedings of the 2016 International Conference on Recent Trends in Information Technology, ICRTIT 2016*, April 2016.

[29] A. Arif, S. T. H. Rizvi, I. Jawaid, M. A. Waleed, and M. R. Shakeel, "Techno-talk: An American Sign Language (ASL) Translator," in *Proceedings of the 3rd International Conference on Control, Decision and Information Technologies, CoDIT 2016*, pp. 665–670, April 2016.

[30] A. K. Tripathy, D. Jadhav, S. A. Barreto, D. Rasquinha, and S. S. Mathew, "Voice for the mute," in *Proceedings of the 2015 International Conference on Technologies for Sustainable Development, ICTSD 2015*, February 2015.

[31] N. P. Nagori and V. Malode, "Communication Interface for Deaf-Mute People using Microsoft Kinect," in *Proceedings of the 1st International Conference on Automatic Control and Dynamic Optimization Techniques, ICACDOT 2016*, pp. 640–644, September 2016.

[32] A. Sood and A. Mishra, "AAWAAZ: A communication system for deaf and dumb," in *Proceedings of the 5th International Conference on Reliability, Infocom Technologies and Optimization, ICRITO 2016*, pp. 620–624, September 2016.

[33] M. Yousuf, Z. Mehmood, H. A. Habib et al., "A Novel Technique Based on Visual Words Fusion Analysis of Sparse Features for Effective Content-Based Image Retrieval," *Mathematical Problems in Engineering*, vol. 2018, Article ID 2134395, 13 pages, 2018.

[34] Z. Mehmood, S. M. Anwar, and M. Altaf, "A novel image retrieval based on rectangular spatial histograms of visual words," *Kuwait Journal of Science*, vol. 45, no. 1, pp. 54–69, 2018.

[35] Z. Mehmood, T. Mahmood, and M. A. Javid, "Content-based image retrieval and semantic automatic image annotation based on the weighted average of triangular histograms using support vector machine," *Applied Intelligence*, vol. 48, no. 1, pp. 166–181, 2018.

[36] N. Ali, K. B. Bajwa, R. Sablatnig, and Z. Mehmood, "Image retrieval by addition of spatial information based on histograms of triangular regions," *Computers & Electrical Engineering*, vol. 54, pp. 539–550, 2016.

[37] Z. Mehmood, S. M. Anwar, N. Ali, H. A. Habib, and M. Rashid, "A Novel image retrieval based on a combination of local and global histograms of visual words," *Mathematical Problems in Engineering*, vol. 2016, Article ID 8217250, 12 pages, 2016.

[38] Z. Mehmood, F. Abbas, T. Mahmood, M. A. Javid, A. Rehman, and T. Nawaz, "Content-based image retrieval based on visual words fusion versus features fusion of local and global features," *Arabian Journal for Science and Engineering*, pp. 1–20, 2018.

[39] S. Jabeen, Z. Mehmood, T. Mahmood, T. Saba, A. Rehman, and M. T. Mahmood, "An effective content-based image retrieval technique for image visuals representation based on the bag-of-visual-words model," *PLoS ONE*, vol. 13, no. 4, e0194526, 2018.

[40] S. Ghanem, C. Conly, and V. Athitsos, "A Survey on Sign Language Recognition Using Smartphones," in *Proceedings of the the 10th International Conference on PErvasive Technologies Related to Assistive Environments*, pp. 171–176, ACM, June 2017.

[41] L.-B. Chen, C.-W. Tsai, W.-J. Chang, Y.-M. Cheng, and K. S.-M. Li, "A real-time mobile emergency assistance system for helping deaf-mute people/elderly singletons," in *Proceedings of the IEEE International Conference on Consumer Electronics, ICCE 2016*, pp. 45-46, January 2016.

[42] R. Kamat, A. Danoji, A. Dhage, P. Puranik, and S. Sengupta, "MonVoix-An Android Application for the acoustically challenged people," *Journal of Communications Technology, Electronics and Computer Science*, vol. 8, pp. 24–28, 2016.

[43] G. Subhaashini, S. Divya, S. DivyaSuganya, and T. Vimal, "Ear Hear Android Application for Specially Abled Deaf People," *International Journal of Computer Science and Engineering*, vol. 3, no. 3, pp. 1108–1114, 2015.

[44] D. Bragg, N. Huynh, and R. E. Ladner, "A personalizable mobile sound detector app design for deaf and hard-of-hearing

users," in *Proceedings of the 18th International ACM SIGACCESS Conference on Computers and Accessibility, ASSETS 2016*, pp. 3–13, October 2016.

[45] M. A. M. Abushariah, "TAMEEM V1.0: speakers and text independent Arabic automatic continuous speech recognizer," *International Journal of Speech Technology*, vol. 20, no. 2, pp. 261–280, 2017.

[46] F. Leu and G. Lin, "An MFCC-Based Speaker Identification System," in *Proceedings of the 2017 IEEE 31st International Conference on Advanced Information Networking and Applications (AINA)*, pp. 1055–1062, March 2017.

[47] K. Mannepalli, P. N. Sastry, and M. Suman, "MFCC-GMM based accent recognition system for Telugu speech signals," *International Journal of Speech Technology*, vol. 19, no. 1, pp. 87–93, 2016.

[48] S. Elouahabi, M. Atounti, and M. Bellouki, "Amazigh Isolated-Word speech recognition system using Hidden Markov Model toolkit (HTK)," in *Proceedings of the International Conference on Information Technology for Organizations Development, IT4OD 2016*, April 2016.

[49] J. P. Bigham, R. Kushalnagar, T. K. Huang, J. P. Flores, and S. Savage, "On How Deaf People Might Use Speech to Control Devices," in *Proceedings of the the 19th International ACM SIGACCESS Conference*, pp. 383-384, October 2017.

[50] M. Gales and S. Young, "The application of hidden Markov Models in speech recognition," *Foundations and Trends in Signal Processing*, vol. 1, no. 3, pp. 195–304, 2008.

[51] S. J. Young and S. Young, *The HTK hidden Markov model toolkit: Design and philosophy*, University of Cambridge, Department of Engineering, 1993.

[52] M. Anusuya and S. K. Katti, "Speech recognition by machine, a review," https://arxiv.org/abs/1001.2267.

[53] D. Gupta, P. Bansal, and K. Choudhary, "The State of the Art of Feature Extraction Techniques in Speech Recognition," in *Speech and Language Processing for Human-Machine Communications*, pp. 195–207, Springer, 2018.

[54] W. Han, C.-F. Chan, C.-S. Choy, and K.-P. Pun, "An efficient MFCC extraction method in speech recognition," in *Proceedings of the ISCAS 2006: 2006 IEEE International Symposium on Circuits and Systems*, pp. 145–148, May 2006.

[55] M. A. Hossan, S. Memon, and M. A. Gregory, "A novel approach for MFCC feature extraction," in *Proceedings of the 4th International Conference on Signal Processing and Communication Systems, ICSPCS'2010*, December 2010.

[56] S. Memon, M. Lech, and L. He, "Using information theoretic vector quantization for inverted MFCC based speaker verification," in *Proceedings of the 2009 2nd International Conference on Computer, Control and Communication, IC4 2009*, February 2009.

[57] M. R. Hasan, M. M. G. Jamil, Rabbani., and M. S. Rahman, "Speaker identification using mel frequency cepstral coefficients," *Variations*, vol. 1, no. 4, 2004.

Hindawi
Wireless Communications and Mobile Computing
Volume 2018, Article ID 5767360, 11 pages
https://doi.org/10.1155/2018/5767360

Research Article

eSkin: Study on the Smartphone Application for Early Detection of Malignant Melanoma

Joanna Jaworek-Korjakowska and Pawel Kleczek

Department of Automatics and Biomedical Engineering, AGH University of Science and Technology, Krakow, Poland

Correspondence should be addressed to Joanna Jaworek-Korjakowska; jaworek@agh.edu.pl

Received 13 November 2017; Revised 23 January 2018; Accepted 4 February 2018; Published 7 March 2018

Academic Editor: Seyed M. Buhari

Background. Malignant melanoma is among the fastest increasing malignancies in many countries. With the help of new tools, such as teledermoscopy referrals between primary healthcare and dermatology clinics, the diagnosis of these patients could be made more efficient. The introduction of a high-quality smartphone with a built-in digital camera may make the early detection more convenient. This study presents novel directions for early detection of malignant melanoma based on a smartphone application. *Objectives and Methods*. In this study, we concentrate on a precise description of a complex infrastructure of a fully automated computer-aided diagnostic system for early detection of malignant melanoma. The framework has been customized for a dermoscope that is customized to attach to the smartphone to be able to carry out mobile teledermoscopy. The application requirements, architecture, and computational methods as well as behavioral and dynamic aspects have been presented in this paper. *Conclusion*. This paper presents a broad application architecture, which can be easily customized for rapid deployment of a sophisticated health application. Mobile teledermoscopy is a new horizon that might become in the future the basis of the early detection of pigmented skin lesions as a screening tool for primary care doctors and inexperienced dermatologists.

1. Introduction

Human cutaneous melanoma, a malignant pigmented lesion, is the deadliest type of skin cancer. It is characterized by a rapidly rising incidence rate among Caucasian populations and every year tens of thousands of people worldwide die of this cancer [1]. Melanoma is among the most aggressive neoplasms and rapidly metastasizes to distant organs. When it progresses to metastatic stage, it establishes powerful mechanisms to resist chemo- and radiotherapy, thus hindering the efficacy of current medical therapies [2]. However, when detected early, melanoma is treatable in nearly all cases with a simple surgical excision [3].

Apart from that, there are also benign types of pigmented skin lesions, the so-called moles, that are natural parts of the skin. Both benign and malignant pigmented skin lesions share similar visual characteristics which makes differentiating between them a challenging problem for nonspecialists [4]. This issue is particularly significant during naked eye examinations, when early stage melanomas (Figure 1(b)) often resembles benign lesions (Figure 1(a)). Due to low public awareness of the importance of skin cancer prevention and insufficient access to dermatologists in many regions of the world, melanoma is often diagnosed only after a tumor grows to a medium size (Figure 1(c)).

In the light of the above data, prevention and early diagnosis of melanoma become extremely important issues. There is a demand to develop computer-aided diagnostic systems facilitating the early detection of melanoma which could be applied by nonexperts and the general public [5]. Based on our previous research, we propose a teledermoscopy system architecture to assess malignancy of a skin lesion as well as to differentiate between micromelanomas and developed skin moles.

The goal of this research is to provide future plans and directions for the early detection of malignant melanoma based on a smartphone application. We also summarize the state of the art in the teledermoscopy applications and outline our conclusions from previous researches. The article opens with a short introduction to the topic of the undertaken

(a) Clark nevus (b) Melanoma in situ (c) Melanoma 0.76–1.5 mm

Figure 1: "Naked eye" images of melanocytic lesions [3].

research, a clinical definition of malignant melanoma, and its epidemiology. It continues with a description of the new technology, mobile teledermoscopy (MTD), which has potential for early skin cancer detection and mortality rate reduction. Furthermore, a new robust review of applications for the detection and analysis of melanoma has been described. In Section 2, we describe a new approach to a fully automated computer-aided diagnostic system for early detection of malignant melanoma. The application requirements and architecture as well as behavioral and dynamic aspects are presented. In Section 3, the eSkin application is presented and the early experiments and results are described. In Section 4, the challenges involved in the processing of skin-lesion images acquired with mobile devices and implementation of a patient-oriented system for analyzing such images are outlined.

1.1. Clinical Definition. Melanoma (also malignant melanoma) is a malignant neoplasm, derived from cells that are capable of forming melanin, arising most commonly in the skin of any part of the body including eyes or even sore throat. The high concentration of the body's pigmenting agent, melanin, is responsible for their dark color. Although melanocytic nevi are very common, their histogenesis is not well understood and still a matter of debate [3]. All we know about the life of melanocytic nevi is based on cross-sectional or cohort studies, because it is still complicated to monitor skin lesions in vivo on a cellular level. Skin moles may be congenital or developed during lifetime. The majority of moles appear during the first two decades of a person's life. The congenital melanocytic nevus is more likely to develop into a melanoma, because of its larger size and influence of UV radiation or chemical substances. Smaller melanomas tend to develop sporadically from a pigmented nevus and occur most commonly in fair-skinned people. Any black or brown spot having an irregular border, pigment appearing to radiate beyond that border, blue, red, or white coloration observable on close examination, or a nodular surface is suggestive of melanoma and is usually excised for biopsy [9]. Melanomas are most commonly located on the upper back and lower legs of fair-skinned and on the palms of the hands and insoles of the feet of dark-skinned individuals. Melanomas may metastasize and are among the most malignant of all cancers. Figure 2 shows the stages of melanoma evolution process.

Prognosis depends on the kind of melanoma, its size, and location and depth of invasion. The most important parameter which predicts the stage of melanoma is the thickness of the examined lesion. Skin moles with the thickness less than 1 mm are nearly 100% curable [3]. Seidenari and coworkers reported the direct correlation between diameter and thickness, and as the diameter of in situ melanomas is smaller than that of invasive lesions, it is reasonable to believe that small melanomas are usually in an initial growth phase [10]. Therefore, the aim of each clinician is to detect malignant melanomas when they are still small and thin. Figure 3 shows dermoscopic images of successive stages of melanoma.

1.2. Epidemiology of Melanoma. Over the past several decades, there has been a significant increase in the incidence and mortality rate from skin cutaneous melanoma among Caucasian populations worldwide (Figure 4) [1]. Despite the fact that only about 4% of all diagnosed skin cancers are melanoma, melanoma is responsible for about 70% of skin cancer-related deaths in the United States and in Australia [11, 12]. Invasive melanoma has an estimated incidence of 73,870 and an estimated total of 9940 deaths in the United States in 2015 [13].

One of the most important factors considered to result in melanoma is the brief, intense sun exposure pattern. Due to a constant depletion of ozone layer in stratosphere, which results in higher exposure to UV radiation, malignant melanoma is likely to become one of the most common malignant tumors in the future, with even 2–10 times higher incidence rate [1, 3]. As no effective treatment of melanoma in advanced stages has been developed so far, its early diagnosis has become an extremely important issue.

1.3. Improving Melanoma Detection Based on Sensing Technologies. Telemedicine which is also called telehealth, online

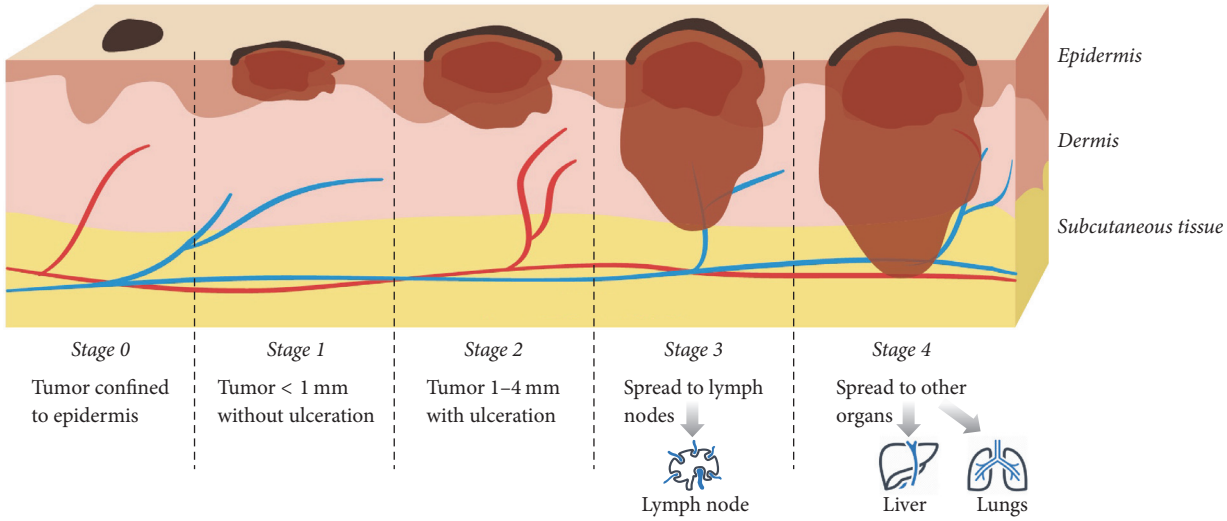

Figure 2: Presentation of five stages in malignant melanoma evolution process.

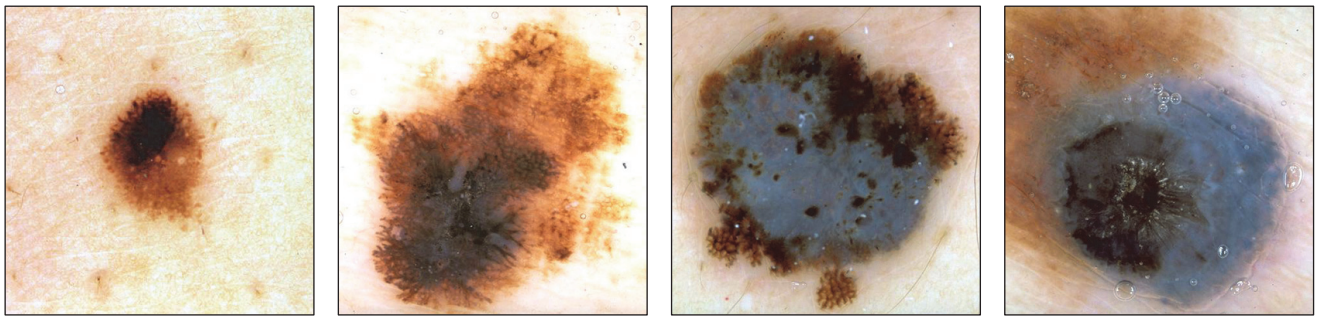

Figure 3: Dermoscopic images of successive stages of melanoma [3].

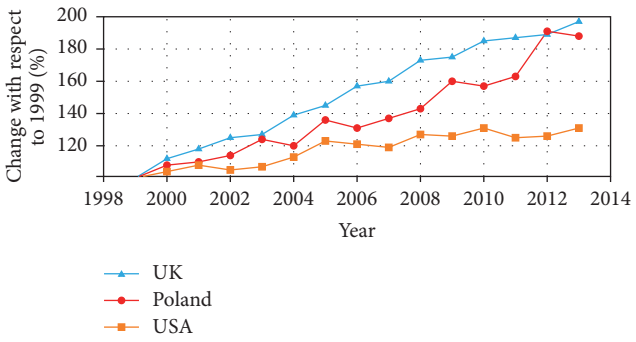

Figure 4: The increase in incidence rate of skin melanoma observed in UK, Poland, and USA between 1999 and 2013 [6–8]. The incidence rate reported in 1999 has been set as a point of reference.

health, e-health, or "medicine at a distance" is a new and rapidly developing field of medicine, providing access to medical knowledge that would be not available at a particular location and time. It is commonly defined as the use of telecommunication technologies for the exchange of medical information over a distance for the purpose of patient management (including triage, diagnosis, and therapeutic suggestions, as well as follow-up) and medical education [14]. Teledermatology has been listed in Norway among priority telemedicine specialities for large-scale implementation underlining the growing interest in this field [14, 15].

The most important question that has to be posed while supporting the early skin cancer detection is *does the teledermoscopy system achieve an adequate accuracy and is it effective?* In this research, we will analyze only two factors including diagnostic reliability and accuracy as well as economic analysis. With no doubt, the most significant parameter while using any computer-aided diagnosis system is the diagnostic reliability and accuracy which have to be compared between the diagnostic system and conventional method (human interpretation) [16]. Diagnostic accuracy assessments for dermatologic disease are still problematic. The histopathological examination constitutes the gold standard for classifying a melanocytic skin lesion as malignant. Although there exist other forms of examination (e.g., dermatoscopy), they yield lower diagnostic confidence than a histopathological examination. Still, numerous studies showed that the misdiagnosis rate of melanoma may be as high as 10–25%. Histopathologic review cannot be universally used to make a definitive diagnosis of all skin lesions. Despite

Table 1: A summary of mobile applications for melanoma risk assessment and diagnosis available on App Store in March 2017.

Application	Main functionality	Image analysis method
DermaCompare	Risk assessment	Image matching
Lūbax	Mole diagnosis	Content-based image retrieval
MySkinApp	Risk assessment	Unknown
SkinVision	Risk assessment	Fractal analysis

this, few studies have analyzed data among patients that underwent biopsy and other diagnostic methods which made it possible to compare the teledermatology systems with the clinic-based examination [16–18]. Teledermatology systems achieved accuracy at about 70–85% which indicates that the computer-based solutions have comparable diagnostic accuracy when compared to conventional clinic-based care [16]. While implementing and deploying a teledermatology system, the economic aspects play an important role. The following criteria are taken into account: dermatology visits that have been avoided, skin biopsies skipped, and consult costs. In study [19], authors have evaluated the proportion of real-time interactive teledermatology consults that avoided a clinic-based visit to a dermatologist. Dermatology clinic visits have been avoided in 54% thanks to the real-time interactive teledermatology. Also the decrease of the number of biopsies is a cost-saving strategy. Based on a quick evaluation of the dermoscopy image, inexperienced physicians will gain knowledge and avoid unnecessary treatment.

1.4. Related Works. According to the estimates by the American Food and Drug Administration, nearly 500 million smartphone users worldwide use eHealth mobile applications. In July 2014, there were 39 dermatology-related mobile applications aimed at general community, patient, and generalist clinician users available on the market [20]. The main functionality of over half of them was to provide information or education about melanoma, UV radiation exposure prevention advice, and skin self-examination strategies. Such applications are usually targeted at students and novice doctors. Another large group of applications were those capable of taking images of moles using mobile embedded camera, tagging them with the body location, and storing them either for review by a dermatologist or for self-monitoring to track changes in mole appearance, an important predictor of melanoma.

In March 2017, there were over 45 mobile applications related to mole diagnosis available on Apple's App Store alone. Most of them ($n = 28$) offered only educational information on melanoma, nearly half of them ($n = 17$) allowed the user to take photos of their moles and track changes over time using simple visual comparison, and only four applications performed melanoma risk assessment or lesion classification based on image analysis (Table 1).

Only the authors of SkinVision and Lūbax made public the results of clinical evaluation of their risk assessment algorithm [21, 22]. Out of 4 applications summarized in Table 1, only two were certified by authorities: SkinVision received the European "CE" Marking and DermaCompare was approved by the US Food and Drug Administration.

1.4.1. SkinVision. The risk assessment algorithm used by SkinVision is based on the analysis of a gray-scale image of a lesion (I_G) and its associated fractal map I_{FM}. The fractal map is generated based on the weighted local fractal dimension (WLFD) proposed in [23] (the WLFD was originally used for computer tomography image enhancement, but authors of SkinVision adapted it to the context of dermatoscopy). To segment the lesion (and thus extract the lesion contour), thresholds t_G and t_{FM} were obtained by applying Otsu's thresholding on I_G and I_{FM}, respectively. The following parameters are calculated on I_{FM}: percentage of pixels with WLFD lower than $t_{FM}/3$, percentage of pixels with WLFD lower than $t_{FM}/2$, number of connected regions with distinct textures found in the interval $[0, t_{FM}/2]$, and t_{FM}, and the following are calculated on I_G: number of connected regions with distinct intensities found in the interval $[0, t_{FM}/2]$, t_G, and circularity index. Based on these parameters, the SkinVision application evaluates lesions to one of the three risk classes: high, medium, or low.

SkinVision was tested on a set of melanocytic lesions images taken using iPhone 4S mobile device equipped with an 8-megapixel autofocus camera. It achieved the overall sensitivity of 73%, specificity of 83%, and accuracy of 81%. The positive and negative predictive values were 49% and 83%, respectively.

1.4.2. Lūbax. The skin-lesion classification system used by Lūbax consists of a proprietary database of nearly 12,000 images of diagnosed lesions and a computer algorithm based on the principles of content-based image retrieval (the algorithm compares characteristics of new images with images in the database to identify the nearest-match diagnosis).

The lesion images were taken using Celestron® (Torrance, CA) hand-held digital microscopes equipped with 2-megapixel cameras with a macro lens surrounded by a ring of white light-emitting diode lights. The consistent lighting conditions and imaging distance were ensured by attaching an opaque 10 cm tube to the front of each camera. The largest diameter for all nonmelanoma and melanoma lesions was at least 10 mm.

Each lesion image in the database was reviewed and diagnosed by at least one of three board-certified dermatologists using standard clinical criteria. The "ground truth" classification was not biopsy-proven, but based on the agreement between the reviewing dermatologists. Only 302 images of melanoma borrowed from the DermNet NZ [24] database were previously confirmed by histopathology.

The algorithm compares new images of skin lesions with the database of diagnosed skin-lesion images. It uses orientation- and artifact-independent image information on

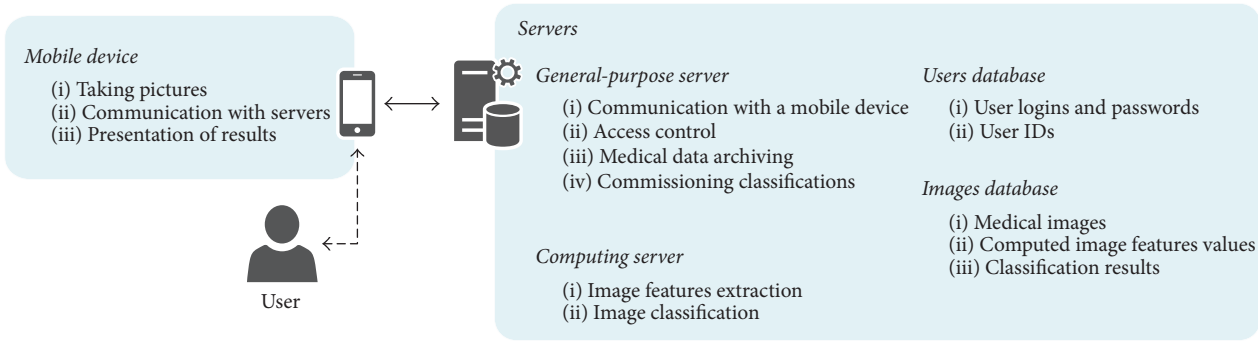

Figure 5: The concept diagram of the proposed system.

lesion size, color, shape, and texture to create a single high-dimensional signature for each image. The "malignant versus nonmalignant" classification is then performed using a k-nearest-neighbor classifier.

Lūbax was evaluated on a set of 337 images queried from the database, out of which 208 were melanomas. It scored sensitivity of 90.4%, specificity of 91.5%, and accuracy of 90.8%. The positive and negative predictive values were 94.5% and 85.5%, respectively.

2. Development of the eSkin Teledermatoscopy System

Based on the above information, there is still a great need in the development and analysis of teledermatoscopy systems. In this paper, we propose a new approach to the analysis of nonmelanoma and melanoma lesions. The innovation is firstly based on the differentiation between micromelanomas which have diameter less than 5 mm and advanced skin moles. Secondly, we propose an additional algorithm for the skin-lesion differentiation that can be applied in a teledermoscopy system and has been described in our work [25]. In this section, we present the system overview and describe the technical requirements, application architecture, and behavioral and dynamic aspects of the system.

2.1. Concept of the System. The purpose of presenting the concept of the system is its better illustration and description of the relationships between the individual modules of the system. While composing the system, overview issues such as safe medical information transfer, fast connection availability, server choice, and database type are analyzed. Figure 5 presents the implemented concept of a system that consists of a smartphone application available to the client (client side) and the server side of the system, consisting of a general-purpose server, computing server, users database, and images database.

2.2. Application Requirement Specification. The most important piece of hardware is a high-quality camera system. Certain dermoscopic features of a lesion, such as pigment network or dots, are clearly visible only under magnification (usually of at least ×10). Moreover, since colors visible in a lesion are important diagnostic clues, it is desirable to take images in appropriate illumination conditions.

Most modern smartphone cameras (this is true, e.g., for all iPhone devices starting from iPhone 5S and all Samsung Galaxy devices starting from Samsung Galaxy S4) are equipped with at least 8-megapixel sensor whose pixel size is at most 1.5 μm, allowing the user to capture high-quality photos. However, smartphone cameras generally lack a quality optical zoom and are not equipped in a source of white light which would uniformly illuminate an examined lesion.

The solution to the above-mentioned deficiencies of bare smartphones is to use either a smartphone dermatoscope or a conventional dermatoscope with a mobile phone case (Figures 6 and 7). A smartphone dermatoscope is an attachment for dermoscopy that provides a detailed view of the skin through magnification and specialized lighting. Most smartphone dermatoscopes currently available on the market provide ×10 to ×40 magnification, work in both polarized and nonpolarized lighting modes, and are capable of performing examinations in both contact and noncontact mode. Some conventional dermatoscopes may be attached to a mobile phone using a special case (e.g., all dermatoscopes from 3Gen's DermLite and Canfield's VEOS series may be used with iPhone 5 and newer and 3Gen's DermLite and MoleScope products can be used with Samsung Galaxy S4 and newer).

2.3. Application Architecture. Like any other complex system, software and essentially medical applications have to be built on solid foundations. During the smartphone application design process, it is important to define a structured solution that meets all of the technical and operational requirements, while optimizing common quality attributes such as performance, security, and manageability. The process involves a series of decisions based on a wide range of factors, and each of these decisions can have considerable impact on the quality, performance, maintainability, and overall success of the application [26]. The proposed system consists of two parts: mobile application and servers (Figure 8).

The tasks of the mobile application include the following:

(i) Friendly user interface with the ability to log in and change basic settings

(a) MoleScope™ (b) DermLite® Connection Kit

Figure 6: Examples of smartphone dermatoscopy solutions for an iPhone: (a) a smartphone dermatoscope; (b) a conventional dermatoscope attached to a smartphone in a case.

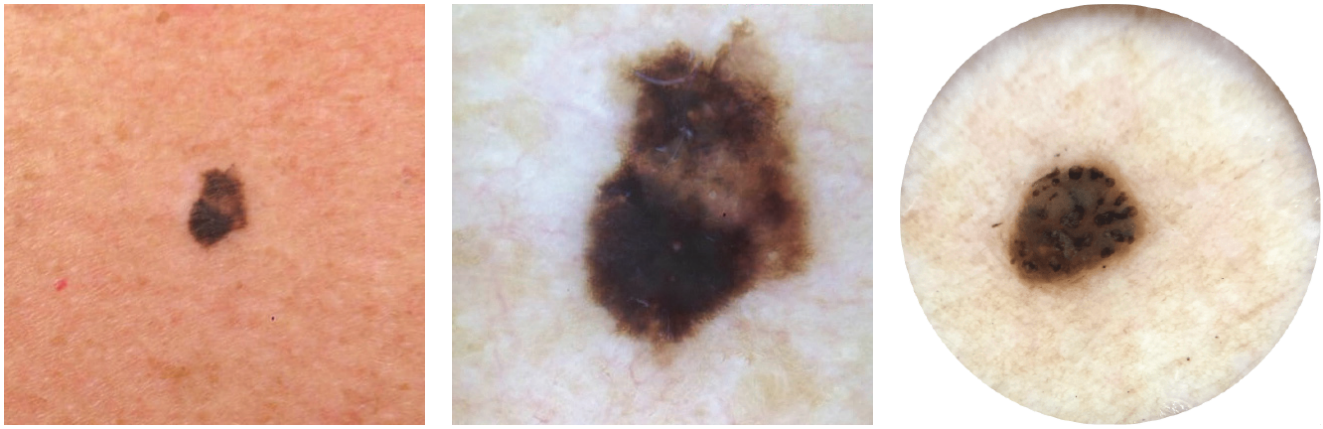

(a) No attachment (b) HÜD™ (c) MoleScope II™

Figure 7: The comparison of the qualities of pictures taken with (a) a bare smartphone and (b, c) a smartphone equipped with a dermatoscopic attachment.

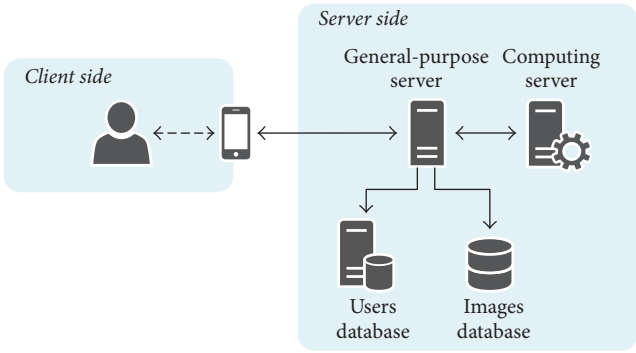

Figure 8: The system architecture diagram of the proposed system.

(ii) The ability to take a picture of a skin mole or select from already saved pictures on the smartphone

(iii) Presentation of results of classification of selected skin mole

(iv) User location for UV hazard rating

(v) Communication with servers including general-purpose server, image database, user database, and computing server

(vi) Checking the Internet connection and data security.

The tasks performed by the server include the following:

(i) Communication with the user mobile device *(general server task)*

(ii) User login (username and password verification) and access control *(general server and user database task)*

(iii) Calculation of feature parameters, image classification, and comparison of ratings *(computing server task)*

(iv) Medical data archiving (medical images, computed skin mole parameters, and classification results) *(image and user database task)*.

2.4. Behavioral and Dynamic Aspects of the System. The activity diagram of the proposed mobile application, capturing its dynamic behavior, is shown in Figure 9. The

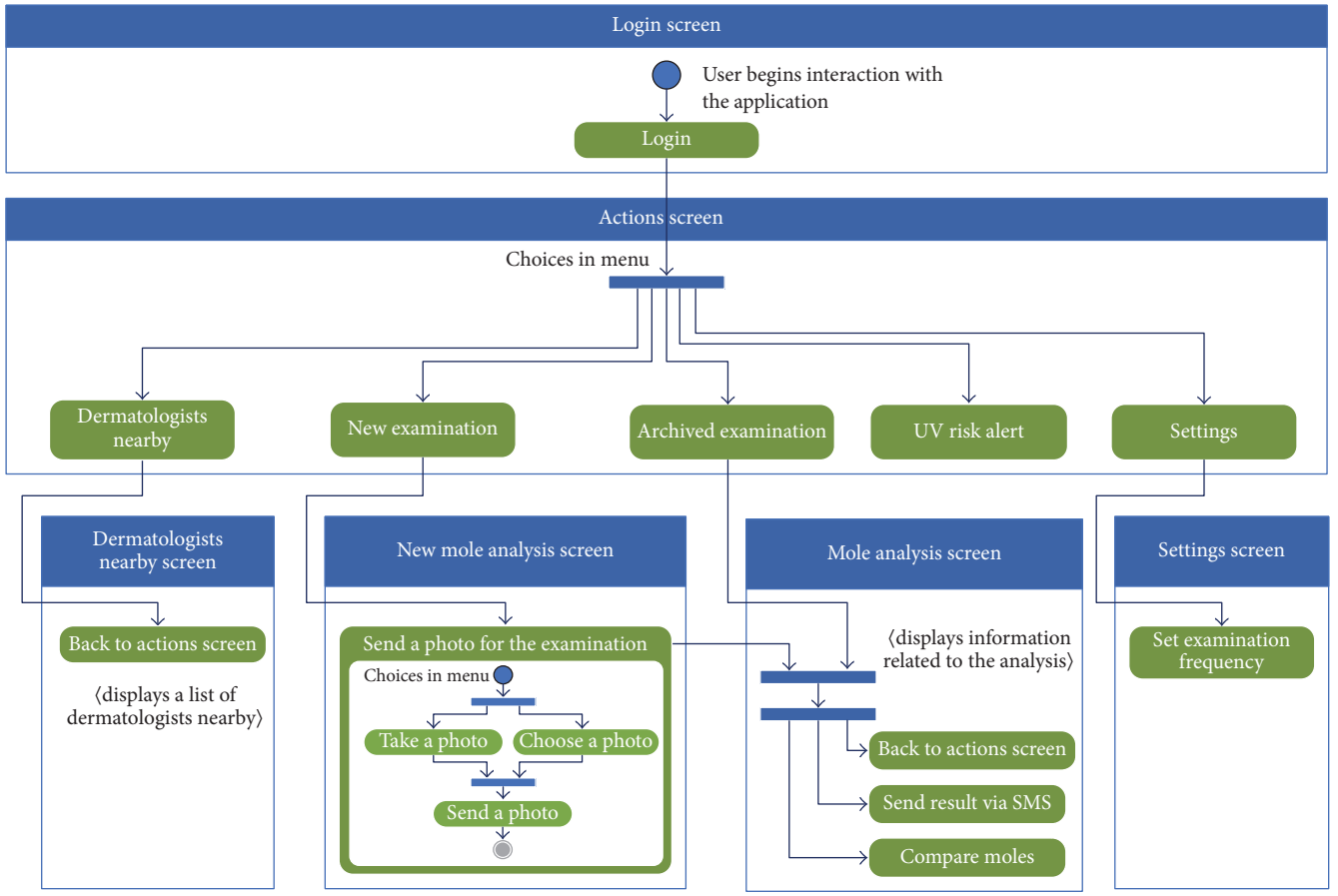

Figure 9: The activity diagram of the eSkin application.

main functionality of the application is to take photos of moles and send them to the server in order to perform melanoma risk assessment. It is also capable of archiving captured photos and browsing through past examinations. Additional features, intended to rise melanoma awareness, include ultraviolet radiation risk alerts, reminders about a subsequent examination, and a tool to easily find the nearest dermatologist.

A data flow diagram (DFD) is a graphical representation of the "flow" of how data is processed by a system in terms of inputs and outputs. It focuses on the flow of information, where data comes from, where it goes, and how it gets stored. It is a picture of the movement of data between external entities and the processes and data stores within a system. Figure 10 presents the proposed DFD diagram. A DFD diagram consists of external entities, processes, and data stores:

(i) *External entities*: origin or destination of data (outside the system): user (mobile application), computing server, and general-purpose server

(ii) *Processes*: work or action performed on data: image evaluation, authentication, image storage, and subcontract image evaluation

(iii) *Data stores*: data that the system stores: users' database and images' database.

2.5. Computational Methods. Analysis and classification of melanoma skin lesions are a complex issue due to the different appearance on various levels of disease progression. Our recent research and experience in the topic of early detection of melanoma have shown that different approach to the classification process should be undertaken to improve the recognition results. The implemented and tested computer-aided diagnostic system has been presented in Figure 11. The first two steps including image preprocessing and segmentation are performed for each of the analyzed medical pictures.

The preprocessing step is essential for dermoscopic images to improve the quality due to the extraneous artifacts, such as skin lines, air bubbles, and hairs which appear in almost every image. The preprocessing step contains three algorithms [27, 28]:

(i) Black frame removal: black frames, introduced to the image during its digitization, are detected using lightness component of the HSL color space.

(ii) Smoothing: Gaussian filter is used for smoothing of air bubbles and light hairs.

(iii) Black hair inpainting: for removing black and thick hairs, we chose the white top-hat transform. Hair line pixels are replaced with values calculated on the basis of the neighborhood pixels.

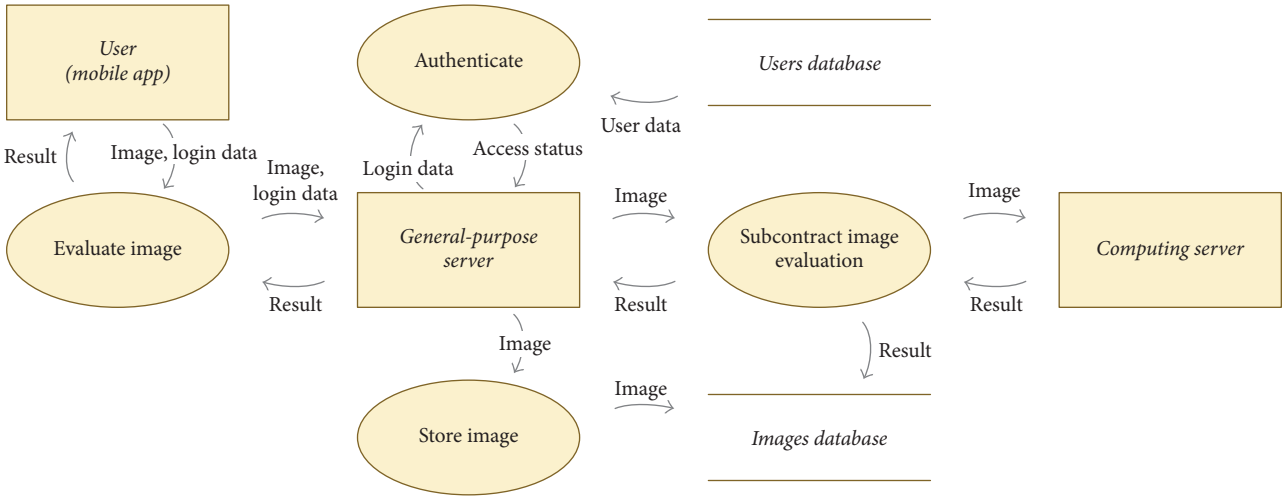

Figure 10: The data flow diagram of the proposed mobile application.

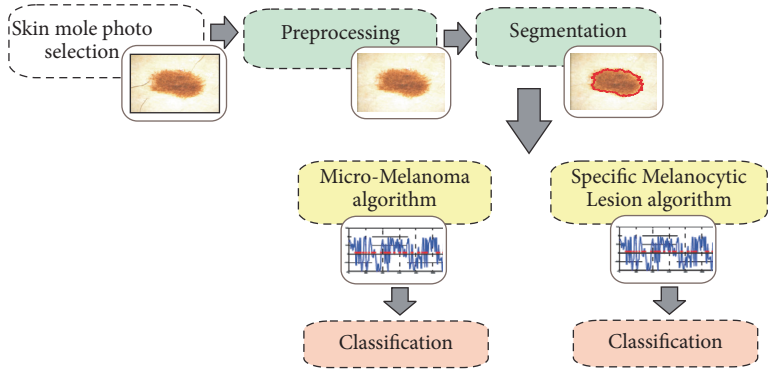

Figure 11: The schema of the implemented and tested computer-aided diagnostic system.

A medical image is one of most complicated images to be segmented; furthermore, this step is crucial for sequential analysis and diagnosis. During our work, we have compared different segmentation methods and on the grounds of the previous outcomes the applied segmentation algorithm for the skin-lesion extraction is based on seeded region-growing algorithm [29, 30].

After the first two steps, the segmented skin mole is ordered to one of the two classification algorithms. The division is done on the basis of the mole diameter. Skin moles with a diameter lower than 5 mm are passed to the *Micro-Melanoma algorithm* and the remaining ones to the *Specific Melanocytic Lesion algorithm*. The diameter of the lesion is provided by the user as it is not possible to assess it only based on the medical image. Micromelanomas represent a minority of diagnosed lesions, their frequency ranging from 1% to 17%. The mean diameter of in situ melanomas is around 1 cm, and invasive melanomas are usually greater than 6 mm. Despite the fact that micromelanomas are in the minority, they are responsible for most errors during the diagnosis. Separation of individual changes allows us to obtain a more accurate and reliable computer diagnosis system. The *Micro-Melanoma algorithm* and the *Specific Melanocytic Lesion algorithm* have been described in detail in [25, 28].

3. Early Experiments

We implemented the application on an iOS smartphone, which most of the people in US use in their daily lives. This small smartphone includes all sensors that can provide enough information needed for realizing this system. The preliminary version of the eSkin application has been implemented in Swift in the Xcode development environment which is dedicated for macOS and contains a suite of software development tools for macOS, iOS, watchOS, and tvOS. Figure 12 presents the proposed version of the graphical user interface. The basic functionality including taking a medical photo and assessing the skin mole as well as medical data archiving have been implemented.

The eSkin application uses a scientifically proven algorithm to detect and analyze the dermoscopy images for visible signs of skin cancer. To measure the diagnostic performance, we calculated sensitivity, specificity, and the area under that

Table 2: A summary of the classification results for the medical algorithms.

Medical diagnosis	TPR [%]	TNR [%]	AUC [%]
Micromelanoma lesions	90	96	93
Blue nevus	100	100	100
Clark nevus	91	96	98
Malignant melanoma	86	96	97
Spitz nevus	94	98	98

Figure 12: The proposed version of the graphical user interface.

plot curve (AUC). The fundamental definitions of these performance measures could be illustrated as follows.

The sensitivity (also called True Positive rate) is the probability that the cell is said to be adherent given that it is. This can be estimated by relative frequency:

$$\mathrm{TPR} = \frac{\#\mathrm{TP}}{\#\mathrm{TP} + \#\mathrm{FN}}, \tag{1}$$

where TP is the True Positive answer and FP is the False Negative answer. The value of sensitivity ranges between 0 and 1, where 0 and 1, respectively, mean worst and best classification.

Specificity (also called False Positive rate), which is defined as the proportion of the True Negatives against all negative results, is defined by the following equation:

$$\mathrm{TNR} = \frac{\#\mathrm{TN}}{\#\mathrm{TN} + \#\mathrm{FP}}, \tag{2}$$

where TN is the True Negative answer and FN is the False Negative answer. Value of specificity ranges between 0 and 1, where 0 and 1, respectively, mean worst and best classification.

Table 2 shows the classification results obtained with the implemented algorithms for microlesions as well as developed skin moles.

For statistical analysis, SkinVision classified histologically proven nevi as low or medium risk and melanoma as high-risk lesion. The statistics included 144 lesions (with a minimum of 3 images per lesion) with the following histological diagnosis: 84 benign nevi (58%), 34 dysplastic nevi (24%), and 26 melanomas (18%).

Images of poor quality (e.g., due to inappropriate imaging angle or distance) and containing other elements not belonging to the lesion (e.g., hair), as well as cases with an equal number of results in two consecutive risk classes (e.g., 1 high risk, 1 medium risk, and 1 low risk result), were excluded from the analysis. In total, 26% of the images initially taken have been dismissed due to improper imaging.

The sensitivity of the SkinVision melanoma detection algorithm compared to the histological result was 73%, the specificity 83%, and the accuracy 81%.

The performance of the melanoma detection algorithm by Lūbax was assessed on a set of 337 images randomly selected from their database. The set included 129 images of nonmelanoma lesions and 208 images of melanoma lesions, all with the largest diameter of at least 10 mm. All melanoma query images were selected from the set of images acquired from DermNet NZ to ensure confirmation of the malignancy by histopathology.

The sensitivity of the Lūbax melanoma detection algorithm was 90%, the specificity 91%, and the accuracy 91%. For the melanoma classification, the sensitivity of the SkinVision algorithm compared to the histological result was 73%, the specificity 83%, and the accuracy 81%.

The conducted results achieved by the implemented classification system are much better than the results described in similar works. Our method allowed classification of skin

moles very precisely and we can confirm that the classification of micro-skin lesions has to be done separately from the classification of developed skin moles. Overall, our experiments clearly show that the classification can be supported by a powerful system based on advanced machine learning techniques.

4. Conclusions and Discussion

In this paper, we propose a new teledermatology system for melanoma diagnosis, based on our previous research on assessing malignancy of a skin lesion as well as on differentiating between micromelanomas and developed skin moles. Our system is built in a client-server architecture and is intended for smartphone users.

In our system, the main functionality of the client application is to take photos of moles and send them to the server in order to perform melanoma risk assessment. By shifting all computations related to image assessment to the dedicated servers, we may analyze dermoscopic images using computationally demanding algorithms. Since the medical data would be archived in a central database, they would provide invaluable aid when working on improvements to the diagnostic algorithm. The client-server architecture would also make the process of implementing changes to the assessment algorithms seamless for the users, since there would be no need for client software updates.

To ensure high quality of images and good visibility of certain dermoscopic features of a lesion, the system is designed to work with smartphone dermatoscopes or conventional dermatoscopes with a mobile phone case. Such a solution would also reduce the negative impact of taking images in appropriate illumination conditions and make it possible to avoid issues with determining the size of a lesion. The latter issue is of particular importance, since our recent research has shown that depending on the size of a lesion different diagnostic algorithms should be used to improve the recognition results.

Although the client side of our system was initially developed for iOS devices, it does not use any functionality specific to either iOS or Apple's smartphones. Therefore, it could easily be ported to work with devices running the Android operating system.

Due to low public awareness of the importance of skin cancer prevention and insufficient access to dermatologists in many regions of the world, there is a demand to develop computer-aided diagnostic systems facilitating the early detection of melanoma which could be applied by nonexperts. However, as of March 2017, there were only four mobile applications performing melanoma risk assessment or lesion classification based on image analysis available to the general public. With teledermatology systems achieving accuracy up to 85%, comparable to conventional clinic-based care, we are convinced that our system would fulfill that demand and allow its users to avoid dermatology visits, to skip skin biopsies, and to cut costs of consultations.

Conflicts of Interest

The authors declare that there are no conflicts of interest regarding the publication of this paper.

Acknowledgments

This scientific work was supported by AGH University of Science and Technology research grant on Decision nos. 15.11.120.883 and 15.11.120.635 to J. Jaworek-Korjakowska.

References

[1] C. Garbe and U. Leiter, "Melanoma epidemiology and trends," *Clinics in Dermatology*, vol. 27, no. 1, pp. 3–9, 2009.

[2] M. Campioni, D. Santini, G. Tonini et al., "Role of Apaf-1, a key regulator of apoptosis, in melanoma progression and chemoresistance," *Experimental Dermatology*, vol. 14, no. 11, pp. 811–818, 2005.

[3] G. Argenziano, P. H. Soyer, V. D. Giorgio et al., *Interactive Atlas of Dermoscopy*, Edra Medical Publishing and New Media, 2000.

[4] K. Korotkov and R. Garcia, "Computerized analysis of pigmented skin lesions: a review," *Artificial Intelligence in Medicine*, vol. 56, no. 2, pp. 69–90, 2012.

[5] R. Tadeusiewicz, "How intelligent should be system for image analysis?" in *Innovations in Intelligent Image Analysis*, H. Kwaśnicka and L. C. Jain, Eds., vol. 339 of *Studies in Computational Intelligence*, pp. V–X, Springer Verlag, Berlin, Heidelberg, 2011.

[6] *englishSkin Cancer Incidence Trends over Time*, Cancer Research UK, 2016.

[7] "Zachorowania i zgony na nowotwory złos'liwe w polsce, Krajowy Rejestr Nowotworów, Centrum Onkologii, Instytut im. Marii Skłodowskiej-Curie, 2016".

[8] *Seer stat fact sheets: Melanoma of the skin*, National Cancer Institute, 2016.

[9] *Mosby's Medical Dictionary*, Elsevier, 10th edition, 2016.

[10] S. Seidenari, C. Ferrari, S. Borsari et al., "Dermoscopy of small melanomas: just miniaturized dermoscopy?" *British Journal of Dermatology*, vol. 171, no. 5, pp. 1006–1013, 2014.

[11] *Cancer Facts & Figures 2016*, American Cancer Society, 2016.

[12] Australian Bureau of Statistics, *Causes of Death, Australia 2015*, 2016.

[13] M. E. Celebi, J. S. Marques, and T. Mendonca, *Dermoscopy image analysis*, CRC Press LLC, 1st edition, 2016.

[14] E. M. T. Wurm, H. P. Soyer, and A. C. Smith, *Telemedicine in Dermatology*, Springer-Verlag, Berlin, Germany, 1st edition, 2012.

[15] J. Norum, S. Pedersen, J. Størmer et al., "Prioritisation of telemedicine services for large scale implementation in Norway," *Journal of Telemedicine and Telecare*, vol. 13, no. 4, pp. 185–192, 2007.

[16] J. D. Whited, H. S. Pak, and K. E. Edison, *Teledermatology: A User's Guide*, Cambridge University Press, Cambridge, UK, 2008.

[17] J. D. Whited, R. P. Hall, D. L. Simel et al., "Reliability and accuracy of dermatologists clinic-based and digital image consultations," *Journal of the American Academy of Dermatology*, vol. 41, no. 5, pp. 693–702, 1999.

[18] S. Markun, N. Scherz, T. Rosemann, R. Tandjung, and R. P. Braun, "Mobile teledermatology for skin cancer screening: A diagnostic accuracy study," *Medicine*, vol. 96, no. 10, p. e6278, 2017.

[19] R. Wootton, M. A. Loane, S. E. Bloomer et al., "Multicentre randomised control trial comparing real time teledermatology with conventional outpatient dermatological care: Societal cost-benefit analysis," *British Medical Journal*, vol. 320, no. 7244, pp. 1252–1256, 2000.

[20] A. P. Kassianos, J. D. Emery, P. Murchie, and F. M. Walter, "Smartphone applications for melanoma detection by community, patient and generalist clinician users: A review," *British Journal of Dermatology*, vol. 172, no. 6, pp. 1507–1518, 2015.

[21] T. Maier, D. Kulichova, K. Schotten et al., "Accuracy of a smartphone application using fractal image analysis of pigmented moles compared to clinical diagnosis and histological result," *Journal of the European Academy of Dermatology and Venereology*, vol. 29, no. 4, pp. 663–667, 2015.

[22] R. H. Chen, M. Snorrason, S. M. Enger et al., "Validation of a Skin-Lesion Image-Matching Algorithm Based on Computer Vision Technology," *Telemedicine and e-Health*, vol. 22, no. 1, pp. 45–50, 2016.

[23] A. Udrea, M. Tanase, and D. Popescu, "Nonlinear deterministic methods for computer aided diagnosis in case of kidney diseases," in *Proceedings of the 9th International Conference on Informatics in Control, Automation and Robotics (ICINCO '12)*, J. Ferrier et al., Ed., 516, pp. 31–511, SciTe Press, 2012.

[24] DermNet NZ, *The dermatology resource*, http://www.dermnetnz.org.

[25] J. Jaworek-Korjakowska and P. Kłeczek, "Automatic classification of specific melanocytic lesions using artificial intelligence," *BioMed Research International*, vol. 2016, Article ID 8934242, 17 pages, 2016.

[26] Patterns and Practices Developer Center, *What is software architecture?*, 2009.

[27] J. Jaworek-Korjakowska and R. Tadeusiewicz, "Hair removal from dermoscopic color images," *Bio-Algorithms and Med-Systems*, vol. 9, no. 2, pp. 53–58, 2013.

[28] J. Jaworek-Korjakowska, "Computer-aided diagnosis of micro-malignant melanoma lesions applying support vector machines," *BioMed Research International*, vol. 2016, Article ID 4381972, 8 pages, 2016.

[29] J. Jaworek-Korjakowska, "Novel method for border irregularity assessment in dermoscopic color images," *Computational and Mathematical Methods in Medicine*, vol. 2015, Article ID 496202, 11 pages, 2015.

[30] J. Jaworek-Korjakowska, *Detection and analysis of local structures in malignant melanoma [Ph.D. thesis]*, AGH University of Science and Technology in Krakow, 2013.